THE BIOLOGICAL ROLES OF GLUTATHIONE TRANSFERASE OMEGA 1

Deepthi Menon

A thesis submitted for the degree of Doctorate of Philosophy

at the Australian National University

March, 2015

The John Curtin School of Medical Research,
Australian National University
Canberra, Australia

Statement of authorship

The results presented in this thesis are, except where otherwise acknowledged, my own original work. The J774.1A macrophage stable transfectants were generated by Dr. Rebecca Coll, Luke O'Neill laboratory, Trinity College Dublin. The cell line characterization results presented in Figure 5.1A, B & C (Chapter 5) were provided by Dr. Coll and have been acknowledged accordingly.

Deepthi Menon
Molecular Genetics group
Dept. of Molecular Biosciences
The John Curtin School of Medical Research
Australian National University

Acknowledgements

I would like to thank my supervisor, Prof. Philip Board, for this fantastic project and for the constant support and enthusiasm. The three of us made a good team (you, me and the project!)

I am very grateful to Prof. Luke O'Neill and his laboratory for hosting my visit at Trinity College Dublin and providing a wonderful and inspiring environment to work in. Special thanks goes to Dr. Rebecca Coll for her efforts in generating the J774.1A stable transfectants. Truly and deeply appreciated!

I am grateful to Prof. Jane Dahlstrom (The Canberra Hospital, Australia) for analysing our pathology samples and for providing us with valuable feedback under such time constraints.

I thank my panel members Dr. Anneke Blackburn, Dr. Stefan Broer and Dr. Marco Cassarotto for their timely advice and suggestions.

I would like to thank Dr. Thy Thuong at the Mass spectrometry facility, RSB for training me up on the use of the mass spectrometer and for her valuable advice on the data analysis.

The technical support provided by the staff at the Biomolecular Research Facility (BRF) and the microscopy division (MCRF), ANU is highly appreciated.

I thank the Australian Phenomics Facility (APF) for doing a fantastic job maintaining the animals used in this study and making them available at our convenience.

I would like to acknowledge the funding bodies that have contributed to this work: Australian National University PhD Scholarship, Boote's Foundation research project grant and the European Molecular Biology Organization for the EMBO Short term fellowship.

I am very grateful to Dr. Dan Liu, Dr. Padmaja Tummala and Santhi Achuthan for proofreading my thesis and providing insightful advice.

Finally, I thank the Molecular genetics group, Cancer genetics and metabolism group and ex-members of the Muscle research group for helping me make it to the end.

I have always wondered how my ma and acha put up with my continuous absence for the past few years. I wouldn't have made it this far without them!

Abstract

Glutathionylation is the reversible redox modification of protein thiols by disulphide formation with glutathione. Glutathionylation can alter protein structure and activity in response to changes in the oxidation state of the protein, thus modulating protein stability. The forward reaction is largely spontaneous while the reverse reaction (deglutathionylation) is predominantly catalysed by the Glutaredoxin (Grx) family of thioltransferases. Glutathione transferase Omega 1 (GSTO1-1) is an atypical glutathione transferase that has minimal functional resemblance with other members of the superfamily. GSTO1-1 has previously been shown to have high thioltransferase activity like glutaredoxins. Interestingly, GSTO1-1 has been reported to be differentially expressed in neurodegenerative diseases. Although the studies reporting these differences speculate on the GST-like activity of GSTO1-1, it is evident from data published by our laboratory that the primary role of GSTO1-1 is yet to be identified. This study investigated the role of GSTO1-1 in the glutathionylation cycle.

Here, we show that human GSTO1-1, with a unique conserved cysteine at its active site, can catalyse the deglutathionylation of protein thiols *in vitro* and in cell lines. The kinetics of the catalytic activity of GSTO1-1 was determined *in vitro* by assaying the deglutathionylation of a synthetic peptide by tryptophan fluorescence quenching and in cell lines by means of immunoblotting and immunoprecipitation. We generated stable GSTO1-1 transfectants in T47-D breast cancer cells which are devoid of endogenous GSTO1-1. The over-expression of GSTO1-1 in these cells resulted in a global abatement of protein glutathionylation. Furthermore, we demonstrated that a mutation in the active cysteine residue (Cys-32) ablates the deglutathionylating activity, confirming the role of GSTO1-1 as a redox switch in regulating protein post translational modification. Mass spectrometry revealed four deglutathionylated targets of GSTO1-1, of which β-actin was validated by extensive immunoprecipitation studies and the physiological impact of deglutathionylated β-actin was confirmed by immunostaining. This study introduces GSTO1-1 as a novel member of the family of deglutathionylating enzymes which is currently restricted to glutaredoxins and sulfiredoxins and identifies specific proteins targeted by GSTO1-1 in cells. Additionally, we have developed and employed a novel and rapid method to quantify global glutathionylation *in vitro* to confirm the catalytic role of GSTO1-1 in the glutathionylation cycle.

GSTO1-1 has been investigated in relation to a number of biologically and clinically significant pathways and disorders including drug resistance, Alzheimer's disease, Parkinson's disease, the action of anti-inflammatory drugs and susceptibility to chronic obstructive pulmonary disease (COPD). Since glutathionylation has also been implicated in the pathology of Alzheimer's disease, Parkinson's disease, COPD and inflammation, it is proposed that GSTO1-1 dependent glutathionylation and/or deglutathionylation could be a common factor. The data gathered from the initial phase of the project directed us to determine whether GSTO1-1 is required for inflammatory signalling in phagocytic immune cells such as macrophages. Inflammatory stimulants such as bacterial lipopolysaccharide (LPS) have been shown to induce the generation of reactive oxygen species (ROS) through the activation of Toll like receptor 4 (TLR4) and the recruitment of downstream signalling proteins resulting in the subsequent induction of pro-inflammatory cytokines such as IL-1β, IL-6, TNF-α and ROS generating NADPH oxidase 1 (NOX1). Following from the previously reported involvement of glutathione GSTO1-1 in the secretion of IL-1β and our recent discovery of its deglutathionylation activity, we have identified a novel role for GSTO1-1 in regulating the generation of ROS following LPS activation of the TLR4 pro-inflammatory cascade. We discovered that J774.1A macrophages deficient in GSTO1-1 do not respond to LPS and fail to elicit pro-inflammatory responses including the generation of ROS via NADPH oxidase 1 and the expression of pro-IL-1β. The present data also show that the suppression of several antioxidant enzymes (catalase, glutathione peroxidase, glutamate-cysteine ligase) that normally protect against the effects of oxidative stress in LPS treated J774.1A cells is dependent on the presence of GSTO1-1. In order to confirm that the redox events unfolding in the presence of GSTO1-1 were due to its catalytic activity, we tested the GSTO1-1 inhibitor ML175 on wildtype J774.1A macrophages. The production of ROS and the suppression of antioxidant enzymes after LPS stimulus were blocked significantly by pre-treating cells with ML175, clearly mimicking the response of GSTO1-1 knockdown cells.

Taken together, our data demonstrate the significant attenuation of ROS in GSTO1-1 deficient cells, thus identifying a novel component of the ROS production pathway in LPS activated macrophages and placing GSTO1-1 in the TLR4 signalling pathway, upstream of NF-κB. TLR4 ligands such as LPS modulate the metabolic activity of macrophages, skewing cells towards a more glycolytic phenotype which is characterized by an increase in metabolic flux through the pentose phosphate pathway

(PPP) and lower oxygen consumption (OCR). We show that the glycolytic switch is significantly attenuated in GSTO1-1 deficient macrophages, which we propose results from an upstream block in the TLR4 signalling pathway. Our studies on GSTO1-1 deficient cells demonstrate that AMPKα, a key metabolic stress regulator is maintained in a phosphorylated (active) state in macrophages after LPS stimulation, supporting its anti-inflammatory role. In addition, *Gsto1* knockdown cells were unable to induce HIF1α in response to LPS, thus indicating their failure to acquire a glycolytic phenotype. This was confirmed by their low extracellular acidification rate (ECAR).

The findings in the cell line studies translated well *in vivo* as the *Gsto1*$^{-/-}$ mice failed to elicit an adequate inflammatory response when injected with sub-lethal and lethal doses of LPS intra-peritoneally. Subsequent studies focused on identifying the target(s) of GSTO1-1 in the TLR4 pathway. We have successfully placed GSTO1-1 upstream of NF-κB and IRAK4 and narrowed down the target(s) to the myddosome complex comprised of TLR4, MyD88 and MyD88 adaptor like protein (MAL). Preliminary data strongly indicate the glutathionylation of MAL on LPS stimulation which is abolished in GSTO1-1 deficient macrophages. The functional implications of the glutathionylation state of MAL are yet to be fully understood. Further studies are in progress to identify the underlying mechanism by which GSTO1-1 regulates TLR4 mediated inflammation *in vivo*.

Publications

Original research publications:

1. **Menon, D**. and P. G. Board (2013) "A fluorometric method to quantify protein glutathionylation using glutathione derivatization with 2, 3-naphthalenedicarboxaldehyde." Analytical Biochemistry **433**(2): 132-136.

2. **Menon, D**. and P. G. Board (2013) "A role for Glutathione transferase Omega 1 (GSTO1-1) in the glutathionylation cycle." Journal of Biological Chemistry **288**(36): 25769-25779.

3. **Menon, D**., R.C. Coll, L.A.J. O'Neill and P.G. Board (2014) "Glutathione transferase Omega 1 is required for the LPS stimulated induction of NADPH Oxidase 1 and the production of reactive oxygen species in macrophages". Free Radical Biology and Medicine **73**: 318–327.

4. **Menon, D,** R.C. Coll, L.A.J. O'Neill and P.G. Board (2015) "Glutathione transferase Omega 1 modulates metabolism in LPS/TLR4 activated macrophages". Journal of Cell Science *(in press)*

Reviews:

5. Board, P. G. and **D. Menon** (2013). "Glutathione transferases, regulators of cellular metabolism and physiology." Biochimica et Biophysica Acta (BBA)-General Subjects **1830**(5): 3267–3328.

6. **Menon, D.** and P.G. Board (2015) "Beyond stress signals: Impact of reversible protein glutathionylation on cell physiology and signalling". *(manuscript in preparation)*

Conference abstracts

Poster presentations:

1. Menon D. and Board P.G. *"A role for Glutathione transferase Omega 1 (GSTO1-1) in the glutathionylation cycle"* presented as a poster at the Lorne Protein Structure and Function conference 2013 (Melbourne, Australia).

2. Menon D., Coll R.C., O'Neill L.A.J. and Board P.G. *"Glutathione transferase Omega 1 is a redox modulator of TLR4 signalling in macrophages"* presented as a poster at the Gordon Research Conference on Thiol-Based Redox Regulation & Signalling 2014 (Girona, Spain).

3. Menon D., Coll R.C., O'Neill L.A.J. and Board P.G. *"Glutathione transferase Omega 1 is a redox modulator of TLR4 signalling in macrophages*" presented as a poster at the 15th International Union of Biochemistry and Molecular Biology (IUBMB) and 24th FAOBMB (Asia-Pacific) Conference 2014 (Taipei, Taiwan).

Oral presentations:

1. *"Glutathione transferase Omega 1 is a redox modulator of TLR4 signalling in macrophages".* Oral presentation at the Australian Society for Medical Research 2014 (Canberra, Australia).

2. *"Glutathione transferase Omega 1 is a redox modulator of TLR4 signalling in macrophages*". Oral presentation at the Thiol-Based Redox Regulation & Signalling Gordon Research Seminar 2014 (Girona, Spain).

3. *"Glutathione transferase Omega 1 is a redox modulator of TLR4 signalling in macrophages*". Oral presentation at the International Union of Biochemistry and Molecular Biology (IUBMB) Young Scientist Program 2014 (Taichung, Taiwan).

4. *"Glutathione transferase Omega 1 is a redox modulator of TLR4 signalling in macrophages*". Oral presentation at the Frank and Bobby Fenner Symposium 2014 (Canberra, Australia).

Abbreviations and symbols

ABI: Applied Biosystems, Inc.
ADP: adenosine 5′ diphosphate
AEBSF: 4-(2-Aminoethyl) benzenesulfonyl fluoride hydrochloride
AMP: adenosine monophosphate
Amp: Ampicillin
ATCC: American Type Culture Collection
ATP: adenosine 5′ triphosphate

BHA: butylated hydroxyanisole
BMDM: Bone marrow derived macrophages

CARD: caspase activation and recruitment domain
cDNA: complementary DNA
CDNB: 1-chloro-2,3-dinitrobenzene
CO_2: carbon dioxide
Cys: cysteine

DMEM: Dulbecco's Modified Eagle Medium
DMSO: Dimethylsulphoxide
DTNB: 5,5'-dithiobis-(2-nitrobenzoic acid)/ Ellman's reagent
DTT: dithiothreitol

EDTA: Ethylenediaminetetraacetic acid
ELISA: enzyme Linked Immunosorbent Assay

FBS: fetal Bovine Serum
FITC: fluorescein isothiocyanate

GAPDH: Glyceraldehyde 3-phosphate dehydrogenase
GC/MS: Gas chromatography mass spectometry
Grx: glutaredoxin
GSH: reduced glutathione
GSSG: oxidized glutathione
GST: glutathione transferase
GSTO1-1: Glutathione Transferase Omega protein
Gsto1: Mouse Glutathione Transferase Omega gene
Gsto1$^{-/-}$: *Gsto1* knockout homozygote
Gsto1$^{+/-}$: *Gsto1* heterozygote

HRP: horseradish peroxidase
H & E: haematoxylin and eosin

IPTG: isopropyl β-D-1-thiogalactopyranoside

JNK: c-Jun N-terminal kinase

Keap1: Kelch-like ECH associated protein 1

LB: luria bertani broth
LC/MS: liquid chromatography mass spectometry

MAPK: mitogen activated protein kinase
ML175: Molecular Libraries compound # 175
mRNA: messenger ribonucleic acid

NADPH: nicotinamide adenine dinucleotide phosphate
NCBI: National Center for Biotechnology Information
NEM: n-ethylmaleimide
NFκB: nuclear Factor Kappa-light-Chain-Enhancer of activated B cells
NMR: nuclear magnetic resonance
Nrf: NF-E2-related factor

PAGE: polyacrylamide gel electrophoresis
PBS: Phosphate Buffer Saline
PCR: Polymerase Chain Reaction
PPAR: Peroxisome Proliferator Activated Receptor
Prdx: peroxiredoxin
PSN: Pencillin/Streptomycin/Neomycin
P-SSG: Glutathionylated protein 'P'
PTP1B: protein tyrosine phosphatase 1B

SDS: sodium dodecyl sulphate
SEM: standard error of the mean
shRNA: short hairpin RNA
Srx: sulfiredoxin

TK: thymidine kinase
Tyr: tyrosine
Trx: thioredoxin

U: units

WT: wildtype

Table of Contents

Figures

Tables

CHAPTER 1
Introduction

1.1 Cellular redox biology

Redox regulation involves mechanisms that make reversible post translational alterations to proteins that confer temporary tolerance to changes in the immediate redox environment [4, 5]. Under normal physiological conditions, reactive molecules such as reactive oxygen species (ROS) and reactive nitrogen species (RNS) are continuously produced by cells. The generation and elimination of these species need to be constantly monitored by cellular defence mechanisms involving glutathione and redox sensitive enzymes including glutathione transferases (GSTs), peroxidases, catalases and superoxide dismutases [6]. Oxidative stress manifests when the delicate balance between the generation and elimination of endogenous and exogenous reactive electrophilic species is disturbed. Basal levels of reactive species are necessary for the normal cellular function and survival. For example, they can act as cell signalling messengers regulating mitochondrial activity and cell death [7, 8]. However, increased generation of ROS can be detrimental to a cell as they destabilize the redox homeostasis leading to post translational modification or/and disruption of proteins, DNA and lipid molecules [9, 10] (Figure 1.1).

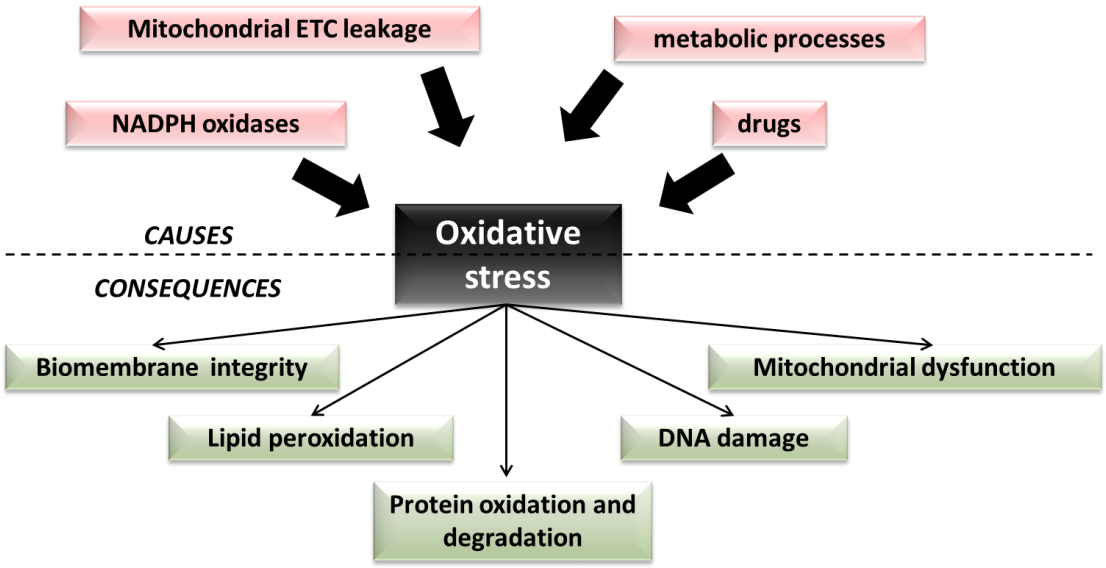

Figure 1.1: Consequences of oxidative stress on cellular components

1.2 Glutathione homeostasis

Glutathione is the most abundant thiol (glutamyl-L-cysteinyl glycine) present in all cells [11, 12]. Glutathione exists in two states: the reduced form referred to as GSH and the oxidized disulphide GSSG. GSH is the predominant form of glutathione occurring in cells, contributing to >98% of the total glutathione pool. The physiological level of GSH is generally maintained at 1-10 mM across different tissues [13, 14]. However, the GSH/GSSG ratio is significantly altered depending on the redox conditions in the cell, with the ratio dropping from 100:1 to 1:100 under increased oxidative stress. The glutathione pool exists mainly in the cytosol though a fraction does occur in the nucleus, contributing to the nuclear glutathione cycle [15]. The redox environment in the ER is more oxidizing than the cytosol to maintain and promote protein folding and post translational modifications (GSH/GSSG = 1:3) [16, 17].

Because of its unique γ-glutamyl linkage glutathione cannot be translated from a glutathione gene and is generated enzymatically. Synthesis of glutathione occurs via two steps (Figure 1.2): In the first step the carboxyl side chain of glutamate is ligated to the amine of cysteine, forming γ-glutamylcysteine. The reaction is catalysed by γ-glutamate cysteine ligase which is composed of catalytic (GCLc) and modulating (GCLm) subunits [12, 14, 18]. In the second step, glutathione synthase (GS) catalyses the addition of glycine to γ-glutamylcysteine generating γ-glutamylcysteinylglycine or GSH. GSH can be transported across the cell membrane via γ-glutamyltranspeptidase (GGT) and recycled back to the source amino acids via the action of GGT and dipeptidases [19].

The antioxidant activity of GSH is mediated by glutathione peroxidases which reduce endogenously produced hydrogen peroxide and lipid peroxides by simultaneously oxidizing GSH to GSSG. The GSSG thus generated is continuously recycled back to GSH by glutathione reductase at the expense of NADPH. However, increased GSSG levels during oxidative stress can glutathionylate protein thiols, (forming P-SSG) transiently protecting them from oxidation. This reaction is predominantly spontaneous though enzymes such as glutaredoxins and glutathione transferase Pi (GSTP) have been demonstrated to catalyse the addition of glutathione to proteins in a target specific manner [20-22].

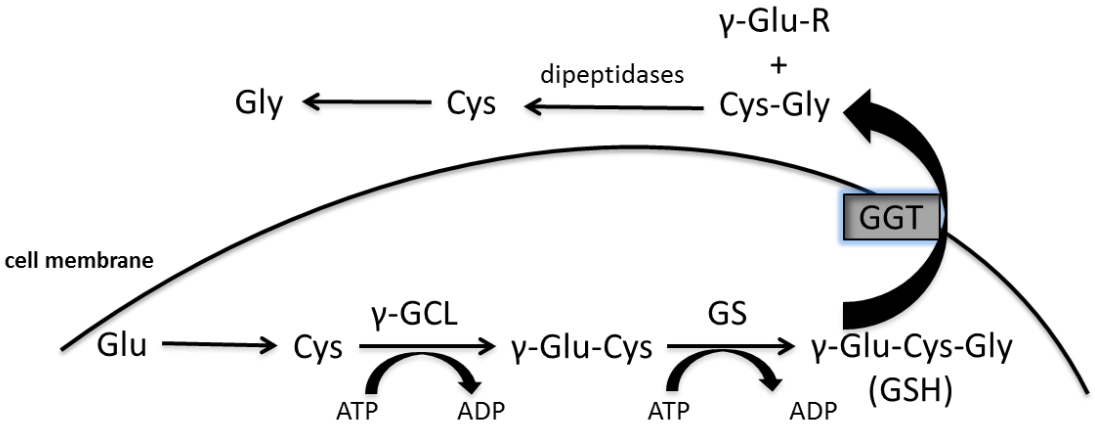

Figure 1.2: Glutathione synthesis pathway
The carboxyl side chain of glutamate (Glu) reacts with the amine group in cysteine (Cys) to form γ-glutamylcysteine (γ-Glu-Cys). This rate-limiting reaction is catalysed by γ-glutamate cysteine ligase (γ-GCL). Glycine (Gly) is added on to γ-Glu-Cys by glutathione synthase (GS) to form glutathione which is transported extracellularly via transporters called γ-glutamyltranspeptidase (GGT) and can be recycled back to the precursor amino acids by dipeptidases.

1.3 Redox modification of proteins

Protein thiols are highly sensitive targets of ROS and redox regulators including glutaredoxins, sulfiredoxin, glutathione peroxidases, glutathione transferases and glutathione are integral to maintaining the integrity and stability of cysteine thiols against oxidative stress induced irreversible damage and subsequent protein degradation. The various redox modifications occurring under normal physiological conditions and under oxidative stress are described in this section (Figure 1.3).

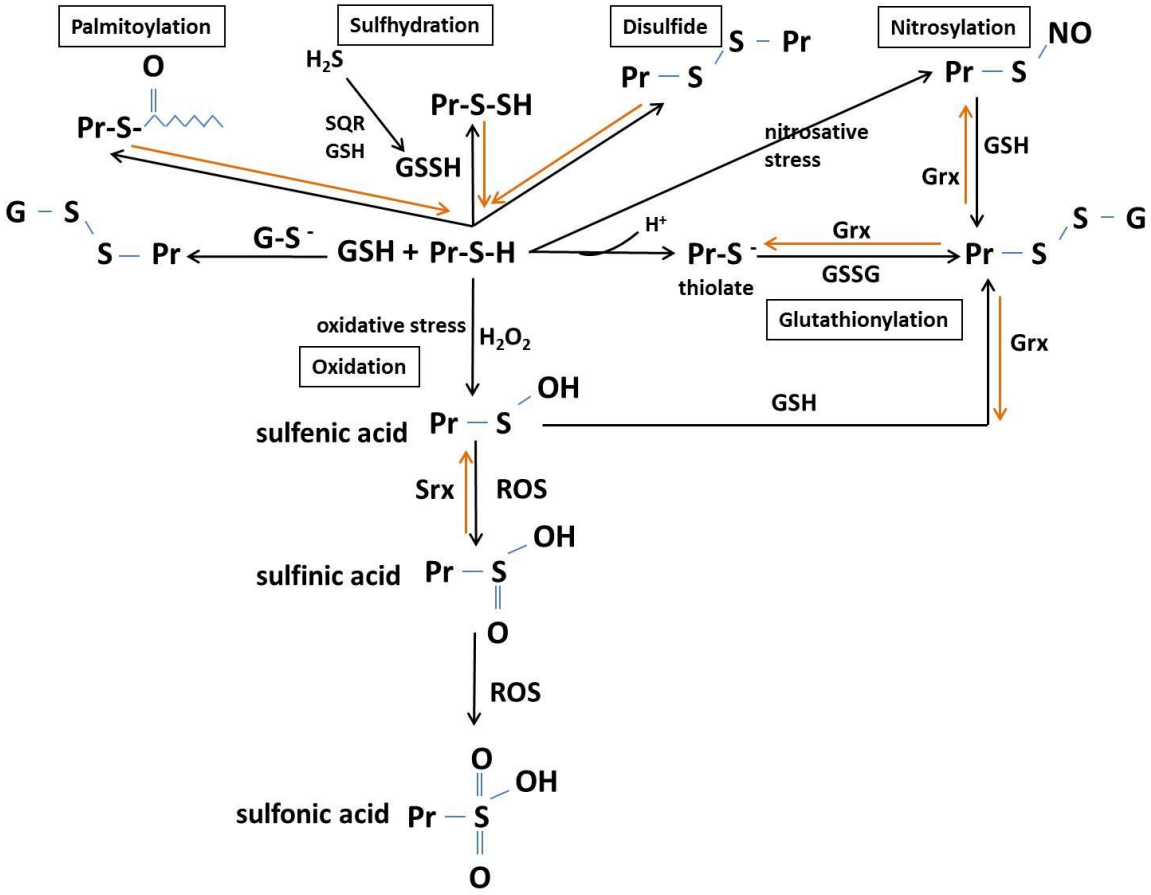

Figure 1.3: Redox modifications of protein thiols

Protein thiol modifications are classified into two categories: irreversible oxidation and reversible modifications.

Irreversible: Reactive oxygen species can induce the oxidation of protein thiols to a sulfenic form which can be reversed by glutaredoxins. Over exposure of sulfenic acid thiol intermediates may result in the further irreversible oxidation into a sulfinic and sulfonic forms. A few studies have demonstrated the reversal of sulfenic acid oxidized thiols via the formation of a thiosulfinate intermediate.

Reversible: These modifications include S-nitrosylation (–SNO) under nitrosative stress, S-glutathionylation (–SSG) can be either spontaneous or catalysed by glutaredoxins (Grx) and GSTP under oxidative stress, either intra- or inter disulphides (Pr-S-S-Pr), sulfhydration (-SSH) by reaction of protein thiols with glutathione persulphide (GSSH) on exposure to hydrogen sulphide, palmitoylation (Pr-S-FA) resulting from the reaction of protein thiols and fatty acids such as palmitate.

1.3.1 Irreversible posttranslational modification

Sulfenylation and Oxidation

Following oxidative insult, protein thiol groups can undergo a series of changes in their oxidation state which can determine the fate of the protein. Cysteines exist as thiols (Cys-SH) with a net charge of –II, referred to as its oxidation state. The Cys-SH group is typically in equilibrium with its deprotonated thiolate form ($Cys\text{-}S^-$) depending on the pKa of the thiol group [23, 24]. Thiols can form disulphide bonds with other thiol containing molecules such as GSH or proteins. Unfortunately, the thiolate form is highly susceptible to oxidation and is readily oxidized to sulfenic acid (R-SOH) (oxidation state: 0) on exposure to oxidative stress (Figure 1.3) [23, 25-28]. Sulfenic acid subsequently can be transformed into two forms- it can either interact with other thiols forming disulphides (oxidation state: -I) or be further oxidized by reactive oxygen species to form sulfinic acid (R-SO2H) (oxidation state: +II) and eventually sulfonic acid (R-SO3H) (oxidation state: +IV) [23, 26-28]. Oxidation of thiols to sulfenic acid and sulfinic acid can be enzymatically reversed by glutaredoxins, thioredoxins and sulfiredoxins though the formation of sulfonic acid is irreversible, targeting the protein for proteosomal degradation [21, 24, 29-31]. Thus, protein thiol groups can be transiently capped with glutathione (P-SS-G) to prevent further oxidation until the redox balance is restored upon which proteins can be enzymatically deglutathionylated by the 'redoxins'. This makes glutathione an indispensable player in the regulation of cellular redox homeostasis.

1.3.2 Reversible modifications

a. Sulfenic acid intermediates

Sulfenic acid intermediates are predominantly formed by the direct interaction of cysteine thiols with hydrogen peroxide and to a lesser extent, alkyl hydroperoxides, peroxynitrites and hypochlorous acid [23, 24]. The susceptibility of thiols is dictated by their ionization state, for instance thiolates are more nucleophilic than their protonated counterparts making them more likely targets of oxidation [24]. Sulfenic acid intermediates can also be formed via the hydrolysis of nitrosylated thiols, disulphides and oxidation of thiyl radicals. The over oxidation of sulfenic acids to sulfinic and further to sulfonic acid is dictated by the immediate oxidative environment. Sulfonic acids cannot be reversed even upon recovery of the normal redox state in a cell. However the same holds generally true for most sulfinic acid intermediates though an extremely low pH (< 4) can reverse the oxidative state to the sulfenic form [32]. It is

relevant to note that though typical redox catalysts such as thioredoxins and glutathione cannot catalyse the conversion of sulfinic to sulfenic acid, recent studies reported the sulfiredoxin mediated rescue of the sulfinic form of peroxiredoxins [33].

b. Thiosulfinates

Oxidation of 2-cysteine peroxiredoxins (2Cys-Prdxs) to the sulfenic oxidized form is catalysed specifically by sulfiredoxin and proceeds by the formation of two distinct intermediates: formation of a sulfinic phosphoryl ester intermediately followed by the reaction of a thiol group with the sulfinic phosphoryl ester to form a protein-thiosulfinate intermediate [33-35]. This intermediate subsequently reacts with reduced glutathione resulting in the generation of sulfenic acid oxidized 2-Cys Prdx. The sulfenic form of 2-Cys Prdx can then be enzymatically reversed by sulfiredoxin [35]. The relevance of the formation of thiosulfinates to other proteins is not fully understood.

c. Sulfenylamide

Sulfenylamide intermediates are relatively lesser known transient modifications of cysteine thiols. A classic example of sulfenylamide formation occurs in Protein Tyrosine Phosphatase1B (PTP1B) which is one of the first identified targets of sulfenylamidation. PTPs are highly susceptible to oxidation and thus cysteine oxidative modifications [36]. Interestingly, the oxidation of PTP1B was found to follow an atypical path involving a previously unidentified oxidative intermediate. The initially formed sulfenic acid form of PTP1B underwent a further reaction with closely available amide nitrogen to form a cyclic ‘sulfenylamide’ intermediate. The sulfenylamide form of PTP1B can interact with other thiols such as GSH, converting it back to the initial thiol active state of the protein. Similar to that seen with other cysteine modifications, the sulfenylamide form can undergo further oxidation to the irreversible sulfinic and sulfonic oxidation forms on prolonged exposure to reactive species [36, 37].

d. Sulfhydration

Increasing evidence strongly indicates that physiological levels of hydrogen sulphide can act as a vasorelaxant [38]. Mice deficient in cystathionine γ-lyase (CSE), an enzyme catalysing the formation of H_2S in cells, are hypertensive albeit the post translational modification of proteins by H_2S was not evaluated [39, 40]. Parallel studies in the impact of H_2S signalling in ER stress have shown the sulfhydration and subsequent inhibition of PTP1B by H_2S can abolish protein activity [41]. This in turn resulted in the

inhibition of the dephosphorylation of protein kinase-like ER kinase (PERK) thereby maintaining phosphorylated/active PERK required for ER stress responses. CSE mutant mice experience constitutive oxidative stress due to the depletion in the glutathione pool [42, 43]. H_2S synthesized by CSE modulated the DNA binding capacity of NF-κB due to the sulfhydration of cysteine 38 of the p65 subunit of NF-κB [44]. Furthermore, the sulfhydration of p65 was demonstrated to enhance the anti-apoptotic activity of NF-κB in wildtype mice on TNFα treatment. Interestingly *CSE* knockout mice failed to induce the sulfhydration of NF-κB and consequently showed diminished NF-κB dependent anti-apoptotic activity [44]. Though predominantly considered a stress response, sulfhydration of several proteins including actin, tubulin and GAPDH, was detected under physiological conditions as well [38]. The physiological role of H_2S induced sulfhydration of GAPDH was further investigated in neural cells in response to IL-1β treatment [45]. IL-1β induces cognitive deficits and memory impairment in brain cells, an effect that was shown to be mediated by H_2S. Increased H_2S production by cystathionine beta lyase led to the sulfhydration of GAPDH consequently promoting its association with Siah (an E3 ligase protein). The association resulted in the physical interaction of the complex with the synaptic scaffolding protein PSD65, labelling the protein for ubiquitination and proteosomal degradation [45]. The loss of PSD65 led to the defective neuro-behaviour induced by IL-1β [45].

e. Palmitoylation

Palmitoylation is the reversible addition of palmitate or other fatty acids to cysteine thiols. The family of palmitoyl acyltransferases (PATs) are generally golgi bound and have been shown to catalyse the reaction of palmitate and to a lesser extent other fatty acids with thiols [46, 47]. Unlike modifications such as glutathionylation and nitrosylation [48-50], palmitoylation does not recognize a specific consensus protein sequence within the target protein. Though palmitate is most common fatty-acid found to react with cysteine thiols, other fatty acids such as oleate, stearate and arachidonate moieties have also been seen to modify thiols in as similar manner. The reaction proceeds by the initial nucleophilic attack by a cysteine thiolate ion on the ester bond of palmitoyl coenzyme A (CoA), resulting in the formation of a thioester bond between the two moieties. The reaction can be reversed by the family of palmitoyl thioesterases (PT) which break the thioester bond and release palmitate, freeing the cysteine residue [46, 47]. There is some evidence for protein target specificity and the balance between palmitoylated and depalmitoylated proteins may be considered as a redox switch

regulating protein function and localization [46]. For example, palmitoylation of membrane bound N-Ras has been shown to influence the cycling efficiency of the protein between the golgi and the plasma membrane [51]. Though not mandatory for the incorporation of membrane bound proteins into the cell membrane, palmitoylation may be considered as a secondary modification that enhances the integration and membrane specific localization of membrane proteins [51, 52].

f. Nitrosylation

Exchange of electrons between reactive species ROS/RNS and protein cysteines can lead to the reversible modification of thiol groups to nitrosothiol (-SNO). Nitrosylation has been reported to modulate the activity of several metabolic enzymes, ion channels, protein kinases, phosphatases, oxidoreductases and signalling intermediates in inflammation and cancer (reviewed in [53, 54]). Nitrosylation of proteins such as ATP synthase has been demonstrated to mediate the cardio protective effects of nitric oxide in cardiomyocytes [37, 55]. During ischemic reperfusion, proteins have been shown to adopt nitrosylation as a mechanism by which they transiently protect their exposed thiols from irreversible oxidative damage. For example, Cys 294 in ATP synthase was found to be nitrosylated during cardiac resynchronization therapy in a canine model [56]. A detailed list of cardiac proteins undergoing various oxidative post translational modifications under different redox conditions is described in [37]. The reversal of nitrosylated thiols to the active thiol form has been shown to be predominantly catalysed by the thioredoxin/thioredoxin reductase system. Though endogenous reactive species can spontaneously nitrosylate thiols, exogenously applied agents such as S-nitrosoglutathione (GSNO) has been shown to selectively induce protein nitrosylation and/or glutathionylation in a target specific manner [57]. The factors that dictate the propensity of a thiol to undergo either nitrosylation or glutathionylation by GSNO are not fully understood. However parameters such as consensus flanking sequence, pKa and steric hindrance have been shown to play a vital role in influencing the preferential glutathionylation or nitrosylation of the same residue under different redox conditions [57, 58]. A typical example of preferential glutathionylation occurs in papain. Cysteine 25 in papain resides adjacent to a histidine residue, which increases the nucleophilicity of the cysteine residue and promotes an attack on the S-NO bond of GSNO, resulting in the glutathionylation of Cys 25 [59]. On the contrary, the cysteine in aldehyde dehydrogenase (ADH) was not activated by histidine and thus the lower nucleophilicity promoted thiol nitrosylation by reacting with the sulphur atom in the

SNO bond [60]. The physiological relevance of nitrosylation is still unclear and open to further investigation.

g. Glutathionylation

Glutathionylation can be defined as the post translational modification of protein thiol groups by the formation of mixed disulphides with glutathione. Glutathionylation can alter protein structure and activity in response to changes in the oxidation state of the protein. The reaction may be spontaneous or can be catalysed by members of the Glutaredoxin (Grx) family of thioltransferases and glutathione transferase Pi (GSTP) [20, 26, 61-65]. Under physiological conditions, glutathione is the most prevalent thiol occurring in the cytosol. On oxidative insult, redox sensitive protein thiol groups are glutathionylated via the formation of generally reversible disulphide bonds with cellular glutathione (capping cysteine residues), thus shielding them from irreversible oxidation [66-68]. Glutathionylation reactions may be reversed depending on the oxidation state of the modified thiol group. Thus, glutathionylation may be seen as a defence mechanism to protect proteins from oxidative stress induced irreversible damage. Though glutathionylation is mainly considered as an oxidative stress triggered protein modification, reversible glutathionylation in the absence of oxidative stress has been shown to have an impact on the functions of proteins as illustrated by its impact on the contractile activity of actin and the phosphatase activity of PTP1B [29, 69]. The redox environment in cytosol is slightly reducing nature, as the GSH:GSSG ratio is normally maintained at 100:1[11]. It would take a steep increase in GSSG to bring the ratio to 1:1 in order to achieve at least 50% glutathionylation under physiological conditions [11]. Thus, most cysteines that are glutathionylated during oxidative stress usually exist in an activated sulfenic acid or thiolate state within pockets of high ROS micro-environment. The typical pK_a of cysteine residues is around 8.5, and a decrease makes them more favourable targets for glutathionylation as they are more likely to exist as thiolates that can undergo nucleophilic substitution with GSSG [70].

Deglutathionylation is the reversal of glutathionylation i.e. removal of protein bound glutathione. Though deglutathionylation was originally identified as a mechanism to reverse oxidative stress induced glutathionylation, there is increasing evidence indicating that some proteins can be actively deglutathionylated in response to oxidative stress [69, 71, 72]. Thus, protein thiols can be transiently modified by glutathione until the redox balance is restored upon which they can be enzymatically deglutathionylated.

The synergistic activity of glutathione, glutaredoxins and thioredoxin may be considered as the major gatekeepers of the cellular cysteine thiol pool [13, 73]. Non-enzymatic glutathionylation occurs under oxidative stress without substrate specificity. On the contrary, deglutathionylation is tightly regulated by enzymes with target specificity even under normal physiological redox conditions [21, 57, 61, 62, 64, 72, 74-76].

1.4 Enzymes that catalyse the glutathionylation cycle

1.4.1 Glutaredoxin

Glutaredoxins are small heat stable 'thioltransferases' discovered as GSH dependent electron donors for ribonucleotide reductase (RNR) in 1976 by Holmgren *et al.* [77]. They were initially considered as a back-up mechanism for the characteristic functions of thioredoxins, the only oxidoreductases known in the early 1960-70s [78-85]. Since glutaredoxins exhibit a classic thioredoxin fold, they may be considered as a class within the superfamily of thioredoxins along with other proteins that share this fold such as protein disulphide isomerase (PDI), glutathione peroxidase (GPx) and the cytosolic GSTs though not all of these enzymes catalyse thioltransferase reactions [86, 87].

Although Glutaredoxins are considered to be the predominant thioltransferases, the most well described being Grx1, other proteins have been shown to catalyse similar reactions, courtesy of their glutaredoxin-domain [31, 73]. Glutaredoxins may be grouped into two classes based on the active site domain that contains either a dithiol motif (CXXC) or a monothiol motif (CXXS) [21, 31, 73, 87] (Figure 1.4). The N-terminal cysteine (cys22) in Grx has a low pKa and catalyses the reduction of disulphides via the nucleophilic attack on the disulphide bond [87]. Grxs have been demonstrated to catalyse dithiol-dependent reduction reactions though not as efficiently as monothiolic reactions. The formation of an intramolecular disulphide between the two cysteines hinders the dithiol cyclic reaction, contributing to the poor efficacy of the enzyme [87].

Monothiol: Grxs most commonly catalyse deglutathionylation reactions via the monothiol mechanism wherein the glutathionylated protein undergoes a nucleophilic attack by the N-terminal thiolate of Grx [63, 87] (Figure 1.4). The resulting glutathionylated intermediate of Grx (Grs-SSG) is recycled by one molecule of GSH, giving GSSG as a product that is subsequently reduced to two molecules of GSH by glutathione reductase and NADPH.

Dithiol: Reduction of protein mixed disulphides via the dithiol mechanism occurs sequentially: first the protein mixed disulphide is attacked by the N-terminal thiolate of Grx, the C-terminal cysteine then reacts with the Grx-protein complex to form an intramolecular disulphide which is subsequently reduced by 2 molecules of GSH, glutathione reductase and NADPH [63]. Albeit thermodynamically all thioredoxin fold containing proteins with low pKa cysteines should catalyse oxidoreductase reactions, an elegant study carried out with mitochondrial proteins demonstrated Grx to be the most effective oxidoreductase in cells [88].

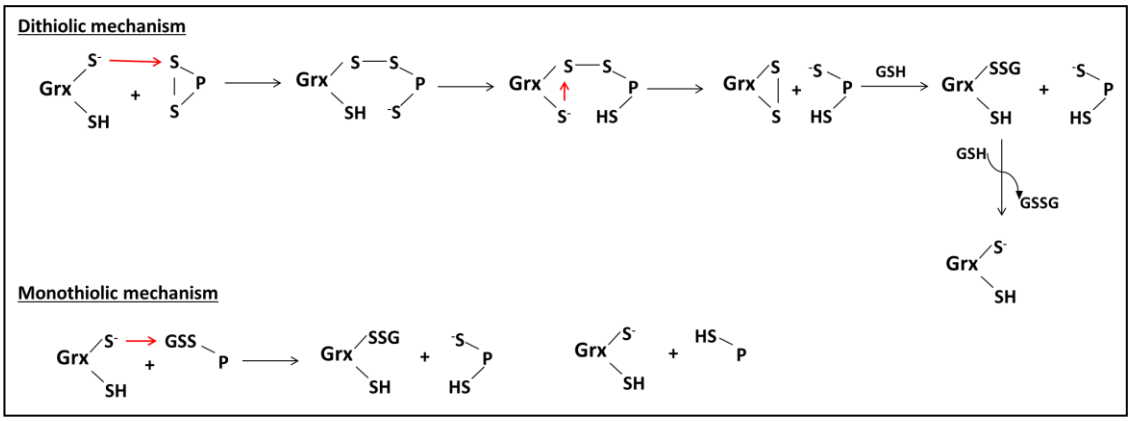

Figure 1.4: Mechanisms of disulphide reduction by glutaredoxin *(modified from [2]).*

Monothiol reactions: The thiolate form of the cysteine in glutaredoxin reacts with target glutathionylated protein (P) resulting in the formation of glutathionylated glutaredoxin. Glutaredoxin is subsequently recycled to the active thiol state by free glutathione (GSH). *Dithiol reactions*: The thiolate form of cysteine in glutaredoxin attacks the disulphide bond within the target protein (P) resulting in the formation of a mixed disulphide bond between glutaredoxin and the target protein. A nucleophilic attack by the thiolate form of the second cysteine in the CXXC domain of glutaredoxin breaks the mixed disulphide bond between glutaredoxin and the protein, forming an intra-disulphide bond between the two cysteines in the CXXC domain. The cysteines in glutaredoxin are then recycled to the active state by two molecules of glutathione.

Deglutathionylation is predominantly catalysed by the glutaredoxin family of thioltransferases though other enzymes sharing the typical 'thioredoxin' fold such as GSTO and CLIC are gradually being characterized with similar glutaredoxin like activity [29, 89, 90]. In mammalian glutaredoxins, the deglutathionylation activities of glutaredoxin 1 & 2 (Grx1 & Grx2) are the most characterized. Unlike Grx1 and Grx2; Grx3, Grx4 and Grx5 are monothiolic and contain only one cysteine residue in the N-terminal [91]. Grx5 contains another cysteine residue that is not conserved across the glutaredoxin family which has been shown to catalyse deglutathionylation reactions [92]. Grx1 and Grx2 share approximately 30% sequence similarity but differ in their cellular localization and target specificity [21, 26]. The active site domain CXXC common to both glutaredoxins bears a proline adjacent to the N-terminal cysteine (-CPXC) in Grx1 while the proline is replaced by a serine in Grx2 [21, 26, 31, 73]. Grx1 occurs predominantly in the cytosol and has been found to be expressed in the nucleus and intermembrane space in the mitochondria [93]. Grx2 is localized to the mitochondria and although less efficient than Grx1, Grx2 is responsible for the deglutathionylation of almost all reported mitochondrial proteins reported to be functionally regulated by the glutathionylation/deglutathionylation cycle [26, 73]. Mitochondrial proteins are more susceptible to redox modifications due to the redox micro environment [94]. The mitochondrial matrix is relatively alkaline, promoting the ionization of protein thiols and reaction with free glutathione [95]. Additionally, constant ROS generation in the mitochondria as a by-product of the electron transport chain (ETC), availability of GSH (~ 5 mM) and the relatively high mitochondrial protein thiol content in the matrix makes the mitochondria suitable for spontaneous protein glutathionylation [94, 95]. This further emphasizes the need for controlled deglutathionylation of proteins in order to reverse glutathionylation and restore protein activity. For example, deletion of Grx2 led to increased glutathionylation of complex I and the subsequent inhibition of ATP production via the ETC [72], enforcing the indispensable role for deglutathionylating enzymes in reversing glutathionylation induced disruption of protein activity even under normal physiological conditions.

Mechanism: The N-terminal cysteine in Grx1 occurs as a thiolate (low pKa) under normal physiological conditions [63, 93]. The thiolate ion attacks the disulphide bond in the target glutathionylated protein (PSSG), transferring the glutathione moiety to Grx1, forming a Grx-SSG intermediate [26, 63, 87] (Figure 1.5). The intermediate can be recycled back to the active thiol by free glutathione, restoring Grx-SH which can

continue catalysing nucleophilic attacks on glutathionylated proteins. A dithiol mechanism mediated via the formation of a transient disulphide bond between the two cysteine residues in Grx1 has also been proposed although it is considered far less efficient due to steric hindrance due to the intramolecular disulphide bond that may disrupt the cycling of glutathione between the interacting protein and Grx1 [63].

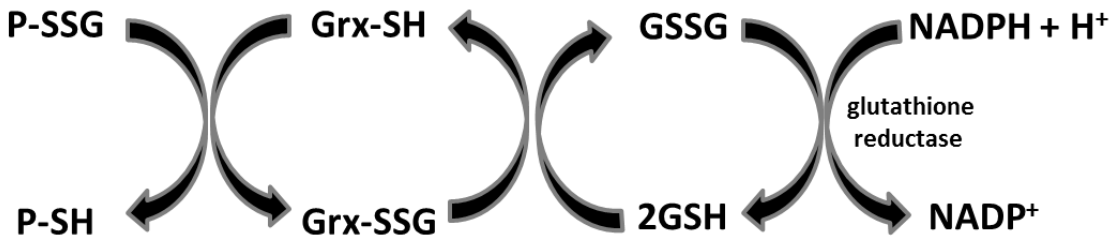

Figure 1.5: Mechanism of deglutathionylation by glutaredoxins
A disulphide exchange between the glutathionylated target 'P' and glutaredoxin (Grx) occurs resulting in the formation of a transient glutathionylated Grx-SSG intermediate. The glutathionylated intermediate is recycled to the active state by reacting with 2 molecules of GSH and producing GSSG. The redox balance is maintained by the NADPH-glutathione reductase system which recycles GSSG back to GSH by oxidizing NADPH.

Although glutaredoxins exhibit substrate specificity in deglutathionylation reactions (refer section 1.6), a review of published literature highlights functional redundancy in targets to a certain extent. This may provide a compensatory mechanism to over-ride the deficiency of one or more proteins and maintain normal redox homeostasis.

1.4.2 Thioredoxin

The founding member of the thioredoxin family was discovered in 1964 as an electron donor for ribonucleotide reductase (RNR) and is structurally made up of 3 α-helices and 4 anti-parallel β-sheets [96-98]. It is important to note that the cis-proline is highly conserved among the family members, a trait shared with the later-discovered glutaredoxins. Albeit the functional and structural similarities of Grxs and thioredoxins (Trx), the two enzyme classes encompass different substrate specificity with minimal overlap [73]. Trxs are mostly associated with reduction of oxidized thiols more than protein mixed disulphides, owing to their lower redox potential [31, 99]. However, a few studies have provided evidence for Trx-dependent deglutathionylation reactions, for

instance in yeast, the deglutathionylation activity of Trx was required to maintain protein glutathionylation levels for the progression of cells from a stationary to a vegetative growth phase [99]. Furthermore, the regeneration system potentiating Trx's catalytic activity is a GSH-independent system comprising Trx reductase and NADPH whereas Grx requires GSH, NADPH and glutathione reductase to recycle its thiolate.

1.4.3 Protein disulphide isomerase (PDI) in glutathionylation as 'misfolded protein response'

Protein folding in the ER is dependent on the redox conditions, which in turn dictates the integrity of protein thiols [100]. The extreme oxidizing environment within the ER provides a suitable balance of GSH/GSSG favouring the spontaneous reaction of protein thiols with GSSG, resulting in an increase in the rate of glutathionylation and the glutathionylated protein pool [16, 101]. The ER provides an intracellular compartment for the post translational processing of proteins with the help of chaperone proteins that prevent the aggregation of misfolded proteins, thus maintaining them in a stable and active form [101, 102]. PDI, the most abundant chaperone protein in the ER, is a member of the thioredoxin superfamily and plays an indispensable role in trafficking proteins and maintaining protein folding and stability through the formation of intra- and/or inter-molecular disulphide bonds [100, 102, 103]. The protein was characterized with five distinct domains, a, a', b, b' and c of which the first two comprise the thioredoxin fold nesting two cysteine residues each [102]. The cysteine residue pairs form two separate active sites and play an important role in protein folding and formation of disulphides (refer review [102]). As a consequence, cysteine modifications have been shown to disrupt protein stability and result in increased turnover of misfolded proteins, characteristic of neurodegenerative diseases such as Alzheimer's and Parkinson's diseases [104, 105]. The activity of PDI is thus kept in check by ER oxidase-1, which maintains the thiols in an oxidized state. Apart from protein chaperoning, PDI has been shown to physically associate with the estrogen receptor (ERα) and form a part of the complex comprising of ERα, Hsp70, Hsp60 [106]. Townsend *et al.* have further demonstrated that glutathionylation of PDI by PABA/NO (a glutathionylation inducing agent) inhibits its activity in cancer cells resulting in the activation of the 'unfolded protein response' (UPR) pro-apoptotic pathway, leading to cell death [107].

1.4.4 Glutathione transferase Pi

The GSTP gene is located on chromosome 11 and spans approximately 3kb in length. Polymorphic variants of GSTP have been implicated in differential susceptibility and drug response in cancer though a definite link is yet to be established (reviewed in [108]). Glutathionylation by GSTP mimics the typical nucleophilic reaction between the electrophilic substrates and the thiolate anion of GSH, previously deprotonated by the active tyrosine residue [20, 109]. This function is based on the catalytic activity of enzyme and is influenced by auto-S-glutathionylation of GSTP itself on two critical residues, Cys 47 and cys101 [110]. Glutathionylation of GSTP causes structural changes in the monomeric subunit which in turn alters the tertiary and quaternary structure of the dimer [20]. The structural changes induced by glutathionylation in GSTP can potentially influence protein-protein interactions of GSTP. The two cysteine residues Cys 47 and Cys 101 have been previously demonstrated to be involved in the physical interaction of GSTP with c-Jun N-terminal kinase (JNK), regulating downstream signalling events in cancer [20, 111]. Hence it is possible that the glutathionylation of GSTP may abolish signalling activated by its interaction with JNK, providing a potential target for the development of GSTP-SSG specific drugs to modulate the activity of GSTP in cancer.

Under physiological conditions, the thiolate anion of GSH reacts with exposed protein cysteinyl thiols thereby undergoing GST-catalysed glutathionylation. However, exposed cysteines may also interact with GSH or GSSG, depending on the redox state of the immediate environment to undergo spontaneous glutathionylation [22, 111]. Independent of its direct glutathionylation activity, GSTP can indirectly contribute to global protein glutathionylation via its GST-like activity by catalysing the metabolism of a diazeniumdiolate-based prodrug to an activated glutathionylating agent PABA-NO which can simultaneously induce both S-nitrosylation and excessive glutathionylation of proteins in cells [111-113].

The structural conservation of the canonical GST thioredoxin fold and the common ability to conjugate electrophilic substrates with GSH suggests that other members of the GST family may catalyse the glutathionylation cycle but apart from GSTM1-1 and GSTP, other GSTs have not yet been shown to catalyse glutathionylation reactions.

1.4.5 Sulfiredoxin

Sulfiredoxin (Srx) was one of the first enzymes shown to specifically catalyse the reversal of protein glutathionylation i.e. deglutathionylation [29]. Sulfiredoxin was first identified in *Saccharomyces cerevisiae* as a protein that was induced as part of the antioxidant responses activated against increased oxidative stress [114]. It is understood that the specificity of sulfiredoxin in deglutathionylating proteins is due to the availability of only one cysteine residue in its active site, unlike most glutaredoxins that contain a CXXC domain at their active site [25, 29]. Sulfiredoxin is the only enzyme that has been shown to catalyse the reversal of oxidation of proteins from the sulfinic form to the further reversible sulfenic form. The sulfinic form of oxidized thiols was previously considered irreversible until sulfiredoxin was found to reverse the over-oxidation of peroxiredoxins (Prdxs) to an active thiol [114]. Prdxs are antioxidants induced in response to the increased generation of hydrogen peroxide in cells [35, 115]. The family of Prdxs consists of 6 members of which Prdx I-IV contain a single cysteine residue at their active site while Prdx V and VI have two cysteines [115]. The reversal of over-oxidation of Prdxs occurs via the formation of two intermediates: first Prdx-SO_2H is converted to the sulfenic form (Prdx-SOH) by sulfriredoxin. As previously mentioned, the sulfenic form of protein thiols can be easily glutathionylated by GSSG and subsequently deglutathionylated by Srx/Grx, restoring the catalytic activity of Prdxs [33]. Alternatively, in the case of Prdxs, the sulfenic form of oxidized Prdx is reduced by the Thioredoxin/Thioredoxin reductase system. This cycle proceeds in cells to maintain the catalytic cysteines in Prdx in a reduced state. However, when Prdx gets over oxidized to the sulfinic form, Srx reverses the oxidation and Trx/TR and recycles Prdx back to the active form [34, 35, 114]. Interestingly, GSTP can also activate Prdx VI by glutathionylation of Cys 47 specifically [111].

Sulfiredoxin contains a single cysteine residue (Cys 99) in the C-terminal domain, which appears to be conserved with the 'non-conserved' C-terminal cysteine residue in Grx5 [29]. Findlay *et al.* have further demonstrated that the deglutathionylating activity of Srx is mediated via Cys 99 and mutating the residue abolishes this activity [29]. Interestingly, a glutathionylated Srx intermediate could not be identified in the disulphide exchange reaction catalysed by Srx, suggesting that Cys 99 did not form a mixed disulphide with glutathione during the reaction. This was unexpected as the crystal structure of Srx confirms the active site region as a FGG**C**HR [116] but the absence of a typical mixed disulphide intermediate at Cys 99 suggests the possibility of

an unknown intermediate or atypical mechanism by which Srx deglutathionylates proteins. Srx was further demonstrated to modulate protein function in cells under oxidative stress [25, 117]. The current list of proteins deglutathionylated by Srx includes actin and PTP1B [29]. The physiological relevance of actin deglutathionylation in cytoskeletal remodelling was also elucidated further confirming the functional implications of the stringent regulatory switch offered by enzyme catalysed reversal of glutathionylation. Apart from the deglutathionylation activity, Cys 99 appears to be involved in the inhibition of glutathionylation reactions as well [29, 117]. The physical interaction between Srx and the target protein interfered with the spontaneous glutathionylation of actin and PTP1B by PABA/NO, thus acting as a target-specific inhibitor of glutathionylation [29].

1.5 Protein specificity of enzymes catalysing the glutathionylation cycle

The target specificity of enzymes catalysing the glutathionylation cycle is very evident from the restricted overlap among their targets [61, 63, 64, 72, 118, 119]. The parameters defining the specificity of enzymes for glutathionylating and deglutathionylating proteins are not fully understood although comparison of the reaction mechanism and kinetics with different protein targets have revealed factors that may influence protein binding and glutathione exchange between the enzyme and target:

1.5.1 Basicity of amino acids adjacent or in close proximity to the target thiol

The occurrence of positively charged residues in close proximity to cysteine thiols in proteins have been demonstrated to promote the formation of reactive thiolates by lowering the pKa of the cysteine thiol [120, 121]. The pKa of cysteine thiols under normal physiological conditions is maintained at 8.5 [121]. Classic examples of proteins that have been shown to be modified by glutathionylation and have either a histidine or a serine residue near-by in the quaternary protein structure include PTPB1 (pKa 4.7-5.4) [122], creatinine kinase (pKa 5.5) [123-125], GAPDH (pKa 5.5) [76, 126], Prdx (pKa 4.6) [70, 127]and protein disulphide isomerase (PDI) (pKa 6.7) [100, 103, 128].

1.5.2 Solvent exposure of target thiols and conformational flexibility of enzymes

The ability of enzymes such as Grxs, Trxs and sulfiredoxin to catalyse the glutathionylation and deglutathionylation respectively also relies on the exposure of the target thiol on the surface of the protein [57, 121]. Steric hindrance may prevent the cysteine thiol from interacting with the active site of the enzyme in order to initiate the

disulphide exchange [63, 129]. On the contrary, although computational modelling predictions on Cyclophilin A place Cys 52 and Cys 161 (out of 4 cysteine residues) on the surface of the protein making them more susceptible to redox modifications, Cys 52 and Cys 62 but not Cys 161 were found to be significantly glutathionylated in T-lymphocytes [130]. This suggests that target specificity cannot be attributed to solvent exposure alone and is dependent on multiple (yet to be fully characterized) parameters.

The structural conformation of the enzyme may also dictate the ability of the target protein to 'dock' into the crevice accommodating the active site of the enzyme to enable transient physical interactions between the two proteins, enhancing the stability of the protein complex [121, 131].

1.5.3 Inter-protein electrostatic and ionic interactions

Several studies have confirmed the participation of inter-protein electrostatic interactions, hydrogen bonds and Van der Waals bonds to contribute to target specificity observed in enzymes catalysing the glutathionylation cycle [120, 131, 132]. Mechanistic studies have provided valuable insight into the enzyme specific interactions that modulate the physical proximity and stability of target proteins that in turn determine the glutathionylating/deglutathionyting ability of the enzyme [120, 132]. One of the studies cited above demonstrated that the electrostatic energy change occurring due to the formation of new bonds during the interaction between two proteins can affect the stability of the transient intermediate complex formed between the target and the enzyme and the susceptibility of the target thiol to glutathionylation [132]. As described above, of the four free cysteines in cyclophilin A, Cys 52 and Cys 62 were glutathionylated in T-lymphocytes [130]. This finding correlated well with the energy change involved in the thiolate formation and reaction with glutathione as well. The energy change was measured to be the least for Cys 52 and the highest for Cys 161 (cys52 < Cys 62 < Cys 115 < Cys 161), favouring the reaction of modification of Cys 52 and Cys 62 [130].

The energy change is additive for the formation of new bonds and alterations of existing bonds (causing enzyme conformational changes) in order to accommodate interacting proteins and disulphide exchanges [63, 131]. Some of the interactions that may contribute to the total energy change and stability are summarized below [119, 120, 131-133]:

- Non-specific backbone-to-backbone hydrogen bonds between the enzyme and the target protein.
- Interactions between γ-Glu of GSH or PSSG: The stabilizing effect exerted by the carboxylate group of the γ-Glu is significantly higher than the effect of the charged amino group.
- The aliphatic linker of the γ-Glu component contributes to the stability.
- Van der Waals interactions between the two interacting proteins contribute to specificity of the enzyme for the interacting protein. For example, the specificity of the glutathionylation reaction between NF-κB and Trx is attributed to the 12 hydrophobic bonds and 9 electrostatic bonds formed between the two proteins.

1.6 Biological significance of Glutathionylation

1.6.1 Metabolism

Two key enzymes participating in energy metabolism pathways that are modified by glutathionylation are Glyceraldehyde-3-phosphate dehydrogenase (GAPDH) and α-ketoglutarate dehydrogenase complex (KGDHC) (reviewed in [27, 134]. GAPDH, a glycolytic enzyme was shown to be inactivated by glutathionylation in an *in vitro* system. Incubating the protein with hydrogen peroxide further enhanced the extent of inactivation. Mitochondrial KGDHC in rat liver was found to be inactivated by glutathionylation on exposure to hydrogen peroxide. It was also shown that the glutathionylation-dependent inhibition was reversed by glutaredoxin [135]. Other metabolic enzymes such as aldolase, triose phosphate isomerase and alcohol dehydrogenase have also been reported to be regulated by glutathionylation in yeast *Saccharomyces cerevisiae* in response to oxidative stress [136].

1.6.2 Apoptosis

Post translational modification of proteins including transcription factors, histones and intermediary signalling molecules has been shown to interfere with the cell proliferation by the activation of apoptotic pathways. A classic example is the disruption of the cell cycle via the glutathionylation of PTP1B and Mitogen-activated protein kinase kinase kinase 1 (MAP3K1/MEKK1) in response to oxidative stress. PTP1B and MEKK1 have been shown to undergo glutathionylation at specific cysteines, which inactivates the enzymes causing adverse downstream effects [27, 29]. The thiol modification interferes with ATP binding which in turn affects the ability of the kinases to phosphorylate their target substrates.

Investigations of the glutathionylation of transcription factors and cell signalling molecules such as NF-κB, TNF-α, p53, GTPase, p21 Ras and Caspase-3 by glutathionylation have revealed inhibitory effects on the cell cycle and on the activation of apoptotic signalling in response to oxidative stress and cytotoxic agents [27, 137].

1.6.3 Regulation of calcium ion channels

The two main calcium channels in muscles are prime targets for glutathionylation under oxidative stress. Sarcoplasmic reticulum calcium ATPase (SERCA) and Ryanodine receptors (RyR) located in the muscle sarcoplasmic reticulum are highly sensitive to the reducing environment generated in the SR even under normal physiological conditions [27]. Glutathionylation of these calcium channels adversely affects their activity during stressed conditions such as myocardial ischemia resulting in irregular intracellular uptake and release of calcium ions and an overall increase in cellular calcium levels [138-140]. The reversibility of glutathionylation dependent inhibition of function was also demonstrated by these studies

1.6.4 Redox regulation of epigenetic DNA modifications

A recently published study identified glutathionylation as an indirect mechanism of DNA manipulation via histone modification [141]. The study demonstrated the significance of glutathionylation in drug response by establishing a link between histone glutathionylation and reversal of resistance to Doxorubicin (Dx) in MCF7/Dx, a Doxorubicin-resistant breast cancer cell line. This is the first study to identify glutathionylation as a mechanism of histone modification that indirectly introduces a novel theory: Is GSTO1-1 translocated into the nucleus to modify nuclear proteins?

1.6.5 Cytoskeletal remodelling

Actin is found in abundance in almost all cell types and is heavily glutathionylated under normal conditions [27, 69]. The glutathionylation of actin plays a significant role in cytoskeletal organization that occurs during cell division and cell adhesion. Remodelling involves the polymerization of actin into filaments and the disassembly of actin-myosin complexes during adhesion, both of which are modulated by glutathionylation (reviewed in [27, 134]. The thiol modification of specific cysteine residues was also found to regulate the contractile activity of actin in the cardiac muscle during ischemic attacks. Paradoxically, oxidative stress induced by artificial agents *in vitro* was found to deglutathionylate actin in A-431 cancer cells affecting actin polymerization during cell division [69].

1.6.6 Inflammation

Many diseases are modified by inflammation and glutathionylation appears to modify the function of many proteins involved in inflammatory pathways. The functional role that glutathionylation plays in several diseases exacerbated by inflammation such as diabetes, Alzheimer's disease, cardiovascular diseases, atherosclerosis and cancer is well elucidated [27, 53, 75, 142-146]. The anti-microbial activity of reactive species generated excessively in response to the presence of pathogens is well-documented [147-150]. The cytosolic source of ROS in phagocytic cells such as macrophages has been attributed to the activity of the family of NADPH oxidases [149, 150]. The functional implications of ROS mediated glutathionylation of proteins involved in inflammatory responses may be the missing link between oxidative stress and inflammation. A few examples of the modulation of inflammation by glutathionylation of specific proteins are presented below:

a. Regulation of chemotaxis: The myeloid related proteins S100A8 and S100A9 are calcium-binding proteins that belong to the S100 family of pro-inflammatory proteins [151, 152]. They are abundantly expressed in phagocytic cells such as neutrophils and monocytes. Both proteins are considered as markers of acute inflammation and are secreted extracellularly during pro-inflammatory responses [153]. The pro-inflammatory activity of neutrophils stimulated by S100A8/A9 is initiated by the association of S100A8 and S100A9 and subsequent polymerization with actin in response to increased calcium levels [153]. This in turn enhances the adhesion and chemotaxis ability of neutrophils. The oxidative burst occurring in activated neutrophils is sufficient to induce the glutathionylation and inhibition of S100A9 [154]. The complex calprotectin, formed by the association of S100A8/A9, is required for the adhesion of neutrophils to fibronectin on activation. The increased ROS has been shown to induce the glutathionylation of S100A9 alone which in turn prevents the adhesion of neutrophils to endothelial cells by inhibiting the oxidation and oligomerization of S100A8/A9 in response to increased ROS. On the other hand, induction of glutaredoxin by inflammatory stimuli has been reported by several studies [21, 61, 62, 64, 75] which suggests that glutaredoxins are required to maintain the redox state of proteins under different inflammatory stimuli. More recently, Bowers *et. al* (2012) have demonstrated the inhibitory effect of Sulfiredoxin-mediated glutathionylation of S100A4 resulting in the disruption of the interaction of S100A4 with cytoskeletal component non-muscle

myosin (NMIIA) [155]. The inability of S100A4 to interact with NMIIA was shown to impact cytoskeletal remodelling and consequently cell adhesion and migration.

ROS produced in immune cells is also responsible for the increased glutathionylation measured by this study and in previously published studies. NOX4-mediated ROS caused an increase in the global levels of protein glutathionylation in monocytes treated with a combination of LDL and high concentrations of D-glucose [156]. The study identified actin as a target of ROS induced glutathionylation which in turn acts as a priming agent accelerating chemotaxis in metabolically stressed monocytes, suggesting a novel role for actin glutathionylation in metabolic disorders associated with increased atherogenesis [156, 157]. MAP kinase phosphatase-1 (MKP-1), another key protein involved in monocyte migration, is similarly glutathionylated in response to intracellular ROS [74]. Glutathionylation of both actin and MKP-1 enhance adhesion and migration of monocytes in response to metabolic stress. The ratio of F-actin to G-actin was also reduced by metabolic stress in unstimulated monocytes, an effect that was further enhanced by MCP-1 stimulation as a consequence of increased glutathionylation of actin [74, 157].

b. TNFα signalling in macrophages: Activation and differentiation of the murine monocytic M1 cell line by IL-6 has been shown to induce expression levels of glutaredoxin which correlated with increased phagocytosis in the cell line [158]. A recent study published by Salzano *et al.* elegantly demonstrated the glutathionylation and consequent secretion of peroxiredoxin by activated macrophages [159]. Glutathionylation was shown to be essential for the secretion of Prdx which in turn induced the secretion of TNFα in the macrophages. Prdx was co-released along with thioredoxin, raising the speculation that this system was in place to maintain the oxidation/reduction of cell surface receptors such as the Toll like receptors (TLRs). The recruitment and activation of several intermediates in the TLR signalling pathways in immune cells have been shown to be influenced by the redox state of the signalling proteins [61, 118, 129, 160]. TLRs mediate pro- and anti-inflammatory responses on activation via signalling cascades that require the recruitment and association of intermediate proteins, most of which are shared among the members of the TLR family (13 in mammals) [161-163].

c. Inhibition of NF-κB dependent transcription of inflammatory genes: Inflammatory responses mediated by TLRs result in the activation of the master regulator of

inflammatory genes, NF-κB by phosphorylation of its subunits p65 and p50 and subsequent nuclear translocation of the subunits in order to activate the transcription of inflammatory genes such as IL-6, TNFα, IL-1β, NADPH oxidase,etc [164-167]. The glutathionylation of NF-κB p50 subunit was shown to inhibit DNA binding by NF-κB [119]. The glutathionylation of upstream IKK complex subunit IKKβ has also been shown to modulate its ability to phosphorylate NF-κB in lung epithelial cells, which was reversible by glutaredoxin [118].

d. Modulation of TLR4 signalling: The downstream recruitment and activation of TNF receptor-associated factor 6 (TRAF6) is essential for LPS stimulated signalling via TLR4/IL-1R in macrophages and B-cells [168]. On LPS stimulation, TRAF6 undergoes K63-linked auto-polyubiquitination which is required for the downstream protein-protein interactions leading to the activation of NF-κB [61]. Under physiological conditions, TRAF6 remains glutathionylated and inactive. When stimulated with LPS, TRAF6 undergoes glutaredoxin-1 catalysed deglutathionylation and subsequent auto-polyubiquitination and activation. However, the identity of the cysteine(s) was not further investigated.

e. Doxorubicin induced protein glutathionylation: Treatment of human monocyte-derived macrophages with the anti-cancer drug doxorubicin resulted in an increase in global glutathionylation levels before causing cell death [169]. Knocking down glutaredoxin aggravated cell death in the macrophages, suggesting that the regulation of deglutathionylation by glutaredoxins is necessary to maintain the increased glutathionylation levels in response to doxorubicin [169]. Interestingly, macrophage dysfunction was reported in adriamycin treated mice though the glutathionylation profile in affected tissues was not investigated [170].

f. Regulation of NOD-like receptor family pyrin domain containing 3 (NLRP3) inflammasome complex activity: The redox protein thioredoxin interacting protein (TXNIP) was shown to disassociate from thioredoxin and directly interact with NLRP3, activating the formation of the NLRP3 inflammasome complex though subsequent studies could not validate this finding further [171]. Caspase 1, a component of the NLRP3 inflammasome complex and a cysteine protease responsible for the proteolytic activation of IL-1β is inactivated by glutathionylation induced by excessive ROS on LPS stimulation [160]. Since NLRP3 activation plays a prominent role in obesity induced inflammation and insulin resistance [172], the modulation of Caspase-1

glutathionylation may provide a novel therapeutic avenue for potential anti-inflammatory drugs. The direct functional implications of protein glutathionylation on different proteins and inflammatory pathways has been extensively reviewed previously [142]. A more detailed discussion of previously published findings that are directly relevant to this study is presented in Chapter 9.

1.7 Clinical avenues for drug development

Nov-002 is a mimetic of GSSG in a complex with cisplatin designed to manipulate the redox homeostasis in cancer cells by targeting the endogenous GSSG/GSH pool and glutathione transferases [173]. Nov-002 is primarily designed for the treatment of non-small cell lung cancer (NSCLC) [174, 175]. Initial rounds of clinical trials revealed the unanticipated effect of Nov-002 on the bone marrow [175, 176]. Preliminary trials showcased improved tolerance of anti-cancer drugs when administered in combination with Nov-002 [174] but in a study which recruited 903 patients with non-small cell lung cancer in 12 countries, Nov-002 along with standard chemotherapy failed to improve overall survival rates.

TLK199, a peptidomimetic inhibitor of GSTP was found to cause unexpected myeloproliferation in rodents [110]. GSTP, apart from its detoxification activity, partakes in protein-protein interactions. The drug induced myeloproliferation was later identified to be due to the interaction of GSTP with pro-apoptotic protein, c-Jun N-terminal kinase (JNK) [110, 111].

1.8 Glutathione transferases (GSTs)

Glutathione transferases (EC 2.5.1.18) are members of a superfamily of detoxification enzymes that predominantly catalyse Phase II conjugation reactions (reviewed in [108, 177-180]). Although some GSTs were known to occur, a Carcinogen binding protein 'ligandin' was studied independently as an all-substrate binding protein, owing to its ability to bind to various non-substrate ligands including steroids, bilirubin and heme [181-184]. The two proteins were later shown to be identical [185-193]. GSTs were then revealed to encompass a superfamily of proteins with demonstrated substrate specificities and detoxification independent activities [177-180, 194-197].

The predominant functions of most, if not all GSTs, centre on their potential to recognize and bind glutathione in their active centres. GSTs constitute approximately 10% of the cellular protein pool in rat liver cytosol. GSTs have been extensively studied

for their catalytic role in the detoxification of electrophilic compounds and in the removal of endogenously produced free radicals (reactive oxygen and nitrogen species) via their glutathione peroxidase activity [195, 198]. GSTs conjugate non-polar compounds including drugs, pesticides and other xenobiotics carrying electrophilic centres (carbon, nitrogen, sulphur) to glutathione, forming water-soluble GSH-conjugates that are either readily transported out of the cell via membrane bound MRP efflux pumps or further metabolised to mercapturic acids and excreted in the kidney. Over the years, advances in GST research have revealed a multitude of substrates specific to individual GST classes (refer [195] and our recent review [180] for a detailed description). While some GSTs catalyse the cis-trans isomerization reactions in the synthesis of steroid hormones, prostaglandins and conversion of maleylacetoacetate (MAA) to fumarylacetoacetate (FAA), others play a regulatory role in switching on cell signalling pathways [89, 110, 199-204]. A relatively new class of GSTs called Chloride Intracellular channel proteins discovered due to sequence and structural similarity with GSTs were found to embed into membranes, forming and modulating membrane-bound ion channels [138, 202, 205, 206]. While GSTs were shown to modulate Ryanodine receptors *in vitro*, the finding that GSTM2-2 is a potent inhibitor of the cardiac ryanodine receptor offers therapeutic avenues to reduce or reverse abnormal channel activity in cardiovascular conditions [199, 207-209]. The Omega class GSTs, considered an atypical class, were shown to exhibit significant thiol transferase and dehydroascorbate reductase activity owing to their active site cysteine and have been implicated in neurodegenerative diseases and cancer [113, 210-217].

1.8.1 Evolution of GSTs

Human cytosolic GSTs (cGSTs) comprise nine classes listed in Table 1.1, that have been categorized on the basis of their sequence similarity and to some extent their common substrate specificities. cGSTs share approx. 40% sequence similarity within a class and over 25% similarity among classes [194, 218].

Protein	**Class**	**Chromosome location**	**Gene**
GSTA1-1 – GSTA5-5	Alpha (A)	6p12.2	*GSTA1-GSTA5*
GSTM1-1 – GSTM5-5	Mu (M)	1p13	*GSTM1-GSTM5*
GSTP1-1	Pi (P)	11q13	*GSTP1*
GSTZ1-1	Zeta (Z)	14q24.3	*GSTZ1*
GSTO1-1 – GSTO2-2	Omega (O)	10q24.3	*GSTO1-GSTO2*
GSTT1-1 – GSTT2-2	Theta (T)	22q11.2	*GSTT1-GSTT2*
GSTS1-1	Sigma (S)	4q22.3	*GSTS1*
CLIC1-CLIC5	Chloride Intracellular Channel	6p21.33 Xq28 (*CLIC2*)	*CLIC1-CLIC5*
GDAP	Ganglioside induced differentiation-associated protein	8q21.11	*GDAP1*

Table 1.1: Classification of human glutathione transferases

1.8.2 Functions of GSTs

a. Drug metabolism

GSTs have been extensively studied for their catalytic role in detoxification of xenobiotic compounds including but not limited to anti-cancer drugs and for their role in the removal of endogenously produced free radicals via their glutathione peroxidase activity (reviewed in [108, 180, 195, 219, 220]). Members of the superfamily of enzymes catalyse the conjugation of glutathione to exogenous and endogenous electrophilic substrates (Figure 1.6). Apart from their well-established functions, many GSTs have specific functions exclusive to their class and to individual members.

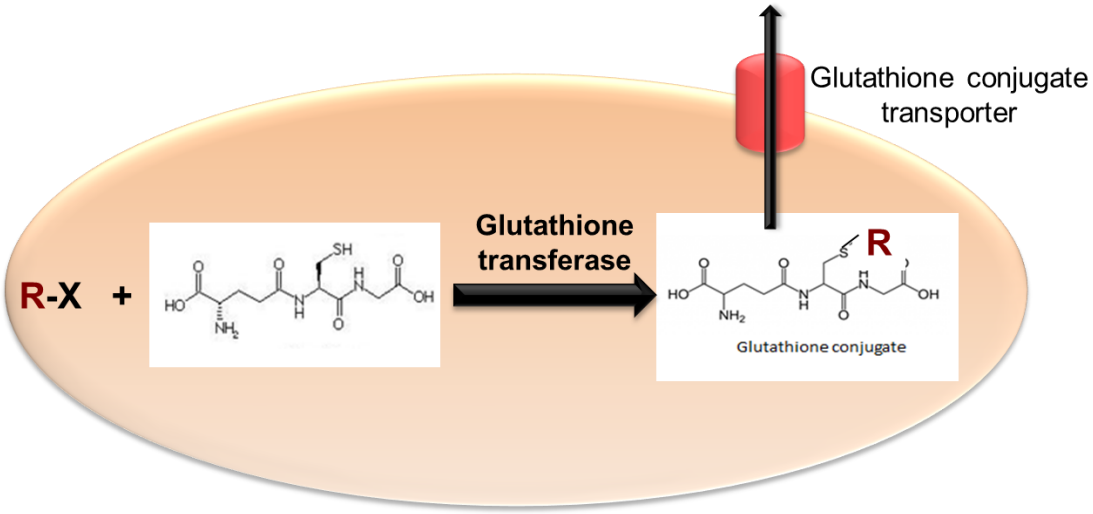

Figure 1.6: Glutathione conjugation reaction catalysed by glutathione transferases

b. Prostaglandin and steroid hormone synthesis

Testosterone and progesterone are two steroid hormones synthesized from a common precursor, 3β-hydroxy-5-pregnene-20-one (cholesterol) via a series of isomerization and oxidation reactions. The isomerization of intermediate 3-keto-Δ^5-steroid metabolites was predicted to be catalysed by 3 β-hydroxy steroid dehydrogenase though *in vitro* studies suggest that GSTA3-3, expressed specifically in steroidogenic tissues such as the testes, adrenal glands and liver, exhibits significantly higher isomerization activity compared to the former [221].

Several cytosolic GSTs including GSTA1-1, GSTA2-2, GSTM2-2, GSTM3-3 and members of the microsomal class (MGST1, prostaglandin E synthase (PGE2 synthase)) have been associated with prostaglandin metabolism [196, 201, 203]. The growth inhibitory properties of Prostaglandin A2 (PGA2) was found to be independent of the cellular glutathione in murine L-1210 cells [222] while contradicting data by Atsmon *et al.* suggest the cellular glutathione dependent regulation of the anti-proliferative property of prostaglandin J2 (PGJ2) in Chinese hamster ovary and hepatoma cells [223, 224]. The stereo-selective conjugation of PGA2 and PGJ2 with GSH is differentially catalysed by GSTA1-1 (R-GSH conjugate selective), GSTA2-2, GSTM1a-1a and GSTP1-1 (S-GSH conjugate selective), [203]. A direct consequence of the GST-dependent prostaglandin metabolism may be associated with the high proliferative

property of tumour cells. Over expression of GSTs is common in tumours, especially GSTP1-1 and the subsequent increased conjugation of PGA2 and J2 by GSTs may stimulate proliferation.

Microsomal PGE2 synthase was primarily identified as the predominant enzyme catalysing the synthesis of PGE2 from precursor PGH2. However, GSTM2-2 and GSTM3-3 (expressed in the brain) have been identified as cytosolic PGE2 synthases, capable of catalysing the formation of PGE2 from PGH2 [201]. This finding could potentially bear functional relevance with respect to the regulation of brain dependent activities including temperature control [201].

GSH-dependent Prostaglandin D2 synthase (GPDS), identified as the only member of the sigma class of GSTs in vertebrates has been shown to possess a unique structural 'cleft' at its active site responsible for its catalysis of the isomerisation of prostaglandin H2 (PGH2) to prostaglandin D2 (PGD2) [196, 225]. GST involvement has also been reported further downstream in the formation of 15d-PGJ2 and its elimination via conjugation with GSH [203].

c. Tyrosine/Phenylalanine degradation pathway

GSTZ1-1, identical to maleylacetoacetate isomerase catalyses isomerization of maleylacetoacetate (MAA) to fumarylacetoacetate in the tyrosine catabolism pathway [204]. Catalysis by GSTZ1-1/MAAI is inhibited by the isomers, maleyloacetoacetate and fumarylacetoacetate via a feedback loop mechanism [204, 226]. Additionally, an exogenous mechanism based suicide inhibitor of GSTZ1-1 was found in dichloroacetate (DCA), a common contaminant in drinking water that is metabolized to glyoxylate by GSTZ1-1 [226-228]. At high levels DCA is a reported carcinogen in rodents but it is not considered to be carcinogenic in humans and is used currently in the treatment of lactic acidosis [227, 229]. Several studies report the anti-cancer and pro-apoptotic properties of DCA and thus characterizing the metabolism of the drug is of prime importance [230-233]. The functional implications of GSTZ1-1 have been previously reviewed in [177, 178].

Although these animals experience constitutive oxidative stress marked with depletion of the cellular GSH pool and lower GSH synthesis capacity *Gstz1* knockout mice (*Gstz1*$^{-/-}$) were shown to have no acute health issues indicating a non-enzymatic bypass in the tyrosine degradation pathway, [204, 219, 234]. The knockout mice were shown to

follow a phenotype consistent with the accumulation of toxic intermediary metabolites, however no detrimental effects like those reported with deficiencies of other upstream and downstream enzymes in the tyrosine catabolism pathway [204, 219, 234]. Deficiency of GSTZ1-1 was also shown to upregulate the expression of other GSTs including GSTP1/2 and GSTM via the activation of the oxidative stress responsive Keap/Nrf2 transcriptional regulation [219]. Gstz$^{-/-}$ mice undergo constitutive oxidative stress which was further exacerbated along with the induction of severe leucopenia when treated with dietary phenylalanine [219, 235]. GSTZ1-1 inactivation in normal mice with DCA resulted in the accumulation of the intermediate MAA though failed to elicit any significant leucopenia in response to dietary phenylalanine [235].

d. Signal transduction

Several GSTs have been shown to be differentially expressed in tumours including non small cell lung (NSCLC), ovarian and prostate [110, 200, 236]. High levels of GSTP have often been shown to correlate with the heightened drug resistance observed in ovarian, NSCLC, breast, colon and lymphomas [237]. Although initial reports suggested the detoxification of anti-cancer drugs by GSTP to be solely responsible for the conferred resistance, several lines of evidence indicate otherwise. GSTP is a potent inhibitor of signalling molecules such as Jun Kinase (JNK), Apoptosis signal-regulating kinase 1 (ASK1) and recently reported TRAF2 via conjugation independent protein-protein interactions [20, 22, 238-240]. In particular, many drugs for which GSTP mediated resistance has been invoked are in fact poor substrates for glutathione conjugation by GSTP. However, the ability of GSTP to regulate kinase pathways such as the Jun-Kinase pathway, indirectly manipulating survival and/or apoptotic signals has been hypothesized to be responsible for the observed drug resistance [238]. Under physiological conditions, a portion of GSTP exists bound to JNK, thus keeping basal levels of JNK in check (Figure 1.7). On sensing excess ROS generation following drug administration, GSTP1 dissociates from JNK and accumulates in the form of oligomers in the cytosol. The release of JNK triggers a cascade of signalling events starting with the activation of Jun-c via phosphorylation leading to proliferation or apoptosis. This would justify the correlation observed between increased GSTP expression in proliferative tissues such as tumours and survival. Up-regulation of GSTP in tumours would result in the over-sequestration of JNK subsequently altering apoptotic signalling pathways and conferring resistance to drug induced cell death. A recent study further demonstrated the physiological downstream effects of GSTP1-1 aided inhibition of Jun-

K on the onset and progression of neurodegeneration in the neurotoxin-based MPTP model of Parkinson's disease [241]. *Gstp1/2*$^{-/-}$ mice treated with MPTP were found to be more susceptible to the neurotoxin resulting in the early onset of degeneration of dopaminergic neurons and striatal fibres. The regulation of the tumour necrosis factor-α (TNF-α) signalling pathway via the activation of TRAF2-enhanced apoptosis signal regulating kinase-1 (ASK-1) [113, 242] provides another example of the regulatory interactions between GSTP and cell signalling pathways. As illustrated in Figure 1.7, GSTP interacts with TRAF2, inhibiting the subsequent activation of JNK and p38 induced apoptotic signalling. Additionally, GSTP hinders the interaction of TRAF2 with ASK1, impeding TRAF2-ASK-1 induced downstream pro-apoptotic signalling (Figure 1.7).

GSTA1-1 is another GST shown to regulate apoptotic signalling pathways via direct protein-protein interaction with JNK [243, 244]. GSTA1-1 over expression was shown to attenuate the Doxorubicin dependent depletion of glutathione in H69 (a small cell lung cancer cell line), reducing the extent of lipid peroxidation [244]. Overexpression of GSTA1-1 significantly decreased the number of cells undergoing apoptosis via the inhibition of JNK-dependent c-Jun phosphorylation, caspase-3 activation and by maintaining Bcl-2 expression levels. The ability of GSTM1-1 in carrying out similar regulatory functions has been shown previously. The association of GSTM1-1 with ASK1 is critical in maintaining the basal levels of downstream phosphorylation targets including stress responsive protein kinase p38 (Figure 1.8). Stress triggers such as heat shock promoted the dissociation of GSTM1-1 from ASK1, resulting in the activation of ASK1 and the phosphorylation-dependent activation of p38 [245]. On the contrary, a recent study reported the suppression of JNK phosphorylation, a mechanism common to *Gstp1/2*$^{-/-}$ mice, and the subsequent inhibition of downstream pro-apoptotic targets in GSTM1-1 knockout mice though the exact mechanism is not well elucidated [240, 246]. Unlike *Gstp1/2*$^{-/-}$ mice, constitutive phosphorylation/activation of ASK1 downstream target, MKK4 was undetectable in both wild type and *Gstm*$^{-/-}$ mice [240]. However, on treatment with Acetaminophen (APAP), phosphorylated MKK4 and downstream target JNK were induced in the wildtype mice alone. The absence of JNK activation is suggestive of the inability of ASK1 to activate intermediary MKK4 in *Gstm*$^{-/-}$ mice though the link between inhibition of JNK activity and APAP induced hepatotoxicity is speculative. The role of cytosolic GSTs in the regulation of cell signalling kinases is clearly of major significance and requires further investigation.

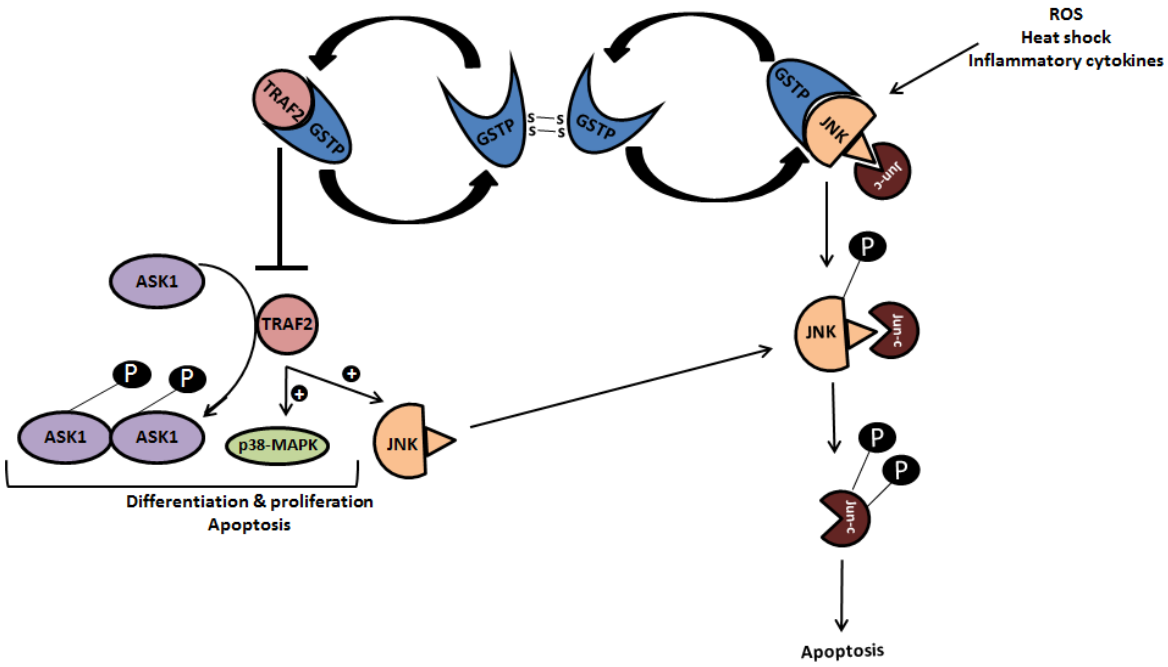

Figure 1.7: The signalling role of GSTP: Under normal non-stressed conditions, JNK and Jun-c are sequestered in an inactive complex with GSTP. Exposure of the cell to a range of stresses can change the redox potential in the cell causing the dissociation of the complex and oligomerization of GSTP. JNK can then be phosphorylated, subsequently leading to the activation of downstream kinases. Similar interactions between GSTP and TRAF2 inhibit the downstream actions of JNK, p38-MAPK and ASK1.

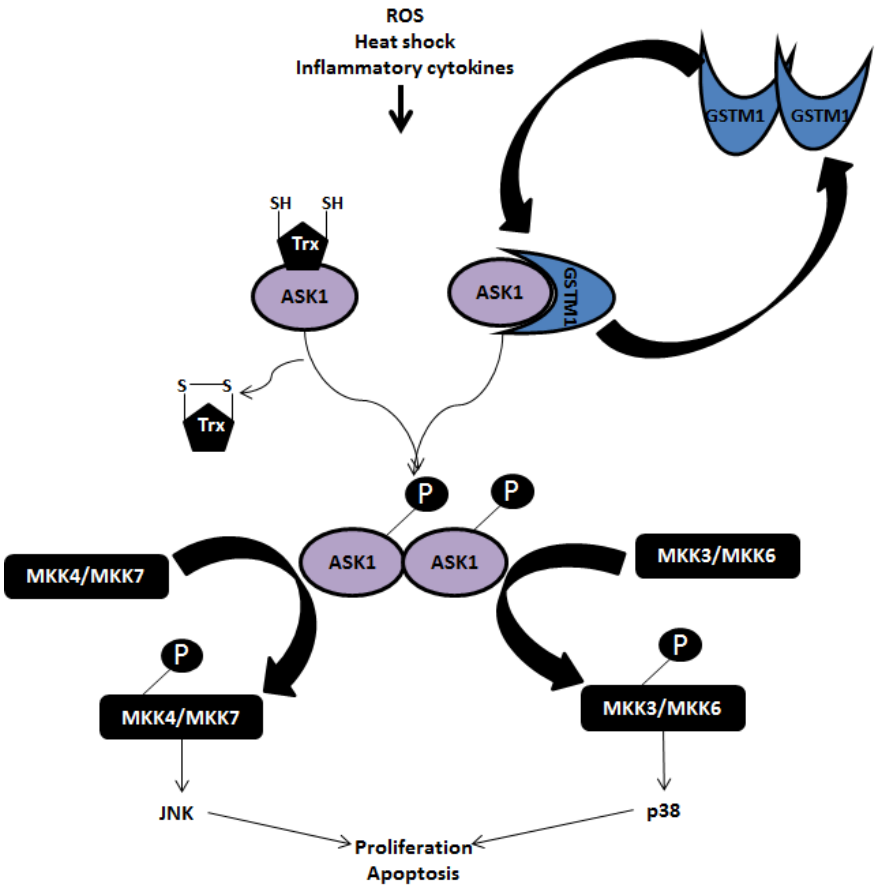

Figure 1.8: The signalling role of GSTM1: GSTM1 and thioredoxin (Trx) can reversibly bind to ASK1 and in the presence of oxidative stress modulate its oligomerization and autophosphorylation. Phosphorylation of ASK1 leads to further downstream kinase phosphorylation and activation leading to cellular proliferation or apoptosis depending on the strength and duration of the oxidative stress.

e. Calcium channels

The regulatory impact on the family of Ryanodine receptors (RyR) is a well-documented property of GSTs and has been extensively reviewed recently [247]. Ryanodine receptors are the major calcium release channels located on the endoplasmic/sarcoplasmic reticulum in muscles. Calcium plays a critical role in cell signalling pathways as a secondary messenger and in cellular processes such as the excitation-contraction coupling required for muscle contraction and relaxation [248]. Intracellular calcium reserves are mainly located in the SR/ER and are constantly released into the cytoplasm via the membrane bound RyRs, thus maintaining the E-C coupling. Disrupting the activity of RyRs results in an imbalance in calcium efflux into the cytosol, destabilizing the membrane potential, resulting in the uncoupling of muscle excitation from contraction and eventually leading to cardiovascular dysfunction or hyperthermia. Deregulation of cardiac RyR (RyR2) is considered a major risk factor for developing cardiovascular disorders and therapies targeting the modulation of RyR2 are currently in demand [249, 250]. The GSTs, tested so far have opposing effects on the cardiac (RyR2) and skeletal ryanodine receptors (RyR1). GSTM2-2 is a potent inhibitor of RyR2 while having minimal effect on RyR1, making GSTM2-2 a viable lead for drug development towards the treatment of arrhythmias and heart conditions presenting with excessive RyR2 activity [208, 209]. Extensive studies on GSTM2-2 have identified helix-6 in the C-terminus to be important for its inhibitory action [208, 251].

GSTO1-1 was found to inhibit RyR2 and activate RyR1 in a concentration dependent manner while CLIC2 exhibited inhibitory effects on both RyR1 and RyR2 [202, 205]. Detailed interaction studies revealed that GSTO1-1 binds transiently to RyRs via its active site cysteine residue (Cys 32). A cysteine→alanine mutation (C32A) abolished its modulatory effects while the weakness/transience of binding was demonstrated with washouts wherein the cytoplasm representative solution was replenished with fresh salt solution minus GSTO1-1, attenuating RyR-GSTO1-1 interaction [205]. Interestingly, the modulatory effect of CLIC2 was found to be redox sensitive. Altering the redox environment on either the cytoplasmic/sarcoplasmic or both by the inclusion of GSH/GSSG in varying concentrations resulted in the reversal of RyR2 modulation in lipid bilayer experiments [138]. CLIC2 was found to exhibit an inhibitory effect on RyR2 under reducing conditions (30:1 GSH:GSSG) while activating the receptor in oxidizing environments. On applying a redox potential mimicking physiological conditions, CLIC2 dependent channel modulation was found to be insignificant

compared to the higher rates measured in similar redox conditions minus CLIC2. The redox-dependent modulation of RyR by other GSTs offers an interesting avenue yet to be explored.

1.9 Significance of GSTs

1.9.1 In cancer

The two major drawbacks encountered with most anti-cancer therapies are acquired drug resistance and relapse. Acquired drug resistance may be attributed to several factors including upregulation of multidrug resistance proteins, drug metabolizing enzymes such as Cytochrome P450s, GSTs and inefficient intracellular uptake of administered drugs. The association of GSTs with acquired resistance may be sourced back to their two distinct activities - the classic conjugation reaction of xenobiotics with GSH and/or through the regulation of apoptotic signalling pathways discussed earlier. GSTP1/2 has consistently been associated with tumor progression and drug response. GSTP expression levels were found to be significantly upregulated in most tumor models and *in vivo* tumour tissues [236, 237, 239, 240, 252]. Conversely, reduced expression of GSTP1 in prostate tumors is considered a marker for tumor progression. However, the poor substrate affinity of GSTP for most anti-cancer drugs fails to account for the observed over expression with drug resistance in both tumors and cancer cell lines selected for resistance. Over expression of GSTP and MGST1, a member of the MAPEG family, have been detected in cancer cell lines resistant to cisplatin, 1,3-bis(2-chloroethyl)-1-nitrosourea (BCNU), Cyclophosphamide, Chlorambucil and Melphalan [113, 220, 253-255]. GSTT1-1 and GSTA1-1 have been linked to increased intrinsic resistance *in vitro*. GSTT1-1 and GSTA1-1 exhibit high substrate affinities for BCNU and chlorambucil respectively, which may explain their resistance dependent over expression [256, 257]. GSTO1-1 was shown to be over expressed in a mouse lymphoma cell line that was resistant to multiple chemotherapeutic agents [258]. A similar study on an ovarian cancer cell line suggested the association of acquired resistance to platinum based anticancer drugs with over expression of GSTO1-1 [259]. Furthermore the artificial over expression of GSTO1-1 was shown to confer resistance to cisplatin induced cytotoxicity in HeLa cells in a concentration dependent manner [260]. Due to the inefficient metabolism of exogenous substrates by GSTO1-1, the possibility of GSTO1-1 driven cisplatin metabolism was ruled out. Alternately, aberrations in cell survival and apoptotic pathways were investigated which identified the activation of Akt and ERK1/2 dependent survival signalling cascades and the inhibition of JNK

phosphorylation dependent apoptotic signalling in GSTO1-1 transfectants, albeit a direct link was not demonstrated [260].

1.9.2 In neurodegenerative diseases

The over expression of GSTO1-1 and its allelic polymorphic variants have been implicated in the age of onset and progression of neurodegenerative disorders such as Alzheimer's and Parkinson's diseases but no direct mechanism for these associations has been identified [210-212, 214, 215]. More recently, Kim *et al.* identified ATP synthase β subunit as an *in vivo* interacting partner of GSTO1-1 in a *Drosophila* model of Parkinson's Disease (loss of function mutation in the *parkin* gene), capable of modulating membrane bound ATP synthase activity [261].

The ability to recognize glutathione and interact with diverse substrates place glutathione transferases central to the regulation of redox sensitive metabolic pathways and cellular processes including oxidative stress response, intrinsic drug resistance, regulation of kinases in apoptotic signalling and protection of proteins susceptible to oxidation via glutathionylation.

1.10 Glutathione transferase Omega 1

Glutathione Transferase Omega is an atypical GST with minimal functional resemblance with the other members of the superfamily [179, 197, 262]. The gene is located adjacent to GSTO2 on Chromosome 10q24.3 and spans 1.5kb in length. GSTO1-1 was identified as a GST a decade ago due to its close sequence and structural similarity with the family and its ability, though minimal, to catalyse classic detoxification reactions with common GST substrates. Over the years, several atypical functions have been discovered (listed in Table 1.2), which will be discussed in detail in the sections to follow. Immunohistochemical studies identified GSTO1-1 in a range of diverse tissues with varied expression levels [263]. Though a surprisingly high expression level was observed in the heart and liver, the functional implications of the tissue-specific distribution are not fully understood. The study also reported the interesting subcellular localization of GSTO1-1 in the nucleus and nuclear membrane in several tissues. The significance of this unusual nuclear translocation is yet to be investigated.

The GSTO1-1 dependent regulation of IL-1β resulting from either the direct post translational modification of IL-1β or interaction with the inflammasome ASC complex offers a potential target pathway to study the deglutathionylating activity of GSTO1-1 [264, 265]. More recently, Kim *et al.* identified ATP synthase β subunit as an *in vivo* target of GSTO1-1 in a *Drosophila* model of Parkinson's Disease (loss of function mutation in the *parkin* gene) [261]. The transgenic fly model constitutively down-regulates the expression of GSTO1-1 and glutathionylated form of ATP synthase β subunit. Over expression of GSTO1-1 in the *parkin* mutants was shown to increase glutathionylation of ATP Synthase and partially restore enzyme activity. Though the study suggests the catalytic role of *Drosophila* GSTO1-1 in glutathionylation, we propose that the deglutathionylating activity of GSTO1-1 may also be physiologically significant.

1.10.1 Atypical functions of GSTO1-1

GSTO1-1 was previously shown to catalyse the reduction of dehydroascorbate and exhibits low thioltransferase activity [262, 266]. These reactions are not catalysed by other GSTs but are characteristic of glutaredoxins. The functions unique to GSTO1-1 are listed in Table 1.2. Recent studies have demonstrated the significance of GSTO1-1 expression in cell defence mechanisms [260, 264, 267]. A study by Laliberte *et al.* identified GSTO1-1 as a target of Cytokine Release Inhibitory Drugs (CRIDs) and hence implicating GSTO1-1 in mechanisms activating proinflammatory Interleukin 1β in monocytes [264]. The exact role of GSTO1-1 in this process is yet to be determined though a recent study in 2011 identified a novel interaction of GSTO1-1 with ASC (Apoptosis associated speck-like protein containing a CARD), a component of the inflammasome complex required for the activation of IL-1β production indicating the probability of an indirect effect of GSTO1-1 on IL-1β via protein-protein interactions within the activation complex [265].

There are several lines of evidence implicating GSTO1-1 in drug resistance in cell lines although no mechanism has been established [258, 259, 268]. Another study successfully linked GSTO1-1 over-expression with increased resistance to Cisplatin in HeLa cells [260]. On a different note, the redox sensitive regulation of cardiac Ryanodine receptor (RyR2) was reported by Dulhunty *et al.* [269]. Though the regulation of ryanodine receptors by GSTs is well established, the presence of cysteine at the active site of GSTO1-1 as opposed to Tyr/Ser increasingly questions the exact mechanism of RyR regulation by GSTO1-1. The redox sensitivity of GSTO1-1

dependent regulation of RyR would be an interesting option to explore with respect to determining the 'mechanism of action' of GSTO1-1.

Due to its structural similarity to glutaredoxin and its inability to recognize and strongly bind to typical GST substrates, we believe that its primary function is yet to be defined. Based on recent findings, my project proposes that GSTO1-1 may regulate a variety of proteins irrespective of their function via a common mechanism. The relevance of this hypothesis to my project is further elaborated in the following sections.

Cell/Tissue/Animal model	**Functional implications**	**Reference**
Monocytes	Activation of IL-1β	[264],[265]
T47-D breast cancer cells, rat hepatic cytosol	Reduction of S- (phenacyl)glutathiones	[270, 271]
HeLa	Resistance to Cisplatin	[260]
Humans	Delay in onset of neurodegenerative diseases such as Parkinson's and Alzheimer's diseases GSTO1-1 is implicated in Chronic obstructive pulmonary disease. Lower levels of GSTO1-1 reported in COPD patients when compared to non-smokers.	[214-216, 272] [213]
Calcium channels in lipid bilayers	Regulation of cardiac Ryanodine receptor RyR2	[269]
Caenorhabditis elegans	Participates in cellular response to oxidative stress	[267]
BALB/c and C57BL/6 mice	Up-regulation on induction of allergic airway disease. Antioxidant properties speculated as cause of up-regulation	[273]
Gsto1 knockout mice (*Gsto1*$^{-/-}$)	Reduction of Monomethylarsenate, Dimethylarsenic acid in the biotransformation of inorganic arsenic	[274, 275]

Table 1.2: Functional significance of Glutathione transferase Omega

1.10.2 GSTO1-1 and Glutathionylation

The crystal structure of GSTO1-1 is suggestive of a novel role of GSTO1-1 in glutathionylation, atypical of the superfamily. GSTO1-1 possesses the typical GST fold comprising of the N-terminal 'thioredoxin' resembling domain embedding the GSH binding site and the C-terminal helical domain [262]. As mentioned earlier, most GSTs possess a tyrosine or serine residue at their active site, responsible for catalysing conjugation reactions between GSH and electrophilic substrates. The active site residue in GSTO1-1 was identified as cysteine (Cys 32) flanked by proline and phenylalanine uncharacteristic of other mammalian GSTs [262]. On detailed dissection of the crystal structure, the active cysteine (Cys 32) was found to form a disulphide bond with GSH, a feature that is characteristic of glutaredoxin. Additionally, the GSH binding site is interestingly positioned in a wide crevice that can potentially accommodate large substrates such as proteins, suggesting potential interactions with molecules apart from GSH [197].

Due to the structural diversity at the substrate-binding site among the members of the GST superfamily and their ability to bind to GSH, it was hypothesized that the enzymes may be involved in protein-protein interactions leading to downstream effects. The enzymatic glutathionylation of proteins *in vitro* by GSTP1-1 was recently demonstrated by Townsend *et al*. using actin as an *in vitro* substrate [20]. However, it is yet to be determined whether other GSTs participate in the glutathionylation cycle.

This section attempts to summarize the literature on GSTO1-1 and justify the relevance of this information to the main objective of my project. There is increasing evidence for the physiological significance of GSTO1-1 in cellular defence mechanisms. Most GSTs are up-regulated by oxidative stress but the uniqueness of the structure of GSTO1-1 with respect to its active site suggests a novel role for this enzyme in physiological and oxidative stressed environments. The close structural resemblance of GSTO1-1 with Glutaredoxin, summarized in Table 1.3 supports the possibility that GSTO1-1 may catalyse glutaredoxin like activities.

Previous data from our laboratory confirm the thioltransferase activity of GSTO1-1 with chemical substrates such as 2-Hydroxyethyl disulphide (HEDS) [275]. Preliminary data from my project take this one step further and demonstrates the deglutathionylation of a glutathionylated cysteine residue in an 8-mer peptide and GSTO1-1 *in vitro*. This observation provides experimental evidence supporting a novel catalytic role of

GSTO1-1 in the deglutathionylation of proteins. In 2006, Sulfiredoxin was identified as a novel regulator of redox sensitive protein modification with the ability to deglutathionylate proteins [29]. Although the protein shares structural resemblance to the glutaredoxin family of enzymes, the catalytic cys-99 responsible for the thioltransferase activity is not conserved between the protein and Grx members. The cys-99 residue is instead in alignment with the non-conserved cysteine residue in Grx5 which is known to possess deglutathionylating activity. In the case of GSTO1-1, Cys 32 is conserved with the catalytic cysteine in Grx, a finding favouring the hypothesis underlying this study. Moreover, sulfiredoxin over-expression was demonstrated to regulate cell proliferation and drug response *in vitro* via the manipulation of proteins involved in regulating the cell cycle [25]. This study has encouraged me to question the possibility that GSTO1-1 may play a role in cell cycle modulation and drug resistance given that deglutathionylation is a common mechanism with the potential to influence global cell signalling.

Structural/functional characteristics	**Glutaredoxin**	**GSTO1-1**
Thioredoxin fold-like structure	+	+
Active site cysteine residue	Two catalytic cysteine residues	One catalytic cysteine residue conserved with glutaredoxin
Glutathionylation activity	Catalyses both glutathionylation and deglutathionylation	To be characterized (Recently published study indicates demonstrates the glutathionylating activity of GSTO1-1 in *Drosophila* while data from our lab suggest deglutathionylation by GSTO1-1*)*
Thioltransferase activity	++	+
Dehydroascorbate reductase activity	++	+
Ability to accommodate large substrates such as proteins in the active site	++	++

Table 1.3: Comparison of the characteristic features of glutaredoxins and GSTO1-1

1.11 Inflammation

Innate immunity is considered as the first line of defence against invading pathogens in mammalian cells. Immune cells mediating innate immune responses such as macrophages, neutrophils and dendritic cells express pathogen recognition receptors on their surface (PRRs) that recognize bacterial components and DNA, collectively called Pathogen Associated Molecular Patterns (PAMPs) [161, 276]. Based on their structural characteristics and ligand specificity, PRRs may be further classified into three distinct classes of receptors: cytosolic C-type lectin receptors, membrane bound Toll like receptors (TLR) and cytosolic NOD (nucleotide-binding oligomerization domain) like receptors [276]. Of the 11 TLRs identified across mammalian cells, TLR4 is highly expressed in macrophages and mediates inflammatory responses when in contact with bacterial cell wall component, lipopolysaccharide (LPS) or nickel metal ions [277].
In macrophages, activation of TLR4 by LPS has been shown to recruit downstream signalling proteins and induce the generation of reactive oxygen species (ROS) and pro-inflammatory cytokines such as IL-1β (Figure 1.9) [162, 278-281]. In addition to their bactericidal activity, their signalling role and their impact on the expression of pro-inflammatory cytokines, the ROS generated by the TLR4 pathway have also been shown to cause tissue damage and are central to the progression and pathology of many inflammatory diseases [280]. TLR signalling is regulated at various levels to maintain a tightly monitored inflammatory response against pathogen infection. Regulatory mechanisms at the transcriptional level by microRNAs and at the proteomic level by post-translational modifications of proteins involved have been shown to play important roles in the activation and maintenance of TLR signalling [161, 163]. Redox modifications of proteins partaking in TLR4 signalling have been discussed in detail in Chapter 9.

The secretion of IL-1β requires the activation of two parallel pathways (Figure 1.9): TLR4-dependent activation of transcription of pro-IL-1β and recruitment of the NLRP3 inflammasome. Transcription of pro-IL-1β is switched on by NF-κB which requires the activation of a cascade of intermediate signalling molecules on TLR4 activation by lipopolysaccharide (LPS) [278, 282-284]. A simultaneous potassium efflux into the cell signals the recruitment of the NLRP3 inflammasome complex comprising NLRP3, ASC and Procaspase-1. Procaspase1 is cleaved to its active form, Caspase-1 which subsequently cleaves pro-IL-1β into mature IL-1β.

The role played by ROS in the parallel activation of the NLRP3 inflammasome is still not clear and there is considerable controversy about if and how ROS acts as a direct stimulus for NLRP3 activation [161, 283]. Cytosolic ROS generated by the activity of NADPH oxidases was previously shown to activate the recruitment and formation of the NLRP3 complex [285]. This directed curiosity towards the possible redox modifications that proteins within and downstream of the NLRP3 inflammasome complex may be undergoing in the presence of ROS. However, subsequent studies on macrophages derived from NADPH oxidase deficient mice demonstrated normal NLRP3 function, indicating that NADPH oxidase dependent ROS may not be the source of ROS-mediated activation of NLRP3 [285, 286].

Following these observations, focus was drawn to the generation of mitochondrial ROS and the role it plays in priming NLRP3. It is now clear that mitochondrial ROS can act as a stimulus for NLRP3 activation and the subsequent secretion of IL-1β in the presence of an appropriate TLR stimulus (LPS) [284, 287-289]. A recent study has further extended the consequences of mitochondrial ROS to other TLRs such as TLR3. It is yet to be fully understood whether ROS directly primes NLRP3 alone or whether it modulates proteins downstream of the multiple pathways activated during inflammatory responses in macrophages. One of the downstream effects activated in macrophages is their ability to phagocytose invading microbes, which has been considered as a reasonable marker to investigate the extent of TLR signalling inhibition by synthetic drugs [290, 291]. In addition, the role of antioxidants in NLRP3 inflammasome function has also been investigated, suggesting the need for a fine balance between the generation of oxidants and the expression of counteracting antioxidants in order to maintain inflammatory responses [149, 160, 292]. As described in section 1.7.6, macrophages deficient in superoxide dismutase 1 (SOD1) were found to have increased ROS and low inflammasome activity due to the inactivation of caspase 1 by the rapid oxidation of susceptible cysteines which is prevented in SOD1 expressing cells by glutathionylation [160]. The effects of redox catalysts such as the glutaredoxins have also been shown to modulate the phagocytic efficiency of neutrophils, and redox post translational modifications of proteins as one of the key regulatory mechanisms in place in phagocytic immune cells [293].

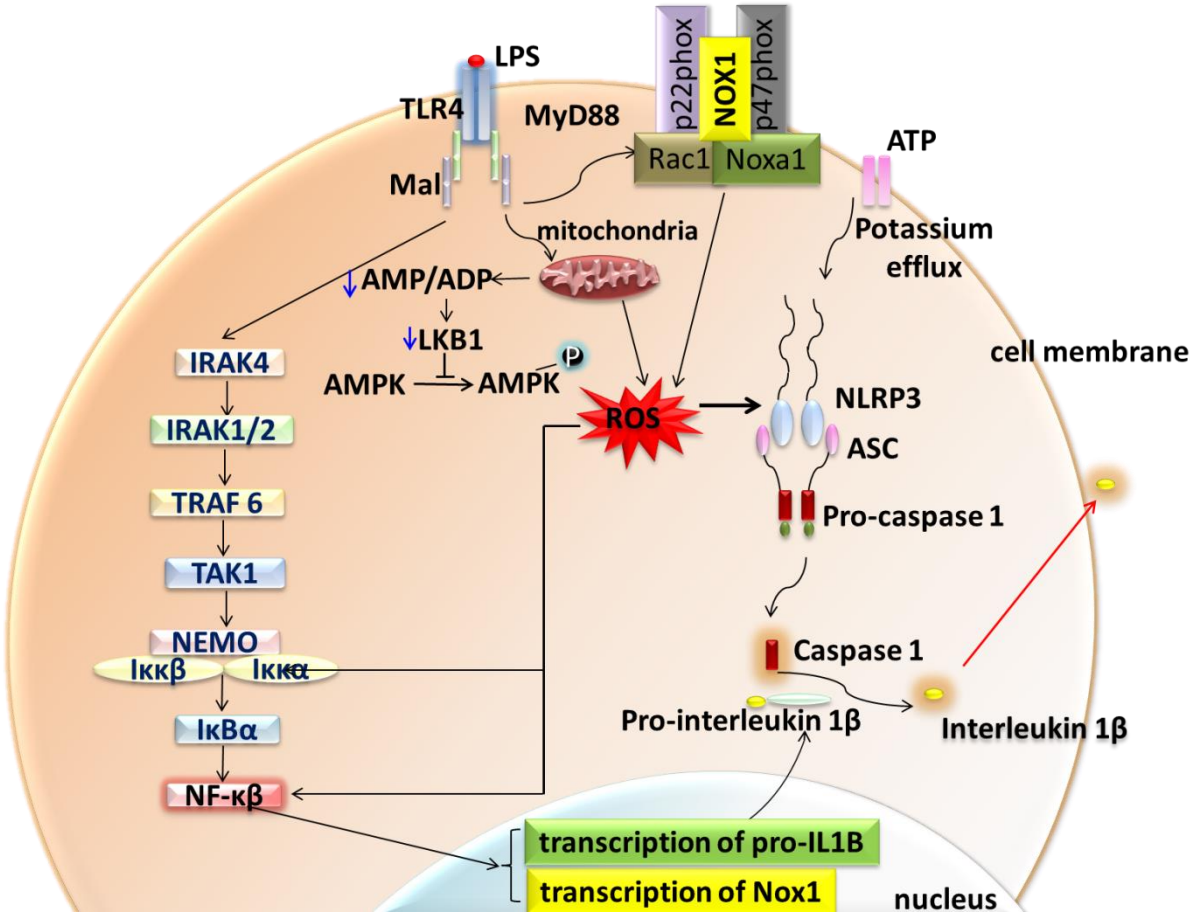

Figure 1.9: Expression and secretion of IL-1β

The secretion of IL-1β requires the activation of two parallel pathways: TLR4-dependent activation of transcription of pro-IL-1β and recruitment of the NLRP3 inflammasome. Transcription of pro-IL-1β is switched on by NF-κB which requires the activation of a cascade of intermediate signalling molecules on TLR4 activation by lipopolysaccharide (LPS). A simultaneous potassium efflux into the cell signals the recruitment of the NLRP3 inflammasome complex comprising of NLRP3, ASC and Procaspase-1. Procaspase1 is cleaved to its active form, Caspase-1 which subsequently cleaves pro-IL-1B into mature IL-1B.

1.12 Investigating the biological role of GSTO1-1

At the start of these studies it was known that GSTO1-1 catalysed reactions that are similar to those catalysed by the glutaredoxins and it was suspected that it may contribute to protein glutathionylation. In addition, there was evidence suggesting that GSTO1-1 had a role in the release of IL-1β. Genetic variation in GSTO1-1 had also been associated with a range of unrelated clinical disorders such as Alzhemier's disease, COPD, Parkinson's disease and cancer suggesting that GSTO1-1 may be mediating its effects through a common process that contributes to the pathology and progress of multiple disorders. With this prior knowledge the following hypothesis and aims were proposed.

Hypothesis

GSTO1-1 regulates proteins and their biological functions by catalysing the glutathionylation cycle and modulates proteins involved in inflammatory signalling in macrophages.

Aims

- To investigate glutathionylation and/or deglutathionylation reactions catalysed by GSTO1-1
- To identify protein targets of GSTO1-1 catalysed glutathionylation or deglutathionylation
- To determine whether GSTO1-1 is a redox modulator of pro-inflammatory responses in macrophages

The results obtained from these experiments led to the development of further aims:

- To expand the development of GSTO1-1 inhibitors as anti-inflammatory agents *in vitro*
- To investigate the effect of GSTO1-1 deficiency on the development of the glycolytic phenotype of TLR4 activated macrophages
- To investigate mechanism(s) by which GSTO1-1 mediates pro-inflammatory signalling mediated via TLR4

CHAPTER 2

Materials and methods

2.1 Commonly Used Materials

Commonly used chemicals are listed in Appendix A1. All chemicals are of analytical grade and were purchased from Sigma Aldrich unless specified otherwise. All restriction enzymes used were purchased from New England Biolabs (NEB).

Culture media, sterile PBS, antibiotics, trypsin and glutamine were obtained from Life Technologies (Gibco). Culture media, buffers and enzymes are listed in Appendix A2-4. Chemicals used for treatment of mammalian cell lines were dissolved in cell culture grade DMSO (Sigma Aldrich). All cell lines were previously purchased from the American Type Culture Collection (ATCC) and maintained as per supplier's recommendations.

2.2 Bacterial Strains and Plasmids

All plasmids were maintained and manipulated in bacterial strain *E.coli* DH5α and were streaked out on Luria broth/Ampicillin (LB/Amp) plates and grown overnight in LB media supplemented with a 100 µg/ml ampicillin at 37°C. Clones were stored in 75% glycerol stocks at -70°C. For protein expression and purification purposes, respective clones were transformed into bacterial strain BL-21 and grown under ampicillin selection.

2.3. Plasmid DNA Preparation

Plasmid DNA was isolated from *E.coli* cells using a miniprep kit (Qiagen Plasmid Purification Mini-Kit, Qiagen Pvt. Ltd., Australia). Cells were harvested and plasmids were extracted by alkaline lysis. Cells were re-suspended and lysed in 250 µl of sodium hydroxide containing Reagent P1 followed by protein denaturation with 250 µl of Reagent P2 containing SDS. The alkaline suspension was neutralized with 350 µl sodium acetate (Reagent P3). The precipitate was then separated from the supernatant by centrifuging the samples at 13000 x g for 10 minutes. The clear supernatant was transferred into Qiagen spin columns. After centrifugation at 13000 x g for 1 minute, DNA was retained on the spin column membrane which was then repeatedly washed

with Ethanol. The membrane was incubated in 50 µl DNase free sterile water for a minute prior to elution by centrifugation.

2.4 DNA Manipulation

2.4.1 Restriction Digestion

Plasmid DNA (250-400ng) was double digested with restriction enzymes as per NEB instructions. The digestion reaction was set up in a suitable buffer, common to both restriction endonucleases. The reaction volume was made up with water to a total of 10 µl for all digestions. The reactions were incubated at 37°C for two hours. Final concentrations of enzymes, buffers and BSA were maintained at $1/10^{th}$ the total volume.

2.4.2 DNA Sequencing

DNA Sequencing was performed on a 3730*xl* DNA automated DNA Analyzer (Applied Biosystems) at the Biomolecular Resource Facility (BRF), JCSMR. The analyzer utilizes a high throughput capillary electrophoresis system to detect and analyze fluorescently labelled DNA sequences that were generated using the *Chain Termination* principle using fluorescently labelled dideoxynucleotides (ddNTPs). A typical 20 µl reaction mix contained 2 µl of ABI PRISM Big Dye Terminator mix, 3 µl of the respective ABI Big Dye Terminator 5X sequencing buffer, 3.2pmol of primer and 300ng of plasmid DNA. The terminator mix contains fluorescently labelled ddNTPs with unlabelled ddNTPs which were incorporated into the DNA fragment during PCR amplification. A clean up with Ethanol/Sodium Acetate is required to remove residual unincorporated terminator dye which may interfere with the capillary electrophoresis procedure (Biomolecular Resource Facility DNA Sequencing Protocol). The sequencing sample is washed with 70% Ethanol twice to get rid of residual nucleotides and vacuum-dried.

Fluorescently tagged DNA fragments are run on an acrylamide gel, separating them based on size. The fluorescent tags on each of the four ddNTPs are of different emission wavelengths. A laser positioned at the bottom of the gel excites the fluorescent tag on each fragment and generates a list of nucleotides in the order of the fragment size. The nucleotides are then read off based on the wavelength of the fluorescence emitted.

2.4.3 Polymerase Chain Reaction (PCR)

a. Primer Design

Primers were designed using NCBI Blast and Amplify 3X. Primer length was restricted to between 18-30 bps with a GC content ≤ 50% for all PCR reactions. Annealing temperatures of primer pairs were in close proximity to one another. Primers were preferably designed to end with a 3′ guanine or cytosine.

b. Cycle conditions

Cycle conditions were altered depending on the DNA template and the primer melting temperature (T_m). A single cycle denatured the DNA template at 95°C followed by annealing of primers at the appropriate temperature which was generally the same as the lowest melting temperature of the primer pair. Extension of DNA strands by Taq Polymerase proceeded at 70°-72C°. The three steps were repeated 30-35 times and completed with a single round of extension for 5 minutes at 70°-72°C.

2.4.4 DNA Ligation

Ligation of insert with vector was carried out by T4 DNA Ligase. In the case of ligation into pGEMT, the insert was tagged with a single adenosine at both ends. An A-tailing reaction mix consisted of 0.6 µl of Taq Polymerase, 1 µl of 2 mM dATP, 0.4 µl MgCl2, 1 µl of ABI Buffer IV and 7 µl of the PCR product. The reaction was incubated at 70°C for 20 minutes. The reaction was stopped and the PCR product was purified using a PCR purification kit (Promega). 150ng of insert DNA was incubated with 50ng of vector and 1 unit of T4 DNA Ligase in a buffered reaction (total volume 10 µl) containing 1 µl of 10X T4 DNA Ligase Buffer overnight at 4°C. Insert to vector ratio was maintained at 3:1 for all ligation reactions.

2.4.5 Transformation of plasmids into bacterial cells

a. Preparation of competent E.coli cells

A primary culture of *E.coli* in 5 ml of LB media was set up overnight at 37°C in a shaker. A secondary culture was set up by inoculating 400 ml of LB media with 2 ml of the primary culture. Cells were incubated until the absorbance at 600 nm reached 0.5-0.9. Half of the culture was aspirated and replenished with fresh LB media. The culture was further incubated till the O.D. of 0.6 was reached. The cells were centrifuged at 4000 x g for 10 minutes at 4°C and the pellet was re-suspended in 40 ml of TfB I buffer (refer recipe in Appendix A5). Centrifugation was repeated and the cells were re-suspended in 40 ml of TfB II buffer (refer recipe in Appendix A5). Cells were then

aliquoted (100 µl) into sterile 1 ml microcentrifuge tubes and snap-frozen on dry ice prior to storage at -70°C.

b. Transformation of plasmids

Ligation reactions were transformed into 100 µl aliquots of competent cells and incubated on ice for 30 minutes. Cells were heat shocked at 42°C for 90 seconds and immediately allowed to recover on ice for 60 seconds. The cells were then incubated in 500 µl of LB media without antibiotics for 40 minutes. Transformed cells were then plated onto LB plates containing ampicillin and incubated overnight at 37°C.

2.4.6 Nucleic Acid Quantification

Nucleic acid concentration and purity was determined using a spectrophotometer (Nanodrop Technology, Biolab). Concentration was measured in terms of the corresponding optical density (O.D.) at a wavelength of 260 nm. Purity of DNA/RNA was estimated by calculating 260/280. A ratio of approximately 1.8 is considered pure for double stranded DNA.

2.4.7 Agarose Gel Electrophoresis

Restriction enzyme digested plasmids, PCR amplification products and colony crack PCR results were analysed by agarose gel electrophoresis. Gels varied from 0.8-1.5% in agarose concentration. Agarose was dissolved in 1X TBE Buffer (refer recipe in Appendix A5) by gradual heating. The solution was allowed to cool to 50°-60°C before adding 0.02% GelRed, a DNA binding dye that allows visualization of DNA by UV illumination. DNA samples were diluted with sucrose loading dye in a 4:1 ratio prior to loading. All gels were run in the 1X TBE buffer used to prepare the gel.

2.5 Protein expression and purification

Histidine tagged hGSTO1-1 allelic variants, hGSTO2-2, hGSTK1-1 and CLIC 2 were expressed from cDNA constructs in the bacterial expression plasmid pQE30 and purified as described previously using nickel affinity chromatography [294]. A starting culture of 5 ml LB broth supplemented with 100 µg/ml of ampicillin (see Appendix A5 for recipe) was inoculated with BL-21 cells expressing the desired plasmid and incubated overnight at 37°C with gentle agitation. The starting culture was added to 500 ml of LB broth supplemented with 100 µg/ml of ampicillin and grown at 37°C till the absorbance at 600 nm reaches approximately 0.6-0.7. Protein expression was induced

with 250 µl of 100 mM IPTG and the culture was incubated for 4 hours at 37°C with shaking. Cells were harvested by centrifugation at 3000 x g for 20 minutes at 4°C and lysed in 25 ml Buffer A (50 mM sodium phosphate buffer pH 7.5, 300 mM NaCl, 10% glycerol) containing 1 mM AEBSF and 80 µg/ml lysozyme. Cells were lysed by 5 x 30 second bursts of sonication. The lysate was extracted by centrifugation at 15000 x g for 20 minutes at 4°C. The clarified lysate was mixed with equilibrated Nickel agarose beads overnight at 4°C. Nickel bound proteins were washed thoroughly and eluted using 50-500 mM of Imidazole. Eluted fractions were run on an SDS PAGE gel and fractions containing the purified protein were pooled. The pooled fractions were dialyzed into Buffer A overnight at 4°C and then concentrated using protein concentrators (Vivaspin 10KDa cut-off). The concentrated protein was dialyzed into 20 mM tris pH 8.0, 1 mM DTT and 10% glycerol and stored at -20°C.

2.6 Proteomics assays

2.6.1 Protein quantification

Protein concentration in cell lysates, tissue homogenates and of recombinant purified proteins was determined using a Bicinchoninic acid assay (BCA) protein estimation kit as per the manufacturer's instructions (Pierce catalogue # 23225).

2.6.2 Polyacrylamide Gel Electrophoresis (SDS-PAGE)

a. Preparing and running a polyacrylamide gel

SDS-PAGE generally preceded Western blots in all experiments. All buffers were prepared prior to use from stock solutions. Buffer compositions are mentioned in Appendix A5. Polyacrylamide gels were prepared in a Biorad gel apparatus as per manufacturer's instructions. The gel plates, plate holders and combs were rinsed thoroughly and wiped with 80% Ethanol to remove gel residues. Resolving gel of the desired percentage was poured into the gel apparatus and allowed to set at room temperature. This was followed by filling the top one-fourth of the gel apparatus with the stacking gel (4%). The comb was gently placed in the stacking gel and allowed to set.

b. Protein sample preparation

Proteins were extracted from cell lines. Cells were spun down and re-suspended in PBS. Cells were lysed by means of an electric pestle and centrifuged at 16000 x g for 10 minutes at 4°C. The lysate supernatant was transferred into fresh tubes and protein

concentration was determined. Lysates were kept on ice throughout the protocol. 100 µg of protein was mixed with SDS-Loading dye in a 2:1 dilution and boiled for 5 minutes. The protein samples were spun down and loaded onto the SDS-polyacrylamide gel.

c. Running SDS-PAGE gels

Polyacrylamide gels were run in Biorad electrophoresis chambers. The gels were run at 150V for approximately one hour. Invitrogen Pre-stained Benchmark ladder (10 µl) was loaded alongside the samples. On completion of a successful run, the proteins were stained with Coomassie brilliant blue stain for an hour followed by destaining the gel 40% methanol, 10% glacial acetic acid overnight.

2.6.3 Immunoblotting

For blotting purposes, an SDS-PAGE gel was transferred onto a nitrocellulose membrane and sandwiched between a set of pre-soaked three filter papers and a porous mat on either side [295]. The sandwich was firmly placed in a blotting cassette and electro-transferred at a constant voltage of 100V for an hour at room temperature. The membrane was blocked in either 5% skim milk or 5% bovine serum albumin (as recommended by specific antibody suppliers) for one hour at room temperature. Incubations with primary and secondary antibodies varied and have been described in Appendix A8. All secondary antibodies used in this project were HRP-tagged and chemiluminescence signal was detected using ECL Rapid detection system (GE Healthcare) on a Fujifilm Chemiluminescence Imager.

2.7 Mammalian Cell Culture

Human cancer cell line T47-D was obtained previously from ATCC and maintained as per supplier's recommendations. Cells were grown in RPMI media supplemented with 10% FBS, 0.1%PSN and 2 mM Glutamine. Cells stably transfected with GSTO1-1 coding plasmids were maintained under Geneticin selection at a concentration of 350 µg/ml. Mouse macrophage cell line J774.1A wildtype and lentiviral transfected cells were kind gifts from Prof. Luke O'Neill and Dr Rebecca Coll (Trinity College, Dublin). Wildtype J774.1A cells were grown in DMEM supplemented with 10% FBS, 0.1% PSN and 2 mM glutamine. Lentiviral transfected cells were maintained in the same media, under Puromycin selection at a concentration of 3 µg/ml. Epstein–Barr virus-transformed human lymphoblastoid cell lines (LCLs) generated from anonymous Red

Cross Blood Bank donors were a gift from Dr. Juleen Cavanaugh (Australian National University) and were cultured in RPMI 1640, 15% foetal bovine serum, 2 mM l-glutamine, 100 IU/ml penicillin and 0.01 mg/ml streptomycin. All cell lines were maintained at 5% CO_2 and 37°C except for the lymphoblastoid cells which were cultured at 10 % CO_2 and 37°C.

2.8 In vitro assays

2.8.1 Cell viability assay

Total cell number was measured quantitatively using neutral red assays. Cells were seeded at ~50% confluency into 96 well plates and treated for desired periods at 37°C, 5% CO_2. Cells were then washed in PBS and incubated with neutral red stain (33 μg/well in media) for 3 hours at 37°C, 5% CO_2 followed by a wash in PBS to remove dead cells. Viable (stained) cells were lysed in a 25% acetic acid: 75% methanol solution and absorbance was read at 540 nm using a plate reader (SpectraMax 190, Molecular Devices).

2.8.2 Peptide synthesis

The peptide used in this study (SQLWCLSN) was synthesized by the Biomolecular Resource Facility (BRF), JCSMR, ANU. The synthesized peptide was dissolved in 0.1 M ammonium acetate, pH 8.0 and glutathionylated by incubation with a 10 fold molar excess of oxidised glutathione for 24 hours at room temperature with constant stirring. The peptide was then diluted in sterile water (3X) prior to freeze drying and purification by HPLC prior to use.

2.8.3 Tryptophan quenching assay

The deglutathionylation assay was based on a previously described procedure that recorded the change in tryptophan fluorescence as glutathione is removed from a model peptide [87]. Fluorescence was recorded at an excitation wavelength of 280 nm and an emission wavelength of 356 nm at room temperature over a time period of 10-30 minutes. For the deglutathionylation reaction, the reaction mix contained McIlvaine's buffer (2 M sodium hydrogen phosphate, 1 M citric acid pH 7.0), 1 mM GSH, 50 μM NADPH, 0.25 U Glutathione reductase (GR), 1 mM EDTA, 0-20 μM peptide, 1.4 μg GSTO1-1. GR and GSTO1-1 were diluted in McIlvaine's buffer containing 1 μg/μl BSA. GSH affinity was similarly measured by varying GSH concentrations from 0-2

mM, maintaining protein concentration constant at 1.4 µg and substrate concentration at 5 µM. Deglutathionylation activities of human GSTO2-2, CLIC2 and GSTK were tested up to an enzyme concentration of 6 µg. All measurements were recorded in triplicate.
Glutathionylation of the peptide was measured as described previously [87] with a modification. The reaction mix was made in McIlvaine's buffer (described above) with 5 mM GSSG, 1 mM EDTA, 5 µM peptide, 6 µg enzyme, 2 mM t-butylhydroxyperoxide and 10 µg of GSTA2-2 were added to the reaction to recycle the GSH to GSSG.

2.9 Quantification of cellular glutathione pool

The assay was carried out as described previously [296]. For oxidized glutathione, 100 µl of sample or GSSG standard were treated with 10% 2-vinylpyridine for one hour followed by pH neutralization with 6% triethanolamine. For reduced glutathione, 100 µl of sample or GSH standard were assayed directly. Samples were incubated with pre-mixed DTNB (0.67 mg/ml) and glutathione reductase (250 µg/ml) for 30 sec - 1 minute as per protocol and mixed with NADPH (0.67 mg/ml) and the reaction rate was immediately measured at 412 nm using a microplate reader (SpectraMax 190, Molecular Devices).

2.10 Immunoprecipitation

T47-D cells were treated in culture with 50 mM N-ethylmaleimide (NEM) for 30 minutes followed by lysis in non-reducing buffer (20 mM tris pH 8.0, 137 mM NaCl, 1% NP-40, 2 mM EDTA, 10 mM NEM, 2 mM AEBSF protease inhibitor). 1 mg of total cell lysate protein was used per sample as measured by BCA protein estimation. Immunoprecipitation was carried out using Pierce crosslinking immunoprecipitation kit. Cellular GSH was removed by precipitating the proteins with 5 times the volume acetone overnight at -20°C. Precipitated proteins were resuspended in lysis buffer as per manufacturer's instructions. Immunoprecipitated proteins were separated on 12% SDS-PAGE and immunoblotted as above.

2.11 Real time RT-PCR

Total RNA was extracted from cells and tissues in trizol as per manufacturer's instructions (Invitrogen). Trizol-lysed samples were incubated for 5 minutes at room temperature and passed repeatedly through a 25 gauge syringe to enhance cell lysis. 200 µl of chloroform was added to each sample and the tube was shaken vigorously for 30

seconds. The samples were centrifuged at 15000 x g for 15 minutes at 4°C and the top clear layer was transferred to a fresh tube followed by the addition of 600 µl of 70% ethanol. The samples were then transferred to RNA spin columns and RNA was isolated as per manufacturer's instructions (Qiagen RNA extraction kit). The extracted RNA was treated with DNase to remove genomic DNA contamination (Ambion DNAse kit) and cDNA was synthesized with an Invitrogen First strand cDNA synthesis kit. Real time PCR was carried out on an ABI 7900HT thermocycler and relative transcript levels were calculated by the ΔΔCt method using GAPDH as an internal control to which all transcripts were normalized.

2.12 Statistical analysis

Data were expressed as the mean ± standard error and analysed using Prism 4 (Graphpad software Inc.). Statistical significance was calculated by standard t-tests. All experiments were performed in triplicate unless otherwise stated.

CHAPTER 3

Developing a novel fluorescence based micro-titre plate assay to quantify protein glutathionylation

3.1 Introduction

Glutathione (L-γ-glutamyl-L-cysteinylglycine) is a tripeptide found in abundance intra-cellularly and has been extensively studied for its diverse functions, ranging from cellular defence mechanisms to cell signalling and metabolism [297]. The most important role of glutathione is in the maintenance and regulation of the redox state of a cell. Occurring freely in either a reduced (GSH) or oxidized (GSSG) state, glutathione concentrations play a critical role in maintaining cell homeostasis. An imbalance in the cellular GSH:GSSG ratio can destabilize the redox environment leading to excessive generation of free radicals, disruption of protein function, dysregulation of redox-sensitive signalling pathways and eventually cell death [140, 141, 268, 298, 299]. Typical functions of glutathione in redox homeostasis include the conjugation of electrophilic compounds including xenobiotics and detoxification of free radicals generated during oxidative stress. Many of these reactions are catalysed by members of the superfamily of enzymes known as Glutathione Transferases (GSTs) [195, 300, 301]. Redox regulation involves mechanisms that confer reversible post translational modifications on proteins to temporarily to tolerate changes in the immediate redox environment [4, 5].

Post-translational modifications can alter both the functional and structural aspects of proteins. This project investigating the biological roles of GSTO1-1 will focus on one such protein modification known as glutathionylation wherein thiol (-SH) groups in proteins are protected from irreversible oxidation by the addition of glutathione via disulphide bonds. The reaction may be spontaneous or can be catalysed by members of the Glutaredoxin (Grx) family of thioltransferases [21]. Under physiological conditions, glutathione is the most prevalent cellular thiol occurring both freely and bound to proteins in the form of mixed disulphides. On oxidative insult, redox sensitive protein thiol groups become glutathionylated via the formation of generally reversible disulphide bonds with cellular glutathione (capping cysteine residues), thus shielding them from irreversible oxidation to sulfonic acids [10, 27, 68]. Therefore,

glutathionylation may be seen as a defence mechanism to protect proteins from oxidative stress induced irreversible damage. Though glutathionylation is mainly considered as an oxidative stress triggered protein modification, reversible glutathionylation in the absence of oxidative stress has been shown to have an impact on the functions of proteins including the contractile activity of actin and the phosphatase activity of Protein Tyrosine Phosphatase 1B (PTP1B) [29, 69]. The current list of proteins that are structurally and functionally modified by glutathionylation, collectively known as the 'Disulphide proteome', is available at http://csb.cse.yzu.edu.tw/dbGSH/ [49].

In recent years there has been increasing interest in the role of glutathionylation in a wide range of cellular processes including, energy metabolism, signalling and apoptosis, cell cycle regulation, ion channel modulation, calcium homeostasis, regulation of cytoskeletal structures, protein folding and gene regulation (reviewed in [25, 67, 141]). As a result of its impact on cellular processes, aberrant glutathionylation has been implicated in the pathology of a number of clinically significant diseases including Alzheimer's disease, Type 2 diabetes, cystic fibrosis, cataracts and cancer [20, 22, 25, 67, 117, 121, 129, 143, 145].

Because of the increasing recognition of the biological and clinical importance of glutathionylation, a range of techniques have been developed to identify, and locate glutathionylated proteins and to determine the level of glutathionylation. This section aims to briefly describe currently available techniques, their merits, inadequacies and most importantly emphasizes the need for a quantitative glutathionylation assay.

3.1.1 Immunoassays with anti-glutathione

Immunoassays targeting protein bound glutathione are the most prevalent methods used to determine protein glutathionylation. The technique has been used to qualitatively measure global glutathionylation by separating proteins on a polyacrylamide gel, transferring them onto a nitrocellulose membrane and probing transferred proteins with an anti-glutathione antibody [29, 302, 303]. A modification to the method is the use of glutathione-based ELISA assays where proteins are probed in 96-well plates using the same principle. The technique offers you the option of quantitatively estimating the amount of glutathione bound to proteins.

3.1.2 ^{35}S radioactive labelling of proteins

One of the oldest and most commonly employed techniques to detect glutathionylation is the use of ^{35}S radioactively labelled glutathione which effectively identifies glutathionylated proteins in an isolated system [304]. The tagged proteins can be located by autoradiography and identified either by probing with protein-specific antibodies or mass spectroscopy [302]. Though the technique provides information about the localization and abundance of glutathionylated proteins, it proves to be a tedious approach involving radiation. Additionally, this approach is confined to *in vitro* labelling and may give rise to experimental artefacts owing to metabolic labelling.

3.1.3 Mass spectroscopy

Another frequently used proteomic approach involves extensive mass spectroscopic measurements [137, 305-307]. Mass spectroscopy efficiently picks up individual glutathionylated cysteine residues in proteins by detecting the mass of the extra bound '–SG' [302]. Though it offers an accurate method to identify glutathionylated proteins, the technique has its limitations. For one, it is neither a quantitative nor economic approach to be considered for preliminary experimentation as the technique requires extensive sample processing which may not be an option for initial data collection. Also, it cannot be used to identify unknown glutathionylated protein targets. Developing a quantitative method for the identification of glutathionylated proteins will provide new insights about the physiological consequences of oxidative protein modifications.

3.1.4 Glutathione transferase Overlay

Cheng *et al.* employed a biotin tagged Glutathione transferase overlay method to detect glutathionylated proteins *in vitro* [308]. Proteins were separated on a polyacrylamide gel and electrophoretically transferred to a Hybond P-membrane. The transferred proteins were probed with biotin tagged GST which binds specifically to the glutathione moieties. Though the method introduces a novel idea of targeting glutathionylated proteins with GSTs, it is not particularly quantitative and it is not clear whether it detects all glutathionylated cysteines.

3.1.5 Biotin labelling of glutathionylated proteins

The concept of protein tagging and biotinylation has been in use for many years to study various cellular processes. Tagging proteins or compounds interacting with target proteins has led to the revelation of a number of proteins undergoing glutathionylation. Several modifications adapting the principle of tagging have been established over the

years. The technique involves the treatment of whole cells with a blocking agent that binds irreversibly to protein thiol groups. The glutathionylated protein sites are then enzymatically reduced followed by labelling with thiol-specific biotinimide [309]. The biotin tag can be detected and traced via a labelled avidin conjugated agent (agarose/sepharose bound avidin or fluorescence tagged avidin), making the technique an alternative to standard immunoblotting with protein specific or GSH specific antibody [306, 309]. Biotin tagged proteins isolated by affinity chromatography with sepharose bound avidin are identified by separating the protein pool on a 2-DE gel and analysing individual proteins by high through-put techniques like MALDI/TOF [306]. A recent study developed a membrane permeable biotinylated analogue of glutathione which could be tracked by Annexin II [310]. Biotin-tagging of N-ethylmaleimide, which specifically binds to sulfhydryl groups, has led to the identification of glutathionylated proteins. A major drawback to this technique is the lack of accurate quantitation of the extent of glutathionylation.

3.1.6 Measuring the enzymatic rate of glutathionylation/deglutathionylation

The kinetics of the catalytic glutathionylation/deglutathionylation activity of glutaredoxin was measured by Peltoniemi *et al.* using an 8 residue long peptide designed to incorporate a single cysteine residue adjacent to tryptophan (XXXW**C**XXX) [88]. tryptophan, an aromatic amino acid fluoresces on excitation at 280 nm. The technique is based on the principle of tryptophan fluorescence quenching. Any change in the immediate environment of tryptophan would alter the fluorescence. For example, when glutaredoxin glutathionylates the adjacent cysteine residue, tryptophan fluorescence is quenched in a time dependent manner. Alternately, the peptide was artificially glutathionylated to measure the deglutathionylation activity of glutaredoxin. On addition of free GSH to the mix, Grx was found to deglutathionylate the peptide, resulting in a time dependent increase in tryptophan fluorescence. The technique is well suited to test the activity of potential glutathionylating/deglutathionylating candidate enzymes such as GSTs.

3.1.7 Fluorescence microtitre-based quantitative assay

Recently a new quantitative technique was described that used recombinant glutaredoxin-3 to reduce protein –glutathione mixed disulphides and capillary gel electrophoresis to detect and measure the eluted GSH [311]. While the method is sensitive and provides a valuable advance in accurate quantification, it relies on the

limited availability of recombinant glutaredoxin-3 and requires a relatively slow capillary electrophoresis fractionation step. The current techniques are highly complex, require intensive optimization and are restricted in the sample numbers that can be measured. In order to better understand the effect of glutathionylation on cellular processes, a more efficient and quantitative approach is needed to analyse glutathionylated proteins in an *in vitro* setting.

This chapter describes a new, highly specific and quantitative assay for the determination of total protein glutathionylation in cell lysates and tissue homogenates by exploiting the specificity of NDA (2,3-napthalenedicarboxaldehyde) for GSH and its precursor γ-glutamylcysteine. In this assay, GSH is eluted from the glutathionylated protein with tris(2-carboxyethyl)phosphine (TCEP) and specifically detected after reaction with NDA [312]. The assay can be undertaken in a 96 well plate format, uses commercially available reagents and only requires a fluorescence plate reader.

3.2 Materials and Methods

3.2.1 Preparation of purified glutathionylated BSA

Glutathionylated bovine serum albumin (BSA) was prepared by treating the protein with 10 mM reduced glutathione and 200 mM hydrogen peroxide for 30 minutes at 37°C. The glutathionylated protein was recovered by precipitation with 10 times the sample volume of ice cold acetone for two hours at -20°C and was resuspended in 20 mM Tris pH 8.

3.2.2 Cell culture

Cells (T47-D, HeLa, HEK 293) were purchased from ATCC and were maintained at 37°C, 5% CO_2 in RPMI-1640 media (DMEM for HEK 293 cells) supplemented with 10% FBS and 1% glutamine as recommended by ATCC. Cells were maintained at 37°C in a humidified incubator at 5% CO_2. Cells were plated at a high density of $5x10^5$ cells grown to 80% confluency in 6-well plates and treated with 0.5 mM hydrogen peroxide in sterile phosphate buffered saline (PBS) for 60 minutes at 37°C in serum free media followed by lysis in non-reducing lysis buffer as described below.

3.2.3 Animals

Balb/c male mice (aged 8-10 weeks) were maintained at the ANU Biosciences facility under controlled animal room conditions. The animals were fed regular animal diet and water *ad libitum.*

3.2.4 Drug administration

Doxorubicin was diluted in sterile saline and administered intra-peritoneally at a dose of 20 mg/kg. Control animals were injected with equal volume of saline. Animals were regularly monitored and sacrificed at 24 hours. Organs including heart, liver, lungs, brain, kidneys, testes and spleen were harvested immediately in sterile PBS and homogenized in a non-reducing buffer (20 mM Tris pH 8.0, 137 mM NaCl, 1% NP-40, 2 mM EDTA, 10 mM NEM, 2 mM AEBSF protease inhibitor) using a Dounce homogenizer. No significant weight loss was observed in treated mice during this experiment.

3.2.5 Sample preparation

The steps involved in this assay are shown schematically in Figure 3.1. In this assay of determining protein glutathionylation, free thiols (predominantly GSH) are blocked by the inclusion of 10 mM NEM in the tissue-homogenizing buffer (20 mM Tris pH 8.0, 137 mM NaCl, 1% NP-40, 2 mM EDTA, 10 mM NEM, 2 mM AEBSF protease inhibitor). Tissue homogenates were centrifuged at 20000xg for 20 minutes and the protein concentration of the supernatant was determined by Lowry protein estimation [22]. For a typical assay, a sample of tissue extract containing 100 µg of protein was precipitated with twice the volume of ice cold acetone at -20°C for 60 minutes to remove the alkylated cellular GSH, free thiols and excess NEM. After centrifugation at 20000 x g for 15 minutes, the supernatant was discarded and the precipitated proteins were washed again in ice cold acetone and then re suspended in 40 µl of 0.5 mM Tris-HCL containing 0.1% Triton X-100 at room temperature.

3.2.6 Protein-SSG reduction

The reducing agent TCEP was added to the protein solution at a final concentration of 5 mM to break the P-SSG bonds and elute the protein bound GSH (10 µl 25 mM TCEP at room temperature for 30 minutes). The deglutathionylated protein was then precipitated by the addition of 25 µl 200 mM sulfosalicylic acid. After incubation on ice for 30 minutes, the precipitated protein was removed by repeating the centrifugation step.

3.2.7 Quantification of GSH

Previous studies have shown that at a high pH NDA reacts specifically with GSH to form a highly fluorescent cyclic derivative [313]. Consequently, GSH in the supernatant was reacted with NDA and the fluorescence quantified by comparison with authentic GSH standards that were run in parallel for each experiment. Specifically, 20

µl of supernatant was combined with 180 µl of NDA derivatization mix for 30 min in the dark at room temperature. The fluorescence was determined in an Optima FLUOstar Fluorescence plate reader with an excitation wavelength of 485 nm and an emission wave length of 520 nm. The NDA reaction mix was prepared immediately before use by combining 1 ml 10 mM NDA in dimethyl sulfoxide, 7 ml 50 mM tris pH 10, and 1 ml of 0.5 m NaOH with gentle mixing.

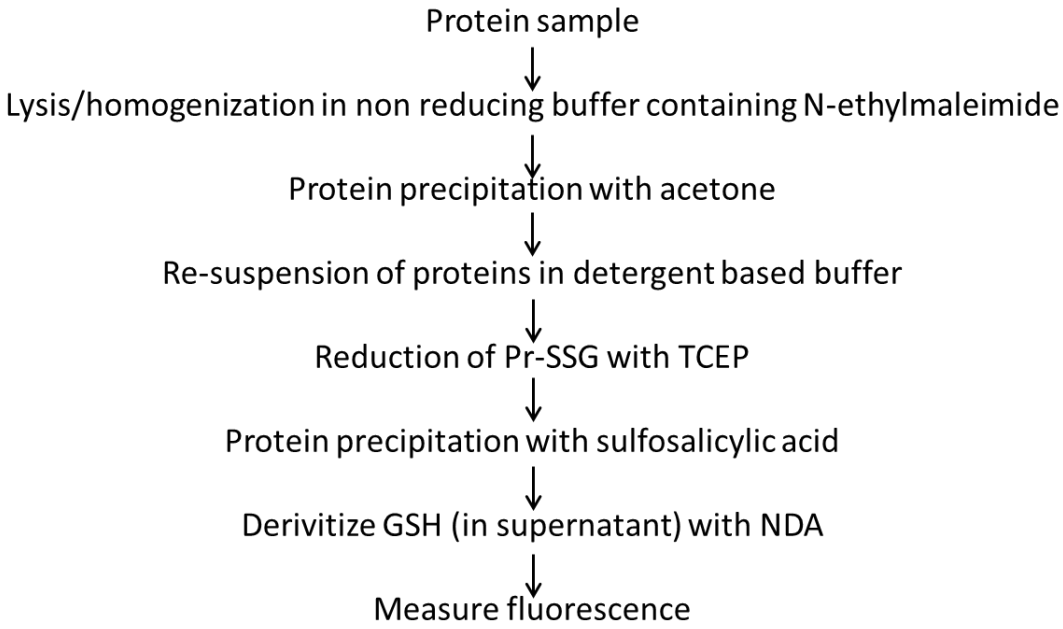

Figure 3.1: Step-wise description of the assay developed to determine total protein glutathionylation

3.3 Results

3.3.1 Optimization of NDA-based fluorescence assay

To develop and validate the method, commercially available Bovine Serum Albumin was artificially glutathionylated (BSA-SSG). Western blotting with an anti-glutathione antibody confirmed that BSA was strongly glutathionylated by treatment with glutathione and hydrogen peroxide (Figure 3.2A). The excess glutathione was removed by precipitating the glutathionylated albumin with ice cold acetone. Initial experiments using 10 μg of BSA-SSG showed that >95% of the mixed disulphide was reduced by 2 mM TCEP (Figure 3.2B). In subsequent experiments, 5 mM TCEP was used to ensure the reduction had gone to completion. In additional optimization experiments, the quantification of GSH derived from BSA-SSG by incubation with TCEP was found to be linear over a range from 0.05- 1.0 mg/ml BSA (Figure 3.2C). This assay determined the quantity of glutathione bound to BSA-SSG to be 54.3 ± 3.8 nmoles of GSH/mg protein compared with 2.3 ± 3.7 nmoles of GSH/mg protein obtained for normal BSA (Figure 3.2D). To confirm that the method measures reversible glutathionylation, the BSA-SSG was pre-treated with dithiothreitol (DTT). This treatment diminished the level of glutathionylation to background levels. The results were calculated as nmoles GSH/mg protein by reference to a standard curve generated with authentic GSH (Figure 3.2E).

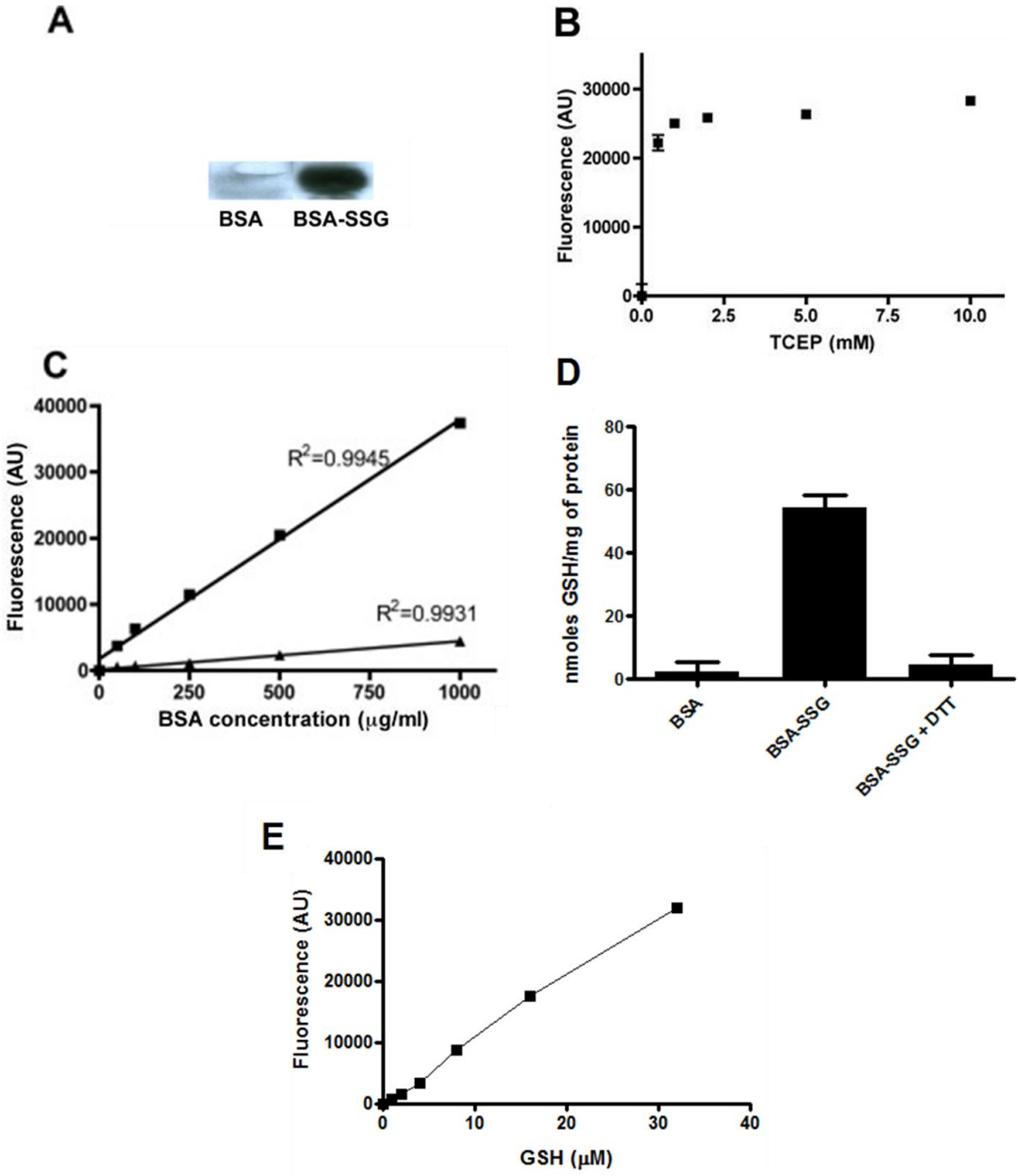

Figure 3.2: Optimization of the glutathionylation assay. (A) shows the glutathionylation level detected in recombinant BSA (control) and glutathionylated BSA (BSA-SSG) probed with an anti-glutathione antibody. (B) shows the quantitative measure of NDA-GSH derived fluorescence from BSA-SSG with increasing concentrations of TCEP. (C) shows the linearity of the fluorescence measurements with increasing concentrations of BSA-SSG (■) and un-glutathionylated control BSA (▲). (D) shows the specificity of the assay for protein bound glutathione by measuring fluorescence levels of BSA-SSG pre and post treatment with DTT. (E) A typical standard curve obtained with authentic GSH.

3.3.2 The effect of oxidative stress on cellular glutathionylation

The level of total glutathionylation was determined in human lymphoblastoid cell lines before and after treatment with the glutathionylating agent GSNO. As shown in Figure 3.3A, the basal level of glutathionylation in untreated cells was found to be 0.9 ± 0.45 nmoles/mg protein, which is well within the detection range estimated for this assay (Figure 3.2C). In contrast, one hour after treatment with 1 mM GSNO, the glutathionylation levels had risen to 16.6 ± 2.5 nmoles/mg protein. The experiment was repeated on separate days to indicate the repeatability of the assay and the cellular response. The level of total glutathionylation was determined in several cell lines and significantly higher levels were found in HEK293 cells compared to T47D and HeLa cells ($p<0.001$). However, treatment with 0.5 mM hydrogen peroxide caused a significant ($p<0.001$) increase in the level of glutathionylation in all cell lines (Figure 3.3B) (Table 3.1) which is similar to thefindings previously reported [302].

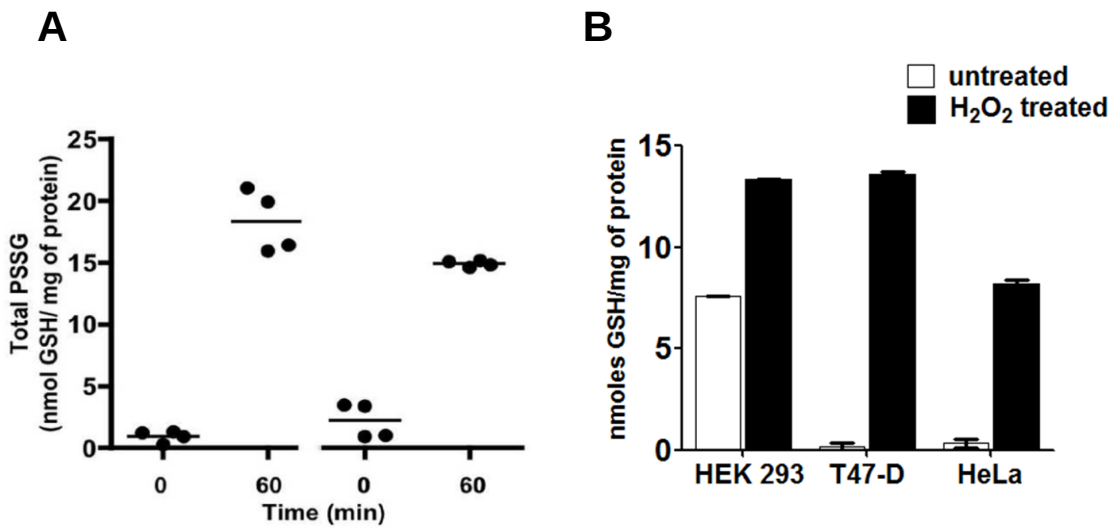

Figure 3.3: Determination of protein glutathionylation in cells
(A) Reproducibility of the assay was determined by measuring the total glutathionylation levels in lymphoblastoid cell lines before and after treatment with 1 mM GSNO on two consecutive days. The mean of individual data points is shown. (B) The assay was exploited to measure glutathionylation levels in basal and oxidative stress conditions in multiple cell lines. The assay consistently detected an increase in total glutathionylation levels in cells treated with hydrogen peroxide across all three cell lines.

	nmoles GSH/mg of protein	
Cell line	**Untreated**	**H_2O_2 treated**
HEK 293	7.57 ± 0.01	13.33 ± 0.05
T47-D	0.18 ± 0.18	13.61 ± 0.12
HeLa	0.33 ± 0.22	8.22 ± 0.19

Table 3.1: Quantification of protein bound glutathione in cell lines

3.3.3 Quantification of global glutathionylation in mouse tissues

Fresh liver, lung, kidney, heart, brain, spleen, testes and skeletal muscle from normal male BALB/c mice were extracted and glutathionylation was measured. The levels of glutathionylation were found to range from 1-2.5 nmoles GSH/mg protein for each tissue except for significantly higher ($p<0.001$) levels in skeletal muscle (Figure 3.4). Treatment of mice with the anti-cancer drug doxorubicin (20 mg/kg IP injection) caused an increase in glutathionylation in most tissues but notably caused a highly significant decrease in the glutathionylation of proteins in skeletal muscle which is still not fully understood. Since doxorubicin has been shown to induce oxidative stress [314-316], it was considered a suitable agent to evaluate and compare glutathionylation levels post doxorubicin treatment.

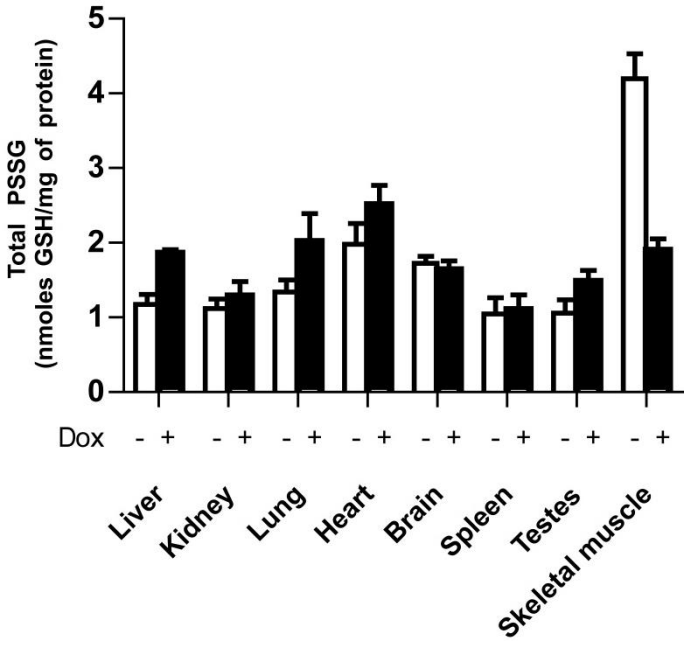

Figure 3.4: Protein glutathionylation levels were measured in mouse tissues pre- and post- treatment with doxorubicin for 24 hours. Data represents mean ± standard error; n=6

3.4 Discussion

Glutathionylation may be spontaneous or can be catalysed by members of the Glutaredoxin (Grx) family of thioltransferases and GSTP [20, 21]. Under physiological conditions, glutathione is the most prevalent thiol occurring both freely and bound to proteins in the form of mixed disulphides. On oxidative insult, redox sensitive protein thiol groups become glutathionylated via the formation of generally reversible disulphide bonds with cellular glutathione (capping cysteine residues), shielding them from irreversible oxidation [10, 67, 68]. Thus, glutathionylation may be considered as a 'hallmark' to characterize the response to oxidative stress. Though glutathionylation is mainly considered as an oxidative stress triggered protein modification, reversible glutathionylation in the absence of oxidative stress has been shown to have an impact on the functions of proteins including the contractile activity of actin and the phosphatase activity of Protein Tyrosine Phosphatase1B (PTP1B) [29, 69].

While many methods for the detection of protein glutathionylation have been described, most are qualitative and at best only semi quantitative. The new method described here for the quantification of protein glutathionylation has several advantages. It is rapid and can be applied to many different tissues and large sample numbers. Unlike a previously described method that uses difficult to obtain or expensive enzymes for the reduction of the Protein-SSG mixed disulphides (P-SSG) [311], this new assay uses commercially available reagents and a standard fluorescence plate reader. The technique can be applied to whole cell lysates and tissue homogenates and has been proven sensitive enough to measure the amount of glutathione bound to proteins in cells under physiological conditions. The specificity and reproducibility of the assay to measure protein bound glutathione alone is due to (a) the high specificity of NDA for glutathione and (b) removal of the cellular glutathione pool in the lysate by acetone precipitation.

The assay was tested *in vitro* with three different cell lines and was found to be sensitive enough to quantitate the increase in total glutathionylation in response to hydrogen peroxide induced oxidative stress. The reproducibility of the assay was determined by measuring the total protein glutathionylation levels in lymphoblastoid cells from different passages on different days. Both the basal and induced glutathionylation levels were remarkably similar, confirming that the assay can be employed routinely to detect protein glutathionylation levels in biological samples. The assay was further employed to establish values for the basal level of glutathionylation *in vivo* in the absence of oxidative stress. The levels of protein bound glutathione measured in the brain of mice

(1.7 ± 0.23 nmoles/mg) by the present assay compared well with the range of 1-12 nmoles/mg observed in various areas of the brain in a previous study [311]. Basal levels of glutathionylation have previously been shown to be necessary not only to protect protein thiols under oxidative stress conditions but also to maintain the activity of proteins such as PTP1B under normal physiological conditions [27, 61, 76, 141].

This method gains its specificity for GSH from the selective capacity of NDA in alkaline conditions to form a novel highly fluorescent cyclic derivative. The formation of a similar derivative is also possible with γ-glutamylcysteine, an immediate precursor in the synthesis of GSH [313]. γ-glutamylcysteine concentrations are normally low in cells as it is rapidly consumed in the synthesis of GSH by glutathione synthetase. In the case of glutathione synthetase deficiency when high levels of γ-glutamylcysteine might be expected to accumulate, it is converted to 5-oxoproline and cysteine by γ-glutamyl-cyclotransferase [317]. Thus it seems unlikely that elevated levels of γ-glutamylcysteine ever occur in normal cells. However if the levels of γ-glutamylcysteine were elevated it would be expected that it would behave like GSH in the glutathionylation process and would be indistinguishable in this assay. O-phthalaldehyde (OPA) has previously been shown to interact with glutathione in a similar manner generating a fluorescent adduct. However, the substrate has several limitations including the slow rate of adduct formation, low fluorescence yield and non-specific interactions with histidine residues [318]. Another limitation of the assay would be the inability to identify individual cysteine residues modified by glutathionylation. In the present study a novel assay has been developed that allows accurate quantification of changes in the level of protein glutathionylation in response to oxidative stress in complex biological samples including cells and tissues as described in the following chapters.

CHAPTER 4

Glutathione transferase Omega 1 (GSTO1-1) catalyses the glutathionylation cycle

4.1 Introduction

The process of protein glutathionylation provides a primary line of defence against irreversible protein damage caused by oxidative stress. Glutathionylation is defined as a post translational modification of protein thiol groups by the formation of mixed disulphides with glutathione [27]. On oxidative insult, redox sensitive protein thiol groups are glutathionylated (capping cysteine residues), thus shielding them from irreversible oxidative damage. This reaction may occur spontaneously, but growing evidence suggests the catalytic involvement of the Glutaredoxin (Grx) family thioltransferases [21, 69]. Additionally, glutathionylation reactions may also be reversed via deglutathionylation i.e. removal of protein bound glutathione. Glutaredoxins and sulfiredoxin are known to catalyse the deglutathionylation of proteins and thus protect protein thiols from oxidation to the oxidized sulfenic acid and sulfinic acid forms [21, 29, 67, 304, 319]. Thus, protein thiol groups can be transiently capped with glutathione until the redox balance is restored, at which time proteins can be enzymatically deglutathionylated. This makes glutathione an indispensable player in the regulation of cellular redox homeostasis. Aside from its well characterised role in oxidative stress, reversible glutathionylation in the absence of oxidative stress has also been shown to affect protein function. Glutathionylation has an impact on the regulation of the cell cycle, apoptosis and inflammation [67, 110, 113, 320], as well as the contractile activity of actin and the phosphatase activity of Protein Tyrosine Phosphatase1B (PTPB1) [29, 69]. Therefore, the mechanisms and enzymatic mediators involved in the glutathionylation cycle are of great interest under both oxidative and non-oxidative conditions.

A role for GSTO1-1 in the glutathionylation cycle is not unexpected given it is an atypical GST, with minimal functional resemblance to other members of the GST superfamily [179, 197, 262]. Most GSTs possess a tyrosine or serine residue at their active site, responsible for catalysing conjugation reactions between GSH and electrophilic substrates. However, the active site residue in GSTO1-1 was identified as

cysteine (Cys-32), flanked by proline and phenylalanine, uncharacteristic of other mammalian GSTs [262]. Previous data from our laboratory have confirmed the glutaredoxin-like thioltransferase activity of GSTO1-1 with chemical substrates such as 2-Hydroxyethyl disulphide (HEDS) [275]. Overall, the crystal structure of GSTO1-1 is suggestive of a novel role for GSTO1-1 in the glutathionylation cycle as the active site is open and could accommodate large substrates such as proteins. In this chapter the capacity of GSTO1-1 to contribute to protein glutathionylation and deglutathionylation reactions has been investigated.

4.2 Materials and methods

4.2.1 Cell culture

Cells lines were purchased from ATCC and were maintained at 37°C, 5% CO_2 in RPMI media supplemented with 10% fetal bovine serum. T47-D cells were previously stably transfected with a *Gsto1* encoding pCDNA3 plasmid [321]. Stable expression was confirmed by immunoblotting with rabbit anti-human GSTO1-1 antibody. The human lymphoblastoid cell lines expressing *Gsto1* variants were a gift from Dr Juleen Cavanaugh.

4.2.2 Preparation of S-nitrosoglutathione

S-nitrosoglutathione was synthesized as described previously [263]. An equimolar amount of reduced glutathione was mixed with sodium nitrite and the pH was adjusted to 1.5 with concentrated HCl. The reaction was allowed to proceed at room temperature for 5 minutes followed by neutralization of the synthesized GSNO with 5 M NaOH. The concentration of GSNO was estimated by measuring absorbance at 544 nm and 332 nm on a Cary UV Spectrophotometer using extinction coefficients of 15 $M^{-1}cm^{-1}$ and 750 $M^{-1}cm^{-1}$ respectively.

4.2.3 Total protein glutathionylation assay

Protein glutathionylation was determined by a previously described method [322] (see Chapter 3) Cells were lysed in a non-reducing buffer (0.5M tris, 300 mM NaCl, 1% NP-40, 50 mM N-ethylmaleimide (NEM), 2 mM AEBSF) and the protein concentration was determined using a BCA protein estimation kit according to manufacturer's instructions (Pierce, Illinois, U.S.A). Cellular proteins (100 μg) were precipitated in ice cold acetone at -20°C for over two hours. Precipitated proteins were collected by centrifugation at 20000 x g for 15 minutes and re-suspended in 0.1% Triton X-100 and

reduced with 5 mM tris(2-carboxyethyl)phosphine (TCEP) for 30 minutes at room temperature. Reduced proteins were precipitated with 200 mM salicylic acid and centrifuged at 20000 x g for 15 minutes. The eluted GSH in the supernatant was assayed with 2,3-naphthalenedicarboxyaldehyde (NDA) and compared with a standard curve. The assay was carried out in duplicate in five independent experiments.

4.2.4 Enzyme assays

a. Dehydroascorbate reductase assay

Reactions were carried out as previously described [323]. Dehydroascorbate was prepared fresh on the day and used within 3 hours. A typical reaction mix contained 200 mM sodium phosphate, pH 6.85, 3 mM GSH and 1.5 mM dehydroascorbate. The reaction was initiated by adding 1 µg of purified protein and the rate of reaction was recorded at 265 nm at 30°C. The specific activity of the enzymes was calculated with an extinction coefficient of 14.7 $mM^{-1}cm^{-1}$. Background rates (sample buffer only) were subtracted from the enzyme catalysed reaction rates.

b. Glutathione transferase assay

Reactions were carried out in 0.1 M sodium phosphate buffer pH 6.5 with 1 mM GSH and 1 mM freshly made 1-chloro-2,4-dinitrobenzene (CDNB). The conjugation reaction was initiated by adding 5 µg of enzyme and recorded at 340 nm at 30 °C for 10 minutes [324]. Specific activity was calculated with an extinction coefficient of 9.6 $mM^{-1}cm^{-1}$.

c. Glutathionylation via thiyl radical formation

The assay was carried out as previously described [325]. The Fe(II)ADP complex was prepared by incubating 20 mM $FeCl_2$ and 100 mM ADP for at least an hour prior to use. The final reaction mix was made up in 0.1 M sodium potassium phosphate buffer and contained 0.2 mM NADPH, 0.5 mM GSH, 2 U/ml glutathione reductase and 50 µM hydrogen peroxide. The reaction was initiated with premixed 0.5 mM $FeCl_2$ and 2.5 mM ADP and recorded spectrophotometrically at 340 nm.

4.2.5 Mass spectrometry

Immunoprecipitation was performed as described in Chapter 2. Glutathionylated proteins were vacuum dried and re- suspended in 7 M Urea, 2 M thiourea, 20 mM tris, 4% CHAPS. Samples were then incubated in DTT (final conc. 100 mM) for 1 hour followed by iodoacetamide (final conc. 15 mM) for 1 hr in the dark and run on a 12% SDS-PAGE. The gel was stained in Coomassie blue R-250 overnight and bands absent

in the T47-D/GSTO1-1 lysates were excised from the T47-D/pCDNA3 lysate. 1D nanoLC ESI MS/MS was carried out at the Australian Proteome Analysis Facility (APAF). Data generated were submitted to Mascot (Matrix Science Ltd, London, UK). Listed proteins were identified with a significance threshold of $p<0.02$ with Mascot cut-off of 34.

4.2.6 G-actin/F-actin assay

Cells were plated in 6-well plates and treated with 1 mM S-nitrosoglutathione as described above. Cells were washed twice with PBS and lysed in 1% Triton X-100. The detergent soluble supernatant (containing globular actin) was collected and the pellet (containing filamentous actin) was washed in PBS and re-suspended in 1X SDS sample loading buffer [326]. Proteins were run on SDS-PAGE and immunoblotted. Actin was detected after incubation with anti-actin (abcam) and the ratio of G/F actin was determined by densitometry. Glutathionylated actin was detected by immunoblotting with anti-glutathione antibody.

4.2.7 Phalloidin staining

Cells were plated on coverslips (5×10^4 cells) and treated with GSNO as described. For immunostaining, the cells were washed with PBS to remove unattached cells and fixed in 3.7% paraformaldehyde (in PBS) for 15 minutes at room temperature. The cells were washed in PBS three times and permeabilized in 0.1% Triton X-100 for 10 minutes at room temperature. Permeabilized cells were washed in PBS and incubated with 50 μg/ml Phalloidin-FITC stain for 1 hour at room temperature in the dark. Samples were washed extensively in PBS and mounted on glass slides with mounting medium with Dapi (Vectashield). Fluorescence was recorded using a confocal microscope (Leica SP5).

4.3 Results

4.3.1 In vitro deglutathionylation by GSTO1-1

To determine if the omega class GSTs participate in the glutathionylation cycle we adapted a peptide based tryptophan fluorescence quenching assay that has been previously used to measure the deglutathionylation activity of glutaredoxin [88]. A synthetic peptide incorporating a single cysteine residue adjacent to a tryptophan residue 'SQLW**C**LSN' was artificially glutathionylated at the cysteine residue (SQLW$\mathbf{C}^{-[\mathbf{SG}]}$LSN) and used as a substrate. Deglutathionylation by GSTO1-1 was then measured by monitoring the change in fluorescence emitted by tryptophan as GSH was

removed from the neighbouring cysteine. Figure 4.1 shows the significant increase in fluorescence in the presence of GSTO1-1 but not with the active site cysteine 32 mutant (C32A). It is interesting to note that the closely related GSTO2-2 isozyme did not exhibit any deglutathionylation activity. Two additional GSTs were included in the study that could potentially catalyse deglutathionylation reactions. Chloride intracellular channel 2 protein (CLIC-2) is a member of the cytosolic GST structural family and like the Omega class GSTs has a cysteine residue in its active site. Despite the presence of an active cysteine residue, no deglutathionylation activity was detected with CLIC2. The Kappa class of glutathione transferases is expressed in mitochondria and is structurally and evolutionarily distinct from the cytosolic GSTs like GSTO1-1. GSTK1-11-1 is structurally related to the prokaryotic disulphide bond forming proteins and can also be considered as a potentially active participant in the gluathionylation cycle. However, recombinant human GSTK1-11-1 did not catalyse the deglutathionylation of the glutathionylated peptide (Figure 4.1).

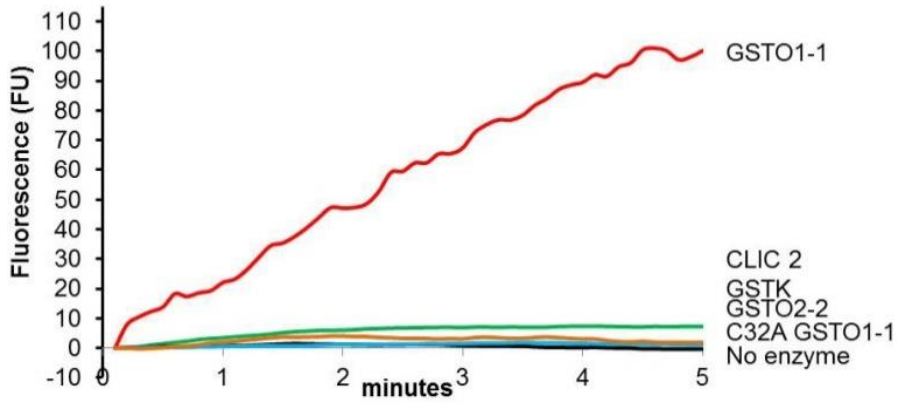

Figure 4.1 GSTO1-1 catalyses the deglutathionylation of a peptide substrate.
The increase in tryptophan fluorescence indicates the rate of peptide (SQLW**C**$^{-}$ $^{[SG]}$LSN) deglutathionylation by hGSTO1-1 in the presence of GSH. Among the GSTs tested, only GSTO1-1 showed deglutathionylating activity. Though GSTO2-2 and CLIC2 have a cysteine residue at the active site, they failed to elicit similar fluorescence spectra with the glutathionylated peptide. Deglutathionylating activity by GSTO1-1 was abolished by mutating the active cysteine residue (C32A). The graph represents the average of three traces.

4.3.2 Determination of kinetic parameters of the deglutathionylation reaction

The tryptophan fluorescence quenching assay was employed to further characterize the GSTO1-1 catalysed deglutathionylation reaction. Previous studies have identified several polymorphic variants of GSTO1-1 that could potentially vary in their substrate affinity and have an impact on the regulation of glutathionylation levels [179, 197, 262]. The specific activity and other kinetic parameters were calculated from V/[S] plots in Figure 4.2 (Table 4.1). The D140 variant had significantly lower deglutathionylation activity and this difference mainly reflected a lower k_{cat} . To confirm that this difference was not due to differential degradation of the enzymes during their preparation, we compared their thioltransferase and dehydroascorbate reductase activities (Table 4.1). These activities were found to be equivalent in agreement with previous studies from this laboratory [197]. A deletion in E155 has previously been demonstrated to be highly unstable and is usually genetically linked to a polymorphism E208K [321]. In this case, recombinant protein with the single K208 substitution was prepared. This enzyme had a significantly lower specific activity when compared to wildtype GSTO1-1. As indicated above, GSTO2-2 had no deglutathionylation activity. However, as shown in Table 4.1, the preparation was not degraded as it exhibited normal thioltransferase activity and the expected high level of dehydroascorbate reductase activity. Previous studies of CLIC-2 have failed to identify any significant enzyme activity so it is not possible to confirm that this protein preparation has not been degraded. We confirmed the viability of the GSTK1-11-1 protein by measuring its glutathione conjugating activity with 1-chloro-2,4-dinitrobenzene. This activity was readily measurable but lower than the specific activity we have previously reported [327].

A

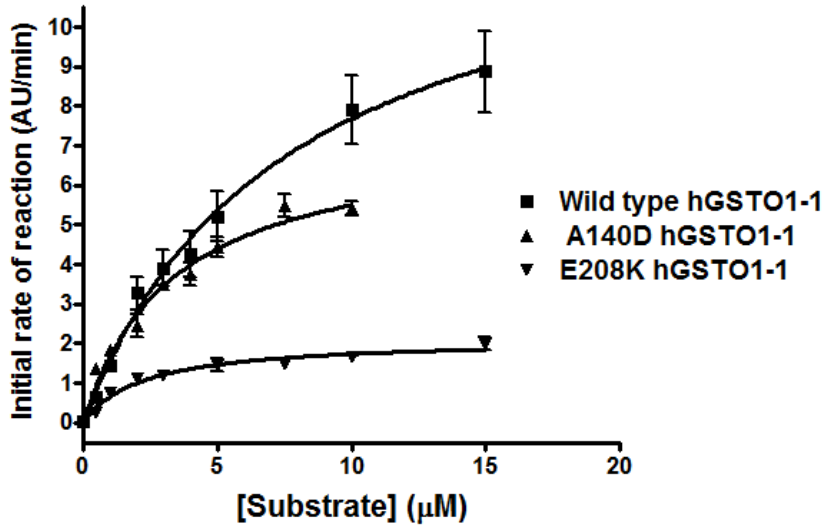

B

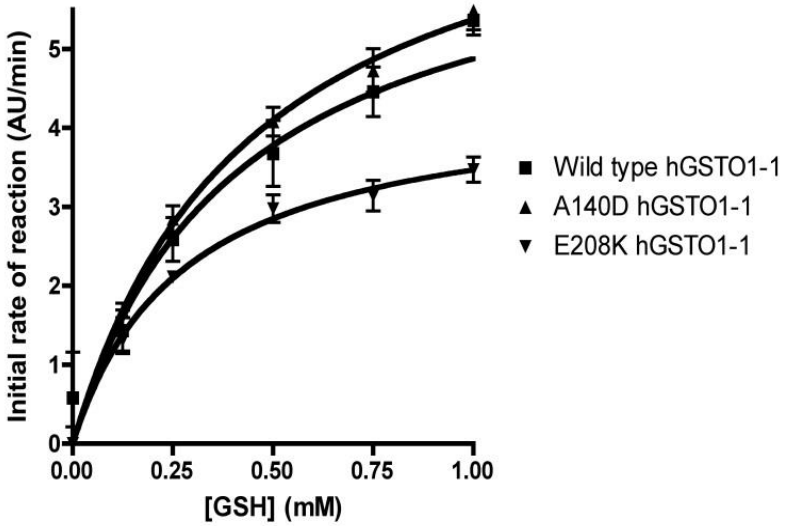

Figure 4.2: Kinetics of GSTO1-1 catalysed deglutathionylation *in vitro*: V/ [S] plots

(A) Increase in the rate of deglutathionylation by GSTO1-1 and its allelic variants with increasing substrate (peptide) concentrations; (B) Increase in the rate of deglutathionylation by GSTO1-1 with increasing GSH concentrations.

Enzyme	K_m Peptide (μM)	k_{cat} Peptide (s^{-1})	k_{cat}/K_m Peptide (μM^{-1} s^{-1})	K_mGSH (mM)	Deglutathionylation specific activity (nmoles/mg of protein/min)	Thiol transferase specific activity (μmoles/mg of protein/min)	Dehydroascorbate reductase specific activity (μmoles/mg of protein/min)
A140/E208/C32	7.9 ± 0.97	2.8 ± 0.28	0.3	0.4 ± 0.09	83.4 ± 4.4	1.0 ± 0.02	0.1 ± 0.03
D140/E208/C32	3.4 ± 0.5	1.3 ± 0.15	0.4	0.4 ± 0.12	48.6 ± 2.9	0.9 ± 0.03	0.2 ± 0.04
A140/K208/C32	2.6 ± 0.49	0.4 ± 0.07	0.1	0.3 ± 0.05	17.8 ± 2.53	1.0 ± 0.03	0.1 ± 0.04
A140/E208/A32	-	-	-	-	nd	nd	0.6 ± 0.09
GSTO2-2	-	-	-	-	nd	1.2 ± 0.02	12.9 ± 0.88
GSTK1-1	-	-	-	-	nd	nd	nd

Table 4.1. Characterization of the kinetic parameters of GSTO1-1 catalysed deglutathionylation *in vitro.*
The allelic variants of GSTO1-1 exhibit significantly different deglutathionylation reaction kinetics. Km: Michaelis constant; K_{cat}: turnover number; K_{cat}/Km: enzyme efficiency
**nd: not detected*

4.3.3 pH dependence of deglutathionylation by GSTO1-1

The dependence of the reaction rate on pH was determined by recording reaction rates in the presence of buffers of varying pHs (4-9). The reaction conditions were found to be optimum at pH 7 with significantly lower rates at both extremes (Figure 4.3).

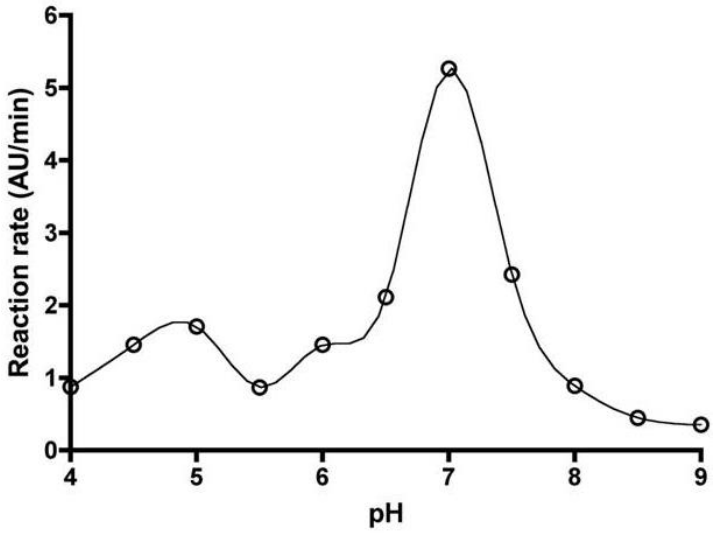

Figure 4.3: pH dependence of deglutathionylation by GSTO1-1

4.3.4 Over expression of GSTO1-1 caused global abatement of protein glutathionylation

T47-D cells are naturally deficient in GSTO1-1 and can be used to evaluate the role of GSTO1-1 in the glutathionylation cycle [321]. Stable expression of GSTO1-1 in T47-D cells was checked prior to use of cells for experiments by immunoblotting (Figure 4.4A). Whole cell lysates from T47-D cells expressing GSTO1-1 and T47-D expressing the empty vector control were separated on a non-reducing gel and probed with an anti-glutathione antibody. In T47-D empty vector transfectants global glutathionylation levels were 2.2 ± 0.49 nmoles GSH/ mg of protein. In contrast 0.9 ± 0.18 nmoles GSH/mg of protein was detected in the GSTO1-1 stable transfectants (Figure 4.4B). A significant decrease in the extent of glutathionylation of proteins as well as a decrease in the number of glutathionylated proteins was seen in the GSTO1-1 stable transfectants (Figure 4.4C). The data suggest that the expression of GSTO1-1 was responsible for the deglutathionylation of at least half the glutathionylated proteins, resulting in low glutathionylation levels.

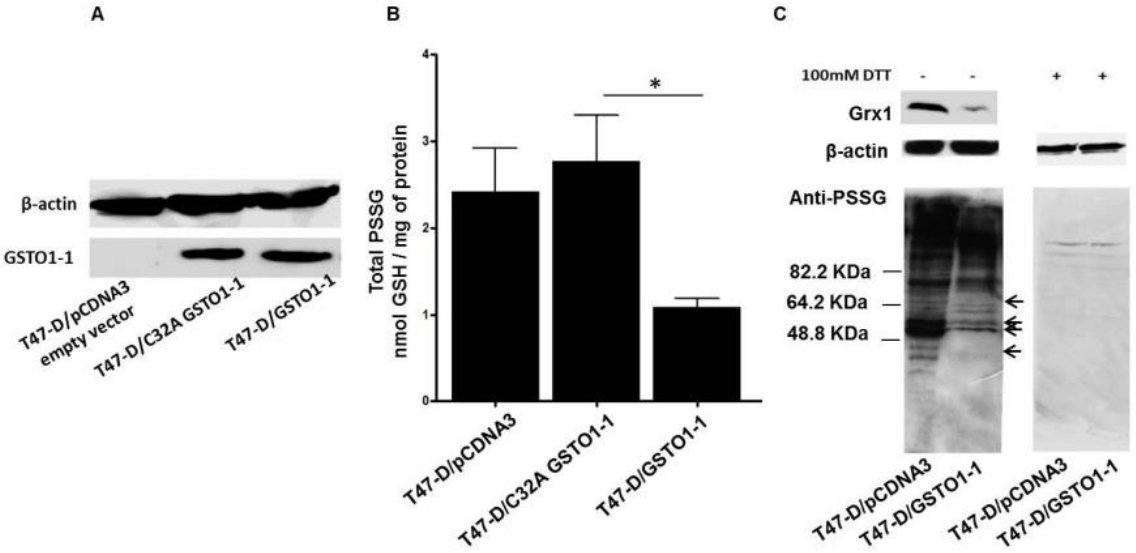

Figure 4.4: Expression of GSTO1-1 causes the deglutathionylation of proteins in T47-D breast cancer cells.
(A) Parental T47-D cells transfected with empty vector are deficient in GSTO1-1 (left lane). The cells were stably transfected with pCDNA3 C32A GSTO1-1 mutant (middle lane) and pCDNA3 GSTO1-1 (right lane). (B) The expression of GSTO1-1 resulted in a significant decrease in the total protein glutathionylation levels. This decrease was seen only in cells expressing wildtype GSTO1-1 and not in the cells expressing C32A GSTO1-1. The C32A GSTO1-1 transfected cells had protein glutathionylation levels comparable to the empty vector transfected cells. (**C**) Total glutathionylated proteins in empty vector and GSTO1-1 transfected cells were qualitatively detected with an anti-glutathione antibody (left panel). Proteins showing a marked decrease in glutathionylation are indicated by arrows. To confirm that the antibody was detecting protein bound glutathione, cell lysates were incubated with DTT and analysed as above. The lower right panel (C) shows that treatment of cellular proteins with dithiothreitol removed the chemiluminescence signal i.e. protein bound glutathione. The upper panel shows glutaredoxin 1 (Grx1) expression in T47-D cells transfected with the empty pCDNA3 vector and lower expression in T47-D cells expressing GSTO1-1.

4.3.5 Identification of targets of GSTO1-1 using mass spectrometry

Glutathionylated proteins that were reproducibly observed to be deglutathionylated in T47-D/GSTO1-1 cells were identified by mass spectrometry. Glutathionylated proteins were immunoprecipitated and separated on a SDS PAGE. Three protein bands present in the T47-D/pCDNA3 cells but absent in the GSTO1-1 expressing cells were excised from the gel, trypsin digested and subjected to mass spectrometry. Four proteins were identified as potential targets of GSTO1-1 catalysed deglutathionylation (Figure 4.5)

(Table 4.2) including β-actin, Heat shock protein 70 (HSP70), Heat shock protein 7C (HSP7C) and Prolactin inducible protein (PIP).

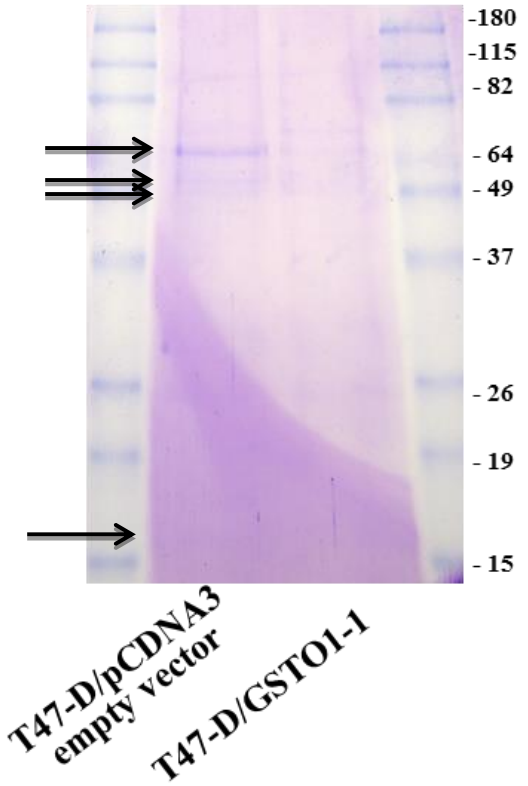

Figure 4.5: Sample preparation for mass spectrometry on glutathionylated proteins. Glutathionylated proteins were immunoprecipitated with anti-glutathione and separated on a 12% SDS PAGE gel and stained with Coommassie blue. Proteins indicated by the arrows were excised and analysed by mass spectrometry.

Protein	NCBI number	Type	Cellular localization	Molecular mass (KDa)
Actin-B	NP_001092.1	Cytoskeleton	cytoplasmic	42
Heat shock protein 70 (GRP75)	NP_004125.3	Stress protein	mitochondrial	70
Heat shock protein 7C (Hsp7C)	NP_006588.1	Stress protein	cytoplasmic	71
Prolactin inducible protein (PIP)	NP_032869.2	Signalling, metastasis marker	Cytoplasmic	16.5

Table 4.2 Proteins deglutathionylated by GSTO1-1 identified by mass spectrometry (Mass Hunter)

Since β-actin is a well-researched target of glutathionylation [27, 29, 69], the role of GSTO1-1 in its deglutathionylation in T47-D cells was validated. β-actin was immunoprecipitated from T47-D cells expressing GSTO1-1 and T47-D cells expressing the empty vector control and probed with anti-glutathione to determine its

glutathionylation state. As shown in Figure 4.6A, glutathionylated β-actin was detected in T47-D/pCDNA3 cells but not in T47-D/GSTO1-1 cells. The equal pull down of β-actin from both cell types was confirmed by probing the membrane with an anti-actin antibody (middle panel). To further validate the deglutathionylation of β-actin by GSTO1-1, glutathionylated proteins were immunoprecipitated from the T47-D cells and the pull down of β-actin was detected with an anti-actin antibody. As shown in the lower panel of Figure 4.6A, β-actin was glutathionylated only in T47-D /pCDNA3 cells and not in GSTO1-1 expressing cells, confirming that GSTO1-1 is required for the deglutathionylation of β-actin.

4.3.6 Physiological implications of GSTO1-1 mediated deglutathionylation of β-actin

The glutathionylation state of actin previously has been demonstrated to influence the ability of the protein to switch from the monomeric globular state (G-) to a filamentous state (F-) which contributes to the cytoskeletal modelling of cells [29]. Hence, the conformational state of actin was evaluated in T47-D/GSTO1-1 cells. As seen in Figure 4.6B, the ratio of G- to F-actin was considerably higher in T47-D/pCDNA3 cells when compared to the ratio in GSTO1-1 expressing T47-D cells. Notably, G-actin was more abundant in T47D/pCDNA3 cells contributing to the shift in the ratio of G-/F-actin. This finding correlates with published literature [29, 69] which states that globular actin is heavily glutathionylated and needs to be deglutathionylated in order to switch to the filamentous form which forms the cytoskeleton. To further understand the modulation of cytoskeletal structuring in the cells, actin was stained with FITC labelled phalloidin (actin-specific dye). Over-expression of GSTO1-1 in T47-D cells was seen to increase the proportion of filamentous actin (Figure 4.6C) which was reversed in GSNO treated cells. Since GSNO is a glutathionylating agent, it is possible that the deglutathionylation of actin was ‘over-ridden’ by the increased oxidative stress.

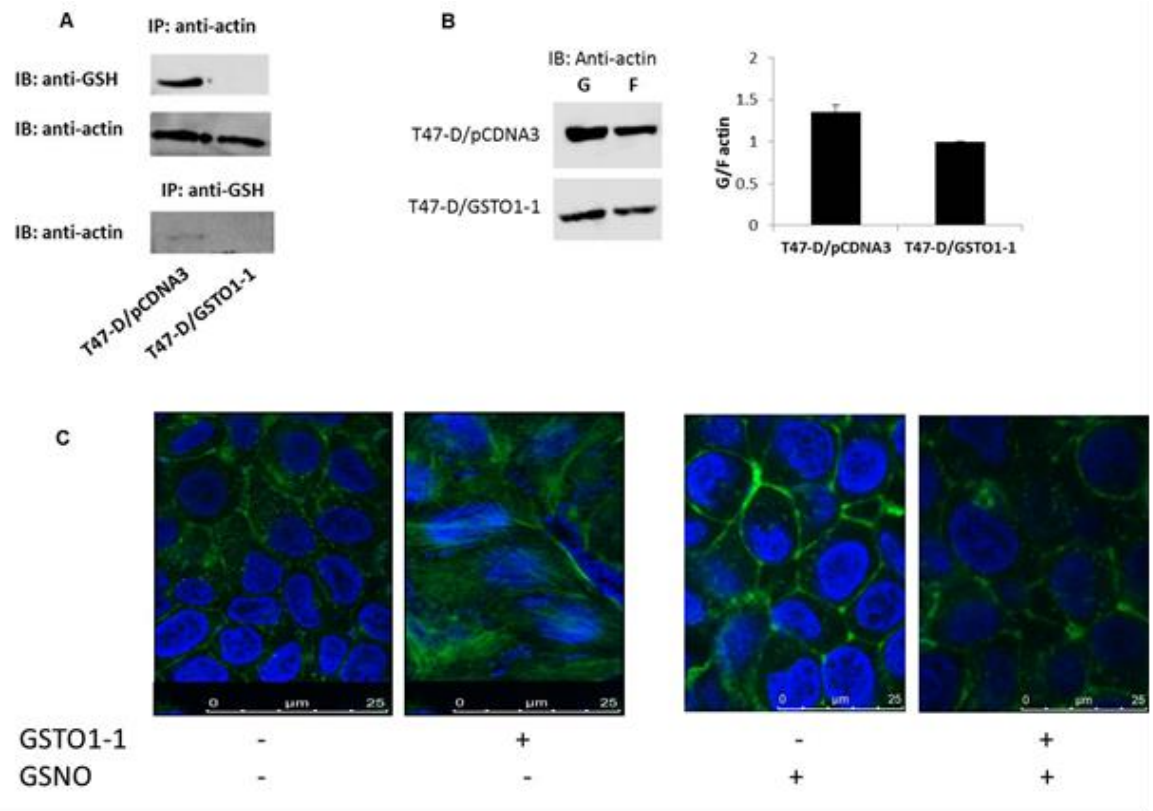

Figure 4.6: GSTO1-1 dependent deglutathionylation modulates the cytoskeletal structure by altering the G-/F-actin ratio.

(A) β-actin was validated as a target of GSTO1-1 dependent deglutathionylation by immunoprecipitation. β-actin was immunoprecipitated with an anti- β-actin antibody followed by immunoblotting with anti-P-SSG (top panel). Glutathionylated actin was detected in the control cells deficient in GSTO1-1 while no glutathionylated β-actin was detected in the GSTO1-1 over- expressing cells. Immunoprecipitation of β-actin in both samples was confirmed by probing with anti- β-actin (middle panel). Glutathionylated proteins were immunoprecipitated with anti-P-SSG and probed with anti- β-actin (lower panel). (B) Globular and filamentous β-actin were extracted from T47-D cells expressing GSTO1-1 and T47-D cells expressing the empty vector control and probed with anti-β-actin. Expression of GSTO1-1 in T47-D cells decreased the G-/F-actin ratio as a consequence of deglutathionylation of actin. Data represent the average of densitometry performed in three independent experiments. C) Fluorescence microscopy revealed increased filamentous actin (green) in the GSTO1-1 expressing cells. Treatment of cells with GSNO resulted in increased glutathionylation and the reversal of filamentous actin to globular actin in GSTO1-1 expressing cells. The nucleus is stained blue with DAPI.

4.3.7 In vitro glutathionylation by GSTO1-1

The glutathionylating activity of GSTO1-1, GSTO2-2, CLIC2 and GSTK1-11-1 was tested using the deglutathionylated form of the SQLW**C**LSN peptide in the presence of high GSSG concentrations. Although the spontaneous glutathionylation rate was high in this experiment (no enzyme control reaction, Figure 4.7), the rate of glutathionylation only increased marginally in the presence of the GSTO1-1, GSTO2-2 and CLIC 2. In contrast GSTK1-11-1 did not affect the reaction rate. Although GSTO1-1 GSTO2-2 and CLIC 2 appear to catalyse the glutathionylation of the peptide under these conditions the absolute rate was insignificant when compared to the deglutathionylating activity of GSTO1-1 (Figure 4.1).

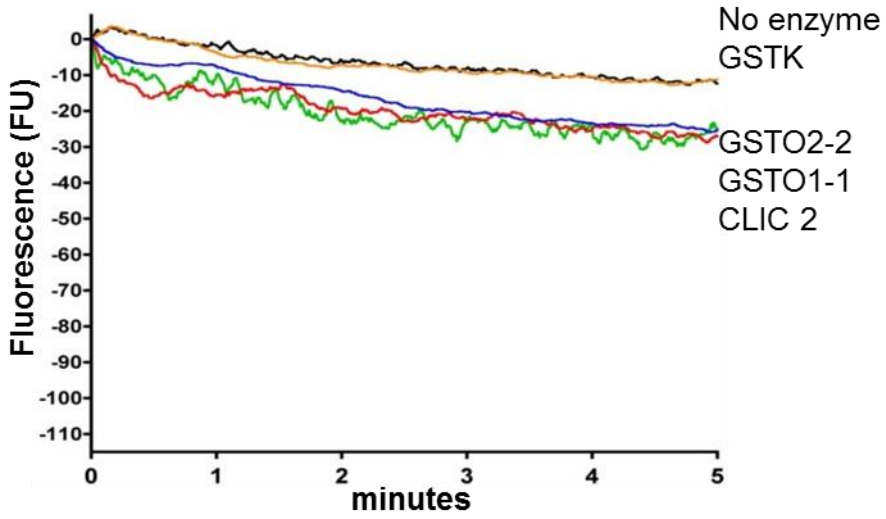

Figure 4.7: GSTO1-1, GSTO2-2 and CLIC2 catalysed the glutathionylation of the peptide SQLW**C**LSN at a poor rate *in vitro*. The graph represents the average of three traces.

4.3.8 Treatment with GSNO increased global glutathionylation in a time dependent manner

S-nitrosoglutathione (GSNO) has previously been shown to be a suitable agent to induce protein glutathionylation in cells with minimal oxidative damage [314]. GSNO was preferred over GSSG in this system as GSSG reacts very slowly with PSH [57]. The degradation of GSNO is dependent on the action of alcohol dehydrogenase class III and can generate several intermediates (Figure 4.8). In the presence of high glutathione concentrations the formation of GSSG is favoured [328]; while low GSH levels favours

the formation of glutathione disulphide-S-oxide (GS(O)SG). Both GSSG and GS(O)SG are capable of glutathionylating proteins directly. Though the S-N bond in GSNO has a slight polarity with a partial negative charge on sulphur and a partial positive charge on nitrogen, there is evidence indicating that protein thiolates react with the partially negatively charged sulphur atom and are glutathionylated and not nitrosylated [28, 58, 126, 329]. This may occur either by direct interaction of P-SSG with GSH or through the denitrosylation of PSNO by GSH.

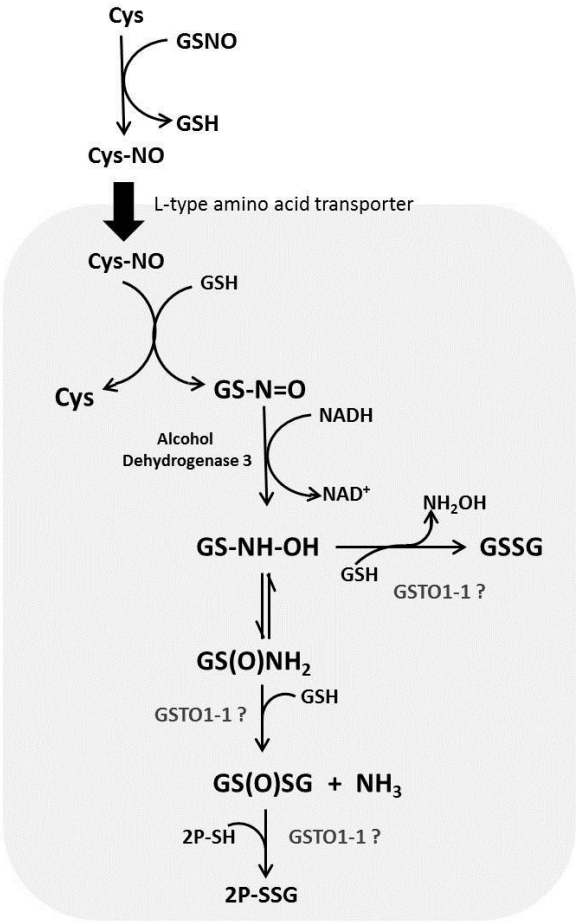

Figure 4.8: Pathways for the GSH dependent metabolism of GSNO. GSNO can be taken up into cells by transnitrosation with cysteine and the L system amino acid transporter [3]. GSTO1-1 could catalyse any of the intermediate steps in the metabolism of GSNO by either catalysing the formation of glutathione disulphide from S-(N-hydroxyamino)glutathione (GS-NH-OH) or the formation of glutathione disulphide-S-oxide (GS(O)SG from glutathione sulfinamide ($GS(O)NH_2$) or the glutathionylation of proteins (P-SSG) by GS(O)SG (shown in grey).

The susceptibility of proteins to glutathionylation versus nitrosylation has been shown to be dependent on various parameters including the polarity of adjacent residues [126]. Protein thiolates adjacent to basic residues such as histidine are more susceptible to glutathionylation. GSNO-induced glutathionylation was shown to be transient in the presence of GSH as an initial increase in total P-SSG was followed by a gradual drop in levels [28, 57, 58, 126, 330]. This was previously attributed to the spontaneous deglutathionylation of P-SSG to PSH.

In this study T47-D transfectants were treated with 1 mM GSNO to determine whether GSTO1-1 expression influences the extent of glutathionylation and the rate of deglutathionylation. Glutathionylation was enhanced significantly by GSNO in both T47-D cells expressing GSTO1-1 and T47-D expressing the empty vector control (Figure 4.9A & B). The cells expressing active GSTO1-1 were found to be more sensitive to GSNO treatment indicated by their higher total glutathionylation levels within 30 minutes (Figure 4.9B) compared with cells not expressing GSTO1-1 or cells expressing the catalytically inactive GSTO1-1 C32A mutant. We expected the expression of GSTO1-1 in T47-D cells would accelerate the rate of deglutathionylation once glutathionylation reached peak levels. T47-D cells over expressing GSTO1-1 demonstrated a marginally higher deglutathionylation rate as compared to the control pCDNA3 transfected cells which suggests that GSTO1-1 may be catalysing the deglutathionylation of proteins and thus helping proteins recover their physiological structure and resume normal cellular function. To investigate the mechanism of the increased glutathionylation in GSTO1-1 expressing cells after GSNO exposure, the endogenous GSSG levels were measured. The GSTO1-1 expressing cells had significantly higher levels of free GSSG that could contribute to the increased glutathionylation of proteins in these cells (Figure 4.9C). This suggests that GSTO1-1 may catalyse an intermediate step in the formation of GSSG in the metabolism of GSNO in cells (Figure 4.8).

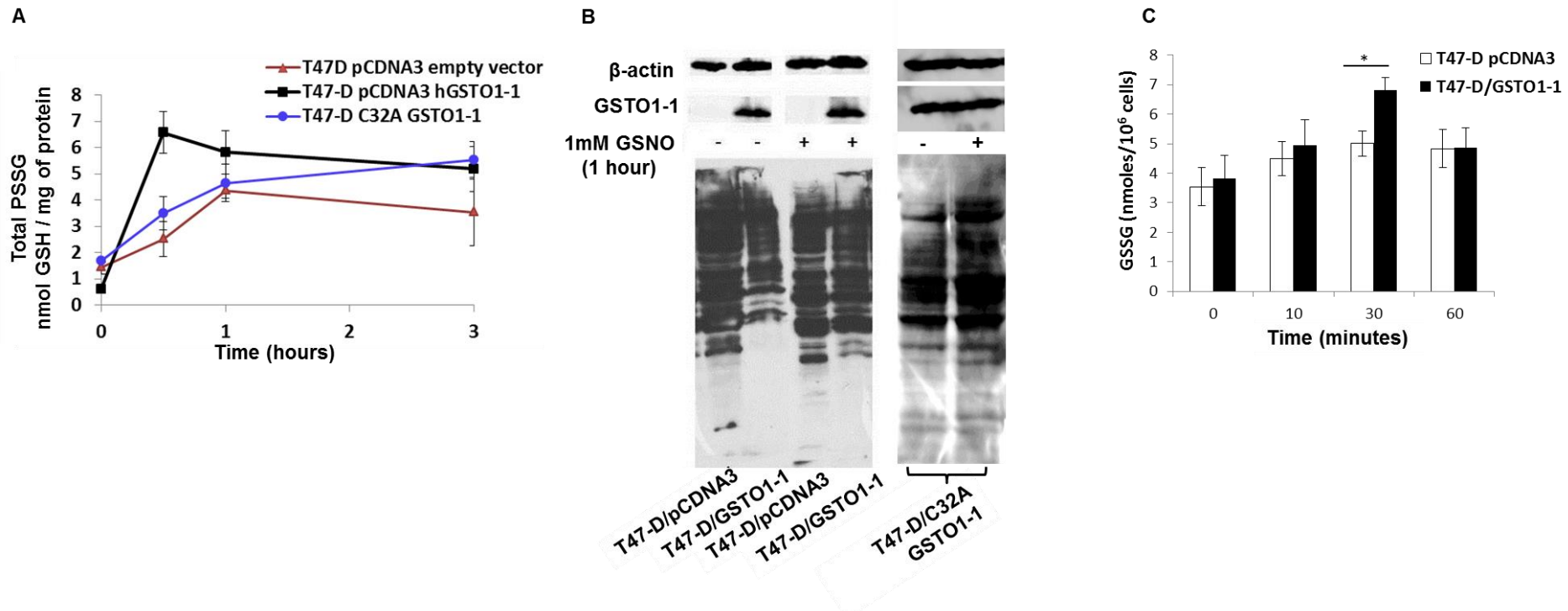

Figure 4.9: GSNO induced protein glutathionylation is dependent on GSTO1-1

(A) Increase in protein glutathionylation after treatment of cells with 1 mM S-nitrosoglutathione (GSNO) is significantly higher in T47-D cells expressing active GSTO1-1 than in GSTO1-1 deficient cells transfected with the empty pCDNA3 vector or the C32A mutant enzyme. The data points represent the mean ± SEM of 3 replicates. (B) Protein glutathionylation increased post treatment with nitrosoglutathione (GSNO) in all cells but the level of glutathionylation was significantly higher in T47-D cells expressing active GSTO1-1 than in cells transfected with the empty pCDNA3 vector or the C32A mutant protein (C) Protein glutathionylation was measured qualitatively in cells treated with GSNO. (D) The levels of GSSG were significantly higher in T47-D cells expressing GSTO1-1 in 30 minutes, correlating with the increase observed in protein glutathionylation. The data points represent the mean ± SEM of 3 replicates

4.3.9 Glutathione thiyl radicals as a GSTO1-1 substrate.

Glutaredoxin (Grx) has been shown to react with glutathione thiyl (GS•) radicals, forming a GRx-SSG•$^{-}$ disulphide anion radical intermediate and transfers the (GS•) to protein thiols or glutathione resulting in the formation of glutathionylated proteins or GSSG. The ability of GSTO1-1 to react with thiyl radicals was tested by incubating purified GSTO1-1 variants with (GS•). Both allelic variants of GSTO1-1 catalysed the formation of GSSG from the thiyl radical. However, the rate of formation of GSSG by D140 GSTO1-1 was significantly higher than the A140 variant (Figure 4.10A). Furthermore, comparing the total glutathionylation levels in lymphoblastoid cells expressing the two allelic variants revealed that cells expressing the D140 variant had slightly higher levels of glutathionylated proteins (Figure 4.10B). This was expected as the deglutathionylation activity of the D140 variant was shown to be significantly lower than the A140 wildtype protein *in vitro*. On GSNO treatment, both cell types showed a similar peaking in total protein glutathionylation followed by a time dependent drop as GSNO is metabolised in the cell. Notably, the difference in total glutathionylation levels was evident between the two variants even in the presence of GSNO, though it was not statistically significant (Figure 4.10B).

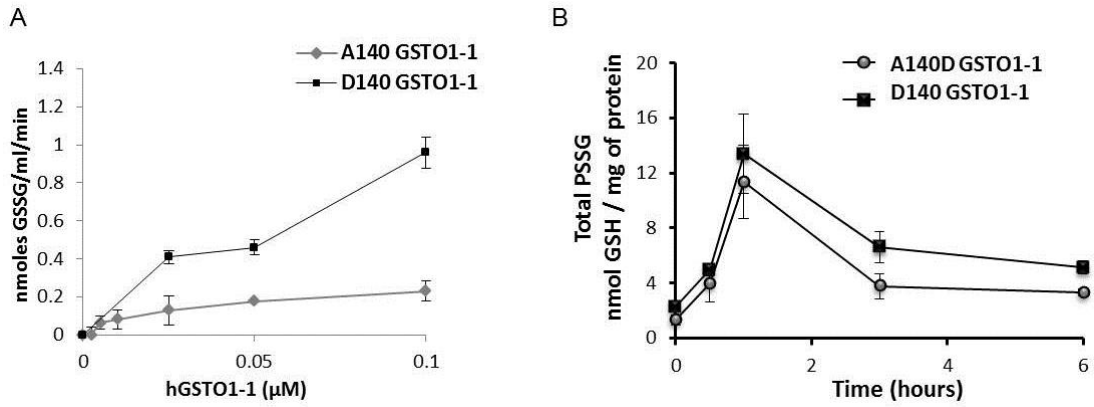

Figure 4.10: Glutathionylation of proteins by GSTO1-1 and its allelic variants
(A) GSTO1-1 catalyses the formation of GSSG from glutathione thiyl radicals. The D140 allelic variant exhibited a higher rate of GSSG formation when compared to the wildtype A140 GSTO1-1. (B) The total protein glutathionylation levels were consistently higher in D140 GSTO1-1 expressing lymphoblastoid cells even after treatment with GSNO.

4.4 Discussion

The impact of post-translational modifications such as phosphorylation and glutathionylation on protein structure and function are of great significance. Phosphorylation has been extensively studied for its role in the regulation of signalling cascades via the modulation of tyrosine kinases. In comparison, glutathionylation is relatively less explored though increasing evidence suggests a growing curiosity in the mechanism and role of protein thiol modification with glutathione [27, 68, 305]. Glutathionylation is the reversible modification of proteins by the addition of a glutathione moiety to thiols exposed on the protein surface. Protein thiols are sensitive to the immediate redox environment and a slight imbalance in redox homeostasis may result in their irreversible oxidation to a sulfonic acid form which may be detrimental to proteins [4]. Glutathionylation may be considered as a primary line of defence raised against oxidative stress and hence the reversal of this thiol modification is equally essential for a cell to recover protein function when rescued from an unfavourable environment. Though glutathionylation is strongly associated with oxidative stress, there are several lines of evidence confirming the occurrence of glutathionylation in normal physiological conditions, acting as a switch regulating protein activity [69, 76, 143]. The reversal of glutathionylation is largely dependent on catalysts, a list that is predominantly restricted to glutaredoxins, thioredoxins and sulfiredoxin [29, 31, 319]. Glutaredoxins are enzymes that rely on their active site cysteine residues to catalyse the glutathionylation and deglutathionylation of proteins [21, 26, 61-65, 76, 87]. Due to the occurrence of two active site cysteines in a conserved CXXC motif, glutaredoxins are capable of glutathionylating proteins via a monothiol mechanism and deglutathionylating via a dithiol mechanism [63]. Glutaredoxins can also catalyse disulphide exchange between the two active cysteines, which forms an intermediate step in the dithiol mechanism. Sulfiredoxins have a single cysteine residue and hence catalyse deglutathionylation reactions via a monothiol mechanism [29, 331].

Members of the Glutathione transferase family have been well characterized with excellent ability to catalyse the conjugation of glutathione with a range of xenobiotics [194, 195]. A relatively new hypothesis proposed previously questioned the possibility of extending GST-catalysed glutathione conjugation reactions to protein substrates [332]. Though GSTs have been shown to regulate signal transduction via direct protein-protein interactions [208, 238, 242, 243, 245, 333], GSTP was the first member identified to catalyse protein glutathionylation. The mechanism of glutathionylation by GSTP was shown to be similar to that of typical GSH-conjugation reaction with

xenobiotics i.e. via lowering the pKa of GSH by the active site tyrosine residue [20, 111]. Though other GSTs haven't been extensively studied, a recent study demonstrated the *in vitro* ability of mammalian GSTM1 and GSTP1 to catalyse the glutathionylation of recombinant AMP- kinase (AMPKα) though the physiological implications were not fully elaborated [334].

Previous studies have established the structural resemblance of the N-terminal domain of GSTO1-1 to the Grx family [197] with a conserved thioredoxin fold. On further analysis, we found that the active site cysteine in human GSTO1-1 aligns with the active site in human Grx1, supporting our findings that GSTO1-1 catalyses deglutathionylation of proteins similar to the glutaredoxins (Figure 4.11). Our data suggest that GSTO1-1 deglutathionylates proteins via a monothiol mechanism through cysteine-32. The reaction proceeds by the following path where the model peptide represents a protein substrate and the enzyme is recycled by the action of GSH:

$$\text{GSTO1 } 32C^{SH} + \text{SQLWC}^{SG}\text{LSN} \rightarrow \text{GSTO1 } 32C^{SG} + \text{SQLWC}^{SH}\text{LSN}$$

$$\text{GSTO1 } 32C^{SG} + \text{GSH} \rightarrow \text{GSTO1 } 32C^{SH} + \text{GSSG}$$

Interestingly, GSTO2-2 (68% sequence similarity to GSTO1-1) and CLIC 2 also contain the thioredoxin fold and similar active site residues but do not exhibit deglutathionylation activity under the conditions used in this study. It must be noted that though GSTO2-2 and CLIC2 have cysteine residues in their active sites, GSTO2-2 does not catalyse the S-phenacylglutathione reductase activity of GSTO1-1 while CLIC2 does not have any measurable catalytic activity. Thus, the inability of the two proteins to catalyse the glutathionylation cycle reactions is not without precedent.

We have characterized the kinetics of GSTO1-1 catalysed deglutathionylation *in vitro* and further confirmed the physiological occurrence of the reaction in cells. Recombinant GSTO1-1 catalysed the removal of glutathione from an artificially glutathionylated peptide in the presence of GSH, which was quantified by measuring the decrease in fluorescence emitted by an adjacent tryptophan residue. The emission spectrum of tryptophan is highly reflective of its immediate environment and an alteration to surrounding residues can modify its fluorescence emission. Thus, when glutathione is catalytically removed from the adjacent tyrosine residue in the

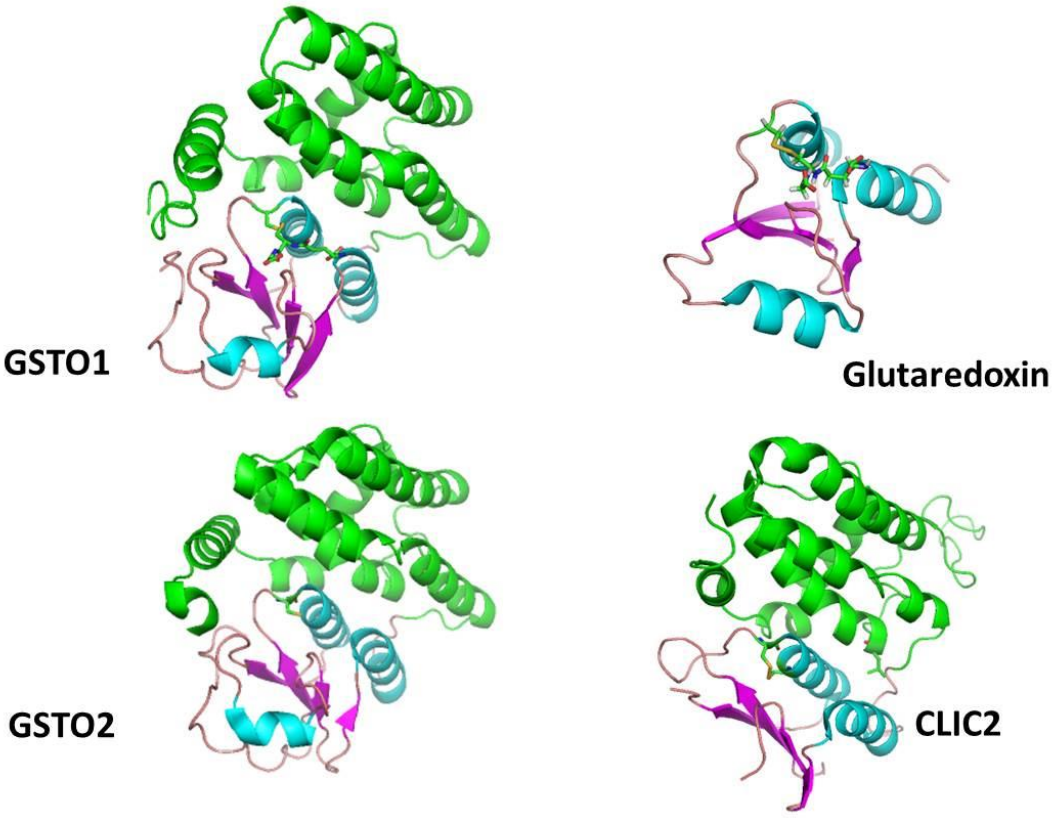

B

```
GSTO1-1     MSGESARSLGKGSAPPGPVPEGSIRIYSMRFCPFAERTRLVLKAKGIRHE 50
GSTO2-2     MSGDATRTLGKGSQPPGPVPEGLIRIYSMRFCPYSHRTRLVLKAKDIRHE 50
CLIC 2      MSG--LRPGTQVDPEIELFVKAGSDGESIGNCPFCQRLFMILWLKGVKFN 48
Grx 1       ---------MAQEFVNCKIQPGKVVVFIKPTCPYCRRAQEILSQLPIKQG 41
```

Figure 4.11: Structural similarities between the glutaredoxin family of oxidoreductases and GSTs

(A) The structures of GSTO1, GSTO2, CLIC2 and Grx1 shown in cartoon form, are drawn from the coordinates in PDB files 1EEM, 3Q18, 2R4V and 1GRX respectively. In the conserved thioredoxin fold domain β-sheet is shown in magenta and helices are shown in cyan. The C-terminal helical domain of GSTO1, GSTO2 and CLIC2 is shown in green. (B) Residues conserved in the active site of the enzymes. (pink: fully conserved, yellow: very similar and blue: weakly similar).

SQLW**C**LSN peptide we measured an increase in tryptophan fluorescence which was normalized to the control (no enzyme) levels for the estimation of its specific activity. The specific activity of GSTO1-1 in deglutathionylation was estimated at 83.4 nmoles/mg of protein/min. The initial rate of the reaction increased with increasing peptide concentration and fitted well to the Michaelis-Menten equation. The Km value obtained for GSTO1-1 was 7.9 ± 0.97 μM which is comparable to that reported for Grx (7.8 μM) [87]. An interesting finding this study revealed was the significant difference in deglutathionylating activity among the allelic variants of GSTO1-1. The polymorphic variant D140 exhibited deglutathionylation activity of almost half that of the more frequent (wildtype) A140 isoform. More significantly, the K208 variant was approximately five times less active than the most common E208 allelic variant. In Europeans the K208 allele is closely linked to a deletion of E155 which destabilizes the protein [335] and its effects would not be apparent *in vivo*. Genetic variation at the *GSTO1* locus has previously been linked to the age at onset of Alzheimer's and Parkinson's diseases however a direct functional mechanism has never been identified [210-212, 214, 272]. It is reasonable to speculate that differences in glutathionylation could play a role in the progression of the pathology of these diseases and this study has shown that there are significant differences in the deglutathionylation reaction kinetics between the common A140 and D140 allelic variants.

In this study, the deglutathionylating activity of GSTO1-1 was evaluated in whole cells. T47-D breast cancer cells were considered ideal to determine the deglutathionylating activity of GSTO1-1 as these cells are devoid of endogenous GSTO1-1 expression due to their hemizygosity for Del E155 allele that results in the expression of an unstable protein.[336]. Thus, T47-D stable transfectants expressing active GSTO1-1 or a catalytically inactive C32A mutant were employed to determine the effect of GSTO1-1 on protein glutathionylation. Expression of GSTO1-1 resulted in an abatement of total protein glutathionylation which complemented the *in vitro* peptide studies. Further investigation into GSTO1-1 catalysed deglutathionylation in T47-D cells identified four protein targets including β-actin. This finding further supports the proposal that GSTO1-1 has target specificity and does not deglutathionylated all proteins at the same rate. Figure 4.12 depicts a proposed mechanism by which GSTO1-1 catalyses the deglutathionylation of proteins and gets recycled by cellular GSH or GSH provided in the *in vitro* reaction mix. Glutathionylation is known to modulate the activity of proteins in various metabolic and signalling pathways [27, 61, 66, 139, 141, 143, 160, 305, 337, 338]. For instance, this study demonstrated that GSTO1-1 dependent

deglutathionylation of actin can modulate the structural modelling of T47-D cells (Figure 4.6).

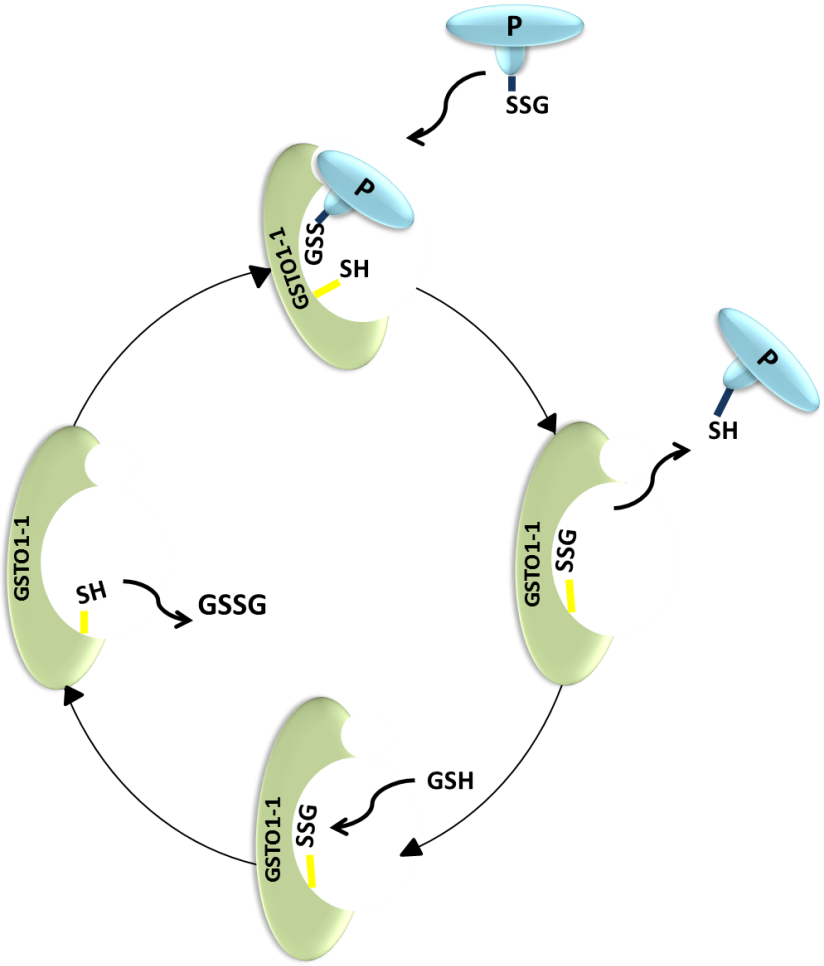

Figure 4.12: Model depicting the reaction pathway of deglutathionylation by GSTO1-1
Glutathionylated protein thiols interact with GSTO1-1 in two steps: First the glutathionylated protein thiol (P-SSG) binds to the GSH binding site of GSTO1-1 via the –SSG group. The –SSG group is exchanged between cysteine 32 (Cys32-SH) (shown in yellow) and P-SSG. The glutathionylated Cys32-SSG is recycled by free GSH and is free to catalyse the deglutathionylation of the next protein substrate.

Thus, it is essential for enzymes catalysing the glutathionylation cycle such as glutaredoxins, sulfiredoxin, GSTP and GSTO1-1 to have substrate specificity to establish a reversible switch to differentially regulate specific pathways under different stress signals. The factors contributing to the observed target specificity of GSTO1-1 are yet to be fully understood.

The *in vitro* experiments performed to measure the potential glutathionylation activity (due to structural and sequence similarity with glutaredoxins) using the peptide 'SQLW**C**LSN' failed to detect any significant activity catalysed by either GSTO1-1 or GSTO2-2. This may be due to several reasons. Fluorescence from the adjacent tryptophan residue was consistently decreasing in the control reaction even in the absence of GSTO indicating spontaneous glutathionylation in the presence of high GSSG concentrations. However it is also known that glutathionylation by GSSG is a relatively slow reaction [57] which may account for the absence of a higher reaction rate for the spontaneous reaction (Figure 4.6). Though glutathionylation is thought to be largely spontaneous, Grxs have been demonstrated to catalyse the reaction with target specificity [21, 26, 62, 63, 76, 87]. Apart from an enzyme's affinity towards a protein target, the susceptibility of the target cysteine residue is also determined by its pKa value which in turn is influenced by the polarity of residues in its immediate environment, either adjacent to the cysteine or in close proximity due to the protein's tertiary structure [30]. Cysteines surrounded by basic amino acids such as histidine have been reported to be more susceptible to glutathionylation by lowering the pKa of the cysteine residue [30, 126]. Since the peptide was 8 residues long, it cannot be argued that the peptide's tertiary structure influenced the poor reaction rates measured. However the absence of suitable basic amino acids within the 8-mer may have contributed to the absence of a significant glutathionylation reaction in the presence of GSSG in the absence of GSTO1-1. Also, it is possible that the sequence of the peptide may not be appropriate for binding to GSTO1-1, hence preventing the interaction of the target thiol with the active site cysteine residue.

GSTO1-1 was also demonstrated to produce GSSG from glutathione thiyl radicals that can in turn glutathionylate proteins. Interestingly, GSTO1-1 may be responsible for glutathionylation of proteins in cells treated with GSNO either by directly catalysing the glutathionylation of specific proteins or by increasing the GSSG levels which in turn glutathionylates proteins. The former could not be proven in this study but after GSNO treatment, GSSG levels were significantly higher in T47D cells expressing GSTO1-1

than in empty vector control cells. This study provides preliminary evidence that GSTO1-1 may catalyse intermediate reactions in the generation of GSSG from GSNO. Consequently GSTO1-1 may indirectly glutathionylate proteins via GSSG formation from glutathionylating agents such as GSNO or by reacting with glutathione thiyl radicals. It is yet to be fully investigated whether glutathionylation by GSTO1-1 has target specificity like Grxs which is affected by other parameters such as the tertiary structure of the protein.

The known impact of glutathionylation on neurodegenerative diseases is not extensive though the activity of critical proteins such as Tau have been reported to be modulated by the oxidative state of their thiols (reviewed extensively in [339]). GSTO1-1 and its allelic variants have been implicated to influence the age at onset of inflammation associated neurodegenerative diseases such as Alzheimer's and Parkinson's diseases. Since the D140 GSTO1-1 variant was shown to exhibit lower deglutathionylation activity both *in vitro* and in lymphoblastoid cells, it is not unreasonable to speculate that GSTO1-1 and its differentially active allelic variants may modulate the function of proteins involved in neurodegeneration by catalysing their deglutathionylation.

CHAPTER 5

Glutathione transferase Omega modulates TLR4 dependent pro-inflammatory responses

5.1 Introduction

A study by Laliberte *et al.* identified GSTO1-1 as a target of Cytokine Release Inhibitory Drugs (CRIDs), implicating GSTO1-1 in pro-inflammatory pathways involved in the activation and processing of interleukin 1β in monocytes [264]. A recent study identified a novel interaction of GSTO1-1 with ASC (Apoptosis associated speck-like protein containing a CARD), which is a component of the inflammasome complex required for the synthesis of mature IL-1β. These results indicate the probability of an indirect effect of GSTO1-1 on IL-1β via protein-protein interactions within the activation complex [265]. We have recently shown that GSTO1-1 has significant deglutathionylation activity like glutaredoxins, both *in vitro* and in cells [90](Chapter 4). Whether this activity has a role in the regulation of pro-inflammatory responses is yet to be determined.

Inflammatory stimulants, such as bacterial endotoxin (Lipopolysaccharide, LPS) have been shown to induce reactive oxygen species (ROS) generation through the activation of Toll like receptor 4 (TLR4) by disturbing the balance between the activation of oxidants and suppression of antioxidants [149, 280, 340-343]. Though LPS induced inflammatory responses largely depend on the activation of TLR4 and recruitment of downstream signalling proteins, the immediate generation of TLR4 mediated ROS has been shown to have an impact on the expression of pro-inflammatory cytokines [279, 340, 343, 344]. The generation of ROS after LPS stimulation has been shown to be dependent on the cytosolic NADPH oxidases [147, 340, 345, 346]. A recent study elucidated the role of NADPH oxidase 1 in LPS induced ROS generation which was significantly attenuated in *Irak1*$^{-/-}$ mice [149]. In this chapter, the indispensable role of GSTO1-1 as a novel regulator of ROS-dependent pro-inflammatory responses in macrophages is described. *Gsto1* knockdown cells were found to be non-responsive to LPS and failed to elicit pro-inflammatory responses including the expression of IL-1β, generation of ROS and the suppression of antioxidants. Since their first description, the Omega class GSTs have been investigated in relation to a number of biologically

significant pathways and clinical disorders including drug resistance [260], Alzheimer's Disease [210, 211, 215, 216, 272], Parkinson's disease [210, 215, 216, 261], vascular dementia and stroke [214], amyotrophic lateral sclerosis [217], the action of anti-inflammatory drugs [264], the disposition of arsenic [274], susceptibility to chronic obstructive pulmonary disease (COPD) [213] and cancer [113, 260, 321]. This study introduces a novel finding that may help elucidate the role of GSTO1-1 in inflammatory disorders.

5.2 Materials and methods

5.2.1 Materials

Ligands for TLR activation including LPS (*E. coli* O111:B4) for TLR4, PAM3CSK4 for TLR1/2, Poly:I(C) for TLR3, R848 for TLR7 and CpG for TLR9 were purchased from Invitrogen. The primers used in this study were purchased from Integrated DNA Technology (IDT). Primer sequences are listed in Appendix A6. ML175 was purchased from Vitas-M laboratory (Netherlands).

5.2.2 Cell lines and treatments

Murine J774.1A cells were stably transfected with *Gsto1* targeting lentiviral shRNA and scrambled non-targeting shRNA as previously described [345] and maintained in DMEM media supplemented with 10% FBS, 3μg/ml puromycin and 2 mM Glutamine. Cells were treated with standard concentrations of 10 ng/ml LPS, 1 μg/ml PAM3CSK4, 1 μg/ml R848, 25 μg/ml Poly:I(C) and 1 μg/ml CpG unless otherwise stated. Cells were treated with varied concentrations of ML175 (0.25 μM- 5 μM) for 2 hours prior to LPS stimulation. For measurement of cytokines, cells were stimulated with indicated ligands for 24 hours and supernatants were collected and frozen at -20°C for ELISAs. For the measurement of ROS and mRNA expression levels, cells were stimulated with LPS for 6 hours.

5.2.3 Measurement of ROS

Total intracellular ROS was determined with the fluorescent probe chloromethyl-2',7'-dichlorofluorescein diacetate (CM-H_2DCFDA) (Invitrogen). J774.1A macrophages were seeded at a density of $1x10^5$ cells in a 6-well plate and treated with LPS (100ng/ml) for indicated time points. The cells were washed twice with PBS and incubated with 10 μM CM-H_2DCFDA (in PBS) for 30 minutes at 37°C. The cells were again washed with PBS and formation of dichlorofluorescein was measured using a

fluorescence spectrophotometer (Fluostar Optima) at excitation/emission wavelengths of 488/525 nm. Raw fluorescence measurements were normalized to unstained cells.

5.2.4 Enzyme assays

a. Catalase: Reactions were carried out as described previously [347]. 5 μg of total cell lysate was added to a reaction mix containing 50 mM phosphate buffer (pH 7.0), 50 mM H_2O_2. The reaction was stopped with 1.25% sodium dichromate for 10 minutes. The reaction rate was measured at 240 nm at 37°C and the specific activity was calculated as moles of H_2O_2 consumed/mg of protein. Baseline samples were prepared by adding sodium dichromate to samples at time 'zero' and background rate was subtracted from the enzyme catalysed reaction rates. Protein concentration was estimated by a BCA protein estimation kit (Pierce).

b. Glutathione peroxidase: 50 μg of total cell lysate was added to a reaction mix containing 50 mM phosphate buffer (pH 7.0), 1 mM GSH, 200 μM NADPH, 0.1 U glutathione reductase and 20 μM cumene hydroperoxide. The reaction rate was measured at 340 nm at 37°C and the specific activity was calculated based on an extinction coefficient of 6.22 $mM^{-1}cm^{-1}$. Background rates were subtracted from the enzyme catalysed reaction rates.

c. Glutathione Reductase: 20 μg of cell lysate was added to a reaction mix containing 0.1 M Tris/0.5 mM EDTA (pH 8.0), 0.2 mM NADPH and 3.3 mM GSSG. The reaction rate was measured at 340 nm at 37°C and the specific activity was calculated based on an extinction coefficient of 6.22 $mM^{-1}\cdot cm^{-1}$. Background rates (sample buffer only) were subtracted from the enzyme catalysed reaction rates.

d. 4-NPG reduction: GSTO1-1 specific activity was determined with S-(4-nitrophenacyl)glutathione (4-NPG) as described previously [348]. Briefly, 5 mM 4-NPG was incubated with 75 μg of cell lysate in 100 mM tris pH 8.0 and 10 mM β-mercaptoethanol. The reduction of 4-NPG was measured spectrophotometrically at 305 nm at 37°C and the specific activity was calculated based on an extinction coefficient of 1.1 $mM^{-1}\cdot cm^{-1}$.

5.2.5 Immunostaining

Cells were plated on coverslips (5 x 10^4 cells), treated with LPS and immunostained as previously described [349]. Briefly, the coverslips were washed with PBS to remove unattached cells and fixed in 3.7% paraformaldehyde (in PBS) for 15 minutes at room temperature. The cells were washed in PBS three times and permeablized in blocking

buffer (1% Bovine serum albumin (BSA)/0.2% Triton-X100/PBS) for 30 minutes at room temperature. Permeabilized cells were washed in PBS and incubated in primary anti-p65 (Santacruz sc109) at a dilution of 1:100 for 2 hours at room temperature. Cells were thoroughly washed and incubated in secondary chicken anti-rabbit FITC tagged secondary antibody (1:200) for one hour at room temperature in the dark. The coverslips were washed extensively in PBS, mounted on glass slides with Dapi containing mounting medium and fluorescence was recorded using a Leica SP5 confocal microscope. The images were analysed using Leica LAS AF software.

5.2.6 Immunoprecipitation

Immunoprecipitation was carried out using Pierce crosslinking immunoprecipitation kit using an anti-IRAK4 antibody (Cell signalling). Immunoprecipitated proteins were separated on 12% SDS-PAGE and immunoblotted as described in Chapter 2. The nitrocellulose membrane was incubated with a mouse anti-phospho-serine and phospho-threonine antibody.

5.2.7 Real time RT-PCR

Total RNA was extracted from cells in trizol (Invitrogen) and a Qiagen RNA extraction kit as previously described (refer Chapter 2 for detailed methods). Primer sequences are provided in Appendix A6.

5.2.8 Phagocytosis assay

Phagocytosis of fluorescently labelled dead *E. coli* (strain K-12) was measured as per manufacturer's instructions (Vybrant phagocytosis kit, Life Technologies). J774.1A cells were seeded in 96-well plates at a density of 10^5/well and allowed to adhere for 2 hours at 37°C, 5% CO_2. Media was removed and the cells were incubated in the fluorescent bioparticle suspension for 2 hours followed by immediate quenching with trypan blue. The supernatant was then aspirated and fluorescence was measured at an Ex/Em wavelength of 480/520 nm using a plate reader (Fluostar Optima). Net phagocytosis of GSTO1-1 knockdown cells was determined by subtracting the average fluorescence of media-only negative control wells and normalized to the average fluorescence of the non-silencing control J774.1A macrophages.

5.2.9 Latex bead phagocytosis assay

Yellow orange 3 micron Fluoresbrite carboxy latex microparticles (Polysciences) were incubated with 30 $\mu g\,ml^{-1}$ LPS overnight at 4 °C in PBS. Beads were then washed

thoroughly in PBS to remove unbound LPS. Cells cultured overnight on coverslips in 12-well plates were incubated on ice for 10 minutes. Coated and uncoated (control) latex beads were added to the cells and allowed to settle on the cells for 10 minutes prior to incubation in warm culture media at 37°C for indicated time periods. Cells were fixed with 3.7% paraformaldehyde for 15 minutes at room temperature, permeabilized with 0.1% Triton-X100/0.2%BSA and stained with Phalloidin-FITC (Sigma) as per manufacturer's instructions. The intracellular uptake of the beads was visualized by confocal microscopy (Leica SP5).Serial z-sections were recorded to confirm intracellular localization of the beads. The number of beads taken up by the cells was counted across 30 cells/coverslip.

5.2.10 In vitro viability assay

Total cell viability was determined with the help of neutral red staining as described in Chapter 2. Cells were seeded in 96-well plates at 50% confluency and treated with increasing concentrations of ML175 for indicated time periods. Cells were washed with PBS and lysed in 25% acetic acid:75% methanol. Absorbance was measured at 540 nm.

5.2.11 Enzyme linked immunoassay (ELISA)

IL-6 was quantified in cell culture supernatant using a murine IL-6 Duoset Elisa kit (R&D Biosystems). Cells were seeded at a density of 10^4 cells/well (in triplicates) in clear bottom 96-well plates and incubated overnight. Post 24 hours of stimulation with TLR-specific ligands, the supernatant was collected and stored at -20°C until further use. Plates (Nunc Maxisorp flat bottom 96 well plates) were prepared by coating each well with 50 µl of 2 µg/ml in PBS of capture antibody (rat anti-mouse IL-6). The plates were incubated overnight at room temperature and washed three times with PBS to remove unbound antibody. Plates were then blocked in 150 µl of 1% BSA/PBS for at least 2 hours at room temperature and the wash step was repeated. 50 µl of cell culture supernatant was added to the wells in triplicates and incubated for 2 hours at room temperature or overnight at 4°C. Recombinant mIL-6 standards were prepared in PBS and added to wells in duplicates. The wells were washed in PBS thoroughly and incubated with the detection antibody (biotinylated goat anti- mouse IL-6) at a final concentration of 150ng/ml (50 µl/well) for 2 hours at room temperature. Plates were washed thoroughly and incubated with streptavidin-HRP for 20 minutes in the dark at room temperature. The wash step was repeated and HRP substrate (Millipore Immobilon western chemiluminescent HRP substrate) was added and incubated for

another 20 minutes in the dark. The reaction was stopped with 50 µl of 2N sulphuric acid and absorbance was measured at 450 nm using a plate reader (Optima Fluostar).

5.3 Results

5.3.1 GSTO1-1 expression profile in immune cells

The expression profile of GSTO1-1 in immune cells was accessed through Immunological Genome Project (Immgen). The levels of GSTO1-1 were significantly higher in phagocytic immune cells such as macrophages, monocytes and neutrophils when compared to non-phagocytic immune cells (Figure 5.1A) whereas the expression of GSTO2-2 in these cells was relatively lower (Figure 5.1B), indicating that GSTO1-1 may be involved in inflammatory responses in macrophages.

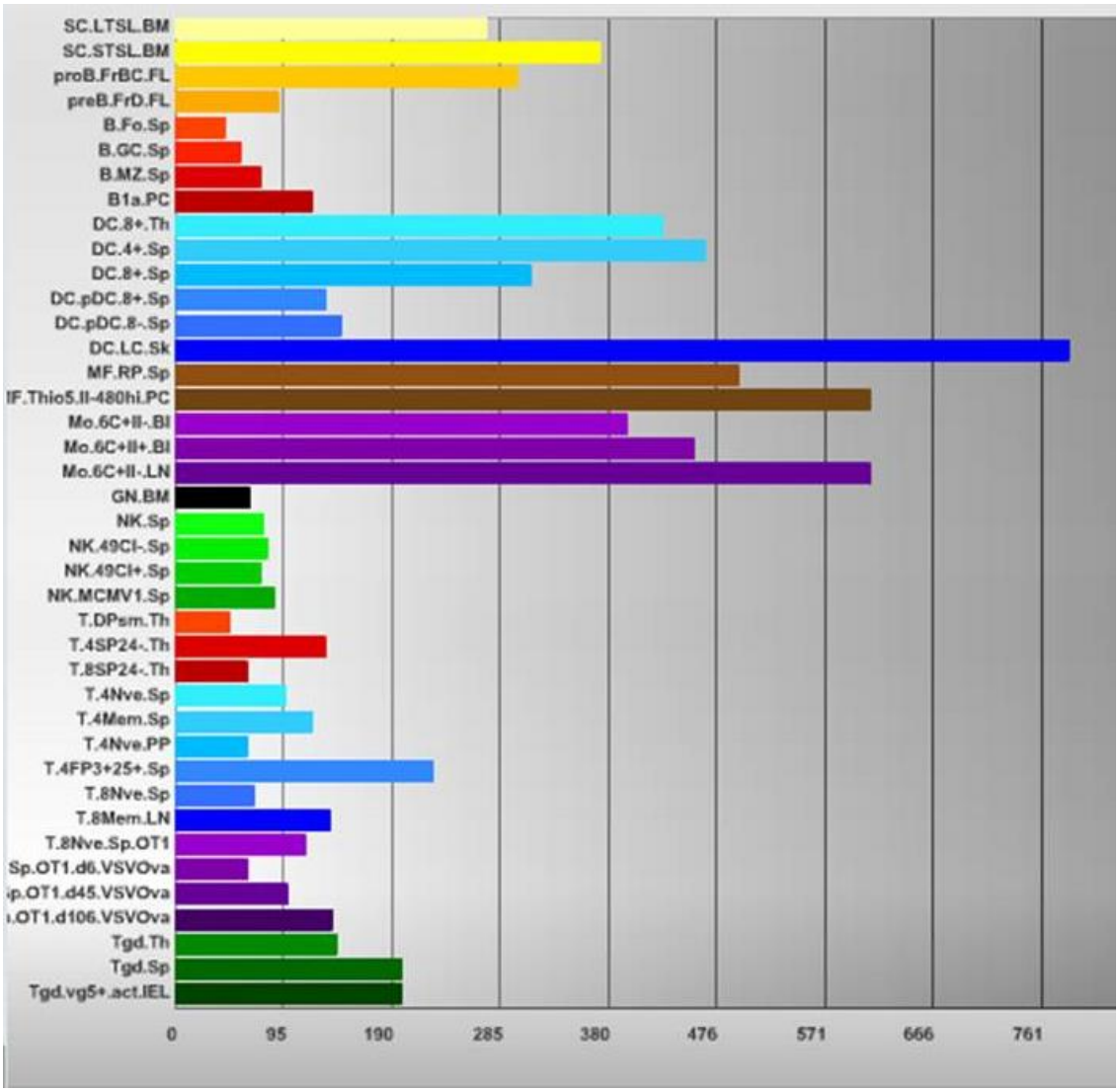

Figure 5.1A: Expression profiling of *Gsto1* in mouse immune cells (Immgen *www.immgen.org*). Cell population description: DC: dendritic cells, Mo: Monocytes, MF: macrophages, NK: Natural Killer cells, T: T-cells, B.: B-cells. Detailed description of subset nomenclature is provided in Appendix A7, Figure 1C.

The data represent relative fold differences in the expression levels (x-axis) of *Gsto1* in indicated cell types (Y-axis).

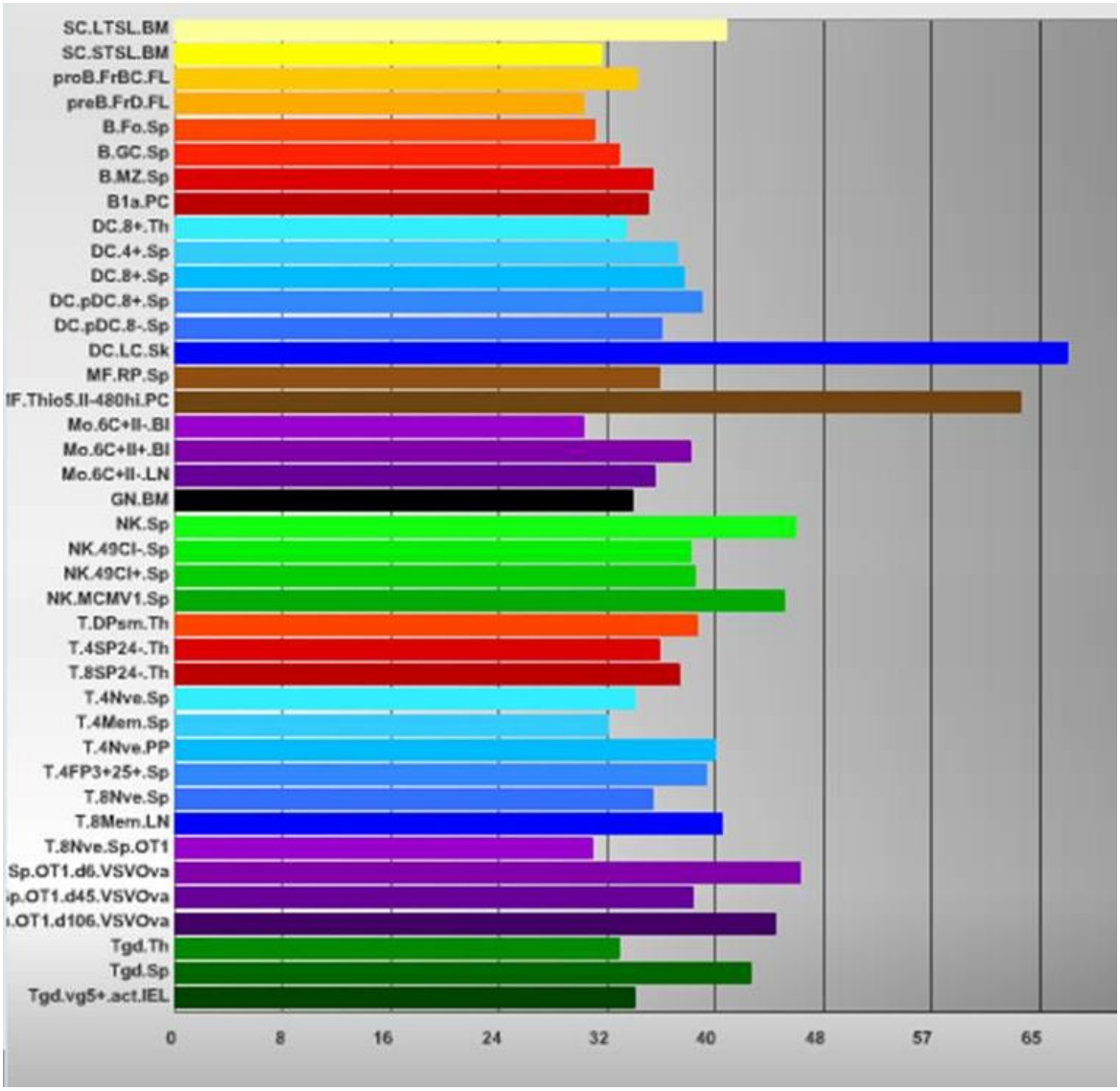

Figure 5.1B: Expression profiling of *Gsto2* in mouse immune cells (Immgen *www.immgen.org*). Cell population description: DC: dendritic cells, Mo: Monocytes, MF: macrophages, NK: Natural Killer cells, T: T-cells, B.: B-cells. Detailed description of subset nomenclature is provided in Appendix A7, Figure 1C.

The data represent relative fold differences in the expression levels of *Gsto1* in indicated cell types (y-axis).

5.3.2 Knockdown and pharmacological inhibition of GSTO1-1

The expression of GSTO1-1 was knocked down by lentiviral mediated shRNA and activity was blocked by chemical inhibitors in J774.1A macrophages. The *Gsto1* knockdown cell line generated by lentiviral shRNA transfection [345] showed >90% reduction in *Gsto1* transcript levels (Figure 5.2A) and no reduction in *Gsto2* (Figure 5.2B). GSTO1-1 protein as measured by western blot, (Figure 5.2C) or by GSTO1-1 activity measured with the specific substrate 4-nitrophenacylglutathione (Figure 5.2D) was also knocked down. The 4-NPG assay was also used to evaluate the efficacy of two pharmacological inhibitors of GSTO1-1, CRID3 [264] (Cytokine release inhibitory drug 3) and ML175 (N-[3-(N-(2-chloroacetyl)-4-nitroanilino)propyl]-2,2,2-trifluoroacetamide) [350]. CRID3 was found to have an IC_{50} of 99.5 μM (Figure 5.2E) that is notably higher than the IC_{50} of 22.8 nM obtained for ML175 (Figure 5.2F). To confirm the specificity of ML175, the effect of the compound was tested on the activity of purified GSTO2-2. As expected, increasing concentrations of ML175 had no effect on the dehydroascorbate reductase (DHAR) activity of GSTO2-2 (Figure 5.2G). ML175 is a well-characterized compound with high specificity for GSTO1-1. However the cytotoxicity of the compound in macrophages specifically was evaluated to determine the optimal range of concentrations for further experiments in cells. Treating J774.1A macrophages with concentrations up to 5 μM for 6 hours did not result in cytotoxicity. However, treating cells with increasing concentrations for ≥ 24 hours resulted in a concentration dependent decrease in cell viability (Figure 5.2H). Based on the cell viability data, concentrations of 0.25-5 μM for no more than 6 hours were used in subsequent experiments with ML175.

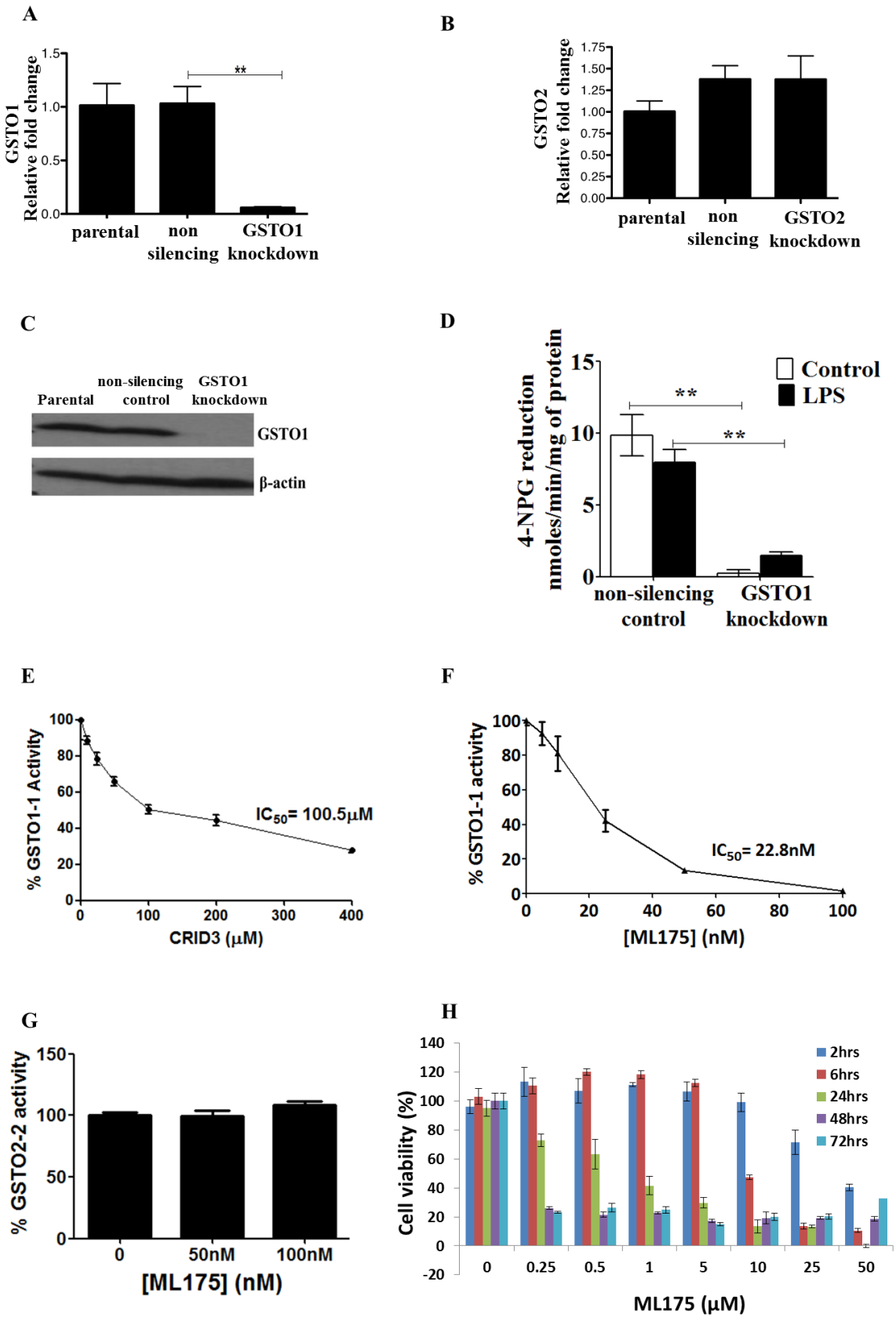
A
GSTO1 Relative fold change
1.5
1.0
0.5
0.0
**
parental
non silencing
GSTO1 knockdown
B
GSTO2 Relative fold change
1.75
1.50
1.25
1.00
0.75
0.50
0.25
0.00
parental
non silencing
GSTO2 knockdown
C
Parental
non-silencing control
GSTO1 knockdown
GSTO1
β-actin
D
4-NPG reduction nmoles/min/mg of protein
15
10
5
0
**
**
Control
LPS
non-silencing control
GSTO1 knockdown
E
% GSTO1-1 Activity
100
80
60
40
20
0
IC50= 100.5μM
0
100
200
300
400
CRID3 (μM)
F
% GSTO1-1 activity
100
80
60
40
20
0
IC50= 22.8nM
0
20
40
60
80
100
[ML175] (nM)
G
% GSTO2-2 activity
150
100
50
0
0
50nM
100nM
[ML175] (nM)
H
Cell viability (%)
140
120
100
80
60
40
20
0
-20
2hrs
6hrs
24hrs
48hrs
72hrs
0
0.25
0.5
1
5
10
25
50
ML175 (μM)

Figure 5.2: Knockdown of GSTO1-1 by gene silencing and chemical inhibitors. (A)* *Gsto1* mRNA levels knocked down by lentiviral transfection of shRNA targeting *Gsto1*. (B)* Specificity of the *Gsto1* shRNA was confirmed by measuring unchanged levels of *Gsto2* in transfected cells. (C)* Immunoblot showing the knockdown of *Gsto1* in J774.1A cells by lentiviral transfection of shRNA targeting *Gsto1* and a scrambled non-silencing control.(D) *Gsto1* knockdown was confirmed by measuring the reduction of 4-NPG, a substrate specific to GSTO1-1. The efficacy of inhibition of the activity of GSTO1-1 by CRID3 (E) and ML175 (F) were determined by measuring the reduction of 4-NPG. (G) The DHAR activity of purified GSTO2-2 remained unaffected by ML175, confirming the specificity of ML175 as a GSTO1-1 inhibitor. (H) Doses over 5 μM of ML175 were observed to cause cell death in macrophages in 6 hours. ML175 concentrations were restricted to 5 μM for 2-6 hours in all experiments.
** Figures 5.2 A, B and C were provided by Dr. Rebecca Coll, Luke O'Neill lab, Trinity College Dublin.*

5.3.3 The role of GSTO1-1 in TLR signalling in macrophages

The requirement of GSTO1-1 in TLR signalling in macrophages was investigated by screening the activation of multiple murine TLRs with their respective ligands in J774.1A macrophages deficient in GSTO1-1 (lentiviral shRNA knockdown of GSTO1-1) and non-silencing control cells (lentiviral scrambled shRNA). All TLRs screened were activated with their respective ligands and the amount of secreted, IL-6 cytokine was measured. TLR1/2, TLR3, TLR7 and TLR9 were functional in the *Gsto1* knockdown cells, secreting IL-6 to the same extent as the non-silencing control cells (Figure 5.3A-B,D-E). However pro-inflammatory signalling through TLR4 on LPS stimulation was found to be severely compromised in the GSTO1-1 deficient cells (Figure 5.3C). The effect of GSTO1-1 on TLR4 signalling was thus further investigated to determine whether GSTO1-1 modulated the redox state of protein(s) involved in the TLR4 cascade.

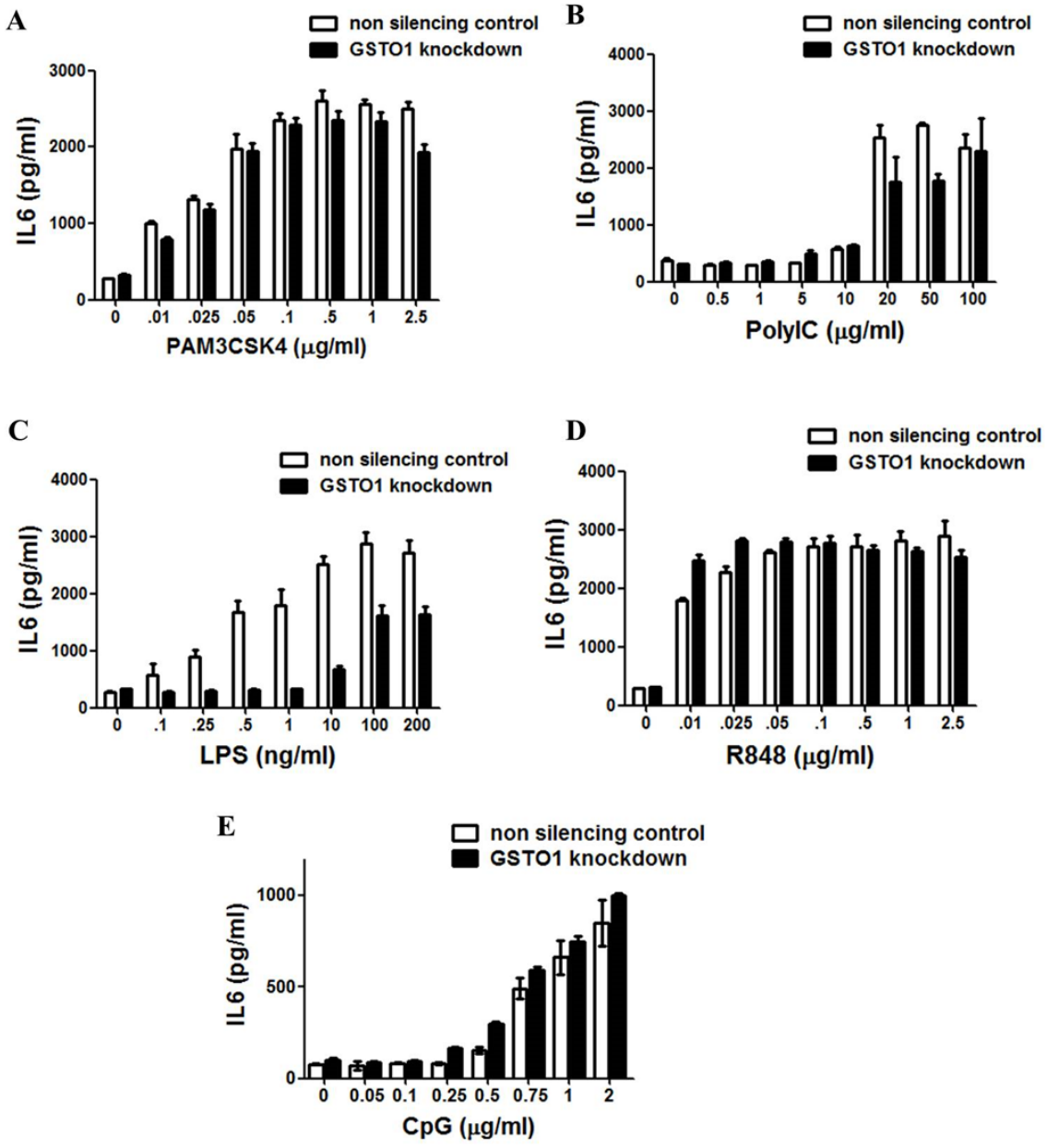

Figure 5.3: Effect of GSTO1-1 deficiency on TLR activation in macrophages. TLR1/2, TLR3, TLR4, LR7 and TLR9 were activated with varying concentrations of their respective ligands in non-silencing control and *Gsto1* knockdown cells. IL-6 secretion on TLR1/2 (A), TLR3 (B), TLR7 (D) and TLR9 (E) activation was similar in both cell types and did not appear to be dependent on the expression of GSTO1-1. (C) GSTO1-1 knockdown cells failed to secrete IL-6 in response to LPS. Higher concentrations (100-200ng/ml) of LPS induced the secretion of IL-6 in the GSTO1-1 deficient cells but to a significantly lower extent as compared to the non silencing control cells.

To determine whether the block in TLR4 signalling was dependent on the catalytic activity of GSTO1-1, wildtype J774.1A macrophages were treated with GSTO1-1 inhibitor ML175 (Figure5.3). ML175 treated cells showed a dose dependent decrease in the secretion of IL-6 on LPS stimulation (Figure 5.4A). Pre-treatment of cells with ML175 did not alter cytokine secretion through the activation of TLR1/2 and TLR7 by PAM3CSK4 (Figure 5.4B) and R848 respectively (Figure 5.4C).

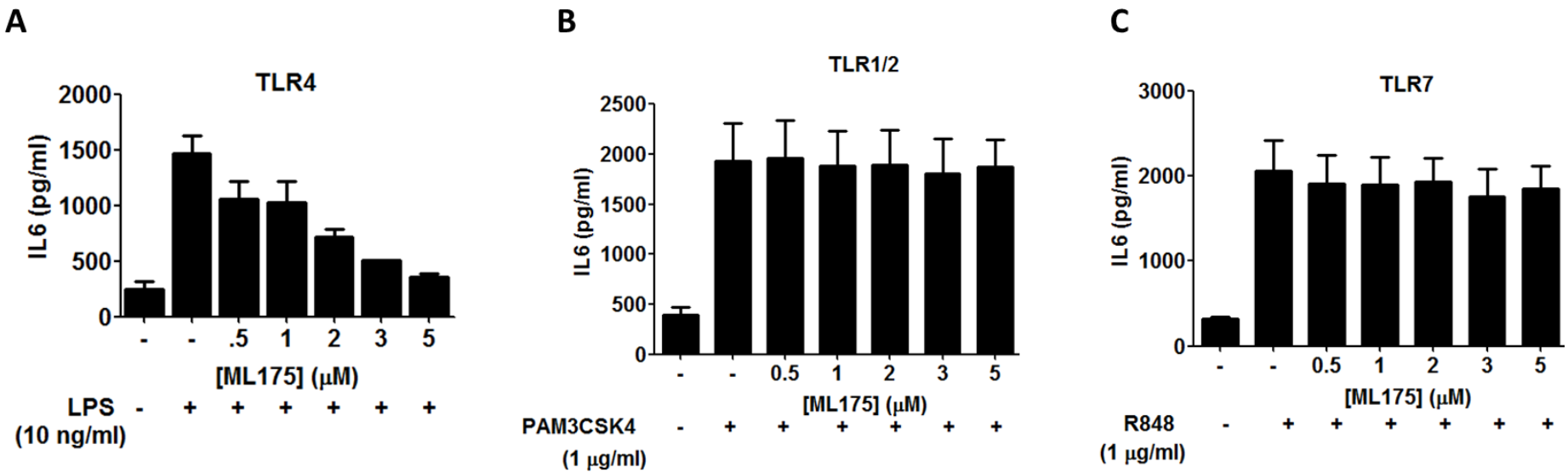

Figure 5.4: Effect of ML175 on TLRs: the specificity of ML175 was tested by screening the activation of TLR1/2, TLR4 and TLR7. (A) TLR4 mediated IL-6 secretion on LPS activation was significantly inhibited by increasing concentrations of ML175. IL-6 secretion activated through TLR1/2 (B) and TLR7 (C) remained unaffected in the presence of ML175. Hence, the inhibitory effect of ML175 is specific to TLR4 activated macrophages. Cells were treated with increasing concentrations of ML175 two hours prior to stimulation with indicated TLR ligands (doses as described in Section 5.2.2).

5.3.4 GSTO1-1 is required for TLR4 mediated pro-inflammatory responses

a. Interleukin 1β

The transcription of pro-inflammatory cytokine IL-1β is activated on LPS stimulation via the TLR4/NF-κB pathway. TLR4 activation with LPS induced the expression of pro-IL-1β, the uncleaved parental form of IL-1β (Figure 5.5A). The GSTO1-1 deficient macrophages failed to elicit this response, suggesting the unresponsiveness of the cells to LPS. To demonstrate that the effect of GSTO1-1 is mediated via its active site cysteine residue, J774.1A wildtype cells were pre-treated with catalytic inhibitor ML175. The cells mimicked the cytokine profile of *Gsto1* knockdown cells and failed to induce the expression of pro-IL-1β (Figure 5.5B). Since the parental form of IL-1β is inhibited, this rules out the possibility that the NLRP3 inflammasome, which is responsible for the cleavage of pro-IL-1β to mature IL-1β, is the prime target of GSTO1-1.

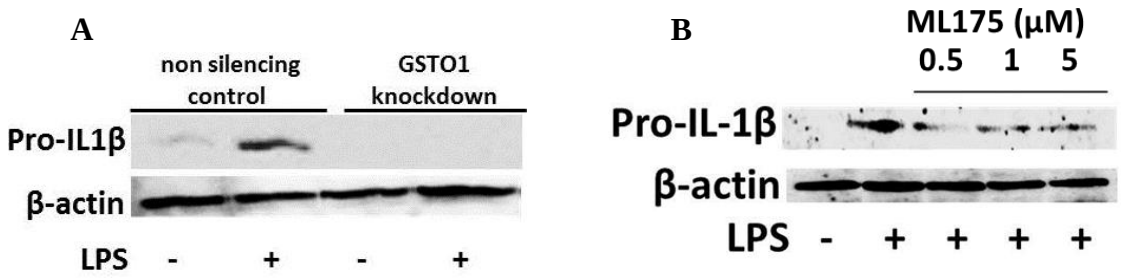

Figure 5.5: Unresponsiveness of GSTO1-1 deficient cells on LPS/TLR4 activation (A) Expression of pro-IL-1β was induced in non-silencing control J774.1A macrophages but not in cells deficient in GSTO1-1 when TLR4 signalling was activated with LPS. (B) Pre-treating wildtype J774.1A macrophages inhibited TLR4 dependent pro-IL-1β expression in a dose dependent manner, suggesting that catalytically active GSTO1-1 is indispensable for the expression of parental IL-1β.

b. Interleukin 10

Along with inducing the expression of pro-inflammatory cytokines, LPS induces multiple negative feedback pathways, one of which is the activation of IL-10. IL-10 limits the expression of pro-inflammatory cytokines such as IL-1β and TNFα [351]. The expression of IL-10 was induced in non-silencing control cells but was largely absent in *Gsto1* knockdown cells (Figure 5.6). The two cytokine profiles taken together suggest

that LPS failed to elicit TLR4 signalling in cells deficient of GSTO1-1 and the effect of GSTO1-1 is mainly on the signalling required for NF-κB nuclear translocation which is a pre requisite for the expression of cytokines.

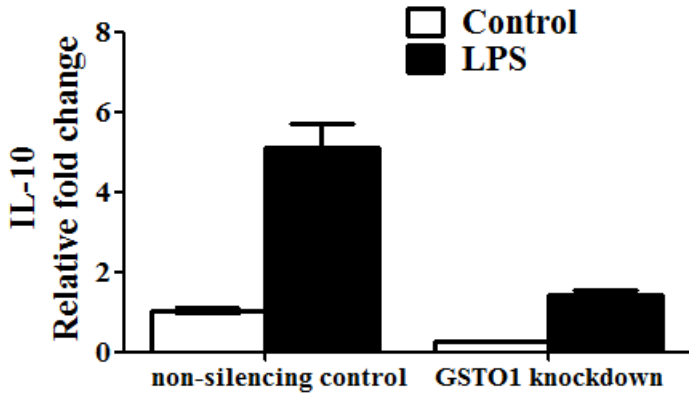

Figure 5.6: The expression of 1L-10 was induced in non-silencing control cells but not in *Gsto1* knockdown cells.

c. Inducible Nitric oxide synthase (iNOS) and Cyclooxygenase 2 (COX2)

Changes in the transcript levels of inflammatory markers that are influenced by oxidative stress were measured in GSTO1-1 deficient macrophages. Increase in ROS levels and/or a decrease in antioxidants such as glutathione have both previously been demonstrated to induce the expression of cyclooxygenase-2 and nitric oxide synthase-2 in LPS treated macrophages. As expected, LPS treated macrophages deficient in GSTO1-1 showed a much reduced induction of COX2 (Figure 5.7A) and iNOS (Figure 5.7B), possibly due to the lack of stimuli in the form of increased ROS/GSH ratio. When LPS activated macrophages were pre-treated with ML175, a potent inhibitor of GSTO1-1, the induction of COX2 and iNOS were significantly abolished (Figure 5.7C-D).

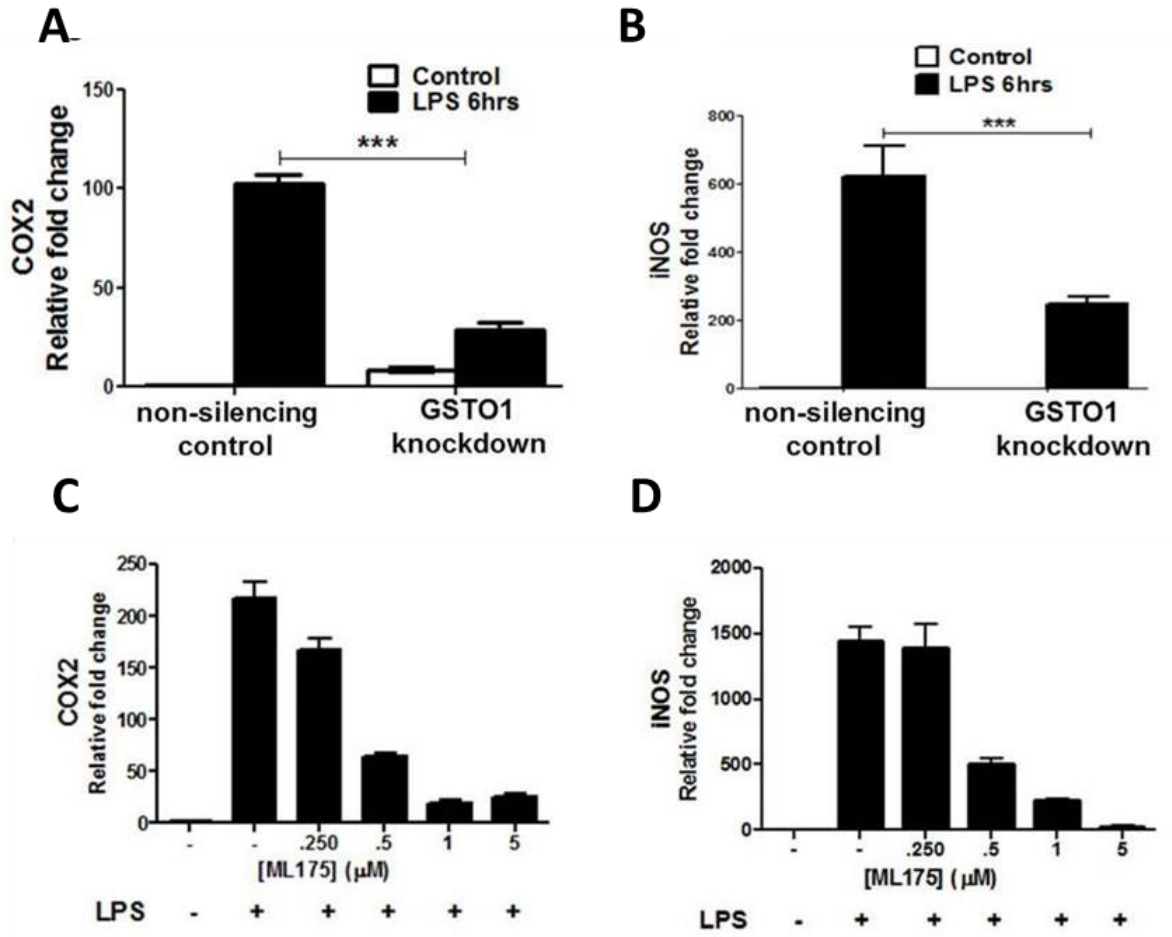

Figure 5.7: Induction of transcript levels of pro-inflammatory markers on LPS stimulation is dependent on GSTO1-1

LPS treated macrophages deficient in GSTO1-1 showed a significantly lower induction of transcript levels of pro-inflammatory markers such as COX2 (A) and iNOS (B). (C-D) The induction of both COX2 and iNOS was abolished in LPS activated macrophages pre-treated with ML175, mimicking *Gsto1* knockdown cells and suggesting the catalytic involvement of GSTO1-1 in LPS signalling.

5.3.5 GSTO1-1 mediates LPS induced ROS generation

To determine the effect of GSTO1-1 on the levels of ROS when the TLR4 signalling pathway is activated, J774.1A *Gsto1* knockdown cells and non-silencing control cells were treated with LPS. As shown in Figure 5.8A there was a significant increase in ROS in a time dependent manner in the non-silencing control cells that was largely absent in the GSTO1-1 knock down cells. In order to determine whether the effect of GSTO1-1 was specific to TLR4 activation, the cells were treated with Poly I:(C) that activates the TLR3 inflammatory cascade. The increase in ROS on TLR3 activation was found to be the same in both non-silencing control and *Gsto1* knockdown cells (Figure 5.8B).

To evaluate the effect of GSTO1-1 inhibitor ML175 on cellular ROS, cells were treated with increasing concentration of ML175 followed by LPS. ML175 significantly blocked the increase in ROS in non-silencing control cells on LPS treatment (Figure 5.8C), mimicking the effect of genetic knockdown of GSTO1-1 in macrophages. However, ML175 did not influence the generation of ROS on TLR3 activation when cells were treated with PolyI(C) (Figure 5.8D).

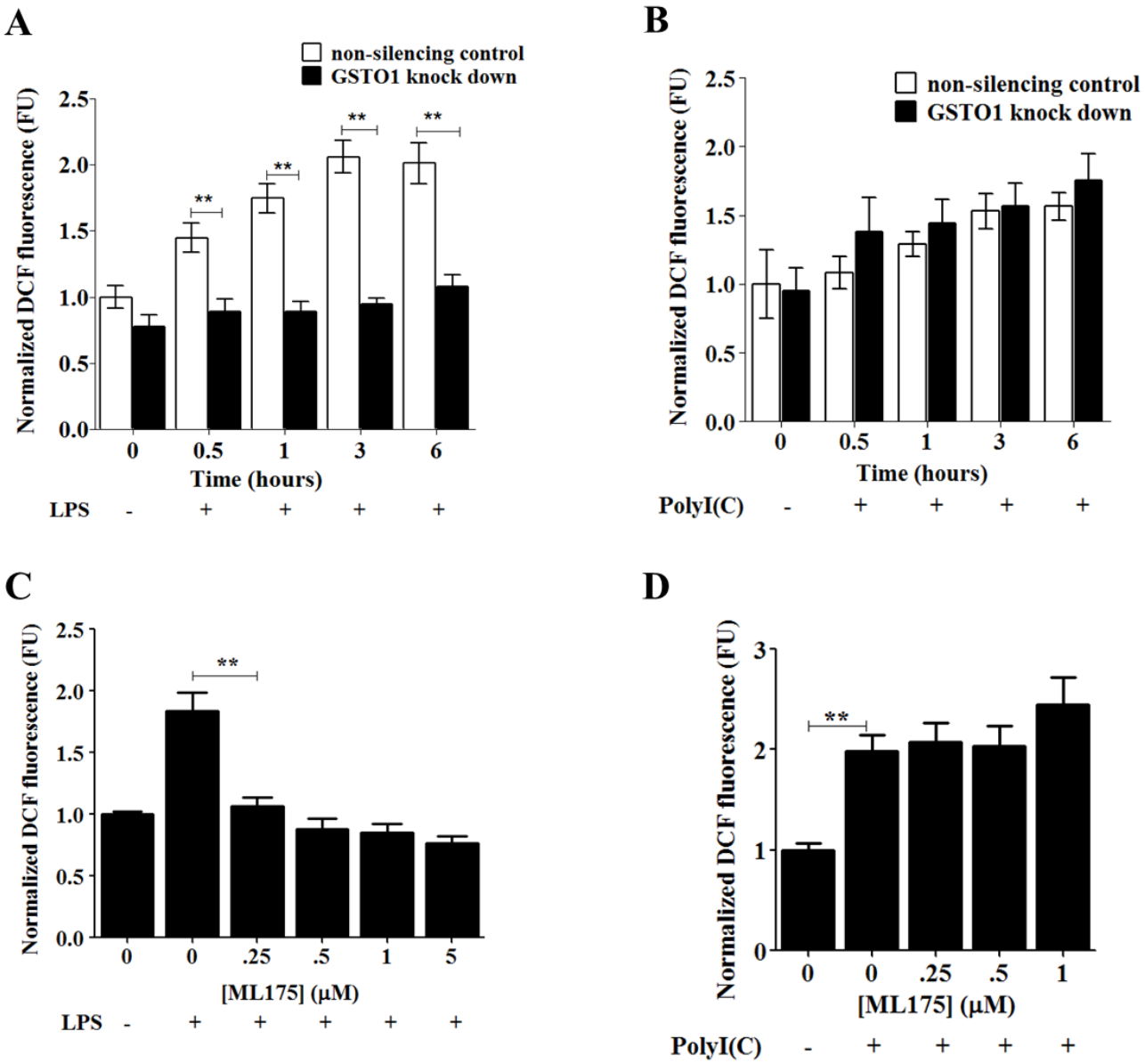

Figure 5.8: GSTO1-1 mediates LPS induced ROS.
A, Knocking down GSTO1-1 attenuates LPS induced TLR4 mediated ROS generation. B, GSTO1-1 dependent ROS generation is TLR4 specific and does not alter poly:I(C) induced TLR3 specific ROS. C, Inhibition of the catalytic activity of GSTO1-1 by ML175 attenuated LPS induced ROS production in a dose dependent manner. Cells were pre-treated with increasing concentrations of ML175 for one hour followed by LPS (100ng/ml) for 6 hours. D, Inhibition of the catalytic activity of GSTO1-1 by ML175 did not attenuate polyI:C induced ROS generation. Cells were pre-treated with increasing concentrations of ML175 for one hour followed by 10 μg/ml polyI:C for 6 hours.

5.3.6 GSTO1-1 mediates the induction of NADPH oxidase 1 (NOX1) after LPS stimulation

Cytosolic ROS is predominantly generated by the family of NADPH oxidases with tissue specificity [147]. NOX1 and NOX2 are primarily expressed in macrophages. Since NOX2 is constitutively transcribed, the expression of NOX1 in LPS activated cells was determined [149]. The expression of NOX1 at both the transcription and protein level was significantly induced in LPS treated non-silencing control cells but largely attenuated in GSTO1-1 deficient cells (Figure 5.9A-B). Similar results were obtained with the inhibitors CRID3 and ML175 (Figure 5.9C and 5.9D). As expected, the effect of CRID3 on NOX1 was less pronounced than that of ML175 due to the relatively poor efficacy of CRID3 as GSTO1-1 inhibitor; hence ML175 was used in subsequent studies to investigate the role of GSTO1-1 in TLR4 signalling.

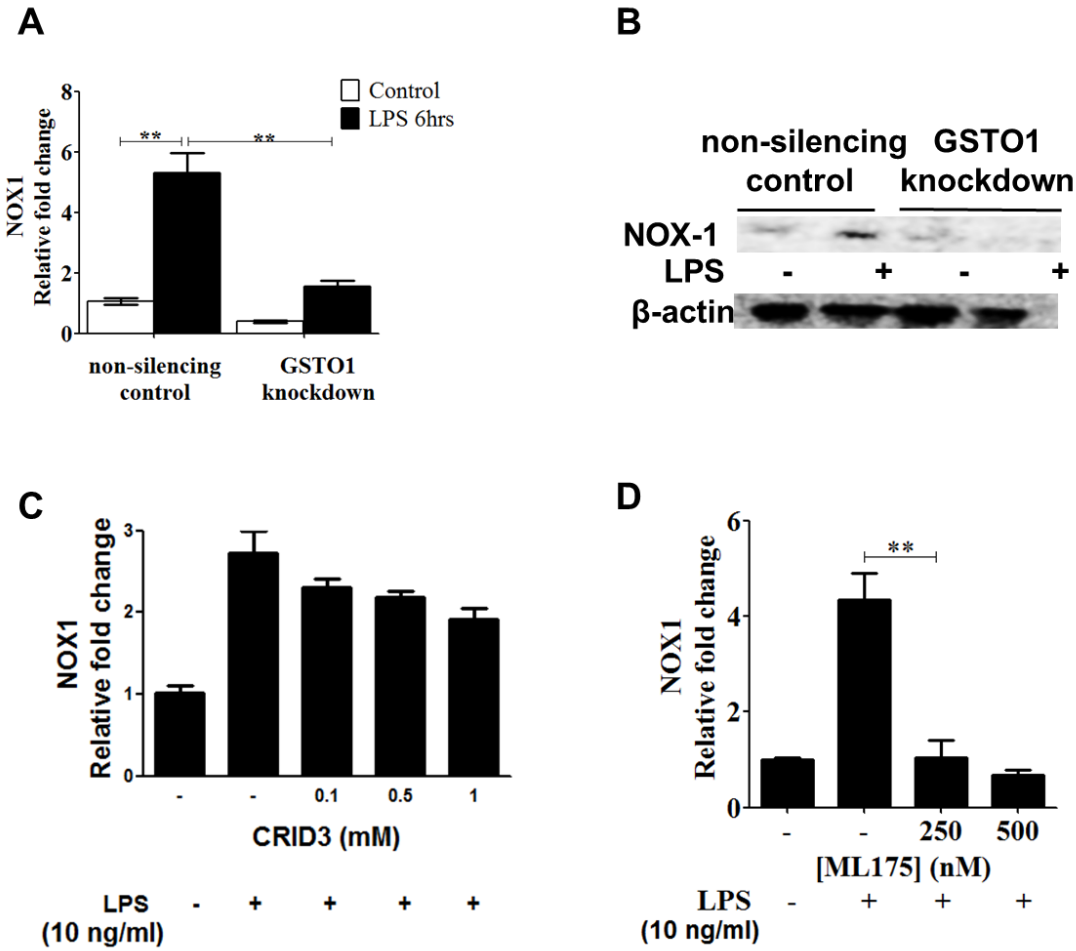

Figure 5.9: GSTO1-1 mediates ROS production via the activation of NADPH oxidase

(A) Activation of NOX1 transcription by LPS is dependent on GSTO1-1 expression in J774.1A macrophages. (B) Induction of NOX1 protein expression was attenuated in *Gsto1* knockdown cells, resulting in attenuated ROS generation. (C) CRID3 decreased the LPS dependent induction of NOX1 transcripts to a moderate extent (at higher concentrations due to its poor efficacy) in wildtype J774.1A cells. (D) Inhibition of GSTO1-1 in J774.1A wild type cells by ML175 decreased the LPS induced activation of NOX1 transcript expression to control levels.

5.3.7 Glutathione homeostasis on LPS activation

As a consequence to increased oxidative stress resulting from the increased cytosolic ROS, a significant shift in the GSH/GSSG ratio was measured in LPS stimulated J774.1A non silencing control cells (Figure 5.10). Interestingly, the GSH/GSSG ratio remained unaltered in *Gsto1* knockdown cells, confirming undisturbed redox homeostasis in these cells under the same condition.

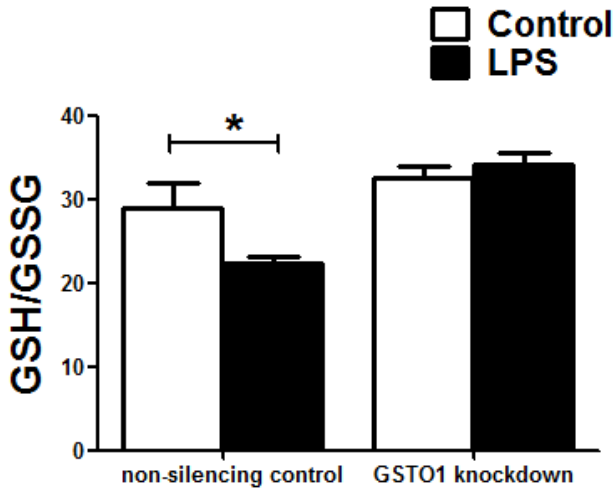

Figure 5.10: Glutathione levels in macrophages
A significant drop in the GSH/GSSG ratio was measured in the non-silencing control cells in response to LPS induced ROS while the ratio remained unchanged in *Gsto1*

5.3.8 The effect of GSTO1-1 knockdown on protein glutathionylation

The deglutathionylation activity of GSTO1-1 has been extensively investigated in the previous chapter and in published data [90]. To further evaluate the redox state of proteins in *Gsto1* deficient cells, the total glutathionylation level under basal conditions was determined. The total protein glutathionylation level in *Gsto1* knockdown macrophages was significantly increased (Figure 5.11A). Treatment of J774.1A non-silencing control cells with LPS caused a significant increase in glutathionylation, presumably as a result of the generation of ROS as the same increase did not occur in *Gsto1*-knock down cells that do not produce ROS. To confirm that the catalytic active site of GSTO1-1 is required to mediate these effects, both non-silencing control and *Gsto1* knockdown cells were treated with ML175 before eliciting pro-inflammatory responses with LPS. As shown in Figure 5.11B, ML175 pre-treatment reversed the up-regulation of total protein glutathionylation on LPS stimulation in the non-silencing control cells in a dose dependent manner. However, ML175 did not have any effect on the *Gsto1* knockdown cells. Interestingly, an increase in the glutathionylation levels in

Gsto1 knockdown cells at 0.5μM of ML175 was observed which could be due to increased cytotoxicity at higher doses.

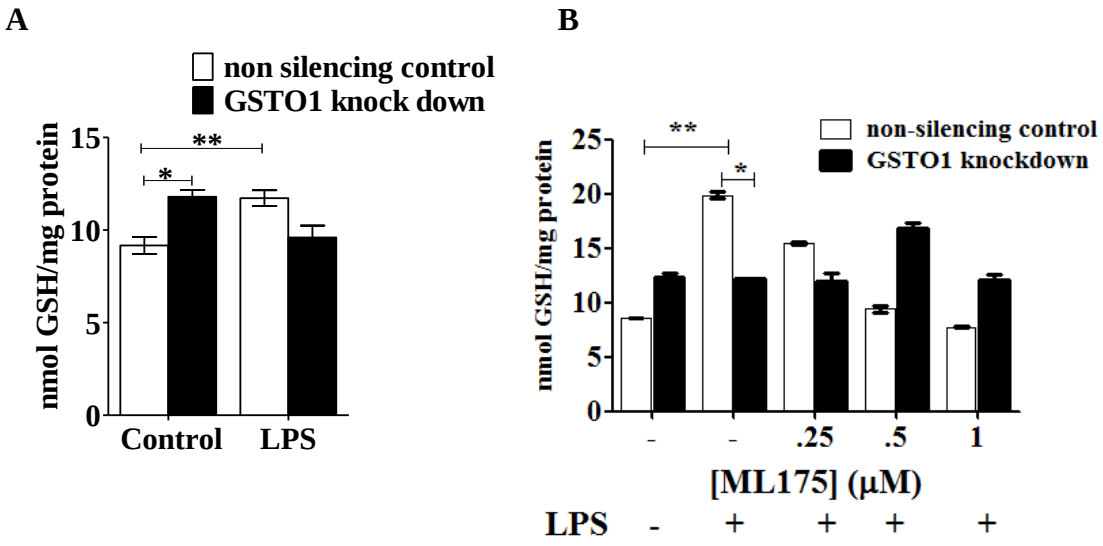

Figure 5.11: Global protein glutathionylation in J774.1A macrophages
(A) Protein glutathionylation was increased in GSTO1-1 knockdown cells compared to non-silencing control cells. When non-silencing control cells were treated with LPS, high ROS levels result in increased protein glutathionylation levels in but low levels of glutathionylation occur in GSTO1-1 knockdown cells that do not generate high ROS levels. (B) Treating non silencing control macrophages with ML175 abrogated LPS induced glutathionylation. ML175 treatment did not alter the glutathionylation levels in GSTO1-1 deficient cells.

5.3.9 Anti-oxidant response to LPS stimulation

The production of ROS in cells would normally be expected to perturb the redox balance and potentially induce increased expression of enzymes that generally protect against oxidative stress. However it has been previously demonstrated that in order to maintain an initial phase of increased ROS, LPS suppresses the antioxidant levels while simultaneously inducing ROS generating enzymes such as NOX1 and NOX4 [147, 149, 346]. Therefore, the effect of LPS stimulation on the transcription and/or activity of catalase, glutathione peroxidase 3 (GPx3), glutamate cysteine ligase catalytic subunit (GCLc), glutamate cysteine ligase modulating subunit (GCLm) and glutathione reductase was evaluated. LPS stimulation of non-silencing control cells caused a significant decrease in the mRNA level of catalase, GPx3, GCLc, Heme oxygenase-1 (HO-1) and NADPH quinone oxidoreductase-1 (NQO1) (Figure 5.12A-C,E-F). In contrast the level of GCLm mRNA was unchanged by LPS stimulation (Figure 5.12D). Notably, knock down of GSTO1-1 by shRNA expression abolished the suppression of

catalase, GPx3, GCLc, HO-1 and NQO1 induced by LPS. The knockdown of GSTO1-1 caused a significant induction of GCLm that was unaffected by LPS stimulation. The activities of catalase, glutathione peroxidase and glutathione reductase were also determined (Figure 5.13A-C). In J774.1A non-silencing control cells the activities of catalase and glutathione reductase were diminished by LPS treatment and this reduction in activity was abrogated in GSTO1-1 knock down cells (Figure 5.13A-B). In contrast, glutathione peroxidase activity was not reduced by LPS treatment (Figure 5.13C). This may be due to the fact that glutathione peroxidase activity is catalysed by multiple isozymes including some glutathione transferases and their genes may not be subject to the same transcriptional regulation as GPx3. Alternatively, GPx3 may turnover slowly and a decrease in transcription may not be reflected in the protein level within six hours in this experiment.

In order to confirm that the redox events unfolding in the absence of GSTO1-1 were due to its catalytic activity, a previously published inhibitor ML175 was tested on wildtype J774.1A macrophages. Similar results were obtained when GSTO1-1 was inhibited by the treatment of non-silencing J774.1A control cells with the GSTO1-1 inhibitor ML175 (Figure 5.14 A-E). The activation of ROS production and suppression of antioxidants on LPS stimulus was blocked significantly by ML175 in a dose dependent manner, mimicking the phenotype of GSTO1-1 knockdown cells.

The results strongly suggest that ML175 is a potent inhibitor of GSTO1-1 both *in vitro* (IC50 in the nanomolar range) and in cells and that the inhibitory effect is mediated via the inhibition of the enzyme activity of GSTO1-1 (as shown in Figure 5.2F)

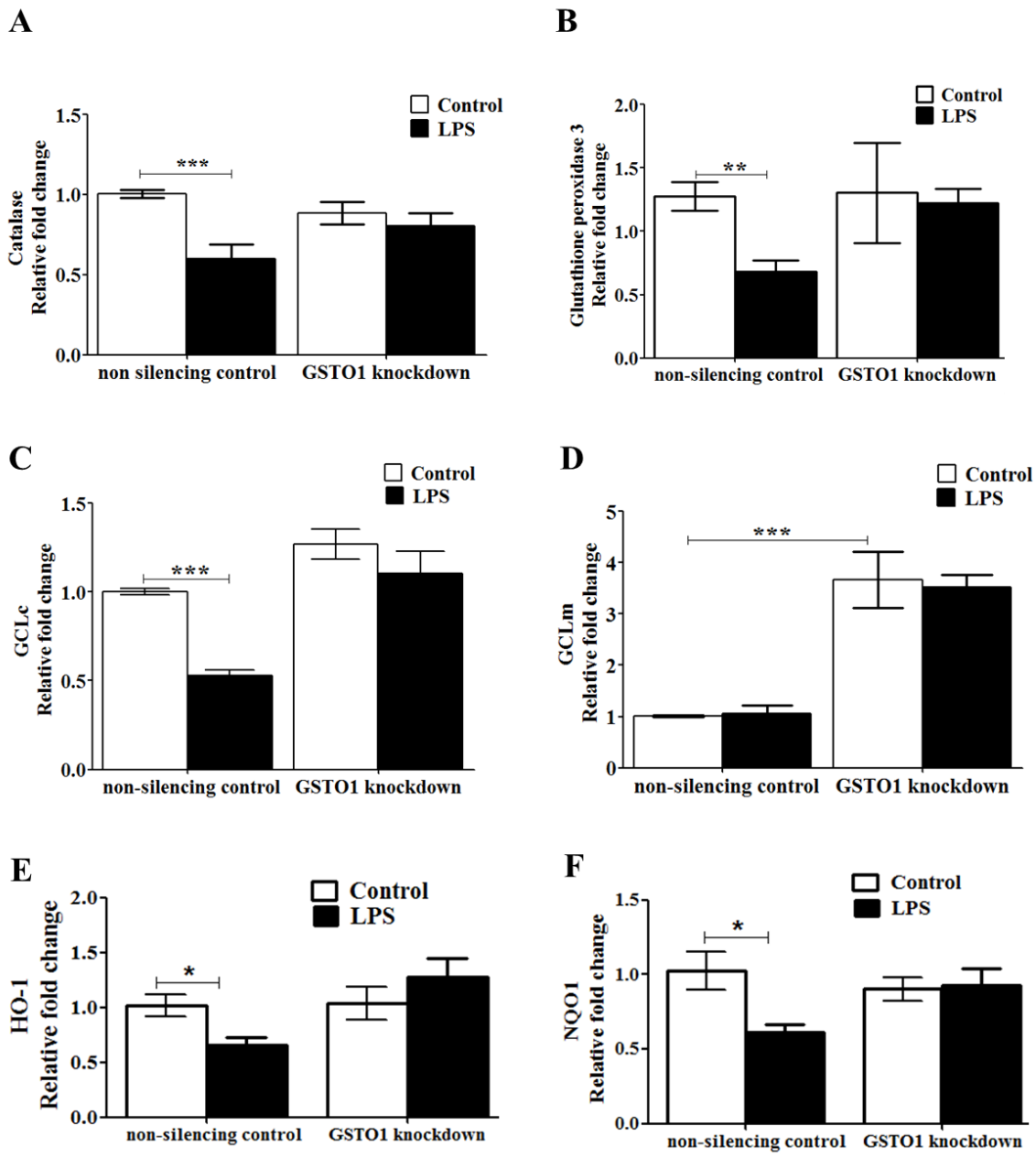

Figure 5.12: LPS modulates the oxidant/antioxidant axis by suppressing antioxidant activity to promote a pro-inflammatory oxidative burst in macrophages Suppression of Catalase (A); Gpx3 (B); GCLc (C); GCLm (D); HO-1 (E) and NQO1 (F) was abrogated significantly in *Gsto*1 knockdown cells.

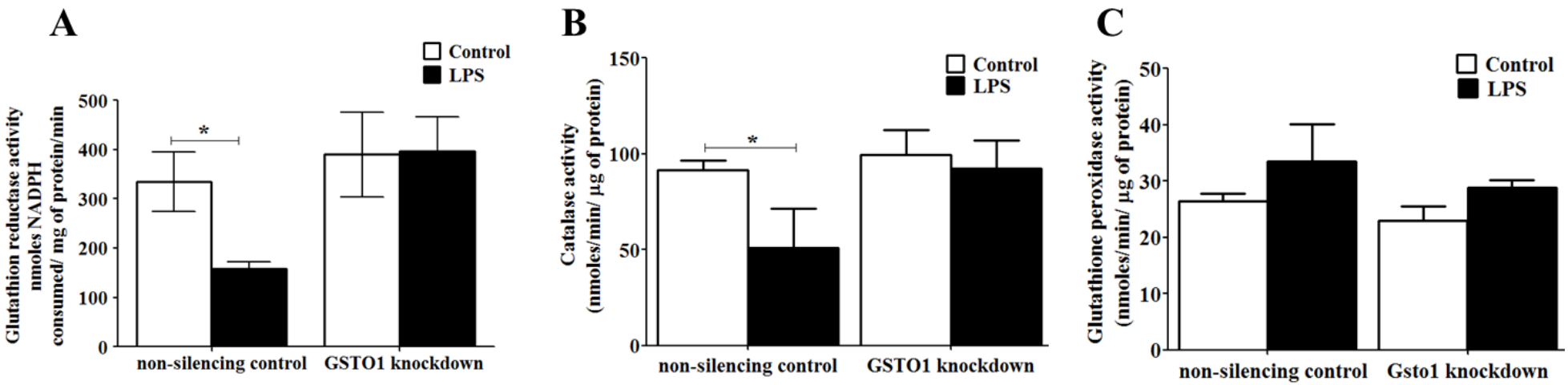

Figure 5.13: Suppression of antioxidants by LPS is abolished in GSTO1-1 deficient J774.1A macrophages
The catalytic activities of catalase (A) and glutathione reductase (B) also showed a decrease in response to LPS in the non-silencing control cells but not in the GSTO1-1 deficient macrophages. (C) Gpx activity did not significantly change in both non-silencing and *Gsto1* knockdown macrophages.

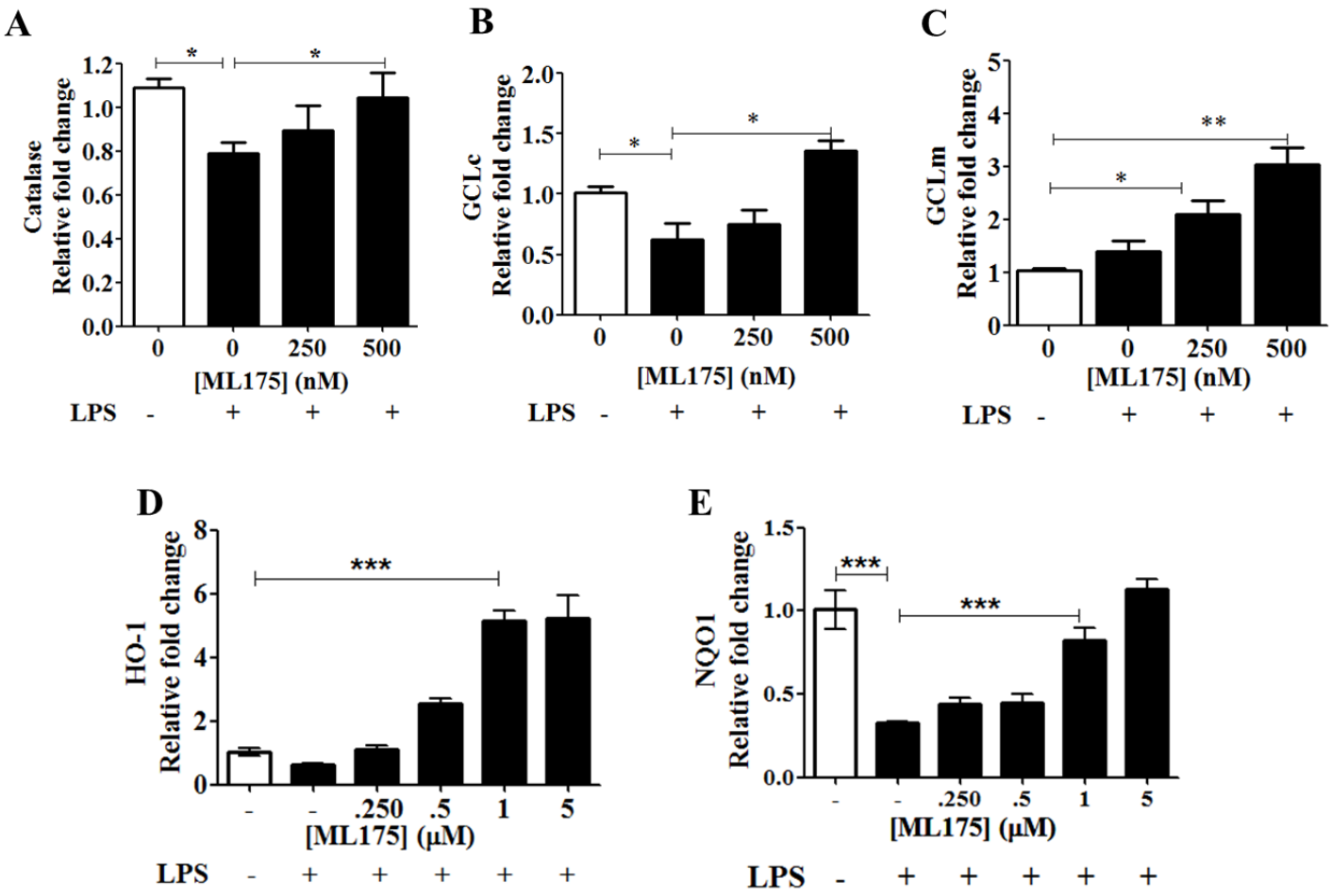

Figure 5.14: The LPS mediated suppression of anti-oxidant enzymes was blocked by inhibition of the catalytic activity of GSTO1-1 with ML175. Transcript levels of Catalase (A); GCLc (B); GCLm (C); HO-1 (D) and NQO1 (E) were measured in ML175 treated J774.1A macrophages.

To investigate the inability of *Gsto1* knockdown cells to suppress the immediate antioxidant responses on TLR4 activation, the role of PPARγ, a key regulator of the Keap1/Nrf2 pathway was determined [352]. Phase 2 genes such as HO-1, NQO1, GCLc and GCLm have anti-oxidant response elements (ARE) and are induced in response to oxidative stress through the Keap1/Nrf2 pathway [352, 353]. As shown in Figure 5.15A, the non-silencing control cells have low levels of expression of PPARγ and this is not significantly altered by LPS treatment. In contrast, *Gsto1* knockdown cells express high levels of PPARγ which would support the induction of genes such as GCLc and GCLm. The expression levels of PPARγ coactivator PGC1β also followed a similar trend in the *Gsto1* knockdown cells. PGC1β levels were suppressed in LPS treated non silencing macrophages as previously reported [354]. However GSTO1-1 deficient macrophages expressed significantly higher levels of the co-factor even in the absence of LPS indicating that the expression of GSTO1-1 mediates PPARγ expression and associated downstream effects albeit the exact mechanism is not known (Figure 5.15B). PGC1β expression was considerably attenuated in response to LPS treatment in *Gsto1* knockdown cells but was not completely abolished. The induction of PPARγ on treatment with GSTO1-1 inhibitor ML175 even in the presence of LPS confirmed the requirement of active GSTO1-1 in the maintenance of PPARγ in a suppressed state in the non-silencing control cells (Figure 5.15C).

Figure 5.15: PPARγ is involved in the inhibition of pro-inflammatory redox responses in LPS stimulated GSTO1-1 deficient macrophages.
(A) PPARγ is induced in J774.1A *Gsto1* knockdown macrophages. (B) PPARγ coactivator PGC1β is induced in *Gsto1* knockdown cells. (C) Pre-treating cells with increasing concentrations of GSTO1-1 inhibitor ML175 induces PPARγ expression in J774.1A macrophages in a dose dependent manner.

5.3.10 GSTO1-1 is required for p65 nuclear translocation

NF-κB is a transcription factor that induces the expression of genes involved in inflammation [164, 355]. A large proportion of cytosolic NF-κB exists as a heterodimer of p65/p50 proteins associated with inhibitory IκB proteins [356]. Activation of pro-inflammatory cascades in macrophages with LPS involves IκκB proteins that phosphorylate IκB and target it for ubiquitinylation and subsequent proteosomal degradation [357-360]. The free p65/p50 heterodimer then translocates into the nucleus and activates the transcription of pro-inflammatory genes [164, 167]. Our data suggest that GSTO1-1 is required for this process. The images in Figure 5.16A-B show the normal increased nuclear localization of p65 in J774.1A non-silencing control cells after LPS treatment. In contrast p65 does not accumulate significantly in the nucleus of GSTO1-1 deficient cells treated with LPS (Figure 5.16C-D). The mean fluorescence intensity was quantified as described in the methods section and confirmed the significant increase in nuclear translocation of p65 in the non-silencing control and not in the GSTO1-1 deficient cells (Fig 5.16E). The failure of p65 to enter the nucleus in GSTO1-1 deficient cells indicates that these cells are unresponsive to LPS and would not induce NF-κB dependent inflammatory genes including NOX1 and other cytokines.

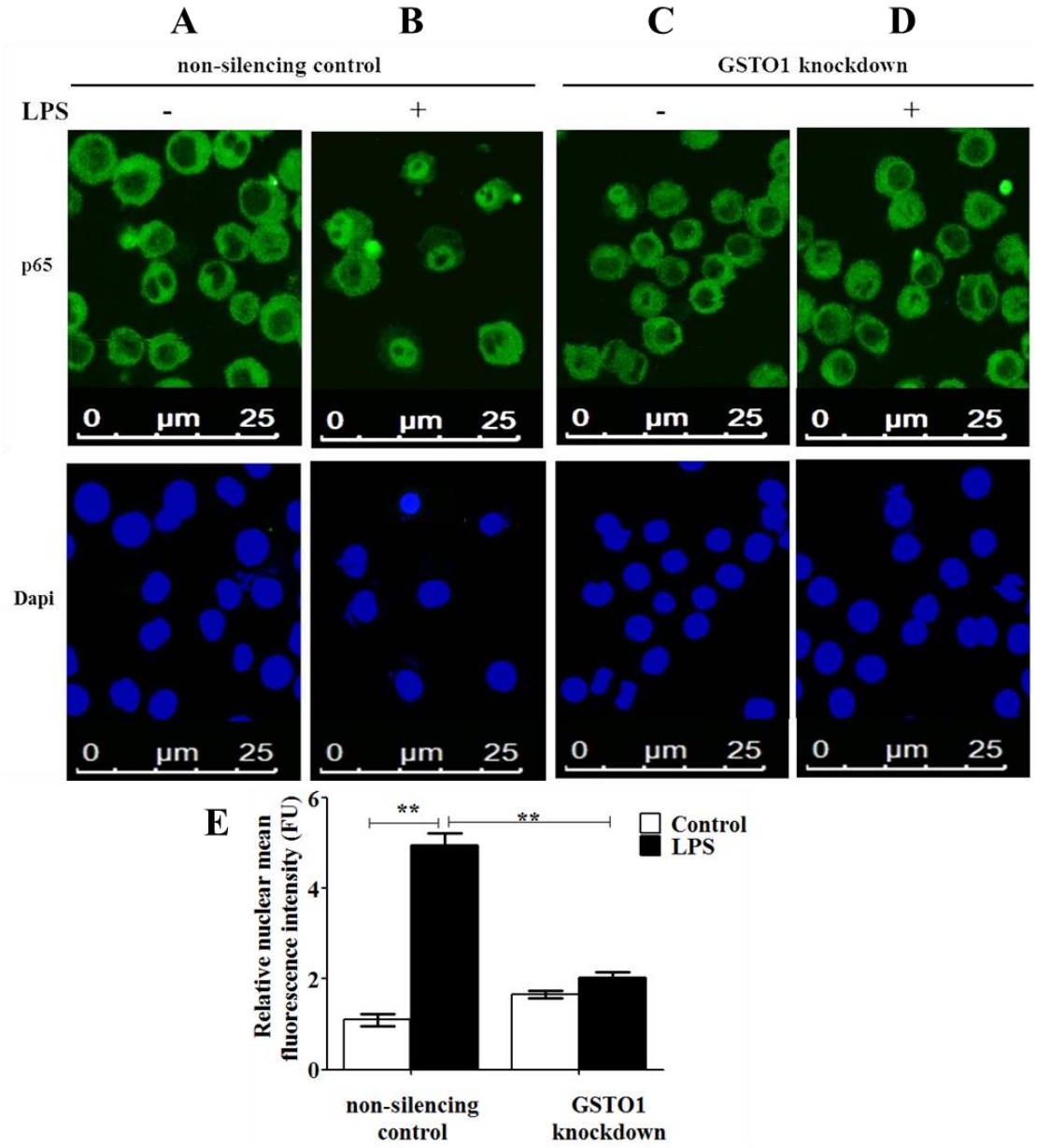

Figure 5.16: Nuclear translocation of p65 on TLR4 activation with LPS is dependent on the expression of GSTO1-1
(A) The p65 and p50 subunits of NF-κB heterodimerize and remain associated with IκB in the cytosol. (B) On LPS stimulation via TLR4, IκB dissociates from the p65/p50 heterodimer allowing the complex to translocate into the nucleus and activate transcription of genes. (C-D) Translocation of p65 into the nucleus on LPS stimulation is attenuated in the absence of GSTO1-1. (E) Fluorescence intensity was quantified using Leica LAS AF software. *Nuclear staining by Dapi is shown in blue; FITC-p65 is shown in green.*

5.3.11 Interleukin-1 Receptor-Associated Kinase 4 (IRAK4) phosphorylation/activation is blocked in GSTO1-1 deficient macrophages

IRAK4 is recruited immediately downstream of the TLR4-myddosome complex after LPS stimulation in macrophages. IRAK4 is auto-phosphorylated on TLR4 activation resulting in the subsequent phosphorylation and heterodimerization of IRAK1/2 (refer Figure 1.9). LPS treatment of the non-silencing control cells resulted in the phosphorylation of IRAK4 in 30 minutes however IRAK4 remained de-phosphorylated in LPS treated *Gsto1* knockdown macrophages (Figure 5.17). Thus the failure to elicit this response in *Gsto1* knockdown cells suggests that the effect of GSTO1-1 is further upstream of IRAK4, narrowing down potential targets of GSTO1-1 dependent modulation to the Myddosome complex and TLR4 itself. This result is inconclusive and slightly complicated to interpret due to the unexpected presence of phosphorylated IRAK4 in the unstimulated non silencing macrophages (though not to the extent of LPS activated macrophages). This may be a technical issue with the generic anti-phospho thr/ser antibody used which may be targeting LPS-independent phosphorylation of other residues on IRAK4. Thus, further experiments with more specific antibodies are required to confirm that GSTO1-1 is upstream of IRAK4.

Figure 5.17: GSTO1-1 influences IRAK4 phosphorylation
IRAK4 was phosphorylated on LPS stimulation in non-silencing control cells in 30 minutes but the extent of phosphorylation was significantly lower in *Gsto1* knockdown cells.

5.3.12 GSTO1-1 deficient cells fail to elicit M1 typical phagocytic phenotype

To evaluate the consequences of disrupted TLR4 signalling in GSTO1-1 deficient cells, the phagocytic ability of the cells was measured both qualitatively and quantitatively using two independent approaches in order to determine whether the cells behave like M1 macrophages upon LPS stimulation. J774.1A non-silencing control cells internalized fluorescently labelled dead bacteria efficiently indicating a collective response of all TLRs to the presence of pathogenic agents in the microenvironment. Further, J774.1A non silencing control cells primed with LPS for two hours prior to incubation with the fluorescently labelled dead bacteria exhibited significantly enhanced phagocytosis (Figure 5.18A). Interestingly, GSTO1-1 deficient cells showed poor efficacy in the internalization of the pathogenic particles and remained unstimulated post priming with LPS as well (Figure 5.18A). Cell viability was evaluated to eliminate any difference in the cell viability post infection (Figure 5.18B). To further narrow down the non-responsiveness of *Gsto1* knockdown cells, latex beads coated with LPS were applied to the cells to specifically activate TLR4. GSTO1-1 deficient cells failed to internalize the LPS coated latex micro particles (in red) to the extent seen with the non-silencing control cells (Figure 5.18 C-D), indicating their inability to respond to pathogenic invasion. On quantification, an average of 2-3beads/cell was counted in the non-silencing control cells on LPS stimulation while the GSTO1-1 deficient cells phagocytosed <1 bead/cell (Figure 5.18 E).

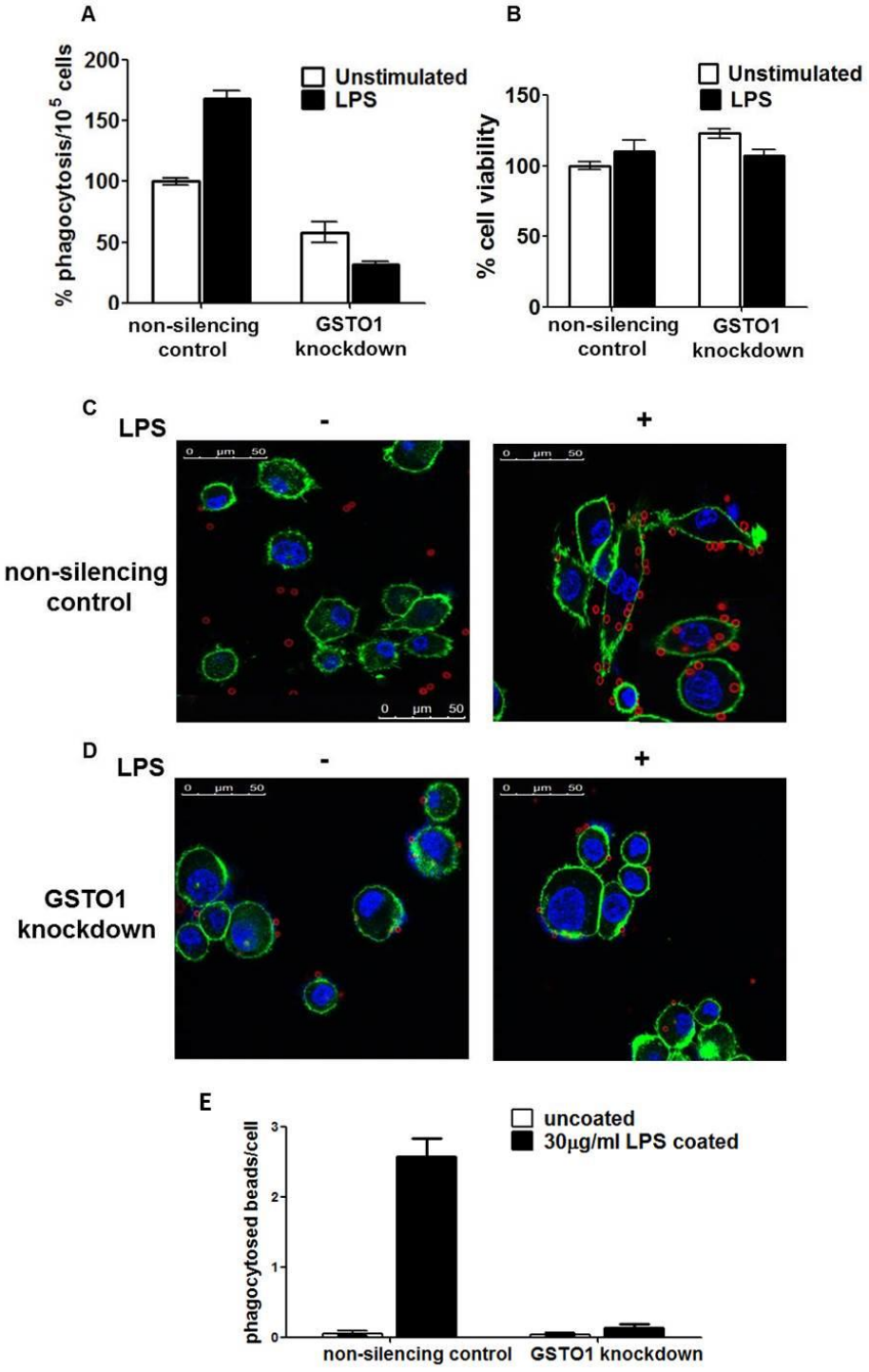

Figure 5.18: Phagocytosis exhibited by classical M1 activated macrophages in response to LPS is attenuated in GSTO1-1 deficient cells.
(A) Phagocytosis of dead bacteria in GSTO1-1 deficient macrophages was significantly attenuated (B) Cell viability remained unchanged between the non-silencing control and *Gsto1* knockdown cells. (C and D) LPS stimulated TLR4 dependent phagocytosis was specifically blocked in GSTO1-1 deficient cells. The nucleus is stained with DAPI (blue), the plasma membrane is indicated by actin staining (green) and LPS coated latex beads are shown in red.(E) The number of phagocytosed beads were counted across 200 cells/group and normalized to the cell count.

5.4 Discussion

Macrophages exhibit pro-inflammatory responses by secreting bactericidal cytokines and reactive oxygen species (ROS). The secretion of TLR4 specific cytokines such as IL-1β requires the activation of two parallel pathways: TLR4-dependent activation of transcription of pro-IL-1β and recruitment of the NLRP3 inflammasome. Transcription of pro- IL-1β is switched on by NF-κB which requires the activation of a cascade of intermediate signalling molecules on TLR4 activation by lipopolysaccharide (LPS). A simultaneous potassium efflux into the cell signals the recruitment of the NLRP3 inflammasome complex comprising of NLRP3, ASC and Procaspase-1 [160, 361-364]. Procaspase1 is cleaved to its active form, Caspase-1 which subsequently cleaves pro-IL-1β into mature IL-1β [364]. The data presented here indicate that the TLR4 mediated expression of cytokines such as IL-1β and production of cytosolic ROS in response to LPS stimulation requires the presence of GSTO1-1. Since GSTO1-1 has been implicated in several inflammatory diseases, it was hypothesized that GSTO1-1 is central to the redox wiring of macrophages. Interestingly, analysis of previously published data on the *Immgen* database also recognized GSTO1-1 and not GSTO2-2 expression to be comparable with other TLR4 signalling proteins such as MyD88 and MAL levels in phagocytic cell types such as monocytes and macrophages (data on MyD88 and MAL are shown in Appendix A7 Figure 1A-B). Redox responses including the excessive generation of ROS and simultaneous down regulation of anti-oxidants has been described by several studies [148, 292, 344, 365]. The exact role of redox changes including protein post translation modifications in response to a pro-inflammatory stimulus such as bacterial infection is not fully understood.

For the purpose of this study, murine macrophage J774.1A cells that were used were stably transfected with either a *Gsto1* targeting shRNA or a scrambled non-silencing control shRNA. These cells were generated in the Luke O'Neill laboratory (Trinity College Dublin) and have served as an excellent platform to investigate the function of GSTO1-1 in TLR4 activation. TLR4 activation by LPS results in the generation of both cytosolic and mitochondrial ROS though the consequences of increased ROS generation on NF-κB dependent activation of cytokines continue to attract speculations. The redox state of macrophages transfected with non-silencing control shRNA and *Gsto1* targeting shRNA was determined by measuring cytosolic ROS levels and protein glutathionylation. Knocking down *Gsto1* in J774.1A macrophages was sufficient to attenuate the generation of cytosolic ROS and inhibit the expression of NF-κB driven

cytokine secretion. Furthermore, *Gsto1* knockdown cells failed to express typical pro-inflammatory markers such as iNOS and COX2 on LPS stimulation. The inhibition of ROS production suggested that GSTO1-1 deficiency disrupted TLR4 signalling and not the NLRP3 inflammasome complex recruitment as TLR4 activation by LPS is required for the transcriptional activation of cytokines and the predominant cytosolic ROS generating enzyme complex NOX1. Previous studies have demonstrated that the oxidant/antioxidant axis is tightly regulated to maintain high ROS levels during the initial phase of LPS stimulation to counteract bacterial infections [292, 343, 352, 354, 366, 367]. The present data show that the suppression of the expression and activity of several enzymes including catalase, Gpx3, HO-1, NQO1 and GCL in order to maintain the initial oxidative stress in response to LPS is dependent on the presence of GSTO1-1.

Increased ROS has been shown to induce the glutathionylation of proteins in order to protect them from irreversible oxidative damage and since GSTO1-1 was found to catalyse the deglutathionylation of proteins, the global glutathionylation status of proteins was determined in *Gsto1* knockdown cells on LPS stimulation. As expected, the total protein glutathionylation in the GSTO1-1 deficient cells was significantly higher than the control cells, suggesting that GSTO1-1 may also catalyse the deglutathionylation of specific proteins in J774.1A macrophages. LPS mediated ROS generation in the non-silencing control cells resulted in an increase in protein glutathionylation as predicted while the glutathionylation levels remained unchanged in the *Gsto1* knockdown cells. The protein glutathionylation levels along with the unaltered oxidant/antioxidant axis and unchanged GSH/GSSG ratio in the GSTO1-1 deficient cells collectively indicates the inability of GSTO1-1 deficient cells to elicit pro-inflammatory and anti-microbial responses mediated by TLR4. The suppression of antioxidants has been previously shown to be mediated via PPARγ and Nrf2 [352, 353, 367, 368]. Though a significant up-regulation of PPARγ and its coactivator PGC1β were measured in GSTO1-1 knockdown cells, the establishment of a direct link between PPARγ and Nrf2 was beyond the scope of this study. Based on published literature [352, 354, 369] and the data discussed here, it is hypothesized that the effects on antioxidant expression and activity may be mediated via the up-regulation of PPARγ due to the block in the activation and nuclear translocation of NF-κB, which in turn maintains Nrf2 in an active state in LPS stimulated macrophages and thus preventing the suppression of antioxidant expression during the initial phase of ROS production (Figure 5.19).

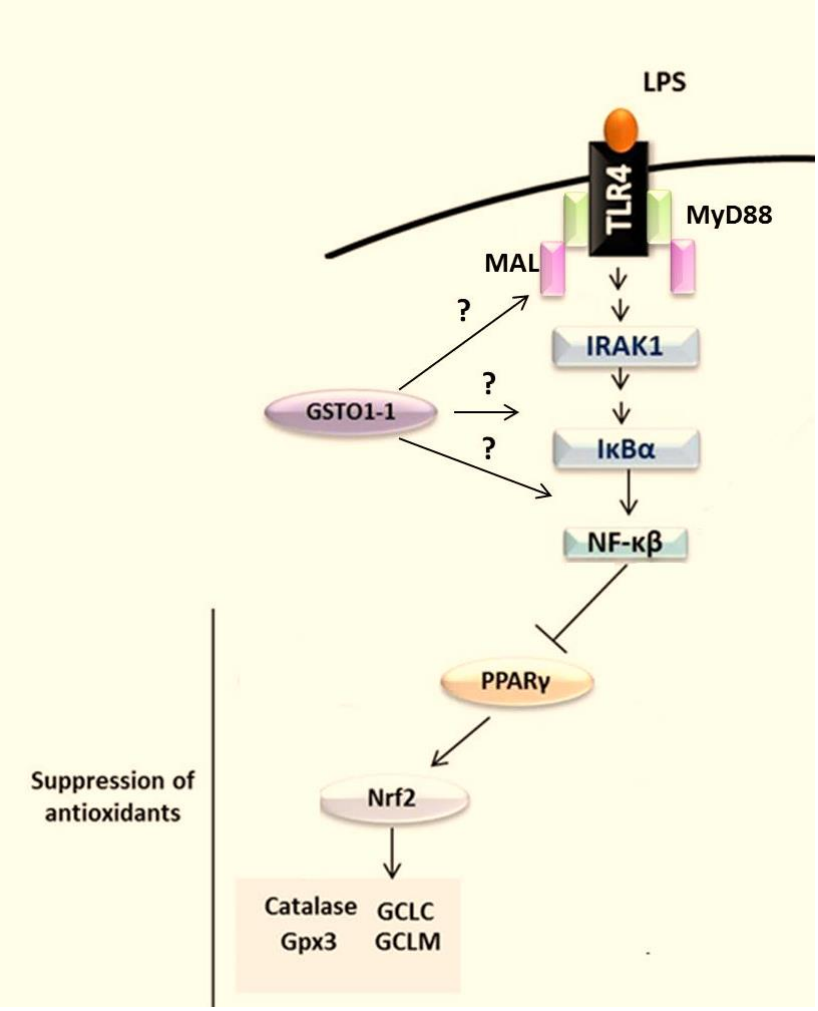

Figure 5.19: TLR4 signalling scheme 1: A scheme describing the key signalling events occurring eventually leading to the nuclear translocation of NF-κB and the PPARγ mediated suppression of antioxidant enzymes.

There are multiple steps involved in the TLR4 activated cascade of signalling molecules leading to the activation of NF-κB and the expression of pro-inflammatory cytokines such as IL-1β [1, 165, 370]. A simplified representation of TLR4 signalling in macrophages and some of the key proteins involved are shown in Figure 5.20. A more detailed description of the pathway has been previously illustrated in Figure 1.9. The work presented in this thesis clearly demonstrates that there are proteins in the TLR4 pathway that are impacted by GSTO1-1. Starting from the downstream key regulator of transcriptional regulation of pro-inflammatory cytokines and NOX1, the disruption in intermediate protein activity was determined. Since the nuclear translocation of NF-κB subunit p65 was blocked in *Gsto1* knockdown cells, the effect of GSTO1-1 was placed further upstream. The activation of proteins partaking in the initial steps of the cascade were also evaluated to determine whether GSTO1-1 acts immediately downstream of TLR4. Since the activation and phosphorylation of IRAK4 (Figure 5.20) was absent in the *Gsto1* knockdown cells, it is hypothesized that GSTO1-1 acts further upstream of IRAK4 which narrows down the site of action to the Myddosome complex. As mentioned in Chapter 1, the Myddosome complex comprises of MyD88, MAL and TLR4. Further investigations into the recruitment and association of these adaptor proteins will help elucidate the role of GSTO1-1 in TLR4 signalling.

Phagocytosis is considered as a classical M1 phenotype marker and is initiated when a macrophage senses the presence of pathogens. When in direct contact with a pathogen, phagocytes such as macrophages and neutrophils form dendrite-like extensions and engulf surrounding pathogens. This phenomenon is further maintained and enhanced by the activation of the TLRs expressed on the phagocyte surface. Interestingly, *Gsto1* deficient cells showed poor efficacy in the internalization of the pathogenic particles and remained unstimulated post priming with LPS as well. The difference in phagocytic ability between the unstimulated J774.1A non silencing control cells and GSTO1-1 deficient cells could be due to the unresponsiveness of the *Gsto1* knockdown cells to TLR4 ligand LPS (pathogen cell wall). This was further validated when the *Gsto1* knockdown cells failed to promote phagocytosis in response to LPS alone (LPS coated beads) determining the response of these cells to LPS alone, without other components contributing to the phagocytic phenotype.

Since a pharmacological inhibitor of GSTO1-1 was found to block the production of ROS via the inhibition of NOX1, it seems likely that the regulatory effect of GSTO1-1

may be mediated by its catalytic activity. A previous study introduced CRIDs as a class of cytokine inhibitory drugs that inhibited IL-1β secretion by interacting with the active site cysteine of GSTO1-1 (cysteine 32). CRID3 was found to be a poor inhibitor of GSTO1-1, with its IC_{50} in the micro molar range. In spite of the poor efficacy of the drug, a moderate decrease in the levels of NOX1 was detected in CRID3 treated cells. Thus, ML175 was determined to be a better chemical inhibitor for the purpose of this study. However since higher concentrations of ML175 resulted in significant cell death, the study was restricted in terms of concentrations that could be used in cells without causing cytotoxicity. The extensive characterization of ML175 undertaken by Tsuboi, K., *et al.*, reported little toxicity and few off target effects. It is possible that the higher toxicity observed in the present study was due to the DMSO used to solubilize the compound [350]. Though the concentrations used were well within the non-toxic range, it is worth noting that the compound may need to be developed further to reduce the cytotoxic effects before applying these findings to *in vivo* models. It is interesting to note that ML175 had a dose dependent effect on the inhibition of TLR4 signalling suggesting that the mechanism of action of GSTO1-1 on TLR4 signalling is 'druggable' and can be tightly controlled to limit excessive inflammation that is associated with various health conditions such as neurodegenerative diseases and metabolic disorders rather than completely abolish TLR4 signalling which could have severe side effects.

Since genetic variation in GSTO1-1 has been shown to be a determinant of the age at onset of Alzheimer's and Parkinson's diseases, it is tempting to speculate that polymorphic variants of *Gsto1* may regulate inflammatory responses and the production of ROS altering the progression of many disorders. It has been shown that that the NLRP3 inflammasome complex is activated resulting in the over-secretion of IL-1β. This in turn resulted in the exacerbation of inflammation associated with the progression of neurodegeneration [371, 372]. Taken together, our data demonstrate significantly attenuation of ROS in *Gsto1* knockdown cells, thus identifying a novel component of the ROS production pathway in LPS activated macrophages. Several studies strongly support the role of ROS in pro-inflammatory responses elicited in activated macrophages and nullifying this effect through pharmacological drugs has been shown to switch macrophages to an anti-inflammatory phenotype. The inhibition of GSTO1-1 by ML175 mediates responses typical of reported anti-inflammatories, hence providing the first evidence supporting the characterization of ML175 as a potential anti-inflammatory agent.

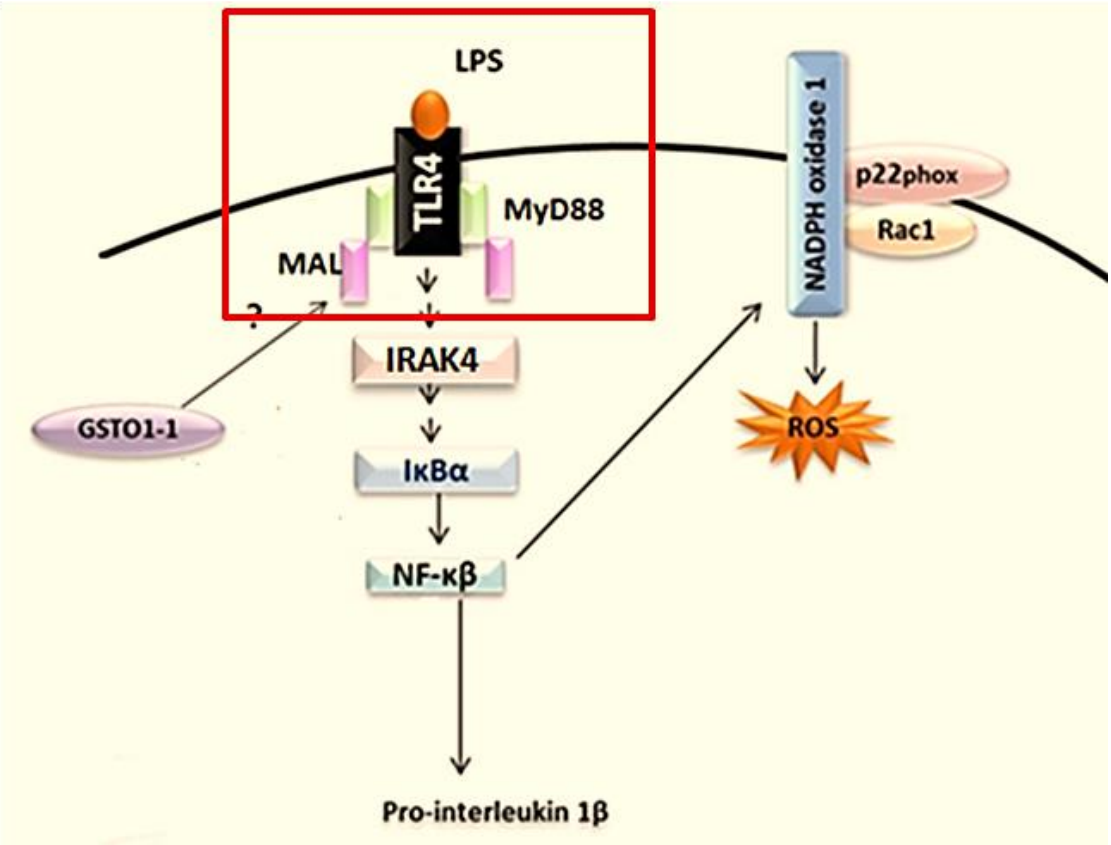

Figure 5.20: TLR4 signalling scheme 2: The absence of immediate phosphorylation of IRAK4 in *Gsto1* knockdown cells places the action of GSTO1-1 further upstream of IRAK4 and possibly in the myddosome complex. The proteins associating to form the myddosome complex are highlighted in the red box.

CHAPTER 6

Glutathione transferase Omega 1 modulates metabolism in activated macrophages

6.1 Introduction

Macrophages are the key players contributing to innate immune responses that recognize foreign pathogens and inflammatory stimulants such as bacterial LPS. LPS has been shown to induce the generation of reactive oxygen species (ROS) and pro-inflammatory cytokines such as IL-1β through the activation of TLR4 and the recruitment of downstream signalling proteins [162, 278-281]. In addition to their signalling role and their impact on the expression of pro-inflammatory cytokines, the ROS generated by the TLR4 pathway have also been shown to cause tissue damage and are central to the progression and pathology of many inflammatory diseases [280]. The role of GSTO1-1 in the activation of the TLR4 pro-inflammatory cascade and the generation of ROS via NF-κB activation was extensively described in chapter 5 [345]. To further understand the mechanism by which GSTO1-1 mediates inflammatory responses in macrophages, the activation of parallel signalling pathways which are independent of NF-κB activation were investigated. In light of recent studies which demonstrate that TLR4 activation by LPS skews macrophages towards a more glycolytic phenotype (Figure 6.1) [1, 373-375], the metabolic profile of GSTO1-1 deficient macrophages was determined. In response to LPS, GSTO1-1 deficient macrophages failed to produce excess lactate and induce HIF1α that plays a key role in maintaining the pro-inflammatory state of activated macrophages. The accumulation of TCA cycle intermediates, succinate and fumarate that occurs in LPS treated macrophages was also blocked in GSTO1-1 deficient cells. These data indicate that GSTO1-1 is required for LPS mediated signalling in macrophages and acts early in the LPS/TLR4 pro-inflammatory pathway.

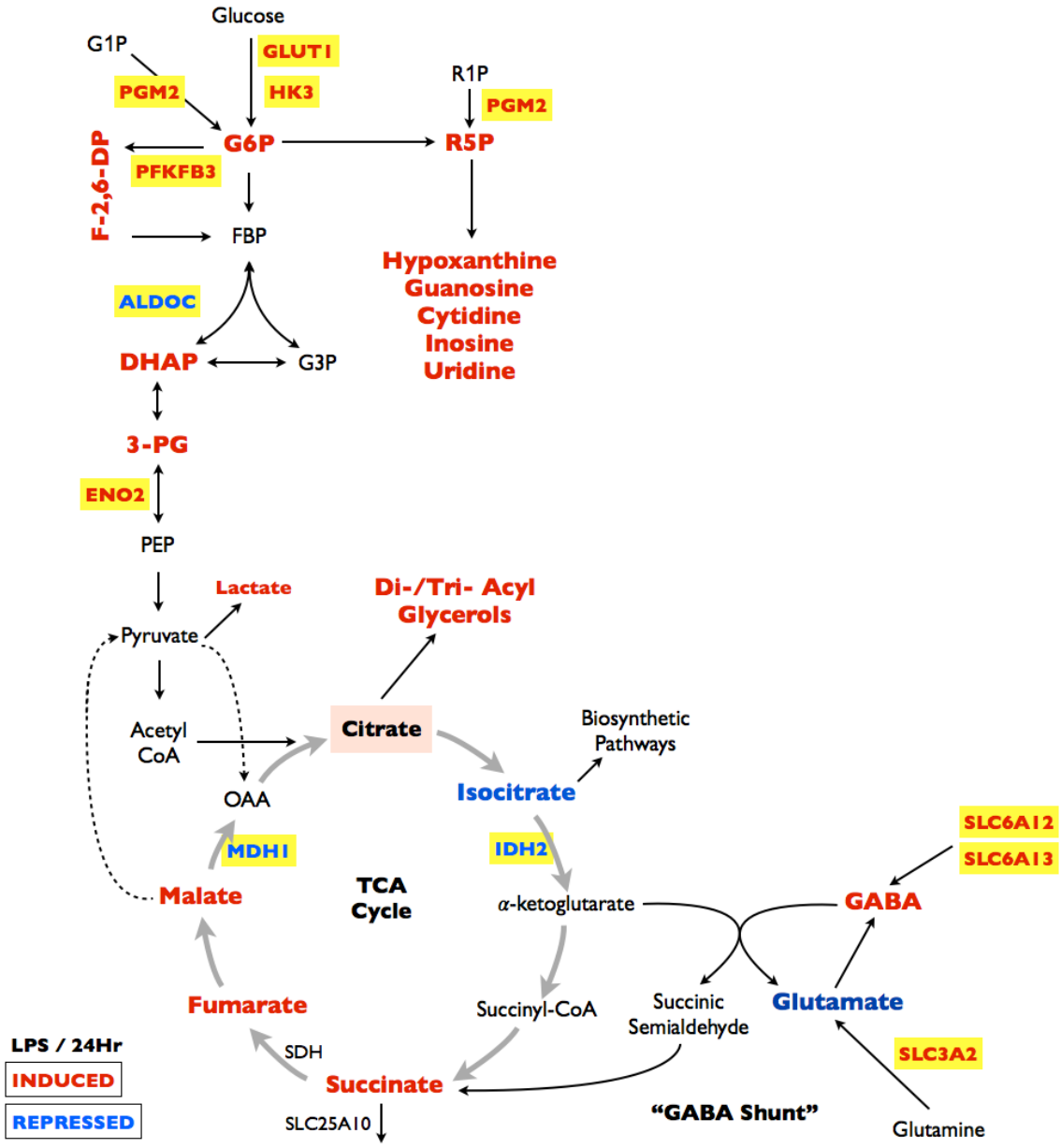

Figure 6.1: Glycolysis and the TCA cycle (adapted from [1])

Intermediates highlighted in red are induced and in blue are repressed in LPS stimulated bone marrow derived macrophages (BMDMs)

6.2 Materials and methods

6.2.1 Measuring mitochondrial ROS

Cells were seeded in six-well dishes at a cell density of $5x10^5$ and treated with LPS as indicated. Cells were washed with PBS and then incubated with MitoSOX/Mitotracker (Life Technologies) for 30 minutes at 37°C [292]. The cells were washed twice and resuspended in PBS and analysed by fluorescence-activated cell sorting analysis (FACS). All measurements were normalized against baseline readings from unstained controls and then to untreated controls from each cell type. Data from three independent experiments were analysed using Flowjo FACS analysis software.

6.2.2 Determining mitochondrial membrane potential

Treated or untreated cells ($1x10^5$), were resuspended in 1ml PBS. As a positive control, cells were treated with 50μM Carbonyl cyanide m-chlorophenyl hydrazone (CCCP) for 5 minutes [292]. Cells were incubated with JC-1 dye (Mitoprobe, Life Technologies) at 37°C, 5% CO_2 for 30 minutes according to the manufacturer's instructions. Cells were then washed with PBS and resuspended in 100 μl of PBS and analysed by FACS with an emission wavelength of 488 nm. Data from three independent experiments were analysed using Flowjo FACS analysis software.

6.2.3 Measurement of extracellular lactate levels

Cells were seeded in 6-well dishes at a density of $5x10^5$ cells and treated with LPS as indicated. Briefly, media was collected at different time points and mixed with 3% perchloric acid. 0.05% methyl orange was then added to the samples (final concentration of 0.00083%) and mixed well. The pH of the samples was raised with 1M K_2CO_3 until the solution turned bright yellow. The volume was adjusted to 400 μl and $1/10^{th}$ of the total volume (40 μl) was then incubated with NAD (1 mM) in a glycine hydrazine buffer (1M glycine, 0.4 M hydrazine sulphate, 5 mM EDTA, 0.5 M NaOH) and initial absorbance was measured at 340 nm at 37°C. The samples were then mixed with 19.8 U lactate dehydrogenase and absorbance was recorded every 10 minutes at 340 nm, 37°C until the reaction was complete. The initial absorbance values were subtracted from the final readings and lactate concentrations were calculated based on the standard curve obtained from standards made from sodium lactate.

6.2.4 Measurement of NADPH/NADP+ levels

Cellular NADPH/NADP levels were estimated by an enzymatic assay (Abnova). Briefly, 10^5 cells were lysed in either NADP or NADPH extraction buffer and heated at 60°C for 5 minutes. Samples were neutralized with the opposite buffer and centrifuged at 16000 x g for 10 minutes to remove all debris. The supernatant was incubated with the reaction buffer (containing 3-(4,5-dimethylthiazol-2-yl)-2,5-diphenyltetrazolium bromide (MTT), glucose and glucose dehydrogenase) and absorbance was immediately read at 565 nm. The reaction was allowed to progress at room temperature and the final absorbance was measured after 30 minutes. The initial absorbance values were subtracted from the final readings and NADPH/NADP ratios were calculated based on NADP standards.

6.2.5 Extracellular flux measurements (OCR and ECAR)

For real-time analysis of the bioenergetics profile of activated macrophages, cells were analysed with an XFe-96 Extracellular Flux Analyser (Seahorse Bioscience) as described previously [373, 374]. Cells were seeded at a density of 130,000/well in XFe 96 plates and treated with LPS as indicated. The cells were washed and allowed to recover in XF media supplemented with 5.5 mM glucose and 1 mM pyruvate for one hour at 37°C without CO_2. The Oxygen Consumption Rate (OCR) and Extracellular Acidification Rate (ECAR) were measured and results were normalized to readings from untreated cells at respective time points.

6.2.6 GC/MS analysis of metabolites in macrophages

Sample preparation: Cells were seeded at a density of $5x10^5$ cells/well in 6-well dishes and treated with LPS as indicated. Post treatment, cells were lysed in 1:1 methanol water solution and derivitized in methoxyamine-HCl in anhydrous pyridine and N-methyl-N-(trimethylsilyl)-trifluoroacetamide. The derivatized samples were analysed by GC/MS with a full scan range of 50-600m/z transition (Agilent 7890A, Agilent 5975C MS inert XL EI/CI MSD with triple axis detector, Inc. Santa Clara, CA, USA). Metabolites were screened using AnalyzerPro and identified against the NSIT library. The peak area of Kreb's intermediates succinate and fumarate were normalized to essential amino acids in each sample. All readings were measured in triplicate.

6.2.7 LC/MS analysis of metabolites in macrophages

Sample preparation: Cells were seeded at a density of $5x10^5$ cells/well in 6-well dishes and treated with LPS as indicated. Post treatment, cells were washed with PBS and

lysed in 1:1 methanol water solution and pre-treated as described above in the GC/MS sample preparation. The supernatant was dried using a vacuum concentrator (Savant Speedvac) and resuspended along with the standards in double distilled degassed water. Samples were vortexed and filtered through a 0.45μm GHP membrane in a Nanosep MF Centrifuge tube (Pall Co., Port Washington, WI, USA) before LC-MS/MS analysis. Sugar phosphates and other metabolic intermediates were analysed using an optimised Agilent 6530 Accurate-Mass Q-TOF LC/MS (Agilent Technologies, Inc. Santa Clara, CA, USA) at the ANU Mass Spectrometry Facility. Samples were subjected to optimised ESI in the Jetstream interface in negative polarity under the following conditions: gas temperature 250°C, drying gas 9 L min–1, nebuliser 25 psig (172.4 kpa), sheath gas temperature 250°c and flow rate of 11 L min–1, capillary voltage 2500 V, fragmentor 145 V, and nozzle voltage 500 V. Mobile phase A consisted of water with 0.1% formic acid and mobile phase B consisted of 90% methanol,10% water and 0.1% formic acid. Samples were injected onto an Agilent Phonomenex Luna 3U HILIC 200A (50 x 2 mm, 3 micron) column and analytes were eluted in mobile phase B. The QTOF was operated in targeted MS/MS mode using collision induced dissociation (CID; N2 collision gas supplied at 18 psi (124.1 kpa), m/z 1.3 isolation window) where the MS extended dynamic range was set from m/z 100–1000 at 3 spectra s^{-1}, and MS/MS m/z 50–1000 at 3 spectra s^{-1}. Data were extracted and analysed using Agilent Technologies Masshunter software. Mass spectrometry was carried out at the Mass Spectrometry Facility, Research School of Biology with the help of Dr. Thy Thuong.

6.3 Results

6.3.1 Mitochondrial dysfunction in LPS stimulated macrophages is abrogated in Gsto1 knockdown cells

LPS has previously been shown to increase mitochondrial ROS generation and contribute to the bactericidal response in macrophages [148, 292, 343, 344, 376]. A significant increase in mitochondrial ROS was detected in LPS treated non-silencing control cells which was absent in the *Gsto1* knockdown cells (Figure 6.2A), suggesting that GSTO1-1 mediates mitochondrial ROS production in addition to its previously demonstrated effect on cytosolic ROS (Chapter 5).

JC-1 is a cationic dye that exhibits potential-dependent accumulation in the mitochondria and consequently is considered a good marker to measure mitochondrial depolarization. Monomeric JC-1 yields green fluorescence (525 nm) which shifts to red (590 nm) when the dye accumulates in the mitochondria forming J-aggregates. Hence, mitochondrial depolarization is indicated by a decrease in the red/green fluorescence ratio. We detected a decrease in the mitochondrial membrane potential (ψ) in LPS treated J774.1A non-silencing control cells. In contrast, the GSTO1-1 deficient cells showed no change in the mitochondrial membrane potential (Figure 6.2B).

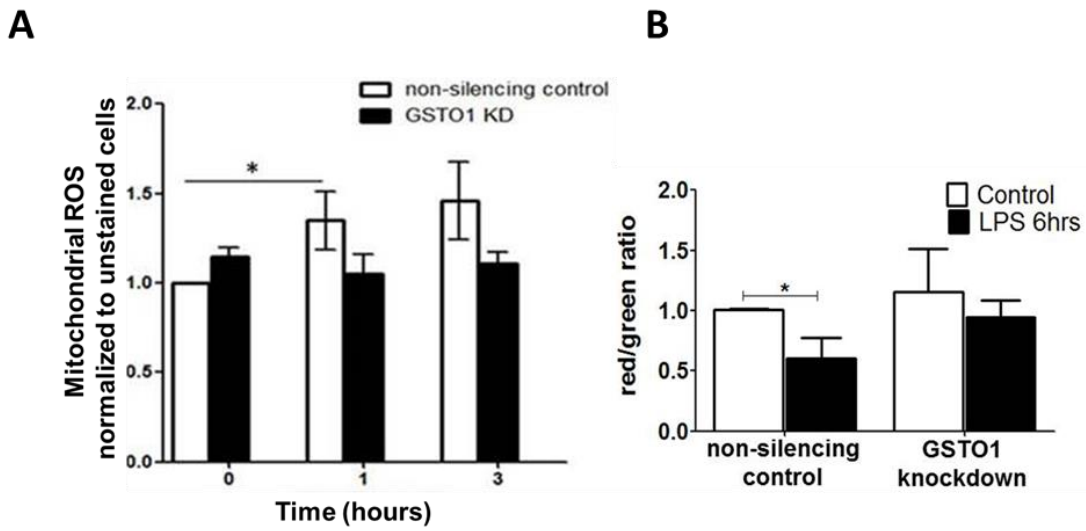

Figure 6.**2:** GSTO1-1 regulates mitochondrial ROS and mitochondrial membrane potential in LPS activated macrophages. (A) LPS treated non-silencing control cells showed a significant ($p=0.05$) increase in mitochondrial ROS which was absent in the *Gsto1* knockdown cells. (B) A significant ($p<0.05$) decrease in the mitochondrial membrane potential (ψ) in LPS treated J774.1A non-silencing control cells was absent in the GSTO1-1 deficient cells.

It has been previously established that an altered mitochondrial membrane potential is associated with an imbalance in the AMP/ADP ratio that is monitored by AMP-activated protein kinase (AMPKα) a major sensor of intracellular energy status [292] As recent evidence suggests a significant link between energy homeostasis and redox state in macrophages [292, 343], we further investigated the role of GSTO1-1 in modulating the LPS stimulated decrease in the mitochondrial membrane potential by evaluating the activation of AMPKα to phospho-AMPKα (p-AMPKα). The results indicate that the activation of AMPKα to p-AMPKα is inhibited by a pro-inflammatory stimulus such as LPS, and this inhibition is blocked in *Gsto1* knockdown cells (Figure 6.3A). By

knocking down GSTO1-1, the cells failed to respond to LPS and p-AMPKα levels remained unchanged. To further determine if the restoration of active AMPKα levels is dependent on the catalytic activity of GSTO1-1, we tested the ability of ML175 to activate AMPKα. As shown in Figure 6.3B, AMPKα activation was restored by GSTO1-1 inhibitor ML175 in a concentration dependent manner. This result further identifies GSTO1-1 as a novel anti-inflammatory target.

To determine whether the downstream effects of GSTO1-1 on ROS production and cytokine secretion are mediated via AMPKα, we tested the hypothesis that the effect of GSTO1-1 on NOX1 expression is dependent on the activation of AMPKα. J774.1A non-silencing control cells and *Gsto1* deficient cells were treated with Compound C (6-[4-(2-Piperidin-1-yl-ethoxy)-phenyl)]-3-pyridin-4-yl-pyrrazolo[1,5-a]-pyrimidine), a synthetic inhibitor of AMPKα. Pre-treatment of *Gsto1* knockdown cells did not reverse the effect of GSTO1-1 on NOX1 transcript levels (Figure 6.3C) suggesting that phosphorylation of AMPKα in LPS treated cells may be an indirect consequence of the upstream regulatory switch provided by GSTO1-1. Hence, it is concluded that the inhibitory effect of GSTO1-1 on NOX1 transcription (reported in Chapter 5) is not dependent on AMPKα.

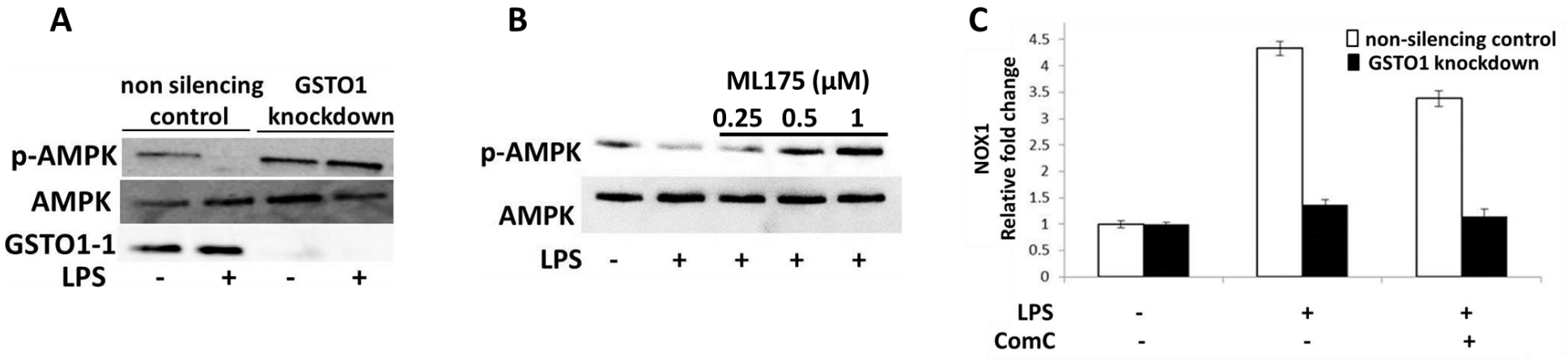

Figure 6.3: GSTO1-1 is required for the inactivation of AMPKα in LPS stimulated macrophages
(A) The inhibitory effect of LPS on AMPKα phosphorylation in J774.1A wildtype macrophages is reversed in GSTO1-1 deficient cells (B) AMPKα activation was restored by ML175 in LPS activated macrophages. (C) Pre-treatment of J774.1A macrophages with AMPKα inhibitor Compound C (ComC) for 2 hours did not reverse the non- responsiveness of *Gsto1* knockdown cells suggesting that the block in the transcriptional activation of NOX1 is independent of AMPKα

6.3.2 Reconfiguration of cellular metabolism during pro-inflammatory (M1) polarization

An imbalance in the energy homeostasis as reflected by the activation of AMPKα was further evaluated by determining the downstream effects of metabolic dysregulation. The two main metabolic pathways, glycolysis and the citric acid cycle (TCA cycle) have been shown to be severely impacted by LPS. LPS activated macrophages acquire a pro-inflammatory M1 phenotype which is associated with a highly glycolytic profile [1, 298, 373, 377]. These activated macrophages tend to secrete excess lactic acid and accumulate high levels of TCA intermediates such as succinate. The accumulation of succinate during the LPS mediated activation of macrophages stabilizes the transcription factor HIF1α and promotes the activation of pro-inflammatory cytokines such as IL-1β [1], thus it appears that the metabolic phenotype is essential for the maintenance of pro-inflammatory responses in LPS activated macrophages. To determine the metabolic state of GSTO1-1 deficient macrophages, the Extracellular Acidification Rate (ECAR) and the Oxygen Consumption Rate (OCR) in response to LPS were measured. The LPS induced increase in ECAR that occurred in J774.1A non-silencing control cells was blocked in GSTO1-1 deficient cells (Figure 6.4A). OCR levels inversely reflected ECAR changes in both control and GSTO1-1 deficient cells. Due to increased glycolysis, the OCR showed a steady decline in control cells whereas the GSTO1-1 deficient macrophages showed no change in the OCR (Figure 6.4B). Complementing the ECAR measurements in GSTO1-1 deficient cells, lactate secreted into the media by the cells on LPS stimulation was quantified. As expected, a significant increase in the extracellular lactate levels in non-silencing control cells was detected in 24 hours (Figure 6.4C). However the *Gsto1* knockdown cells did not alter their lactate secretion, indicating that the cells were unresponsive to LPS and failed to acquire a glycolytic phenotype (Figure 6.4C). To determine if the unresponsiveness to LPS is dependent on the catalytic activity of GSTO1-1, cells were treated with ML175 prior to LPS. Pre-treatment with ML175 decreased the level of extracellular lactate secreted by wildtype J774.1A macrophages in a dose dependent manner (Figure 6.4D). Since increased flux through the Pentose Phosphate Pathway (PPP) generates NADPH that is required by NADPH oxidases to generate high levels of ROS after TLR4 activation, the effect of LPS on the PPP was investigated in *Gsto1* knockdown cells. We found that NADPH levels were significantly increased in LPS stimulated macrophage

cells but no increase was observed in *Gsto1* knockdown cells (Figure 6.4E) or in wildtype cells treated with ML175 (Figure 6.4F).

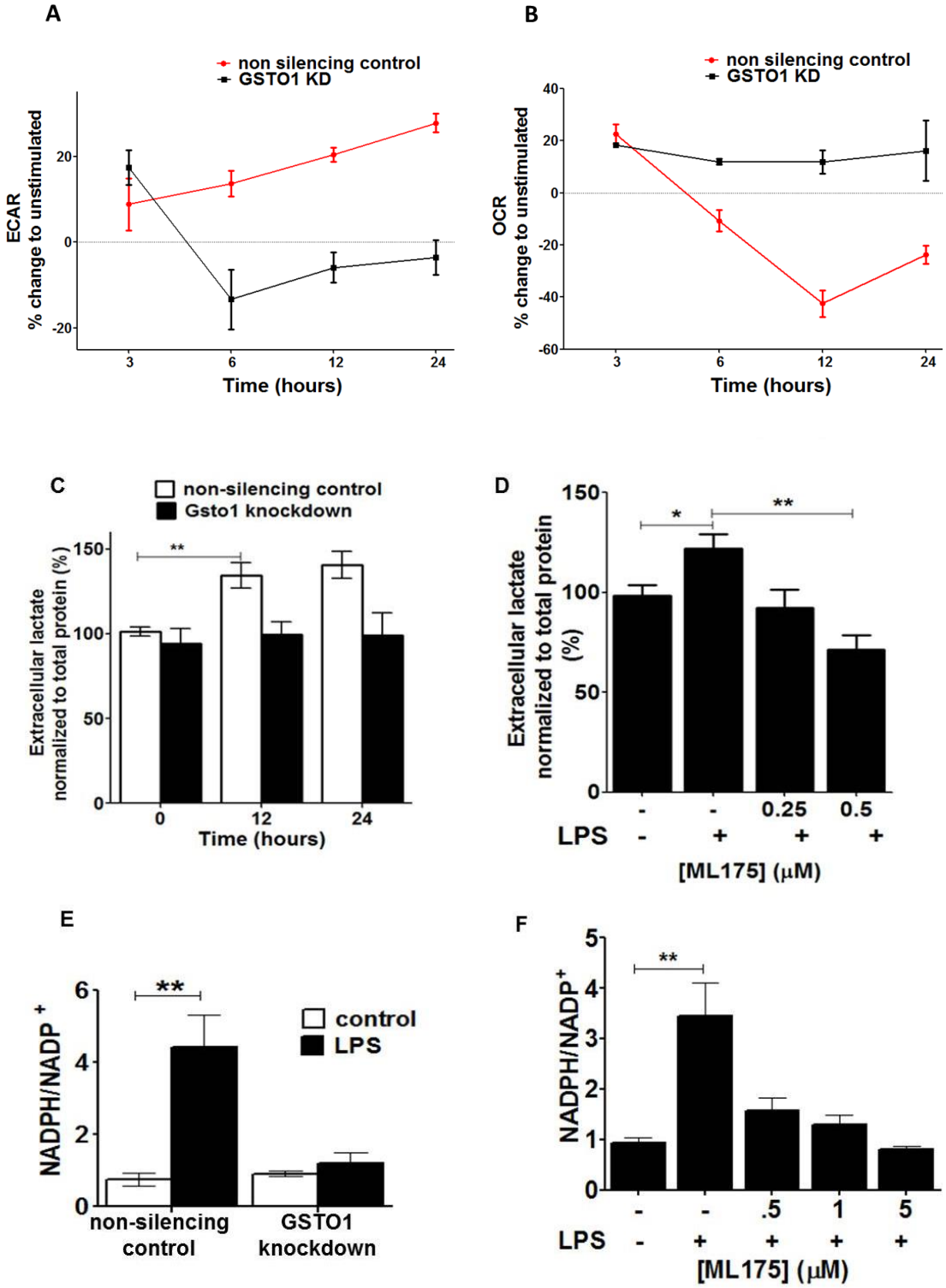

Figure 6.4: GSTO1-1 deficiency prevents macrophages from acquiring a glycolytic phenotype in response to LPS. (A) The LPS induced increase in ECAR in non-silencing J774.1A macrophages over 24 hours was blocked in the GSTO1-1 deficient macrophages. (B) The LPS induced decrease in OCR measured in non-silencing J774.1A macrophages did not occur in GSTO1-1 deficient macrophages. (C) The extracellular lactate levels in the media collected from the LPS treated non silencing control J774.1A macrophages were significantly increased over 24 hours. This trend was largely absent and the media lactate levels remained unchanged in *Gsto1* knockdown cells treated with LPS. (D) Wildtype J774.1A macrophages treated with LPS showed a significant dose dependent decrease in the extracellular lactate level when GSTO1-1 was inhibited with ML175. (E) NADPH levels were significantly ($p<0.01$) increased in LPS treated J744.1A non-silencing macrophages but no increase was measured in the GSTO1-1 deficient cells. (F) Pre-treatment with ML175 maintained unchanged levels of NADPH in LPS treated wildtype J774.1A macrophages.

6.3.3 LPS induced accumulation of succinate and the stabilization of HIF1α

It has been previously shown that there is a significant increase in the intermediate metabolites funnelling into glycolysis and TCA cycle such as fructose-6-phosphate, succinate, fumarate, after LPS activation (Figure 6.1) [373]. Metabolomics performed after LPS activation of J774.1A cells revealed a build-up of TCA intermediates succinate and fumarate (Figure 6.5 A-B). The increase in the abundance of succinate, fumarate and citrate in LPS treated macrophages was abolished in GSTO1-1 deficient cells, complementing the absence of a glycolytic phenotype in these cells (Figure 6.5A-C). The abundance of TCA metabolites was normalized to the total number of cells and to the essential amino acids detected in the cell lysates. A similar trend was observed in the levels of upstream glycolytic intermediate glucose-6-phosphate in GSTO1-1 deficient cells (Figure 6.5D). This trend in sugar phosphates was previously reported to dampen the pro-inflammatory responses of TLR4 activated macrophages [373].

Activation of HIF1α has been shown to play a key role in maintaining the pro-inflammatory state of activated macrophages [1]. Bone marrow macrophages from *Hif1α*$^{-/-}$ mice were unresponsive to LPS and did not secrete IL-1β on TLR4 activation. The succinate build-up on LPS stimulation inhibits Prolyl Hydroxylase (PHD) resulting in the stabilization of HIF1α [1]. In this study the activation status of HIF1α was evaluated in GSTO1-1 deficient macrophages to determine if the observed absence of succinate accumulation in these cells resulted in the suppression of HIF1α activation.

The results indicated that the induction of HIF1α stimulated by LPS is significantly attenuated in GSTO1-1 deficient cells (Figure 6.6A). Furthermore, the inhibition of GSTO1-1 with ML175 decreased the expression of HIF1α in a dose dependent manner (Figure 6.6B).

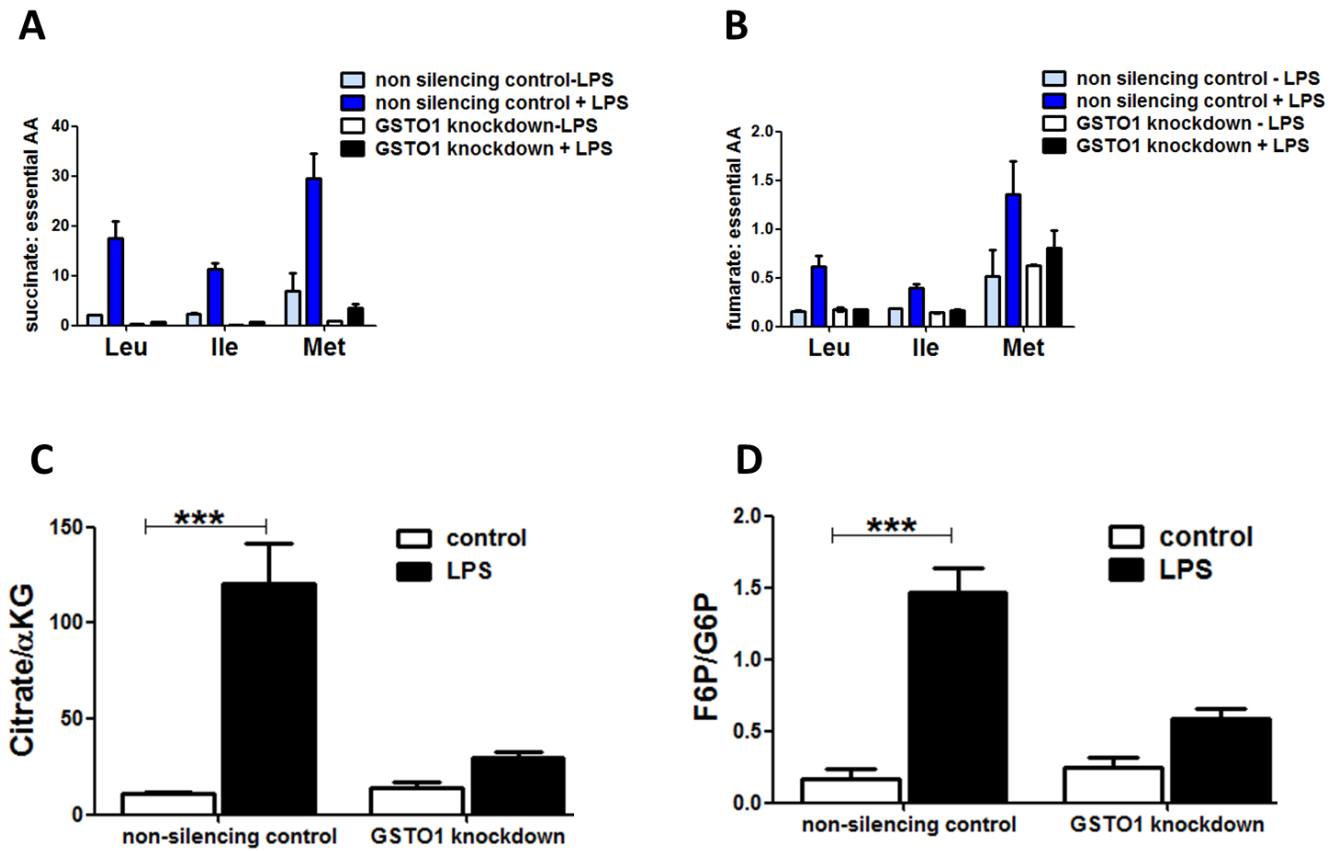

Figure 6.5: LPS dependent re-programming of the TCA cycle in M1 macrophages is altered by *Gsto1* knockdown. (A-B) The accumulation of succinate and fumarate intermediates in LPS treated J774.1A non-silencing macrophages was significantly attenuated in GSTO1-1 deficient cells. (C) Citrate levels were not induced in response to LPS in *Gsto1* knockdown macrophages. (D) The ratio of glycolytic intermediates fructose-6-phosphate (F6P) to glucose-6-phosphate (G6P) was significantly higher in LPS treated non silencing J774.1A macrophages as a result of the glycolytic phenotype acquired by the cells. This trend was absent in *Gsto1* knockdown cells suggesting a failure to acquire a glycolytic phenotype in response to LPS.

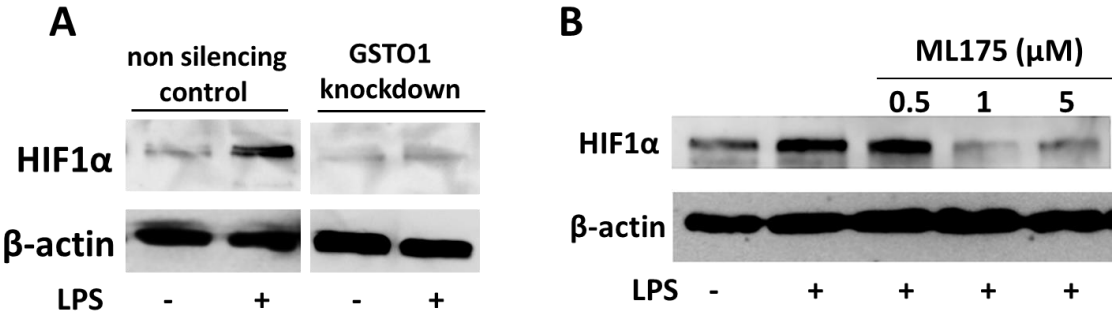

Figure 6.6: LPS induced stabilization of HIF1α
(A) Induction and stabilization of HIF1α by LPS in macrophages was notably attenuated in GSTO1-1 deficient cells. (B) Pre-treatment with ML175 blocked the LPS induced stabilization of HIF1α in wildtype macrophages, mimicking the phenotype observed in GSTO1-1 deficient cells.

6.4 Discussion

Innate immunity is considered as the first line of defence against invading pathogens in mammalian cells. Macrophages are the key players contributing to innate immune responses that recognize foreign pathogens and inflammatory stimulants such as bacterial LPS. LPS has been shown to induce the generation of reactive oxygen species (ROS) and pro-inflammatory cytokines such as IL-1β through the activation of TLR4 and the recruitment of downstream signalling proteins in macrophages. Previous studies have established that macrophages activated via the LPS/TLR4 pathway produce ROS and develop a glycolytic phenotype characterized by the increased production of lactate and the accumulation of succinate that stabilizes HIF1α and regulates the expression of IL-1β [1, 373-375]. Macrophages deficient in GSTO1-1 are non-responsive to LPS and do not activate NF-κB after TLR4 activation (Chapter 4). In this chapter, the impact of GSTO1-1 on TLR4 signalling occurring in parallel with the activation of NF-κB-dependent transcriptional regulation of pro-inflammatory genes was further elucidated. GSTO1-1 was found to be required for the production of mitochondrial ROS which contributes significantly to the total cytosolic ROS measured in the previous chapter. As a consequence of the high mitochondrial ROS, the mitochondrial membrane potential was significantly affected resulting in an imbalance in AMP/ADP which in turn leads to the phosphorylation/activation of AMPKα. ROS are major mediators of cytotoxicity and are directly responsible for much of the pathology that is associated with inflammation. As inflammation contributes to the pathology and exacerbation of a

range of metabolic disorders and neurodegenerative diseases, it is possible that the implicated role of GSTO1-1 and its allelic variants in diseases such as Alzheimer's disease, Parkinson's disease, vascular dementia and stroke, amyotrophic lateral sclerosis, and chronic obstructive pulmonary disease (COPD) [210, 212-215, 272], is due to the modulation of the redox state of proteins involved in the disease-associated inflammatory responses.

Several lines of evidence suggest that LPS induces metabolic reprogramming in macrophages in response to pathogen infection [1, 298, 363, 373, 374, 378]. Additionally recent evidence demonstrates that the secretion of cytokines on LPS stimulation depended on the inhibition of Prolyl Hydroxylase (PHD) and subsequent stabilization of HIF1α in response to the accumulation of succinate through the TCA cycle in the mitochondria [1]. The previous chapter detailed the consequences of GSTO1-1 deficiency on the typical pro-inflammatory responses elicited in LPS stimulated macrophages. The findings were further strengthened by characterizing the metabolic profile of GSTO1-1 deficient cells to determine whether GSTO1-1 could alter the glycolytic reprogramming reported by others.

Published literature strongly suggest that LPS causes a glycolytic switch in macrophages, directing them towards a more catabolic phenotype characterized by increased generation of glycolytic intermediates such as Fructose-6-phosphate and increased channelling of glycolytic intermediate glucose-6-phosphate through the PPP shunt [1, 373]. GSTO1-1 deficient macrophages failed to switch towards a glycolytic phenotype and therefore no increase in glycolytic and PPP shunt intermediates was detected. Furthermore, the findings correlated well with published data on the responses mediated via the TCA cycle. LPS stimulation led to a build-up of TCA intermediates including succinate which in turn activated HIF1α by inhibiting PDH. However the *Gsto1* knockdown cells showed no disruption in the TCA cycle and consequently failed to stabilize HIF1α. These findings bring us back to the initial results suggesting an overall unresponsiveness of GSTO1-1 deficient macrophages towards LPS. Since LPS did not lead to the stabilization of HIF1α (Figure 6.6), pro-IL-1β levels also remained un-induced (Figure 5.5). Additionally, it is also speculated that accumulation of citrate would result in an increase in acetyl-CoA in the cytosol of macrophages as a direct by-product of citrate metabolism in macrophages [379]. The acetyl-CoA generated could then be channelled into phospholipid biosynthesis resulting in the production of

arachidonic acid, a substrate for prostaglandin synthesis. The NF-κB dependent induction of COX2 has already been described in Chapter 5. Taken together, the two pathways merge to initiate and maintain inflammatory responses stimulated by LPS in macrophages. It was also hypothesized that another product of citrate metabolism, oxaloacetate, could potentially contribute to ROS generation though a mechanism wasn't elaborated further [379]. This part of the study indicates that GSTO1-1 is required for most LPS dependent TLR4 signalling in macrophages and plays a critical role in maintaining internal energy and redox homeostasis. Indeed, immune signalling is a metabolically expensive process and is severely impacted under metabolically starved conditions [298, 378]. The metabolic changes unfolding in response to pathogen invasion would allow for an up-regulation in the production of biosynthetic intermediates to meet the energy demands of pro-inflammatory macrophages.

Since the pharmacological inhibitor of GSTO1-1, ML175 was found to inhibit cells from acquiring a glycolytic phenotype, characterized by the alterations in glycolytic and TCA intermediates. This supports the contention that the regulatory effect(s) of GSTO1-1 may be mediated by its catalytic activity.

The pro-inflammatory responses activated by LPS are orchestrated via several parallel pathways that include the activation of NF-κB, and the metabolic reprogramming to a glycolytic phenotype (similar to cancer cells). Both these pathways promote anti-bacterial responses through the production of ROS and the secretion of pro-inflammatory cytokines. These findings support the hypothesis that GSTO1-1 is an indispensable upstream modulator of TLR4 mediated responses and is necessary for orchestrating the metabolic and redox re-profiling of LPS activated macrophages. Since all the parallel pathways are disrupted by GSTO1-1 deficiency, it further supports the hypothesis that the target of GSTO1-1 is a protein early in the pathway and probably within the Myddosome complex (Figure 6.7)

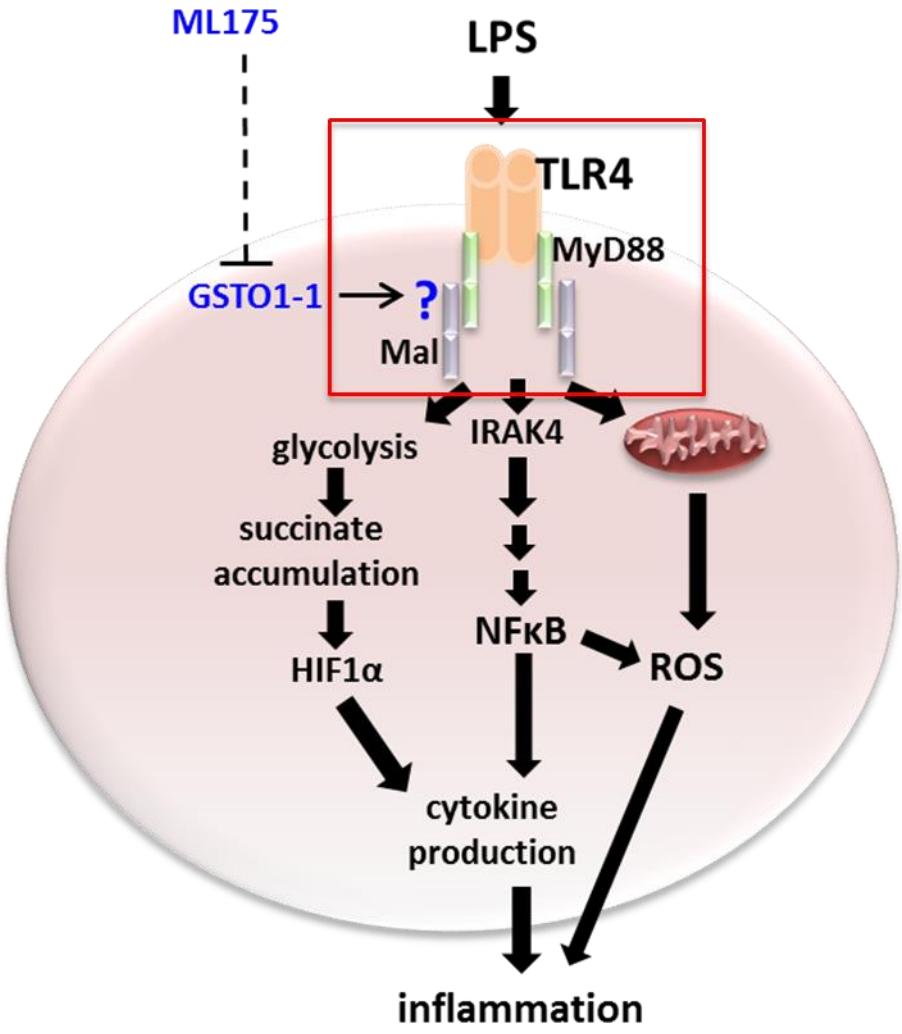

Figure 6.7: A scheme linking the metabolic pathways involved in maintaining a pro-inflammatory state in macrophages with the downstream expression of cytokines. Inhibition of GSTO1-1 with ML175 blocks the activation of multiple pathways originating at TLR4 and diverging downstream of the TLR4/Myddosome complex (highlighted in red).

Chapter 7

Characterization of *Gsto1*$^{-/-}$ mice and their response to bacterial endotoxin

7.1 Introduction

Stimulation of macrophages with LPS results in the production of various cytokines such as TNFα, IL-1, IL-6, IL-10 and enzymes contributing to ROS production [168, 292, 345, 380]. LPS in appropriate quantities can activate pro-inflammatory responses resulting in unfavourable conditions for pathogens. However, hyper-activation of macrophages by either excessive LPS or prolonged exposure to LPS can lead to endotoxic shock [380-384]. In the present study, mice were injected with *E.coli* O55:B5 LPS to evaluate the role of GSTO1-1 in the response to LPS *in vivo*. LPS is a mixture of polysaccharide and lipid A, and much of LPS responses are mediated by the lipid A portion [168, 385]. Since the deficiency of GSTO1-1 resulted in the attenuation of TLR4 signalling in macrophage cell line J774.1A, it was hypothesized that *Gsto1*$^{-/-}$ mice would tolerate an LPS challenge.

7.2 Materials and Methods

7.2.1 Animals

Gsto1 knockout mice were generated by Taconic Biosciences (U.S.A) and became available late in the course of the project (November 2014). Heterozygotes were mated to generate knockout and wildtype control littermates. Due to the poor number of homozygote knockouts born from heterozygote x heterozygote breeding (9 *Gsto1*$^{-/-}$ from 328 progeny), knockout siblings were mated and wildtype littermates from the heterozygote x heterozygote crosses were also mated to generate two strains of *Gsto1*$^{-/-}$ and *Gsto1*$^{+/+}$ mice. The phenotype of the *Gsto1*$^{-/-}$ mice used in this study was not fully characterized due to unforeseen difficulties in the breeding and the resulting scarcity of mice. The *Gsto1*$^{-/-}$ mice bred well when the homozygote line was established and it remains unclear why they could not be produced from the heterozygote mating. Mice were maintained at the ANU Biosciences facility under controlled animal room conditions. The animals were fed regular animal diet and water *ad libitum.*

7.2.2 Enzyme assays

Biochemical assays were carried out as described in Chapter 2-5.

7.2.3 Organ collection and homogenization

Organs were harvested in assay specific buffers. For immunoblots and biochemical assays, tissues were extracted, washed in PBS and homogenized in T-PER (Thermo Scientific) using an Ultraturux homogenizer. Homogenates were centrifuged at 20000 x g at 4°C to remove tissue debris and stored at -20°C until further use. For assays requiring low denaturing and non-reducing conditions, tissues were homogenized in 20 mM tris pH 7.2, 1% NP-40, EDTA, 100 mM N-ethylmaleimide as above and used immediately upon preparation. Tissues for histological analysis were washed thoroughly in PBS and fixed immediately in 10% neutral buffered formalin.

7.2.4 Histology

Tissues for histochemical analysis were fixed in 10% neutral buffered formalin and embedded in paraffin at the Microscopy and Cytometry Research Facility (MCRF). Tissue sections were cut at a thickness of 4 microns and stained with hematoxylin-eosin. Tissue embedding, sectioning and H&E staining were carried out by Ms. Anne Prins (MCRF) and histological analysis was carried out at the Canberra Hospital by Professor. Jane Dahlstrom.

7.2.5 Haematology

Mice (8 weeks of age) were left untreated or injected with 50 mg/kg LPS for 12 hours and 200-220 µl of blood was collected into heparin-coated sterile tubes by retro-orbital bleeding. Blood samples were immediately analysed using ADVIA Haematology systems (Siemens) at the Australian Phenomics Facility.

7.2.6 Injections and treatments

Indicated doses of LPS (Sigma) were intra-peritoneally injected (5-50 mg/kg). For body temperature measurements, temperature-recording probes (DAS-7009 smart reader, BMDS) were inserted sub-cutaneously 24 hours prior to LPS injections. The body temperature was monitored over 24 hours to confirm that no infection occurred due to the insertion of the probe. For LPS experiments, body temperature of less than 24°C was considered as 'death as an endpoint' and mice were euthanized immediately by CO_2 asphyxiation if the body temperature dropped to 24°C or less for 2 consecutive readings in accordance with the ANU animal ethics protocol.

For experiments with butylated hydroxyanisole (BHA), female mice (between 7-8 weeks of age) were fed *ad lib*. either regular chow (control) or chow supplemented with 0.5% (w/w) BHA (Sigma) for 14 days. Mice were euthanized by CO_2 asphyxiation as recommended by the ANU animal ethics committee.

7.2.7 ELISA

Cytokine specific ELISAs were carried out as described in Chapter 5.

7.2.8 Isolation of Bone marrow derived macrophages

Bone marrow macrophages were isolated and differentiated as previously described. The femur and tibia from mice were extracted at the hip joint and placed in cold DMEM media (DMEM Glutamax from Gibco Life technologies). Attached muscle tissue was removed and the femur was separated from the tibia. The ends of each bone were cut to expose the bone marrow. The bone marrow was flushed out of each bone using a 10ml syringe fitted with a 23G needle into a 50ml tube. Cells were centrifuged at 800 x g for 5 minutes and the supernatant was discarded. The pellet was incubated in RBC lysis buffer (Sigma) for 5 minutes. Lysis was stopped by resuspending the cells in DMEM media. The centrifugation step was repeated and the supernatant was discarded. The cell pellet was re-suspended in DMEM media supplemented with 20% L-929 conditioned media seeded in three 10 cm petri dishes (non tissue-culture grade sterile plastic dishes) and allowed to differentiate for 7 days at 37°C, 5% CO_2. At the end of 7 days, cells were washed, counted and re-seeded as required.

7.3 Results

7.3.1 Characterizing GSTO1-1 deficiency in Gsto1$^{-/-}$ mice

The general characteristics of *Gsto1*$^{-/-}$ mice including body weight and organ weights were evaluated in order to determine whether GSTO1-1 deficiency caused any developmental/growth abnormalities. As shown in Figure 7.1A, the total body weight of *Gsto1*$^{-/-}$ mice (8 weeks of age, males) clustered well within the limits set by the wildtype littermates. Furthermore, the major organs were visually normal and the organ weights did not differ from the wild type controls (Figure 7.1B), suggesting no organ deformities in the *Gsto1*$^{-/-}$ mice under normal physiological conditions.

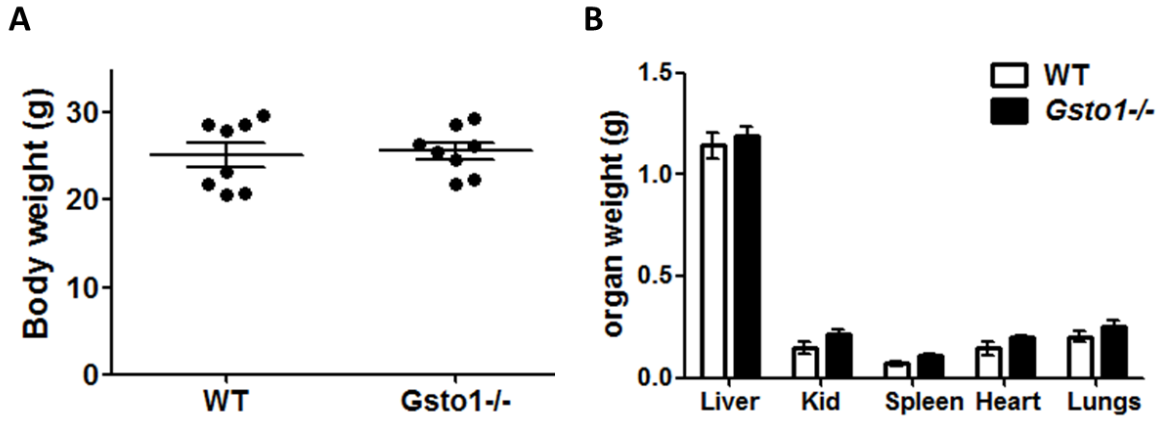

Figure 7.1: Body and organ weights of *Gsto1*$^{-/-}$ mice
(A) The body weights of *Gsto1*$^{-/-}$ and wildtype littermate controls were similar at 8 weeks of age. (B) Individual organ weights were comparable between *Gsto1*$^{-/-}$ mice and wildtype controls.

Immunoblotting of liver extracts revealed that GSTO1 was absent in *Gsto1*$^{-/-}$ mice while the *Gsto1*$^{+/-}$ mice expressed half the amount detected in wildtype mice (Figure 7.2A). To further confirm that the expression of GSTO1-1 was completely absent, the enzyme activity of GSTO1-1 with 4-NPG as substrate was determined and was undetectable in the liver of *Gsto1*$^{-/-}$ mice (Figure 7.2B) (n=3) while the heterozygotes exhibited half the activity measured in wildtype mice. The distribution of GSTO1-1 across a range of tissues was also determined to evaluate tissue specificity. Immunoblotting for GSTO1-1 in tissue extracts from various organs showed that GSTO1-1 is expressed in comparable amounts in in the liver, kidney, heart, lungs and spleen (Figure 7.2C).

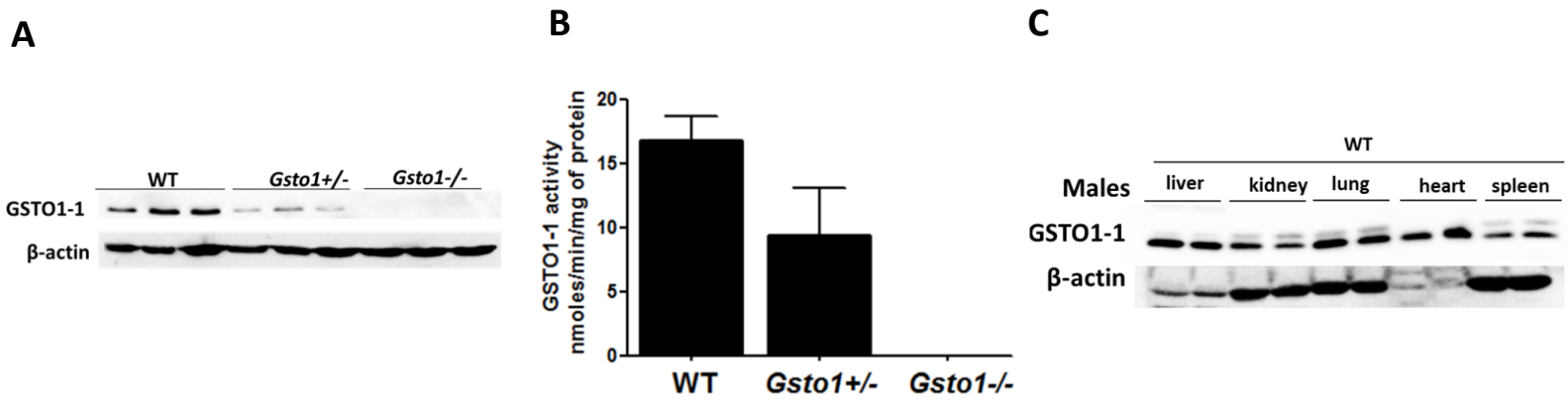

Figure 7.2: Characterization of *Gsto1*$^{-/-}$ mice (n=3)
(A) Knockout of GSTO1-1 expression in liver homogenates of *Gsto1*$^{-/-}$ mice was confirmed by immunoblotting. (B) GSTO1-1 specific 4-NPG reductase activity was undetectable in *Gsto1*$^{-/-}$ mice while the activity in liver homogenates of *Gsto1*$^{+/-}$ mice was significantly halved compared to the wildtype. (C) GSTO1-1 is expressed in abundance in all the tissues evaluated in wildtype mice.

7.3.2 Expression profile of glutathione transferases in Gsto1$^{-/-}$ mice

Previously published studies on *Gstz1* knockout mice revealed an induction in the proteins levels of other GSTs as an antioxidant response to the increased oxidative stress in these mice [386]. To determine whether *Gsto1*$^{-/-}$ mice encountered a similar increase in oxidative stress, liver lysates were extracted and proteins were separated by SDS PAGE. Interestingly, screening the expression levels of GSTs in male *Gsto1*$^{-/-}$ mice revealed a consistent decrease in the expression of Nrf2 driven GSTs including GSTA1/2, GSTT1, GSTT2 (Figure 7.3 A). However, the expression of GSTs such as GSTM2, GSTP, GSTK and GSTO2-2 remained the same as the wildtype mice. The expression levels of NQO1, considered a good indicator of oxidative stress in cells and a target of Nrf2 dependent regulation, were also seen to be significantly lower in the knockout mice. The trend in GST expression levels was maintained in both male and female *Gsto1*$^{-/-}$ mice however females showed a more prominent decrease in the expression of GSTA4, GSTA1/2 and NQO1 (Figure 7.3B).

Because 1-chloro 2,4-dinitrobenzene (CDNB) is a good substrate for some of the GSTs that showed lower expression levels in the livers of *Gsto1*$^{-/-}$ mice, the GST activity of the liver cytosolic extracts was measured with CDNB. Wildtype mice (*Gsto1*$^{+/+}$) had CDNB activity of 11.9 ± 2.05 μmol/mg protein/minute compared with 7.3 ± 1.2 μmol/mg protein/minute in *Gsto1*$^{-/-}$ mice (Figure 7.2C). This difference in GST activity between the wildtype and *Gsto1*$^{-/-}$ mice correlated well with the difference in protein expression reported in Figure 7.3A-B. The residual GST activity measured in the *Gsto1*$^{-/-}$ mice may be due to the unchanged GSTP expression. To support this hypothesis, the GST activity in *Gstp1/2*$^{-/-}$ mice was measured (Figure 7.3C). The activity in *Gstp1/2*$^{-/-}$ mice was significantly diminished (0.3 ± 0.82) which would suggest that GSTP may be a major contributor of the GST activity measured in the liver of *Gsto1*$^{-/-}$ mice.

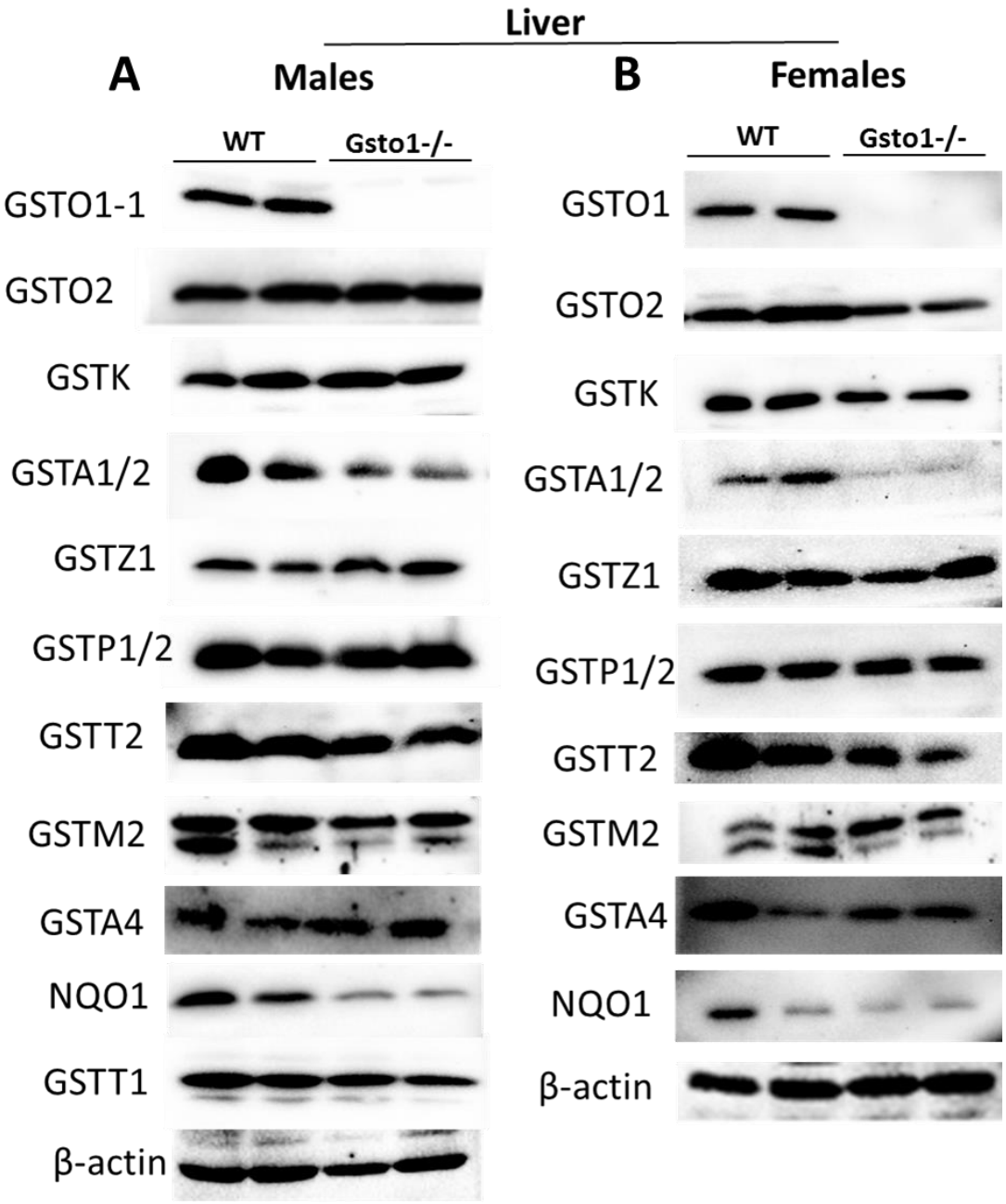
Liver
A
Males
WT
Gsto1-/-
GSTO1-1
GSTO2
GSTK
GSTA1/2
GSTZ1
GSTP1/2
GSTT2
GSTM2
GSTA4
NQO1
GSTT1
β-actin
B
Females
WT
Gsto1-/-
GSTO1
GSTO2
GSTK
GSTA1/2
GSTZ1
GSTP1/2
GSTT2
GSTM2
GSTA4
NQO1
β-actin

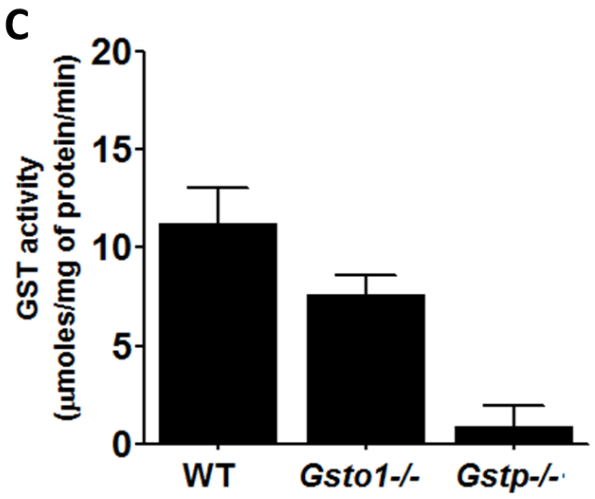
C
GST activity
(µmoles/mg of protein/min)
20
15
10
5
0
WT
Gsto1-/-
Gstp-/-

Figure 7.3: Expression profiling of GSTs in *Gsto1*$^{-/-}$ mice
(A) GST expression in male mice; (B) GST expression in female mice; (C) GST activity with CDNB was moderately lower in *Gsto1*$^{-/-}$ mice than the wildtype mice (WT). GST activity with CDNB was significantly attenuated in *Gstp1/2*$^{-/-}$ mice homogenates of *Gsto1*$^{+/-}$ mice was significantly halved compared to the wildtype (C).

7.3.3 Gsto1$^{-/-}$ *mice are resistant to LPS induced endotoxic shock*

LPS responsiveness was demonstrated by *ip* injection of age matched *Gsto1*$^{-/-}$, *Gsto1*$^{+/-}$ and wildtype *Gsto1*$^{+/+}$ mice with high doses of LPS and monitoring their survival. At a dose of 10 mg/kg, almost all wildtype mice died within 96 hours post LPS injection (12.5% survived) (Figure 7.4A). The *Gsto1*$^{-/-}$ and mice showed high resistance to LPS induced endotoxic shock and survived while the *Gsto1*$^{+/-}$ mice showed intermediate survival rates in between those of wildtype and the *Gsto1*$^{-/-}$ mice (66.7% survived). At a sub-lethal dose of 5 mg/kg, almost all wildtype mice died (37.5% survived) while all the *Gsto1*$^{-/-}$ and *Gsto1*$^{+/-}$ mice survived (Figure 7.4B). To monitor the deterioration in the animal's health, each mouse was subcutaneously implanted with a temperature-transmitting probe 24 hours before LPS injection. The temperature of the mice, which was considered as a direct readout of the response of the animal to the injected LPS, was recorded every 3 hours. As shown in Figure 7.4C and D, the body temperature readings across the three groups correlated well with their respective survival rates. The *Gsto1*$^{-/-}$ mice showed no significant drop in body temperature in response to LPS. On the other hand, the wildtype mice underwent hypothermia within 12 hours after LPS injection at both doses. The lethality of the doses was also reflected in the extent of temperature drop recorded in the wildtype mice. An average drop of 7°C was recorded in wildtype mice injected with 5 mg/kg LPS while the drop was >10°C in wildtype mice injected with 10 mg/kg LPS. Interestingly, the *Gsto1*$^{+/-}$ mice presented an intermediate response. Their survival was considerably higher than the wildtype mice at both doses of LPS and their body temperature decreased within the first 24 hours (Figure 7). However, their rapid recovery from LPS induced systemic inflammation was reflected by the gradual increase in body temperature and other physical characteristics including activity and response to touch. Some of the wildtype mice did recover slightly from LPS induced hypothermia though not to the extent seen with the heterozygotes.

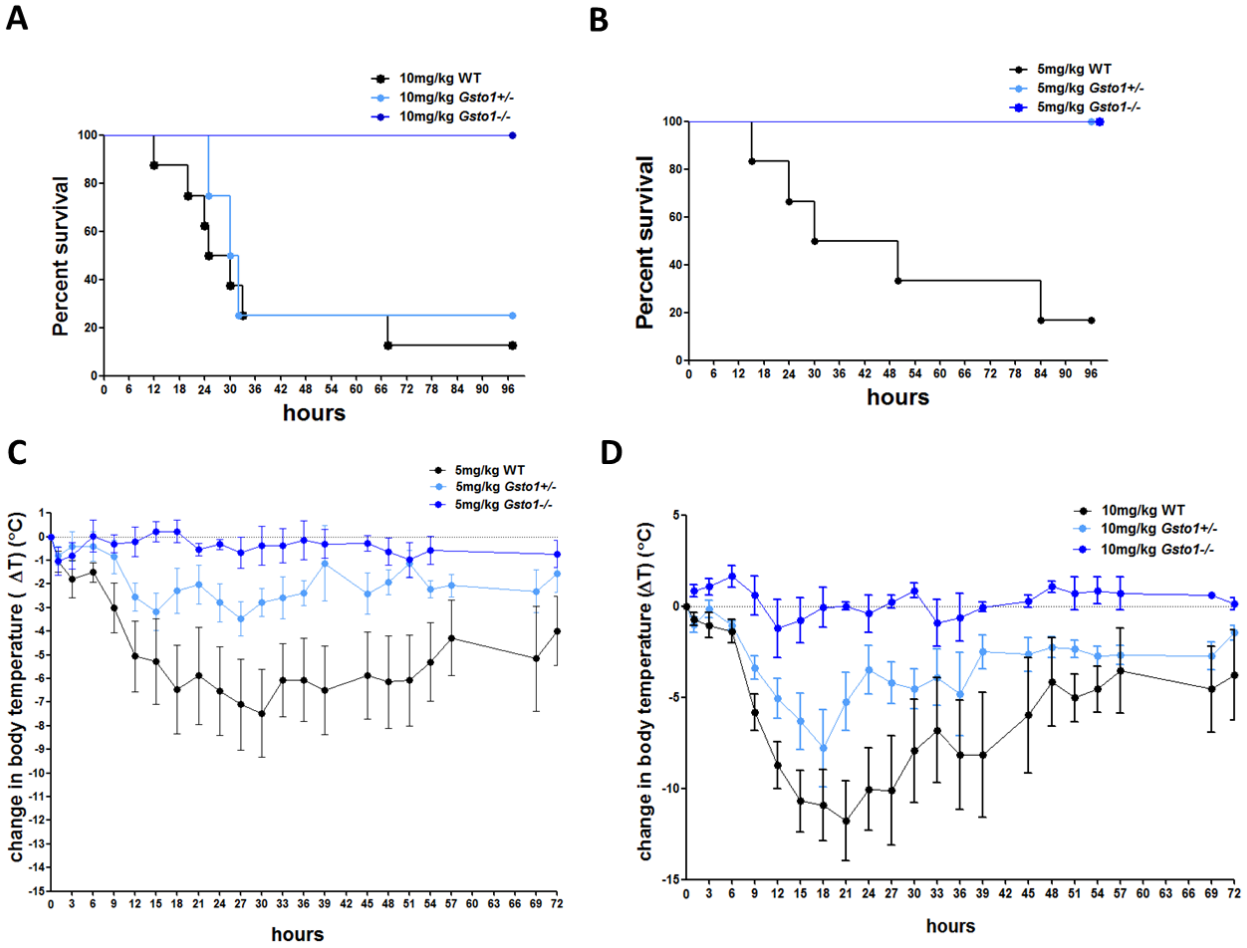

Figure 7.4: Susceptibility of *Gsto1*$^{-/-}$ mice to LPS induced endotoxic shock

(A) Wildtype mice and *Gsto1*$^{+/-}$ mice were highly susceptible to a lethal dose of 10 mg/kg *E.coli* O55:B5 LPS and died within 96 hours due to septic shock while the *Gsto1*$^{-/-}$ mice survived the treatment. (B) *Gsto1*$^{-/-}$ and *Gsto1*$^{+/-}$ mice survived a sub-lethal dose of 5 mg/kg LPS but the wildtype mice died due to severe systemic inflammation. LPS induced hypothermia in mice treated with 5 mg/kg LPS (C) and 10 mg/kg LPS (D) was monitored until the mice were euthanized.

7.3.4 Pathological changes associated with GSTO1-1 deficiency

Light microscopy on tissues showed that 5 mg/kg LPS had no significant effect on the heart, lung, kidney and spleen. The liver in three out of five wildtype mice showed mild inflammation. None of the *Gsto1*$^{-/-}$ mice showed any signs of inflammation in the liver. Two of the five wildtype mice showed marked changes in the spleen with significant recruitment and accumulation of macrophages in the germinal centres of the spleen, showing tingable body macrophages which is considered as a marker of LPS toxicity [387]. The remaining three mice did not show this severe damage. Two of the five wildtype mice also showed reduced red pulp. However, none of the knockout and heterozygotes showed any difference.

Time course of LPS treatment:

Liver: Mice were injected intra-peritoneally with 50 mg/kg LPS and euthanized at 0.5,1,3,6 and 12 hours post injection. The 30 minutes time point showed no signs of inflammation in the liver in both wildtype and *Gsto1*$^{+/-}$ mice. At 1 hour post LPS, all the wildtype and *Gsto1*$^{+/-}$ mice showed significant necrosis in the liver (Figure 7.5A, C-D). , which was completely absent in the livers of the *Gsto1*$^{-/-}$ mice (Figure 7.5B). All wildtype mice showed severe liver damage in terms of necrosis and acute inflammation and one *Gsto1*$^{-/-}$ mouse showed minimal damage though it was considered insignificant when compared to the extent of liver damage observed in the wildtype mice. More significant differences in the liver between the wildtype and *Gsto1*$^{+/-}$ mice were seen at 6 hours post LPS. Two of three wildtype mice showed necrosis and acute inflammation in the liver (Figure 7.5E) but none of the heterozygotes showed any liver damage (Figure 7.5F). To summarize, all but one wildtype showed severe liver necrosis when injected with LPS for greater than 30 minutes and the *Gsto1*$^{+/-}$ mice did not show an inflammatory phenotype when exposed to LPS indicating that *Gsto1*$^{+/-}$ mice are less susceptible to endotoxic shock while the *Gsto1*$^{-/-}$ mice are resistant to LPS induced septic shock.

Spleen: In the time course experiments conducted, no significant changes were seen in the tissues harvested from mice treated with 50mg/kg LPS for 30 minutes in both wildtype and Gsto1 heterozygous mice. At 1, 3 and 6 hour time points, one of three wildtype mice showed Tingible body macrophages (Figure 7.6A-B) in the spleen while none of the *Gsto1*$^{-/-}$ mice showed any abnormalities at 1 and 3 hours post LPS (Figure

7.6C). However, one of two mice at 6 hours showed a similar phenotype as the wildtype mouse.

In terms of red pulp changes in the spleen, there were no significant changes observed in both groups at 30 minutes and one hour post LPS injection. At 3 hours, one of three wildtype mice showed abnormal red pulp changes while none of the heterozygote mice developed any abnormalities. At 6 hours post LPS, all three wildtype mice showed abnormal changes in the red pulp in the spleen while only one of two heterozygotes showed similar changes (Figure 7.6D-E). The Gsto1$^{-/-}$ mice showed no signs of inflammation at both 3 hours and 6 hours post LPS injection.

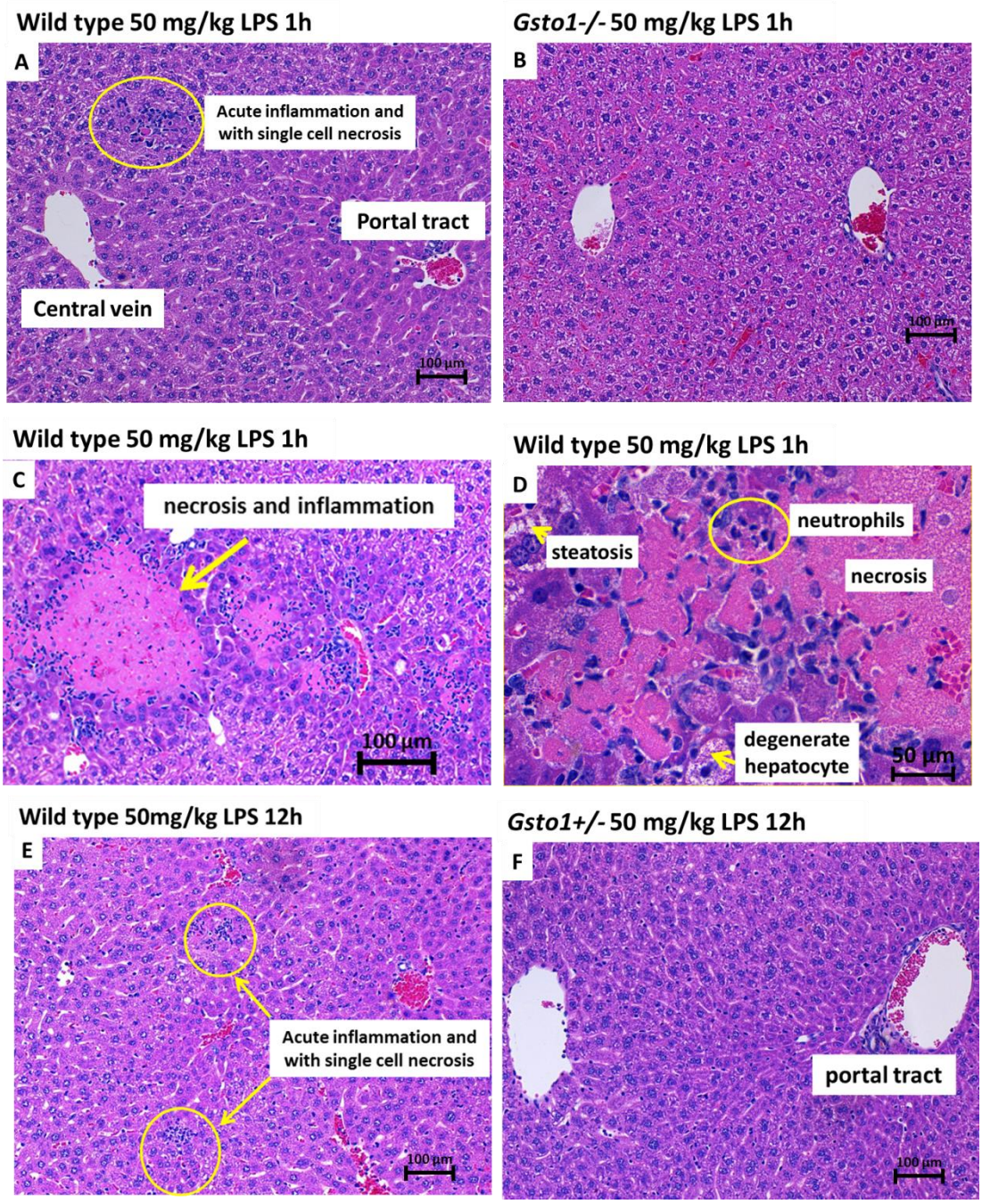

Figure 7.5: Light microscopy showing liver pathology in *Gsto1*$^{-/-}$ mice.
(A) Wildtype mouse injected with 50 mg/kg LPS shows acute inflammation and necrosis (highlighted in yellow) within 1 hour post injection. (B) Gsto1$^{-/-}$ mouse injected with 50 mg/kg LPS (1 hour) showed normal liver histology. (C) Wildtype mouse injected with 50 mg/kg LPS shows acute inflammation and necrosis (yellow arrow) within 1 hour post injection. (D) Magnified view of the necrotic tissue shown in (C) reveals presence of infiltrating neutrophils in wildtype mouse (50µm). (E) Wildtype mouse injected with 50 mg/kg LPS shows acute inflammation and increase in number of single cell necrotic foci in 12 hours post injection (highlighted in yellow). (F) Gsto1$^{-/-}$ mouse injected with 50 mg/kg LPS (1 hour) showed normal histology 12 hours post LPS injection.

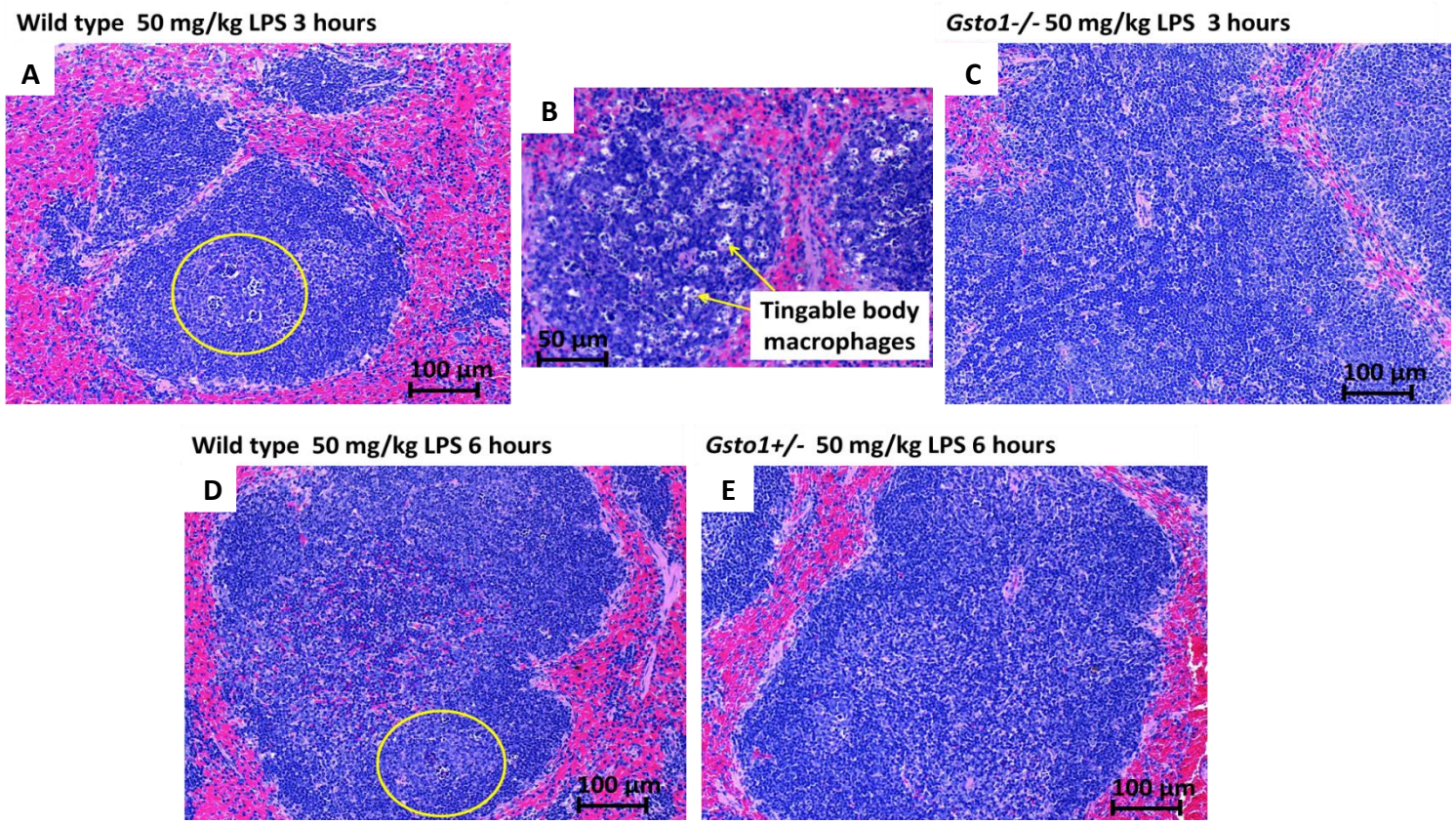

Figure 7.6: Light microscopy showing spleen pathology in *Gsto1*$^{-/-}$ mice.
(A) Wildtype mouse injected with 50 mg/kg LPS shows acute inflammation (highlighted in yellow) within 3 hour post injection. (B) Magnified view of the inflamed pockets reveals tingable body macrophages in wildtype mouse spleen. (C) Gsto1$^{-/-}$ mouse injected with 50 mg/kg LPS (3 hours) showed normal spleen histology. (D) Wildtype mouse injected with 50 mg/kg LPS shows acute inflammation 6 hours post LPS injection while Gsto1$^{-/-}$ mouse showed normal spleen histology (E).

7.3.5 Haematological changes associated with GSTO1-1 deficiency

To characterize the impact of GSTO1-1 deficiency, the haematology profile of *Gsto1*$^{-/-}$ mice was evaluated. Mice (8 weeks of age) (n=4) were left untreated or injected with 50 mg/kg LPS for 12 hours. There were no significant differences in the red blood cell indices of wildtype and *Gsto1*$^{-/-}$ mice left untreated and treated with LPS (Table 7.1). LPS caused a marked reduction in the platelet and total white blood cell counts in both LPS treated groups. The absolute cell count of neutrophils was increased in both the LPS treated groups though there was no notable difference between the wildtype and *Gsto1*$^{-/-}$ mice. Interestingly, though other WBCs including basophils, eosinophils and lymphocytes were depleted in the LPS treated mice (both wildtype and *Gsto1*$^{-/-}$), the monocyte profile was considerably different between the wildtype and *Gsto1*$^{-/-}$ mice. The monocyte count in untreated *Gsto1*$^{-/-}$ mice was significantly lower than the wildtype counterparts under normal physiological conditions. LPS caused a significant depletion in the monocyte cell count in the wildtype mice. In contrast, the monocyte count remained unchanged in LPS treated *Gsto1*$^{-/-}$ mice (Table 7.1). Similarly, eosinophil count in *Gsto1*$^{-/-}$ mice was also lower than the wildtype counts in the untreated groups. In summary, the differential leucocyte counts were affected to a similar extent in both the LPS treated wildtype and *Gsto1*$^{-/-}$ mice. However, the monocyte counts remained unresponsive to LPS in the *Gsto1*$^{-/-}$ mice. Monocytes differentiate into resident macrophages in tissues, which exacerbates inflammation in the affected tissue and are considered the prime cause for septic shock culminating in lethality. Since the data presented in this study thus far demonstrate increased tolerance of *Gsto1*$^{-/-}$ mice to LPS, it is not unexpected that the monocyte counts in *Gsto1*$^{-/-}$ mice did not show any difference on LPS injection. The lower monocyte and eosinophil counts in the *Gsto1*$^{-/-}$ mice under normal physiological conditions is curious and warrants further investigation.

	WT	WT + 50 mg/kg LPS	*Gsto1-/-*	*Gsto1-/-* + 50 mg/kg LPS
WBCP (x10E03 cells/µl)	10.3 ± 1.06	3.4 ± 0.36	9.8 ± 0.44	4.7 ± 0.24
RBC (x10E06 cells/µl)	11.7 ± 0.57	11.6 ± 0.17	11.6 ± 0.31	12.3 ± 0.07
HGB (g/L)	209 ± 9.33	210 ± 2.58	209 ± 6.45	218 ± 2.94
HCT	0.5 ± 0.02	0.5 ± 0.01	0.5 ± 0.01	0.5 ± 0.01
MCV (fl)	45.9 ± 0.91	44.9 ± 0.57	45.9 ± 0.17	44.5 ± 0.43
PLT (x10E03 cells/µl)	934 ± 63.21	613.3 ± 87.69	1013.5 ± 33.97	706 ± 31.99
neutrophils (x10E03 cells/µl)	1.1 ± 0.19	2.4 ± 0.35	0.9 ± 0.05	2.8 ± 0.44
lymphocytes (x10E03 cells/µl)	8.3 ± 0.85	0.6 ± 0.02	8.1 ± 0.42	0.9 ± 0.16
monocytes (x10E03 cells/µl)	0.4 ± 0.05	0.1 ± 0.02	0.2 ± 0.04	0.2 ± 0.04
eosinophils (x10E03 cells/µl)	0.2 ± 0.04	0.1 ± 0.01	0.1 ± 0.01	0.1 ± 0.01
basophils (x10E03 cells/µl)	0.04 ± 0.02	0.005 ± 0.005	0.045 ± 0.03	0.02

Table 7.1: Haematology profile of *Gsto1*$^{-/-}$ mice
WBC: white blood cell count peroxidase method; RBC: red blood cell count; HGB: haemoglobin; HCT: haematocrit; MCV: mean corpuscular volume; PLT: platelet count. Data are presented as mean ±standard error of n=4.

7.3.6 Cytokine profile in LPS treated Gsto1$^{-/-}$ *mice*

The LPS response of *Gsto1*$^{-/-}$ mice was further examined by determining the serum cytokine levels in mice injected with 50 mg/kg LPS. Wild-type mice produced high levels of cytokines TNF-α, IL-6 and IL-1β in response to LPS which peaked in 30-60 minutes (Figure 7.7 A-C). In contrast, the *Gsto1*$^{-/-}$ mice remained relatively unresponsive to LPS and produced significantly lower levels of all three cytokines measured in this study (Figure 7.7 A-C). The peak in serum cytokine levels in the wildtype mice was similar to the trend reported by published data [380, 381]. The data at each time point are based on three mice and duplicate measurements. Additional mice need to be added to this experiment when they become available to address the statistical errors. Since infiltrating macrophages were observed in wildtype mice treated with 50 mg/kg LPS within 6 hours, we determined the expression level of IL-1β in LPS treated liver samples. Increased IL-1β transcript levels were measured in wildtype mice treated with 50 mg/kg LPS for 12 hours (Figure 7.7D). In contrast, IL-1β transcript levels remained un-induced in the livers from *Gsto1*$^{-/-}$ mice suggesting the absence of a pro-inflammatory response in the *Gsto1*$^{-/-}$ mice. The increased survival reported in the *Gsto1*$^{-/-}$ mice treated with LPS may be attributed to the lack of liver necrosis together with the failure to elicit cytokine expression in response to LPS.

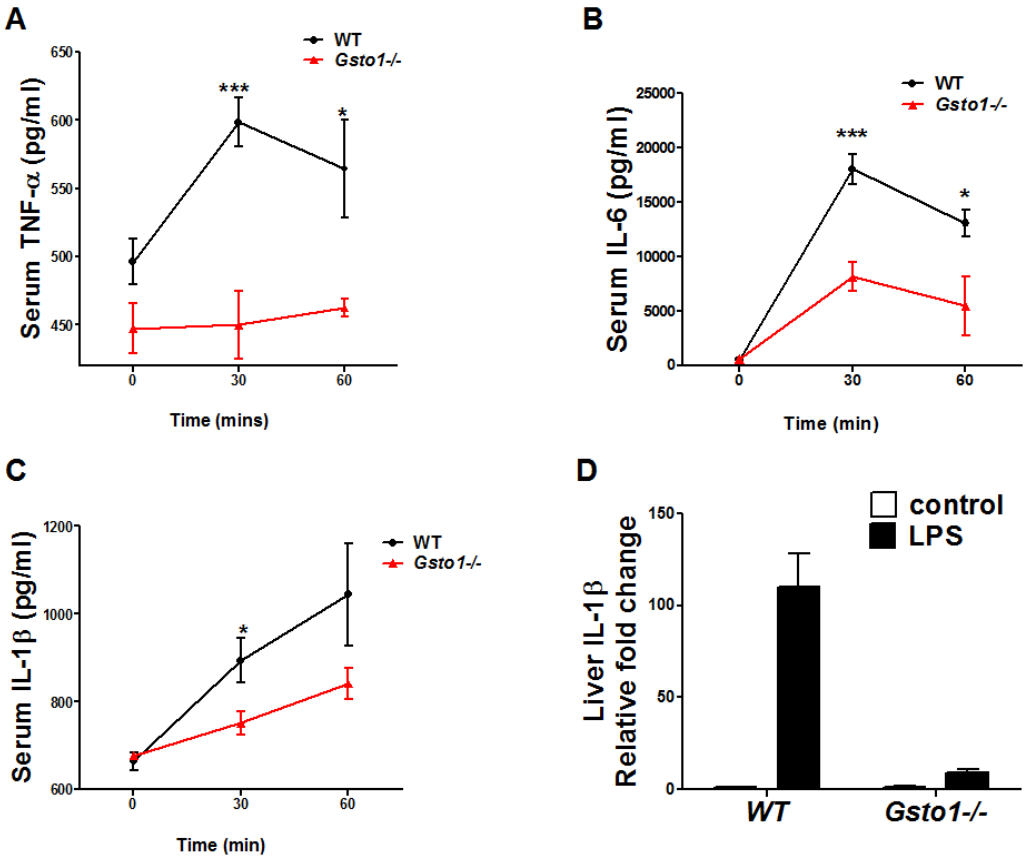

Figure 7.7: Impaired response to LPS in *Gsto1*$^{-/-}$ macrophages.
Mice were injected with 50 mg/kg of *E.coli* O55:B5 LPS for indicated time periods. Concentrations of TNF-α (A), IL-6 (B) and IL-1β (C) in the serum were measured by ELISA. The serum cytokine levels were significantly lower in *Gsto1*$^{-/-}$ mice suggesting hypo-responsiveness of the mice to LPS. (D) IL-1β transcript levels were significantly induced in response to LPS treatment in the liver of wildtype mice. The induction of IL-1β was absent in the *Gsto1*$^{-/-}$ mice. Data are presented as mean ±standard error of n=3.

7.3.7 LPS induced NADPH oxidase 1 transcript levels were attenuated in Gsto1$^{-/-}$ mice

The induction of NOX1 and the resulting increased ROS production in J774.1A macrophages was described in Chapter 5. The study further demonstrated the absence of NOX1 induction in GSTO1-1 deficient macrophages. In order to understand the LPS mediated changes in the liver of LPS injected mice, we determined whether hepatic NOX1 was induced in wildtype and *Gsto1*$^{-/-}$ mice in response to LPS. As shown in Figure 7.8, NOX1 transcription was induced in the liver of wildtype mice injected with 50 mg/kg LPS for 12 hours. However, the NOX1 transcript levels remained unchanged in LPS injected *Gsto1*$^{-/-}$ mice. This result further confirmed the previously reported role of GSTO1-1 in LPS mediated ROS generation via induction of NOX1 (refer Chapter 5).

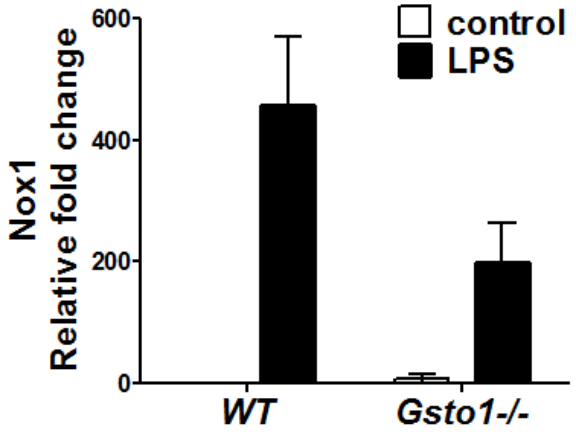

Figure 7.8: Induction of hepatic NADPH oxidase 1 in the liver by LPS is dependent on GSTO1-1. Data are presented as mean ±standard error of n=3.

7.3.8 Anti-oxidant enzyme profile of Gsto1$^{-/-}$ mouse liver remains unaltered in response to LPS

The expression of the rate-limiting enzyme in GSH synthesis, GCLc was previously shown to be inhibited by LPS in macrophages (Chapter 5). GSTO1-1 deficient macrophages were found to be unresponsive to LPS and maintained unchanged levels of antioxidants including GCLc, NQO1 and HO-1 in the presence of LPS. The antioxidant response in *Gsto1*$^{-/-}$ mice post LPS was characterized to determine whether the LPS mediated suppression of Nrf2 driven genes was attenuated in *Gsto1*$^{-/-}$ mice (as observed in GSTO1-1 deficient macrophages).

The transcript levels of all the antioxidant enzymes measured, GCLc, NQO1 and HO-1 were significantly suppressed by LPS (50 mg/kg LPS) in wildtype mouse livers (Figure

7.9A-C). However, the suppression of the transcription of all three Nrf2 driven genes was abolished in the LPS treated *Gsto1*$^{-/-}$ mouse liver which is similar to the trend demonstrated in GSTO1-1 deficient J774.1A macrophages. Interestingly, the transcript levels of GCLc and NQO1 were notably lower in untreated *Gsto1*$^{-/-}$ mouse livers (Figure 7.9A-C). This was not unexpected given the previous finding that the protein expression of most Nrf2 driven GSTs such as GSTA1/2, GSTT1, GSTT2, and GSTA3 were markedly decreased in *Gsto1*$^{-/-}$ mouse livers (Figure 7.3). The data taken together suggest the regulation of Nrf2 induced antioxidant enzymes may be dependent on the expression of GSTO1-1.

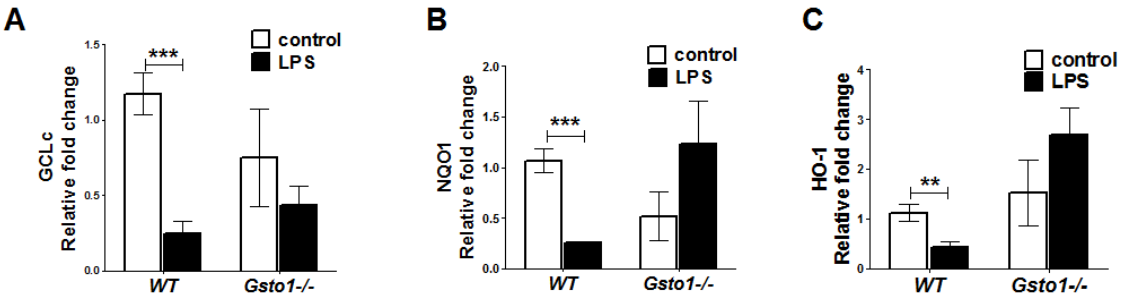

Figure 7.9: Suppression of LPS mediated hepatic antioxidants is abolished in *Gsto1*$^{-/-}$ mice

Transcription of hepatic GCLc (A), NQO1 (B) and HO-1 (C) were significantly suppressed in wildtype mice. The transcript levels of the antioxidants were consistently lower in *Gsto1*$^{-/-}$ mouse liver and remained unaltered post LPS treatment. Data are presented as mean ± standard error of n=3.

7.3.9 ML175 inhibits TLR4 mediated cytokine expression in bone marrow derived macrophages (BMDMs)

Since *Gsto1*$^{-/-}$ mice did not suffer from LPS induced endotoxic shock and even the heterozygote *Gsto1*$^{+/-}$ mice were partially protected, we investigated the possibility that the GSTO1-1 inhibitor ML175 would suppress the production of pro-inflammatory cytokines in primary wildtype BMDMs.

Media concentrations of inflammatory cytokines including IL-6 and pro-IL-1β were measured after LPS challenge in BMDMs derived from wildtype mice. The cells were treated with ML175 as described in Chapter 5 followed by LPS stimulation. As shown in Figure 7.10A, ML175 inhibited IL-6 secretion in wildtype primary BMDMs in a dose dependent manner. Since the effect of ML175 on primary BMDMs is similar to that

measured previously in ML175 treated J774.1A macrophages (Chapter 5 Figure 5.4), it is reasonable to conclude that the J774.1A GSTO1 knockdown cell line is a suitable model to study the mechanism of action of GSTO1-1. The specificity of ML175 for TLR4 inhibition was further investigated by measuring cytokine secretion on activation of TLR1/2, TLR7 and TLR9 in primary BMDMs. IL-6 expression determined by ELISA showed no difference in the levels of IL-6 in ML175 treated BMDMs when stimulated with PAM3CSK4 (TLR1/2), R848 (TLR7) or CpG (TLR9). However a moderate decrease in IL-6 expression was observed in TLR7 activated macrophages at higher doses of ML175 (Figure 7.10B-D). Furthermore, the expression of parental pro-IL-1β was determined in ML175 treated BMDMs as well. The expression of pro-IL-1β was significantly inhibited in ML175 treated BMDMs, confirming that TLR4 signalling are targeted by ML175 (Figure 7.10E). Signalling downstream of NF-κB resulting in the activation of MAPKK and MAPK eventually leading to the phosphorylation of p38 was also blocked in ML175 treated macrophages (Figure 7.10F).

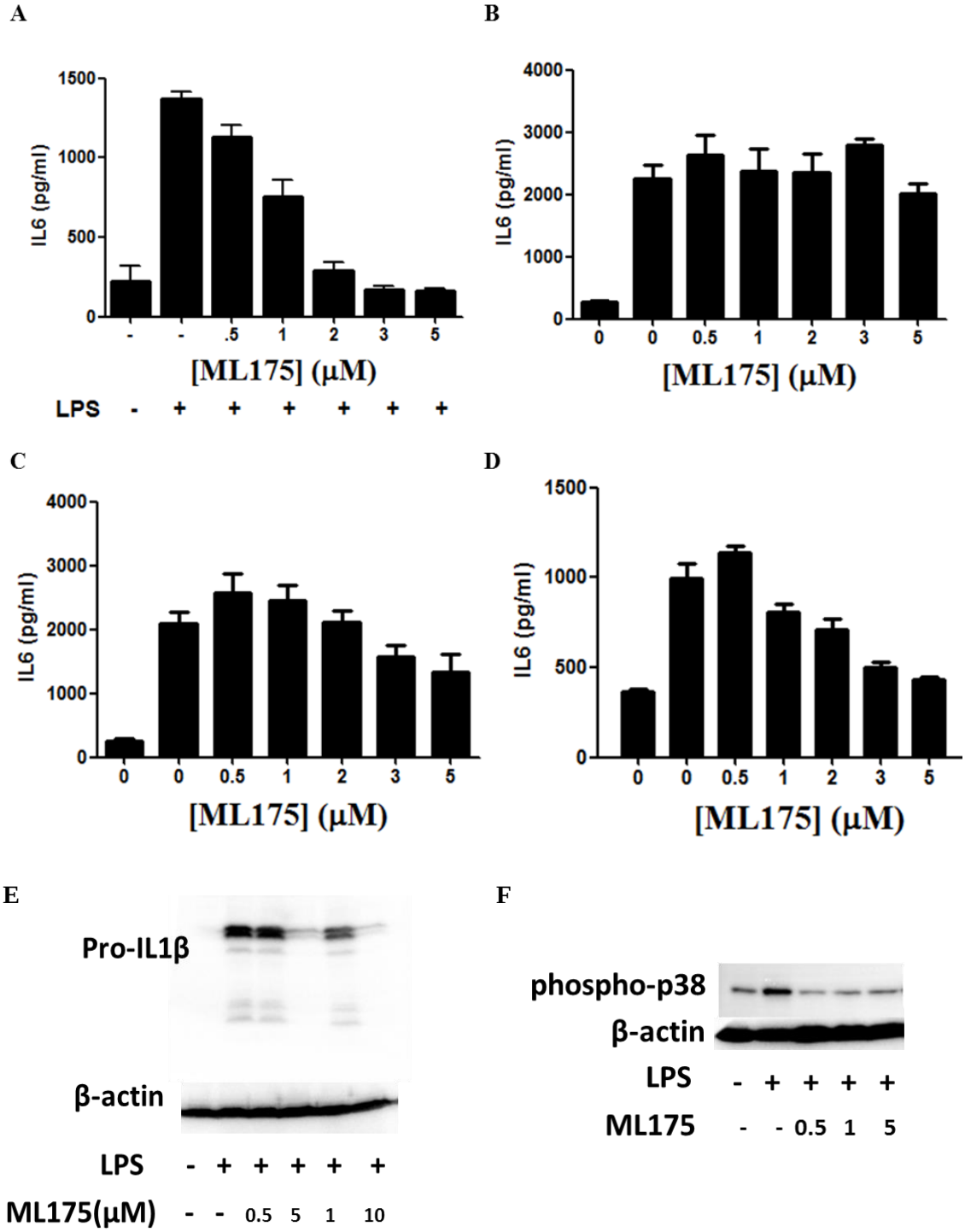

Figure 7.10: ML175 inhibits TLR4 activation in primary bone marrow derived macrophages

(A) LPS induces the expression of IL-6 via TLR4. TLR1/2 (B), TLR7 (C) and TLR9 (D) dependent IL-6 expression remained unchanged when the BMDMs were stimulated with their respective ligands. (E) Activation of pro-IL-1β by LPS is significantly attenuated in ML175 treated BMDMs. (F) Activation/phosphorylation of p38 by MAPK was blocked in ML175 treated macrophages. Data are presented as mean ±standard error of n=3. Immunoblots are representative of three replicates.

7.3.10 GSTO1-1 deficiency suppresses Nrf2 driven antioxidant enzyme expression in the liver under normal physiological conditions

The relatively lower constitutive expression of antioxidant enzymes including GSTA1/2, GSTT1 and GSTT2 in *Gsto1*$^{-/-}$ mice was an unexpected finding. Since the constitutive and butylated hydroxyanisole (BHA) inducible expression of these antioxidants is known to be dependent on transcriptional activation by Nrf2 [388, 389], the responsiveness of *Gsto1*$^{-/-}$ mice to Nrf2 inducer BHA was determined. Mice were fed BHA supplemented chow for 14 consecutive days and the food intake was monitored daily. Though a previous report suggested inconsistency in food consumption in BHA treatment groups due to the taste of dietary BHA [390], this study recorded comparable consumption rates of BHA supplemented chow by wildtype and *Gsto1*$^{-/-}$ mice (Figure 7.11A). Female mice were used in this experiment based on previous studies on the differential regulation of Nrf2 between sexes [388, 389]. Expression of Nrf2 driven GSTs including GSTA1/2, GSTA4, GSTT1, and GSTT2 in the livers of female wildtype and *Gsto1*$^{-/-}$ mice showed significant induction with BHA (Figure 7.11B-C). Additionally, the expression of other Nrf2 dependent genes such as NQO1 and glutathione synthesis protein GCLm also showed considerable induction with BHA suggesting that the inducible expression of Nrf2 driven antioxidants by dietary BHA in the liver is not dependent on the expression of GSTO1-1 (Figure 7.11B). Due to unexpected difficulties in breeding of the *Gsto1*$^{-/-}$ mice, the availability of mice was restricted and hence the number of mice used in this experiment was limited to 2/group.

7.4 Discussion

The role of GSTO1-1 in inflammatory signalling activated via TLR4 in J774.1A macrophages was extensively described in the previous chapters. We generated *Gsto1*$^{-/-}$ mice in order to further investigate the physiological relevance of the downstream effects of GSTO1-1 deficiency *in vivo*. The phenotype of *Gsto1*$^{-/-}$ mice including body weight and organ weight were found to be comparable to the wildtype mice. The expression of other GSTs in the *Gsto1*$^{-/-}$ mice was also evaluated to confirm the specificity of the targeted knockout approach employed to generate the *Gsto1*$^{-/-}$ mice and to determine whether the knockout of Gsto1 resulted in the induction of other GSTs, a trend observed previously in Gstz1$^{-/-}$ mice [386].

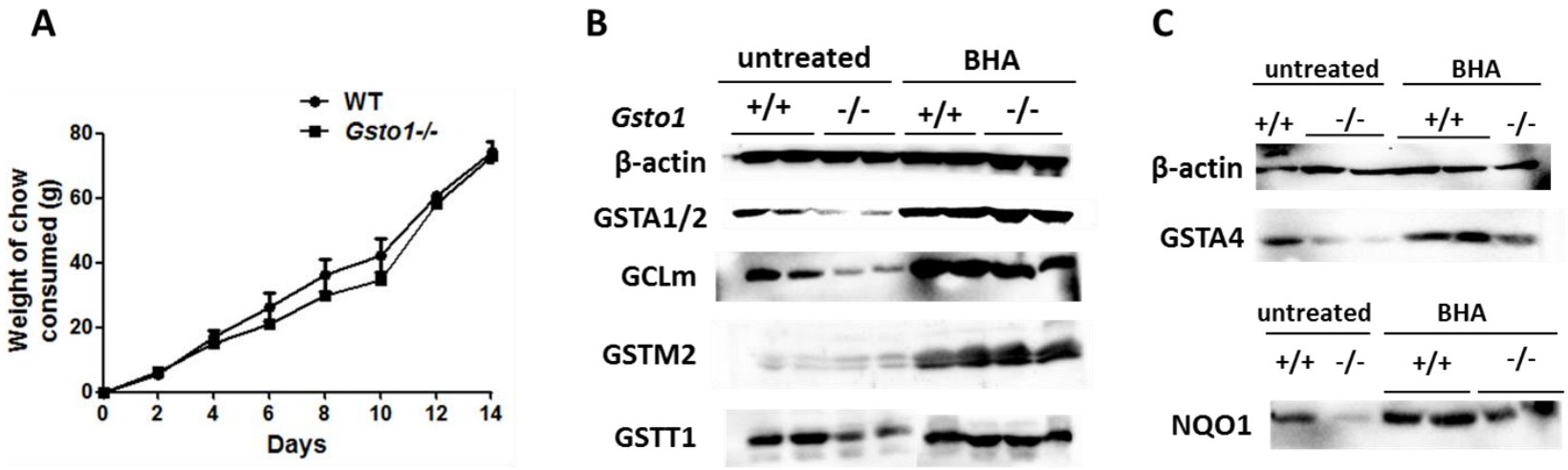

Figure 7.11: Induction of Nrf2 driven genes by butylated hydroxyanisole (BHA) (n=2)
(A) Consumption of BHA supplemented chow was comparable between the wildtype and *Gsto1*$^{-/-}$ mice. (B) Wildtype and *Gsto1*$^{-/-}$ mice fed on a BHA supplemented diet for two weeks showed remarkable induction of Nrf2 driven antioxidants including GSTA1/2, GSTT1, GCLm and GSTM2 in the liver. (C) Nrf2 dependent expression of GSTA4 and NQO1 were also induced in the liver lysates from wildtype and *Gsto1*$^{-/-}$ mice to a similar extent.

Unlike the Gstz1$^{-/-}$ mice, the *Gsto1*$^{-/-}$ mice were found to express a few GSTs, namely GSTA1/2, GSTT1 and GSTT2 in lower abundance in the liver lysates compared to their wildtype counterparts. A previous study by Hayes *et al.* reported a similar trend in GST expression in Nrf2$^{-/-}$ mice, which was more pronounced in females than in the males [388]. Here, we show a similar gender-based difference in the expression of GSTA1/2, GSTT1 and GSTT2. Since Nrf2 has been shown to be regulated by the glutathionylation of its interacting protein Keap-1 [391], it is speculated that the redox state of Keap-1 may be modulated by GSTO1-1 which in turn resulted in the differential expression of GSTs in the *Gsto1*$^{-/-}$ mouse livers. This was further supported by the finding that a non-GST Nrf2 driven gene, NQO1 also showed lower expression levels in *Gsto1*$^{-/-}$ mice. To further investigate this theory, *Gsto1*$^{-/-}$ mice and their wildtype littermates were placed on a BHA supplemented diet for 2 weeks. Since BHA is a potent inducer of Nrf2 signalling, it was hypothesized that while the GST profile would be induced in the wildtype mice, the expression levels would remain unaltered in the *Gsto1*$^{-/-}$ mice as seen in the Nrf2$^{-/-}$ mice [388, 389]. Though the lower expression levels of GSTs and NQO1 remained consistent across *Gsto1*$^{-/-}$ mice, the BHA fed mice showed comparable induction of the tested Nrf2 driven enzymes proving the hypothesis false. However, due to restricted animal numbers used in this study and the lack of analysis of the Keap-1/Nrf2 association and subsequent Nrf2 nuclear localization, this study remains inconclusive and warrants further investigation.

Since GSTO1-1 deficient macrophages were unresponsive to TLR4 activation by LPS, the susceptibility of *Gsto1*$^{-/-}$ mice to LPS induced systemic inflammation was evaluated. This study was divided into two independent parts:

- Survival rate of *Gsto1*$^{-/-}$ mice injected with a sub-lethal doses of LPS (5 mg/kg and 10 mg/kg) was compared to their wildtype counterparts
- A time line was constructed to examine LPS induced tissue damage and the extent of inflammation in mice treated with a lethal dose of 50 mg/kg LPS for up to 12 hours.

Comparison of the survival rates of Gsto1$^{-/-}$ *mice versus Gsto1*$^{+/+}$*:*

In the 5 mg/kg LPS treatment group, the wildtype mice showed a higher lethality rate with all the mice being euthanized in 24-96 hours while mice from *Gsto1*$^{+/-}$ and *Gsto1*$^{-/-}$ treated groups survived the sub-lethal dose of LPS. In the 10 mg/kg LPS treatment group, the wildtype and *Gsto1*$^{+/-}$ mice showed similar survival rates but the *Gsto1*$^{-/-}$

homozygotes tolerated the higher dose as well. The survival rate and body temperature curve of the heterozygotes was found to lie in between those of the wildtype and the *Gsto1*$^{-/-}$ mice. The observation that heterozygotes showed partial protection from LPS mediated inflammation strongly suggests that the inhibition of GSTO1-1 by synthetic compounds could provide a novel avenue for drug development targeting TLR4 associated inflammatory disorders such as rheumatoid arthritis.

Time course of LPS treatment:

To further understand the progression of TLR4 mediated inflammation in *Gsto1*$^{+/+}$ and *Gsto1*$^{-/-}$ mice, mice were injected with 50/kg LPS and euthanized at different time points ranging from 0.5 hours-12 hours. Since cytokine expression and ROS production peak immediately after exposure to LPS [380, 381], it was necessary to accommodate shorter time points in the study. The parameters analysed over 12 hours included:

a. *Histological changes in affected tissues such as liver and spleen:*

   Liver and spleen were the primary tissues that showed signs of LPS induced damage. Analysis of tissue sections revealed significant necrosis and inflammation in the liver of wildtype mice. The extent of damage in the heterozygote mice varied from minimal to none. The *Gsto1*$^{-/-}$ mice showed no necrosis or inflammation suggesting that they were tolerant to LPS induced sepsis. The spleen in wildtype mice showed pockets of inflammation and the occurrence of 'Tingable macrophages' was prominent (a sign of acute inflammation). The *Gsto1*$^{-/-}$ mice showed no significant changes in the spleen morphology supporting the results obtained from the survival rate experiments and confirming that GSTO1-1 is required for TLR4 a mediated inflammatory response

b. *Serum cytokines induced in response to LPS:*

   The serum TNF-α, IL-6 and IL-1β levels were significantly induced in the wildtype mice within 30-60 minutes. The immediate peak in TNF-α and IL-6 levels in response to LPS was largely absent in the *Gsto1*$^{-/-}$ mice. The serum cytokine levels observed in Gsto1$^{-/-}$ mice confirmed the results obtained from the GSTO1-1 deficient J774.1A cells and provides conclusive data that GSTO1-1 deficiency impairs TLR4 mediated cytokine signalling *in vivo*.

c. *Alterations in the haematology indices:*

   The haematology profile of the *Gsto1*$^{-/-}$ mice was similar to the wildtype mice with no notable difference in the individual blood counts except for the

monocyte counts which were markedly depleted in normal *Gsto1*$^{-/-}$ mice. It is interesting to note that while the wildtype and *Gsto1*$^{-/-}$ mice showed comparable decrease in the differential cell counts of leucocytes in response to LPS (12 hours 50 mg/kg), the monocyte counts remained unaffected in LPS treated *Gsto1*$^{-/-}$ mice for reasons not fully understood. It is important to note that monocytes differentiate into resident macrophages found in the different tissues and thus the difference in the precursor cell count may contribute to the unique inflammatory profile observed in the *Gsto1*$^{-/-}$ mice.

d. Modulation of the oxidant/antioxidant axis due to LPS induced ROS generation:

ROS production in response to LPS is an immediate event triggered via the induction of NOX1 (cytosolic source) and from the mitochondria as previously described in Chapter 5-6. Excessive ROS generation in response to inflammatory stimuli such as LPS acts not only as an anti-bacterial response but has also been shown to exacerbate inflammation associated tissue damage [8, 147, 148, 341, 344, 376]. Since the oxidant/antioxidant axis is tightly regulated to enhance ROS production via the suppression of antioxidants and the deficiency of GSTO1-1 abolished this response in LPS treated macrophages, the oxidant and antioxidant levels were determined in the liver tissue of *Gsto1*$^{-/-}$ mice. NOX1 transcription was induced over 100-fold in the liver of wildtype mice while the induction was significantly blocked in the *Gsto1*$^{-/-}$ mouse livers. Complementing the increased oxidant levels, the transcript levels of GCLc, NQO1 and HO-1 were suppressed in the liver of wildtype mice (to enhance ROS production) while the *Gsto1*$^{-/-}$ mice showed no change in the antioxidant levels suggesting the absence of ROS in the liver. The increased NOX1 levels and consequently ROS generation may be a major contributor to the severe necrosis observed in the liver sections obtained from the LPS treated wildtype mice. Due to technical difficulties associated with the detection of ROS (both cytosolic and mitochondrial) in tissues, the total ROS produced in the liver samples was not quantified.

It is interesting to note that though Srx and GSTO1-1 are efficient deglutathionylating enzymes, the deficiency of the two proteins appears to have opposite downstream consequences *in vivo*. Planson *et al.* (2011) have reported that though *Srx*$^{-/-}$ mice have no phenotypical abnormalities under normal physiological conditions, the mice are hyper-responsive to LPS [392]. The pro-inflammatory responses in *Srx*$^{-/-}$ mice were delayed by several hours (20 hours) but remained intense even after the inflammatory

responses subsided in the wildtype mice. However, further investigations revealed that the deficiency of Srx in mice resulted in the constitutive inhibition of the anti-oxidant activity of Prx2. As described in sections 1.3.2(a) and 1.4.5, the sulfinylated form of Prdx2 is functionally inactive and is reduced to the active form specifically by Srx. The absence of Srx in the mice resulted in the inactivation of Prdx2 and subsequently led to the exacerbation of LPS mediated ROS accummulation over a period of time causing the reported delay in inflammatory responses and lower survival rates in the *Srx*$^{-/-}$ mice. Additional experiments identified gene expression changes occurring in the *Srx*$^{-/-}$ mice that were typical of the wildtype mice except that the changes were also induced in the late stages rather than in the early phase of the pro-inflammatory responses. In contrast, *Gsto1*$^{-/-}$ are unresponsive to LPS indicating the absence of an early/immediate response to the presence of LPS. Since our in vitro data on macrophages revealed a significant attenuation in ROS generation in GSTO1-1 deficient macrophages, it is not unreasonable to speculate that the in vivo oxidant/anti-oxidant status of *Gsto1*$^{-/-}$ mice will be similar to the *Srx*$^{-/-}$ mice. However, the mechanism and pathway targeted by the absence of Srx is most likely unrelated to the mechanism(s) modulated by GSTO1-1. Our findings strongly support the hypothesis that GSTO1-1 is required upstream of the TLR4 pathway, possibly at or immediately downstream of TLR4.

Due to unavoidable delays in the generation and breeding of the *Gsto1*$^{-/-}$ mice, the tolerance of *Gsto1*$^{-/-}$ mice to LPS was not fully characterized and work is currently in progress to investigate the mechanism by which *Gsto1*$^{-/-}$ mice remain unresponsive to LPS. The inflammatory profile of *Gsto1*$^{-/-}$ mice is yet to be fully understood and the specificity of GSTO1-1 to TLR4 *in vivo* needs to be demonstrated. In parallel, the specificity of GSTO1-1 to TLR4 *in vivo* will be studied by administering the small molecule inhibitor of GSTO1-1, ML175, *in vivo*. The data gathered in this study demonstrated that ML175 is a potent inhibitor of TLR4 signalling in wildtype bone marrow derived macrophages. However, higher doses of ML175 were found to inhibit TLR9 and TLR7 although to a lesser extent. Thus this study recognizes the need for the development of more specific and potent inhibitors of GSTO1-1 for *in vivo* applications. The observation that the response of *Gsto1*$^{+/-}$ heterozygote mice to LPS was in between the wildtype and *Gsto1*$^{-/-}$ mice and the finding that ML175 can inhibit the expression of pro-IL-1β in a dose dependent manner, strongly suggests the potential for a novel avenue for the therapeutic applications for GSTO1-1 inhibitors.

CHAPTER 8

Redox modulation of TLR4 signalling: Cysteines in MAL are critical for TLR4 activation by LPS

8.1 Introduction

Recent studies have shown that GSTO1-1 catalyses the glutathionylation cycle. Our current results show that GSTO1-1deficiency increases the overall level of protein glutathionylation (Chapter 4). The data in Chapter 4 also indicate that there may be some specificity in the proteins that are deglutathionylation substrates for GSTO1-1. A number of studies have suggested that protein glutathionylation can provide a reversible switch that can regulate protein function and potentially regulate pathways in a manor analogous to protein phosphorylation [67, 69, 75, 129, 305]. Since the GSTO1-1 inhibitor ML175 has recapitulated all the effects of *Gsto1* knockdown in Chapters 5 and 6 it was reasonable to speculate that GSTO1-1 may regulate the TLR4 pathway by the reversible glutathionylation of key protein(s). Previous studies have shown that TRAF6, Iκκβ, NF-κβ and Caspase 1 within the TLR4 signalling and IL-1β release pathways can be glutathionylated and therefore may be targets for GSTO1-1 mediated regulation [61, 64, 118, 160]. However, the results in chapters 5 and 6 indicate that the regulation of TLR4 signalling by GSTO1-1 appears to occur upstream of these proteins. TLR4 activation by LPS requires the recruitment of adaptor proteins (Figure 1.9) called MyD88 and MyD88 adaptor like protein (MAL), collectively called the Myddosome complex [361, 393]. The inhibition of IRAK4 phosphorylation in GSTO1-1 deficient cells (Chapter 5) and the common effect of GSTO1-1 deficiency on parallel activation pathways strongly suggest that the target or site of action of GSTO1-1 is a component of the Myddosome complex.

Since MyD88 is shared among all TLRs it seems unlikely that it is the target of GSTO1-1 as signalling via most TLRs is not dependent on GSTO1-1 (Chapter 4). Since MAL is specific to TLR4 and TLR1/2, the glutathionylation of MAL was evaluated to determine if LPS altered the glutathionylation of MAL and if GSTO1-1 was required to catalyse the reaction.

Based on the previously published crystal structure of MAL, there are eight cysteine residues of which two pairs have been predicted to be engaged in disulphide bonds with one another and of the remaining four, two residues are exposed on the protein surface and hence may be susceptible to oxidative stress induced modifications [282]. The two exposed cysteine residues C91 and C157 are more than 5Å apart and hence are unlikely to interact with one another via a disulphide bond unless there are conformational changes in solution that are not evident in the crystal structure. Thus, it is possible that GSTO1-1 may modulate the glutathionylation state of cysteines C91 and C157 and disrupt the recruitment and interaction of MAL with TLR4 or MyD88. The inability of MAL to form the Myddosome complex could contribute to all aspects of the GSTO1-1 dependent TLR4 signalling phenotype observed in macrophages and *Gsto1* knockout mice in Chapters 4, 5 and 6. In this Chapter the role of cysteines C91 and C157 in MAL function and their susceptibility to glutathionylation or deglutathionylation by GSTO1-1 has been investigated.

8.2 Materials and methods

8.2.1 Materials

Purified proteins MAL, C157A MAL and C91A MAL were kind gifts from Prof. Bostjan Kobe, University of Queensland, Australia. plasmids pMAL, pC157A MAL, pEV, pC91A, pC91A/C157A were provided by Prof. Luke O'Neill, Trinity College, Dublin. GSTO1-1 and its allelic variants were expressed and purified as described in Chapter 2.

8.2.2 Cell culture

HEK293/TLR4/MD2 cells were maintained in DMEM media with 10% FBS, 2 mM glutamine and a cocktail of antibiotics (HG Gold/Blasticidin/Normomycin). J774.1A cells were maintained as described previously. HEK293T cells were grown in DMEM media with 10% FBS and 2 mM glutamine.

8.2.3 Peptide synthesis

The peptide sequence 'QDPW**C**KYQ' was synthesized by ChinaPeptides Co. Ltd. (Shanghai, China). The peptide was glutathionylated and purified by HPLC at the BRF, JCSMR,ANU.

8.2.4 In vitro deglutathionylation assay

10 µg of purified wildtype MAL (WT MAL), C157A MAL and C91A MAL were precipitated in ice cold acetone at -20°C overnight to remove DTT in the protein buffer. The proteins were resuspended in 20 mM tris pH 8.0 and glutathionylated with 10 mM GSSG for 1 hour at 37°C. The excess GSSG was removed by repeating the precipitation step. The proteins were resuspended in 20 mM tris pH 8.0 and incubated with 1µg of GSTO1-1 for indicated time points at 37°C. The reaction was stopped by adding 4X Laemmli sample loading buffer and the two proteins were separated on a 4-12% gradient gel (Biorad) using the Biorad iBolt system due to the similar molecular weights of MAL and GSTO1-1. The proteins were transferred onto a nitrocellulose membrane and probed for glutathionylation using anti-glutathione and GSTO1-1 using our in-house rabbit anti-GSTO1-1 serum. The membranes were developed as previously described in Chapter 2.

8.2.5 Transfections

HEK293/TLR4/MD2 cells were transfected using Genejuice (Millipore). Cells were seeded at a density of $3X10^5$ cells/well in 6-well dishes and incubated overnight in supplemented DMEM media. On the day of transfection, indicated plasmids and transfection reagent were added in a 3:1 ratio in serum free media and incubated for 15 minutes at room temperature. The transfection mix was added to each well drop-wise and the cells were incubated for 24-48 hours. LPS was added to cells 24 hours post transfection and incubated further for 24 hours (wherever indicated).

8.2.6 NF-κB luciferase assay

HEK 293T cells were transfected with 60ng of plasmid encoding NF-κB luciferase and 20ng of plasmid encoding Thymidine kinase (TK) promoter driven renilla luciferase control reporter gene as described above using Genejuice in 96-well flat bottom plates. Plasmids encoding wildtype MAL, C157A MAL, C91A MAL and empty vector (pEV) were co-transfected with the NF-κB/renilla plasmids in triplicates in concentrations ranging from 0 - 80ng. 24 hours post transfection, the media was removed from each well and cells were lysed in 1X Passive lysis buffer and luminescence was measured as per manufacturer's instructions (Promega Glomax Dual reporter luciferase assay kit). All luciferase readings were normalized to their respective TK renilla luciferase readings.

8.2.7 Cysteine oxidation detection assay

The sulfenic acid form of cysteines was detected using a biotin conjugated DCP probe (Millipore). HEK 293/TLR4/MD2 cells were seeded in 10 cm culture dishes overnight and treated with LPS for 24 hours. Cells were washed with PBS and lysed in 1 mM DCP-Bio1. The lysates were centrifuged at 16000 x g for 10 minutes to remove cell debris and incubated on ice for 2 hours. Unreacted DCP-Bio1 was removed by precipitating the proteins in ice cold acetone at -20°c overnight. Proteins were resuspended in 1% SDS lysis buffer. DCP-Bio1 bound proteins were pulled down using streptavidin beads and immunoblotted as before. Over expressed MAL proteins were probed with a rabbit anti-HA antibody (Sigma).

8.3 Results

8.3.1 In vitro deglutathionylation of MAL by GSTO1-1

The Myddsosome complex is comprised of TLR4, adaptor proteins MyD88 and MyD88 adaptor like protein (MAL). Since MyD88 is common to most TLRs and MAL is specific to TLR4 and TLR1/2, we decided to investigate the 'active' state of MAL in LPS stimulated *Gsto1* knockdown cells. Since LPS induces oxidative stress in macrophages as an anti-microbial response, it is not unreasonable to hypothesize that the ROS generated may modulate the redox state of proteins in the TLR4 pathway. To determine if GSTO1-1 can catalyse the deglutathionylation of MAL, a synthetic peptide representative of the flanking sequence surrounding cysteine 157 (C157) of MAL 'QDPW**C**KYQ' was synthesized. The peptide was artificially glutathionylated as described previously and the ability of GSTO1-1 to deglutathionylate the peptide was determined by measuring the fluorescence emitted by the adjacent tryptophan as glutathione was removed from the cysteine residue. Wildtype GSTO1-1 (A140) deglutathionylated the modified cysteine residue in MAL more efficiently than the D140 GSTO1-1 polymorphic variant (Figure 8.1A). A similar study of Cys 91 was not undertaken because a suitable reporter tryptophan residue was not present in the natural sequence. In additional studies, we tested the ability of GSTO1-1 to deglutathionylate artificially glutathionylated MAL (whole protein) by incubating the two proteins together for increasing time periods. The deglutathionylation of cysteines in MAL was studied with whole purified wildtype MAL and two cysteine mutants C157A and C91A. All three proteins were glutathionylated to a similar extent by incubation with GSSG (Figure 8.1B Time 0). As shown in Figure 8.1B, GSTO1-1 deglutathionylated wildtype MAL within 60 minutes (Figure 8.1B middle panel). MAL mutants bearing single mutations of the two cysteine residues C91 and C157 were found to be highly unstable

in solution and degraded over time at 37°C (Figure 8.1B lower panels). Consequently it was not possible to determine if there were differences in the rate of deglutathionylation of these specific residues.

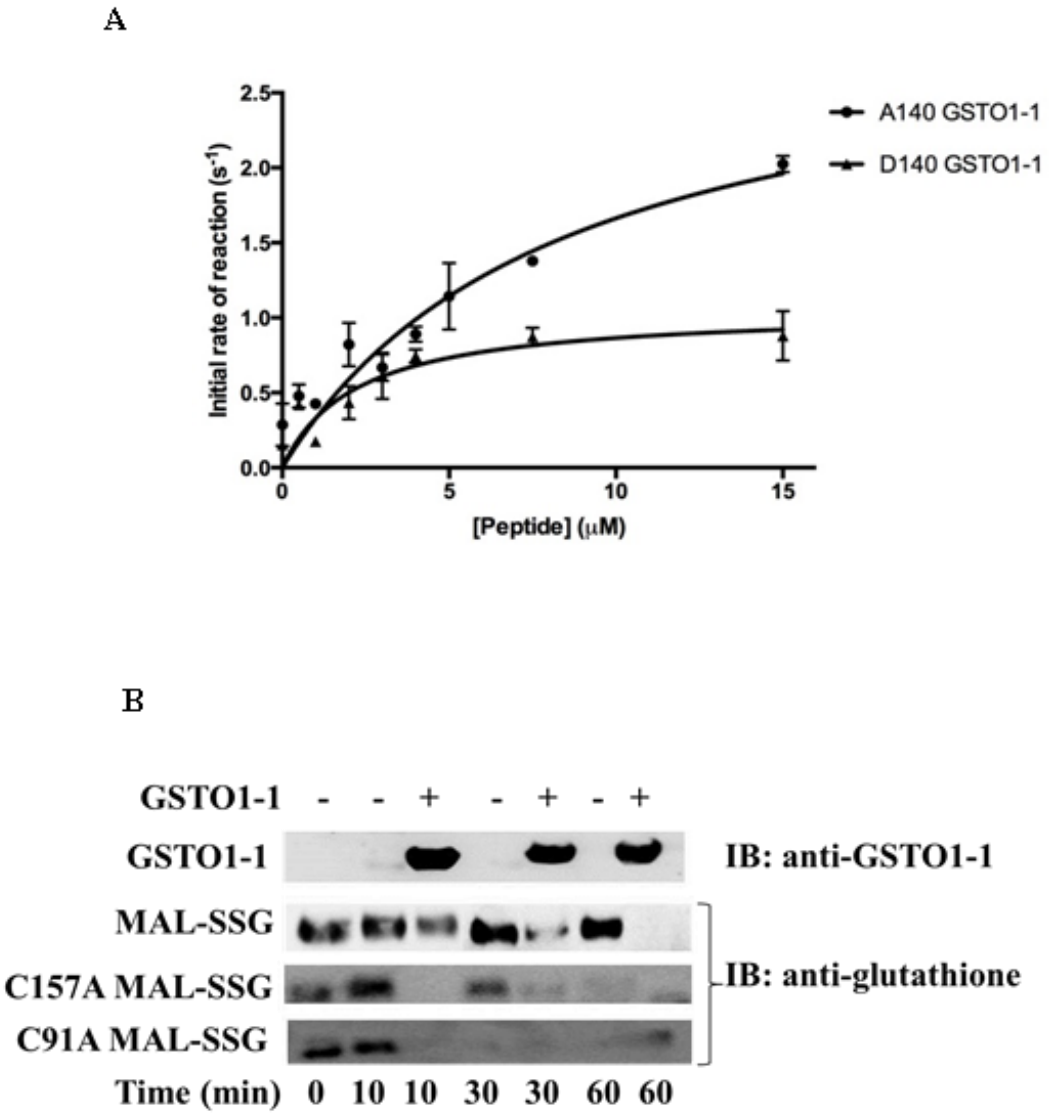

Figure 8.1: *In vitro* deglutathionylation of MAL by GSTO1-1
(A) A peptide sequence spanning MAL residues 'QDPW**C**KYQ' (153-160) was synthesized and glutathionylated at Cys 157 artificially. The intrinsic fluorescence of the Trp residue adjacent to C157 increased significantly in the presence of wildtype GSTO1-1 and to a lesser extent with the D140 allelic variant of GSTO1-1, as a result of the deglutathionylation of C157. (B) Purified MAL, C91A MAL and C157A MAL were glutathionylated and incubated with GSTO1-1 for indicated time periods. The glutathionylation levels of the blotted MAL proteins were detected with an anti-glutathione antibody. Wildtype MAL was enzymatically deglutathionylated by GSTO1-1 in 60 minutes.

8.3.2 Cysteines are critical for MAL to function as an adaptor for TLR4 activation

MAL function was quantitatively assessed by its ability to drive the expression of luciferase from a NF-κB reporter construct. HEK293T cells were co-transfected with NF-κB driven luciferase reporter construct, a TK renilla luciferase coding construct (internal control) and with increasing concentrations of pMAL or MAL cysteine mutants C91A, C157A and a C91A/C157A double mutant in order to determine if mutations in the cysteine residues affect MAL function. The stable expression of wildtype MAL and the cysteine mutants was confirmed by immunoblotting for the HA-tagged protein in whole cell lysates extracted from transfected HEK293T cells (Figure 8.2A). As shown in Figure 8.2B, wild type MAL was sufficient to activate NF-κB transcription indicated by the expression of luciferase. The C91A mutant failed to elicit a similar response suggesting that C91 is critical for the activity of MAL while the C157A mutant was able to drive NF-κB expression to a small extent that was significantly lower than wildtype MAL. As expected, expression of the double mutant also failed to activate NF-κB expression.

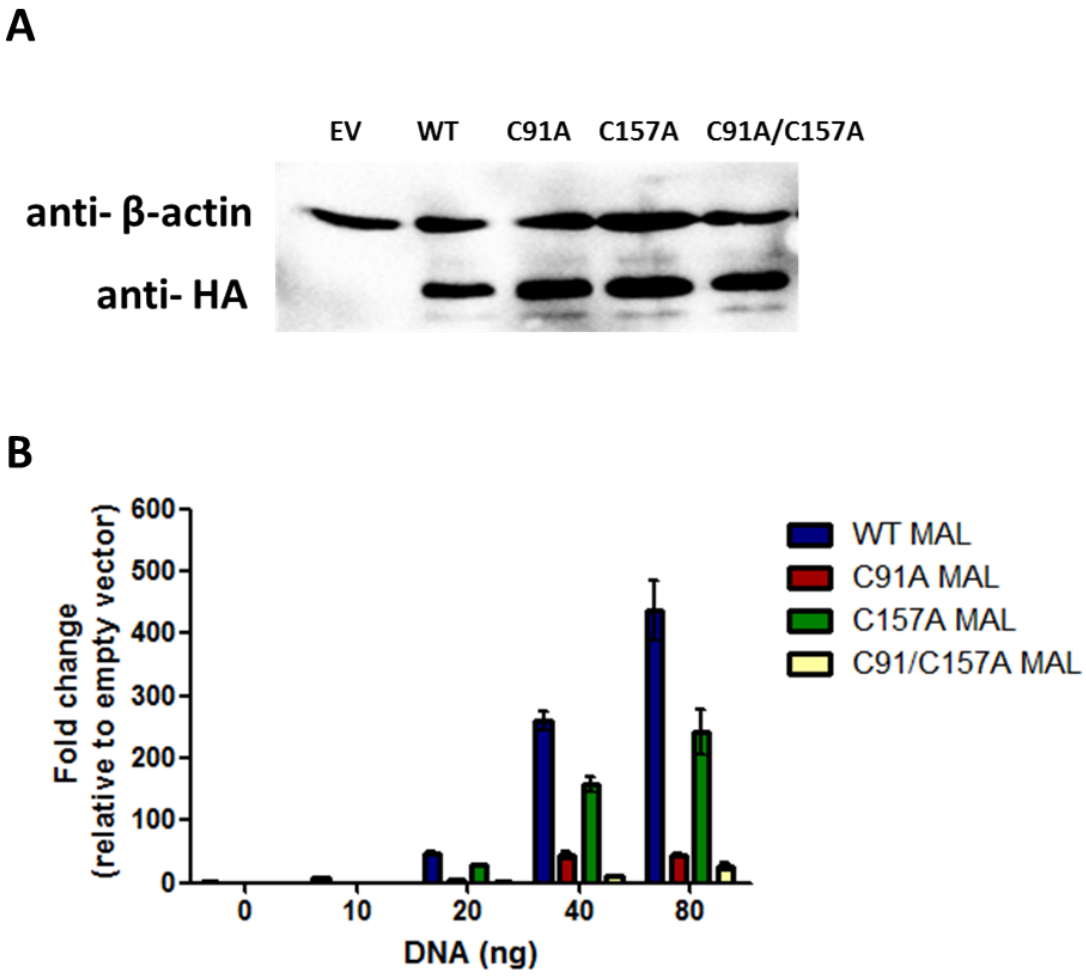

Figure 8.2: Functional relevance of cysteine modifications in MAL
(A) Over expression of MAL and the cysteine mutant encoding plasmids in HEK 293T cells. (B) Expression of wildtype MAL was sufficient to switch on the expression of NF-κB promoter-driven luciferase reporter gene but the single mutant C91A, failed to activate the reporter gene transcription in HEK293T cells while the C157A mutant had a significantly lower activity at higher DNA concentrations. Mutating both cysteine residues abolished the activity of MAL completely.

8.3.3 LPS induced glutathionylation of MAL is dependent on GSTO1-1

Recent structural analysis of the Toll/interleukin-1 receptor homology domain (TIR) of MAL has revealed several cysteines that are likely to be susceptible to oxidation and/or post translational modifications [282] . In this study MAL and its mutants C91A, C157A and C91A/C157A were tagged with HA and expressed in HEK 293/TLR4/MD2 and immunoprecipitated under non-reducing conditions to determine the glutathionylation state of MAL cysteines. Wildtype MAL was heavily glutathionylated in the cells irrespective of TLR4 activation with LPS while the individual cysteine mutants and the double mutant C91A/C157A were glutathionylated to a lesser extent (Figure 8.3A).

Glutathionylation of endogenous MAL was detected in J774.1A non-silencing control cells after LPS stimulation (Figure 8.3B-C). In contrast MAL was only weakly glutathionylated in GSTO1-1 deficient cells after LPS stimulation suggesting that GSTO1-1 is required for the glutathionylation of MAL.

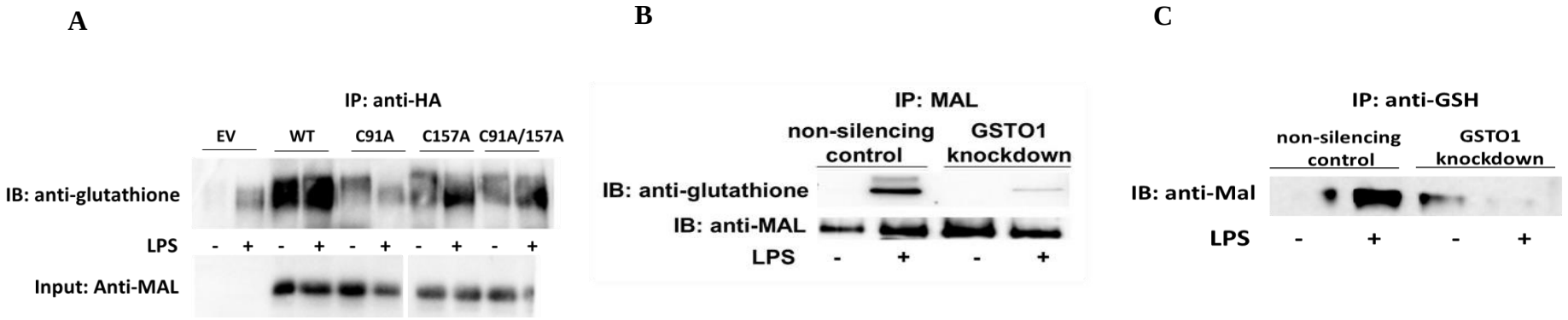

Figure 8.3: Redox state of MAL in cell models

(A) HEK293/TLR4/MD2 cells were transfected with HA tagged MAL and cysteine mutants C91A, C157A and C91A/C157A . Glutathionylation of MAL was detected in HA-MAL expressing cells in both untreated and LPS treated conditions. The glutathionylation of transfected MAL was considerably lower in the cells transfected with the three mutants suggesting that C91 and C157 are glutathionylated in this cell model. (B) Endogenous MAL was immunoprecipitated and probed for glutathionylation with an anti-glutathione antibody in J774.1A cells $^{+/-}$ GSTO1-1. MAL was glutathionylated in response to LPS in the non silencing control cells but not in the *Gsto1* knockdown cells. The membrane was probed with anti-MAL to confirm equal pull down of MAL in both cell types. (C) Glutathionylated proteins were isolated using an anti-glutathione antibody from J774.1A cells $^{+/-}$ GSTO1-1 and probed for MAL. Glutathionylated MAL was detected in LPS stimulated non silencing control cells but not in *Gsto1* knockdown cells, confirming that MAL is glutathionylated in response to LPS in macrophages.

8.3.4 Cysteines in MAL are susceptible to oxidation on LPS stimulation

The redox balance between oxidation and glutathionylation was further investigated by evaluating the oxidative state of cysteines in MAL over expressed in HEK293/TLR4/MD2 cells (stable transfectants expressing TLR4 and MD2) post LPS. Proteins oxidized on LPS treatment were detected using a biotin tagged- 3-(2,4-dioxocyclohexyl)propyl 5-((3aR,6S,6aS)-hexahydro-2-oxo-1H-thieno[3,4-d]imidazol-6-yl)pentanoate (DCP-Bio-1) probe that has high affinity for the sulfenic acid form (-SOH) of cysteine residues [394]. DCP bound proteins were isolated using streptavidin beads. A detailed outline of the assay is described in Figure 8.4A. The sulfenic acid oxidized state (oxidation state +1) was detected in the single mutants C91A and C157A and the double mutant C91A/C157A (Figure 8.4B). Interestingly, oxidation of wildtype MAL cysteines was not detected in this cell model. The absence of significant oxidation of the double mutant suggests that other cysteines in MAL may not be oxidized. In the C157A mutant expressing cells, MAL is significantly oxidized and since C91 is the only cysteine available on the surface of the mutated protein, this suggests that C91 is functionally critical for TLR4 signalling. These findings complement results obtained on the glutathionylation state of MAL described in Figure 8.3. The oxidation of cysteines in the mutants may also explain the inability of the mutant MAL proteins to drive NF-κB dependent transcription of the luciferase reporter gene described in Section 8.3. This study demonstrates that the cysteines in wildtype MAL are glutathionylated in the different cell models in order to protect them from oxidation from ROS generated on LPS stimulation and consequently protein degradation.

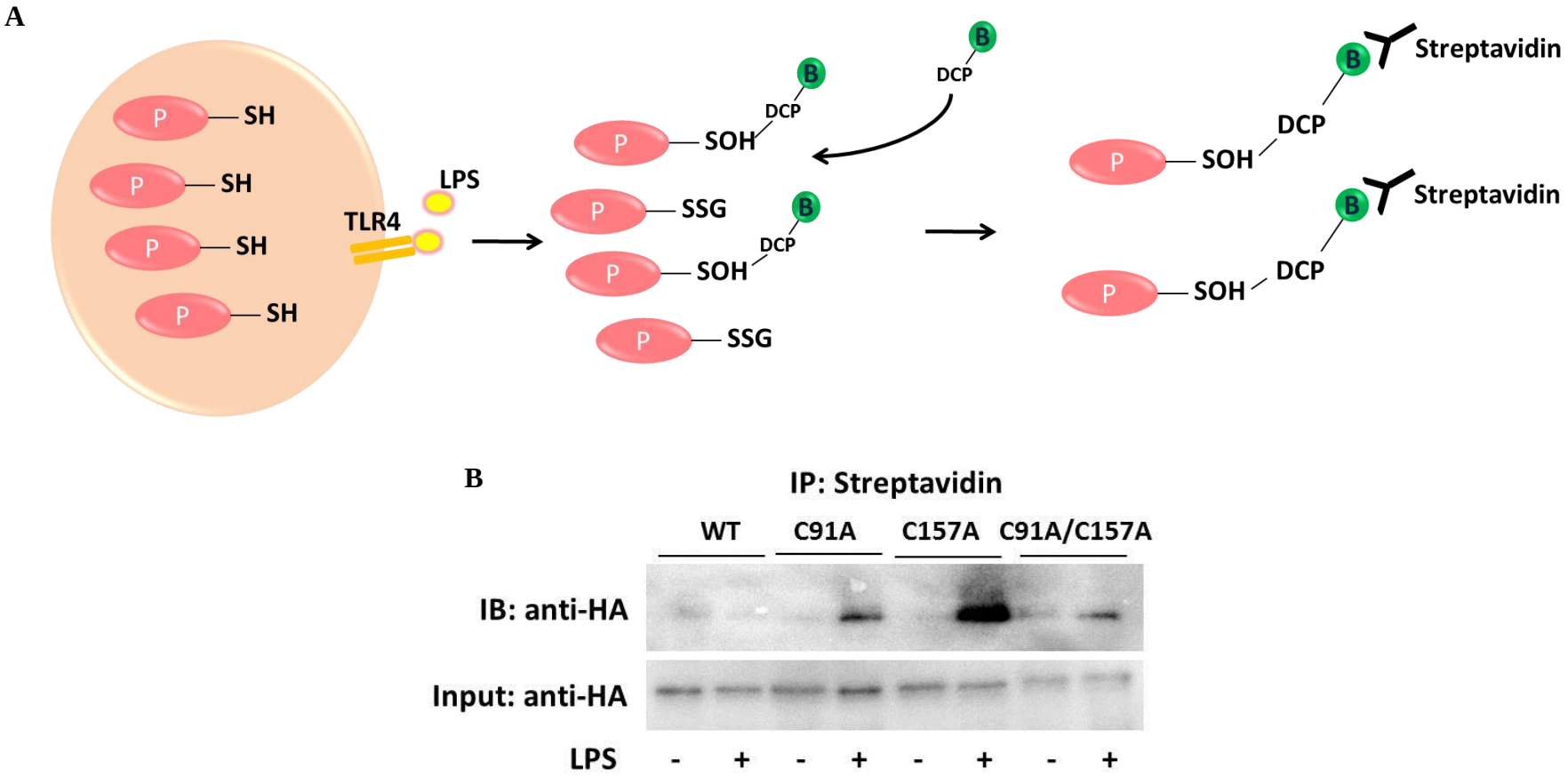

Figure 8.4: Cysteines in MAL are susceptible to LPS induced oxidation

(A) Detection of sulfenic acid form of cysteine residues in cells using a biotin tagged- 3-(2,4-dioxocyclohexyl)propyl 5-((3aR,6S,6aS)-hexahydro-2-oxo-1H-thieno[3,4-d]imidazol-6-yl)pentanoate (DCP-Bio-1) probe. (B) HA-tagged wildtype MAL did not undergo oxidation in response to LPS in HEK293/TLR4/MD2 cells. The C157A was considerably oxidized to the sulfenic acid form on LPS treatment.

8.3.5 Cysteines are critical for the interaction between MAL and MyD88

The recruitment and interaction of MAL and MyD88 with TLR4 are essential for the activation of the downstream signalling molecules (Figure 1.9). HA tagged MAL and its cysteine mutants were co-expressed in HEK293 cells with Myc tagged MyD88 to determine whether C91 and C157 play a role in the physical interaction between the two proteins. It is important to note that the cell model used (HEK293) was not ideal as these cells do not express TLR4 and hence do not respond well to LPS. In spite of technical issues, HA-tagged MAL was found to interact with Myc-tagged MyD88 consistently across 3 biological replicates (Figure 8.5). However, there was a marked decrease in the association of MyD88 with the mutant MAL proteins suggesting that the cysteines may be required for the formation of the Myddosome complex by partaking in the association of MAL with MyD88.

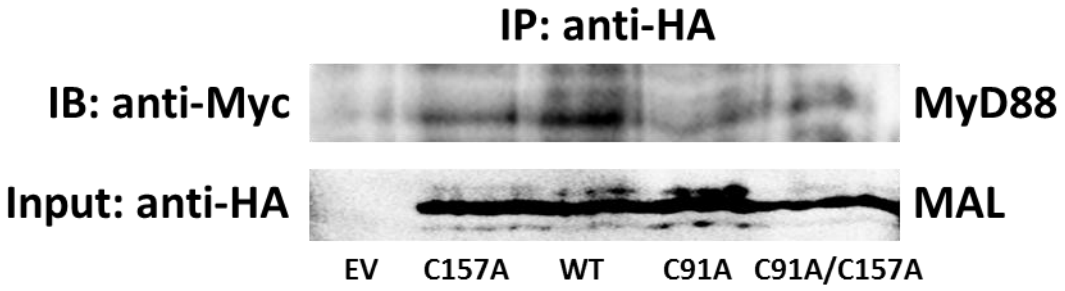

Figure 8.5: Cysteines are critical for the interaction between MAL and MyD88
HA-MAL and its cysteine mutants were co-transfected into HEK293 cells with Myc-MyD88. MAL was immunoprecipitated using an anti-HA antibody and immunoprecipitated proteins were probed with anti-Myc. The interaction of MyD88 with wildtype MAL was detected in cells transfected with wildtype MAL but the interaction was less obvious in the cysteine mutant transfected cells. The blot is representative of three independent experiments.

8.4 Discussion

The catalytic role of GSTO1-1 in the glutathionylation and deglutathionylation of proteins has been investigated in Chapter 4. It is interesting to note that the deglutathionylation activity of GSTO1-1 was detected *in vitro* and was also clearly evident in cells, Furthermore, a peak in glutathionylation levels was measured in T47-D cells over expressing GSTO1-1 under oxidative stress conditions indicates that GSTO1-1 may also catalyse the forward glutathionylation reaction under suitable redox conditions (refer Figure 4.9A). In order to understand the implications of this novel function of GSTO1-1, it is interesting to consider the diseases and physiological conditions in which GSTO1-1 has been implicated in prior studies. In the last decade, a series of studies strongly suggested that GSTO1-1 plays a previously uncharacterized role influencing a range of unrelated diseases whose progress and severity is modified by inflammation. Thus, one of the aims of this project was to understand the mechanism(s) by which GSTO1-1 modulates inflammatory responses.

In previous chapters, the downstream effects of GSTO1-1 deficiency were extensively characterized in macrophages and it was revealed that GSTO1-1 is essential for the activation of TLR4 and switching on the downstream pro-inflammatory responses against infection. Hence, it was hypothesized that GSTO1-1 may be modulating inflammatory responses via TLR4 by catalysing the glutathionylation/deglutathionylation of proteins partaking in the TLR4 signalling cascade after LPS stimulation. Since LPS induces ROS generation in macrophages and we have shown that this increase in both cytosolic and mitochondrial ROS is mediated by GSTO1-1, it is possible that GSTO1-1 may glutathionylate proteins under the ROS induced oxidative stress in the cell. Taken together, all the results presented in the previous chapters support the theory that GSTO1-1 modulates the TLR4 pathway upstream of IRAK4 and NF-κB, potentially placing it in the Myddosome complex. As described earlier, the Myddosome complex is formed by the recruitment of MyD88, and MAL to TLR4.

Since the effect of GSTO1-1 is specific to TLR4 (refer Figure 5.3), MyD88 seemed to be an unlikely target as it is shared among multiple TLRs. On the other hand, MAL is known to be specific to TLR4 and the heterodimer TLR1/2. Though TLR1/2 signalling was not affected by GSTO1-1 deficiency (see Figure 5.3), MAL was still considered as a prime target of GSTO1-1 for the purpose of this study as it is possible to have

differences in signalling and interactions between the proteins downstream of the two TLRs. TLR4 was also considered as a potential target of GSTO1-1 as it has been shown that a synthetic compound TAK-242 (Resatorvid) can inhibit TLR4 signalling by physically binding to the TIR domain and blocking Cys747 which is critical for TLR4 dimerization and activation [362, 395].

Purified MAL protein and the two surface-exposed cysteine residues C91A and C157A could be artificially glutathionylated *in vitro* with high concentrations of GSSG suggesting that there are other cysteine residues in MAL that are susceptible to glutathionylation. However this cannot be confirmed as the C91A/C157A double mutant purified protein was not available to test its susceptibility to glutathionylation. GSTO1-1 was demonstrated to deglutathionylate MAL *in vitro* although the effect did not appear to be physiologically relevant in subsequent studies carried out in whole macrophages.

In the macrophage cell model J774.1A, endogenous MAL was found to be maintained in a deglutathionylated state in non-silencing control and *Gsto1* knockdown cells but was glutathionylated in response to LPS stimulation only in the non-silencing control cells expressing GSTO1-1. MAL remained deglutathionylated in the absence of GSTO1-1 in LPS treated *Gsto1* knockdown cells. This suggests that GSTO1-1 either directly catalyses the glutathionylation of MAL on LPS stimulation or MAL is an indirect target of spontaneous/catalysed glutathionylation that occurs in response to the ROS generated on LPS activation in macrophages. Since this study did not determine the glutathionylation status of TLR4, it is possible that GSTO1-1 modulates TLR4 either through a physical interaction or by (de)glutathionylating TLR4 and activating the TLR4 cascade which in turn would result in ROS production. On analysing the activity of MAL i.e. its ability to drive NF-κB dependent gene expression, it was concluded that cysteine 91 (C91) was critical for the functioning of MAL as both the single mutant C91A and the double mutant C91A/C157A failed to induce NF-κB activated luciferase expression in HEK293T promoter expression system. The C157A single mutant was capable of driving NF-κB activity to a lower extent, suggesting that MAL remained functionally active without C157. Since cysteines in MAL are functionally important, MAL undergoes glutathionylation to protect the cysteines from irreversible oxidation. If MAL is directly glutathionylated by GSTO1-1, we may consider MAL as the redox switch under the regulation of GSTO1-1. However, if MAL

glutathionylation in GSTO1-1 expressing macrophages is a consequence of LPS induced ROS, MAL is not the direct target of GSTO1-1 and further studies should be directed towards investigating the dimerization and activation of TLR4 in GSTO1-1 deficient cells.

Since J774.1A macrophages are relatively difficult to transfect by standard transfection methods (liposomal reagent based), HEK293/TLR4/MD2 cells were used an 'over-expression' model to further investigate the glutathionylation of MAL and the cysteine mutants. Cells over expressing wildtype MAL maintained the over expressed protein in a glutathionylated state even in the absence of LPS unlike endogenous MAL in J774.1A cells where MAL was glutathionylated only in response to LPS. Interestingly, a similar observation was reported in relation to the phosphorylation of MAL in over-expression systems where in MAL was phosphorylated irrespective of LPS stimulation [396]. The C91A single mutant was also glutathionylated, though to a significantly lower extent when compared to the wildtype. Furthermore, the C157A mutant was more glutathionylated than the C91A which was reflected in their relative activity (Figure 8.2). The activity of the C157A mutant was comparable to the wildtype protein whereas mutating C91 abolished MAL's activity. Taken together, it can be concluded that though other cysteines are susceptible to glutathionylation; C91 appears to be critical for the activity of MAL and its glutathionylation protects it from irreversible ROS induced oxidative damage. To further support the hypothesis, the oxidation state of MAL was evaluated. Since wildtype MAL was glutathionylated in LPS treated HEK293T cells, no oxidized MAL was detected in the cells over expressing the wildtype protein. However, MAL was shown to be oxidized in cells transfected with the single mutants and the double mutant. This gives rise to the possibility that the cysteines may be important for the correct folding and maintaining the quaternary structure of MAL and mutating the residues may be making other cysteines including C91 more susceptible to oxidation by increasing steric hindrance and preventing glutathione from binding and/or GSTO1-1 from catalysing the glutathionylation of cysteines, especially C91. There is evidence showing that the C91A and C157A purified proteins may be unstable (Figure 8.1B) though transfected cells show considerable expression of both mutants in HEK 293T cells indicating that the lack of activity of the C91A mutant is not completely attributed to the loss of protein (Figure 8.2A). Establishing a J774.1A stable transfectant expressing the active site mutant C32A would be an ideal system to confirm whether the catalytic activity of GSTO1-1 is responsible for regulating TLR4 signalling.

However this was beyond the scope of this study and will be considered for further investigation. Due to technical difficulties transfecting J774.1A cells, the ability of TLR4 to homodimerize in the absence of GSTO1-1 was not investigated and is still considered a potential target of GSTO1-1.

The disruption of the LPS triggered MAL-MyD88 interaction in the C91A and C157A expressing is additional evidence supporting the functional relevance of the two cysteines in the formation of the myddosome complex. The GSTO1-1 dependent cellular glutathionylation of MAL observed in LPS treated cells may be explained either by the excessive ROS generation in GSTO1-1 expressing macrophages on TLR4 activation, consequently leading to MAL glutathionylation or by the direct catalysis of MAL glutathionylation by GSTO1-1. If the former explanation holds true and MAL is glutathionylated as a result of the ROS generated by the TLR4 signalling cascade, then it may be concluded that the glutathionylation of MAL is not the GSTO1-1 mediated switch regulating the pathway. However, it is evident from the work carried out here that the target of GSTO1-1 lies in the myddosome complex warranting the need to investigate the glutathionylation state of other proteins recruited to the complex. If MAL is a direct glutathionylation target of GSTO1-1 as strongly suggested by our previous findings that GSTO1-1 catalyses the glutathionylation of proteins under oxidative stress, the cysteines undergoing GSTO1-1 catalysed glutathionylation should be identified. The data presented here on the excessive oxidation of cysteines in C157A mutant expressing HEK293T cells and the lack of activity of the C91A mutant collectively identifies C91 as a functionally essential cysteine in MAL and a suitable target of glutathionylation by GSTO1-1.

CHAPTER 9

Discussion

9.1 Significance of results

Glutathione transferase Omega (GSTO1-1), a member of the glutathione transferase (GST) superfamily of Phase II detoxification enzymes, has been characterized as an atypical GST with minimal functional resemblance with other GSTs [179, 197, 262]. GSTO1-1 has previously been shown to exhibit dehydroascorbate reductase activity and glutaredoxin-like thiol transferase activity with chemical substrates such as 2-hydroxyethyl disulphide (HEDS) [262, 275]. Due to its structural similarity to glutaredoxin, a thiol transferase catalysing enzyme, and its inability to recognize xenobiotic substrates typical of other GSTs, it was clear that its primary function remained to be elucidated. Tissue distribution studies identified GSTO1-1 in diverse tissues with varied expression levels albeit the expression of GSTO1-1 was remarkably high in phagocytic immune cells such as macrophages, neutrophils and dendritic cells when compared to non-phagocytic immune cells including B-cells (*www.immgen.org*). Though a significantly high expression level has been observed in the heart and liver, the link between the tissue specific expression and its functional significance is not fully understood. Interestingly, unlike other members of the GST family (except for GSTP), immunostaining of GSTO1-1 revealed the translocation of the protein into the nucleus and localization in the nuclear membrane for reasons yet to be understood [197, 263].

GSTO1-1 was identified as a GST a decade ago due to its close sequence and structural similarity with the family and its ability, though minimal, to catalyse classic detoxification reactions with common GST substrates. GSTO1-1 possesses the typical GST fold comprising of the N-terminal ‘thioredoxin’ resembling domain, embedding the GSH binding site, and the C-terminal helical domain [262]. Most GSTs possess a tyrosine or serine residue at their active site, responsible for catalysing conjugation reactions between GSH and electrophilic substrates [179, 262]. The active site residue in GSTO1-1 was identified as a cysteine (Cys-32) flanked by proline and phenylalanine, uncharacteristic of mammalian GSTs [262]. On detailed dissection of the crystal structure, the active site was found to be in a wide crevice that can potentially

accommodate large substrates suggesting potential interactions with protein- glutathione mixed disulphides (P-SSG).

There have been a few studies published over the years describing oxidative stress dependent activity of GSTO1-1 in nematodes and in *Drosophila* [261, 267, 397]. A loss of function mutation in the *parkin* gene in *Drosophila* has been established as a model for neurodegeneration caused by mitochondrial dysfunction [261]. The mutant shows defective mitochondrial functioning owing to impaired mitochondrial ATP synthase activity. The study demonstrated that over expression of GSTO1-1 in *parkin* mutants partially restored the activity and assembly of the mitochondrial F_1F_0-ATP synthase by the glutathionylation of the β subunit of ATP synthase and hence protecting it from oxidative stress induced damage [261, 397]. This study was published in parallel with our findings that GSTO1-1 deglutathionylates proteins under normal physiological conditions in mammalian cells. Since we also showed that increased oxidative stress led to higher global glutathionylation levels in GSTO1-1 expressing T47-D breast cancer cells, we can argue that the GSTO1-1 catalysed glutathionylation of ATP synthase reported in *parkin* mutants by Kim *et al.* may be due to the preferential catalysis of glutathionylation over deglutathionylation by GSTO1-1 under the high oxidative stress observed in the *parkin* mutants.

A study carried out by Gabel *et al.* identified GSTO1-1 as a target of Cytokine Release Inhibitory Drugs (CRIDs) [264]. The study suggested the involvement of GSTO1-1 in the posttranslational processing of IL-1β in human monocytes. Since the C32A GSTO1-1 mutant failed to elicit responses similar to the wildtype protein, the study speculated that the catalytic activity is key to IL-1β processing. The occurrence of a GSH/ P-SSG binding site on GSTO1-1 and the striking similarity between the crystal structures of the protein and glutaredoxin raises the question whether GSTO1-1 participates in the posttranslational glutathionylation or deglutathionylation of protein(s) involved in the activation and secretion of IL-1β in macrophages.

Co-incidentally, a recent study identified the induction of GSTO1-1 transcription by HMGB1 (high-mobility group protein 1) in response to LPS/GalN-triggered mouse liver injury [398]. HMGB1 is a nuclear component involved in the transcriptional regulation of genes and has also been shown to act as a late mediator of lethality when secreted extracellularly as observed in LPS/GalN-triggered mouse liver injury. The study revealed increased binding of HMGB1 to the promoter sequence of *Gsto1* in

LPS/GalN injected mice. Since HMGB1 directly interacts and activates TLR4/MD2 on the surface of macrophages when secreted extracellularly [399], it may regulate the expression of GSTO1-1 and modulate protein transcription and activity in response to LPS in macrophages. This serves as another line of evidence supporting the speculated but previously uncharacterized role of GSTO1-1 in inflammation.

Aside from the well characterized role of reversible glutathionylation in the protection of proteins against oxidative stress, glutathionylation in the absence of oxidative stress has also been shown to affect protein function. Glutathionylation has been shown to have an impact on the regulation of the cell cycle, apoptosis and inflammation [20, 22, 27, 142], as well as the contractile activity of actin and the phosphatase activity of Protein Tyrosine Phosphatase1B [29, 69]. Therefore, the mechanisms and catalytic mediators of the glutathionylation cycle are of great interest under both oxidative and non-oxidative conditions.

In this study, GSTO1-1 was found to catalyse the deglutathionylation of protein thiols *in vitro* and in a human breast cancer cell line, T47-D. We have identified targets specifically deglutathionylated by GSTO1-1 in T47-D cells, including β-actin and two members of the family of heat shock proteins; Hsp70 and Hsp7c by mass spectrometry though the identity of the exact cysteines was not further investigated at this stage. We validated the deglutathionylation of actin by GSTO1-1 with immunoprecipitation and immunoblotting in cells overexpressing GSTO1-1. The finding that GSTO1-1 deglutathionylated a limited number of proteins in the total glutathionylated protein pool suggests that GSTO1-1 exhibits target specificity though the parameters conferring this specificity are not clear. It is important to note that the GSH-binding site in GSTO1-1 lies in a relatively open crevice that is large enough to fit interacting proteins. This would raise the possibility that the specificity of GSTO1-1 towards protein targets arises from the physical (transient) association of the protein target with GSTO1-1, thereby allowing the glutathionylated residue to bind with the GSH-site and transfer the glutathione moiety to form a disulphide with Cys 32 of GSTO1-1 (Figure 4.12). GSTO1-1 is then recycled to its active state by free GSH in the immediate environment. Also, parameters contributing to the reactivity of the target cysteine thiol such as its pKa, basicity of its flanking residues or residues in close proximity may add to the substrate specificity. The substrate specificity of GSTO1-1 in deglutathionylation is very important since the data presented in this study indicate a regulatory role for GSTO1-1 in inflammation. Our work suggests that the inhibition of GSTO1-1 could be

a suitable target for therapeutic intervention in curbing inflammatory diseases characterized by hyperactivity of TLR4. Target specificity would rule out off-target effects of GSTO1-1 manipulation by synthetic drugs such as ML175 and increase drug efficacy with minimal side effects.

Significantly, T47-D cells overexpressing GSTO1-1 were found to undergo rapid glutathionylation on treatment with S-nitrosoglutathione (GSNO), a known glutathionylating agent. This suggests the possibility that GSTO1-1 may also catalyse glutathionylation of proteins under physiological oxidative conditions. However the present data do not exclude the possibility that the reaction is indirect and results from the generation of GSSG by reactions catalysed by GSTO1-1. Since the glutathionylation and de glutathionylation of proteins has previously been predominantly attributed to Grx family thioltransferases, the current results add a novel protein to the limited list of enzymes catalysing glutathionylation cycle reactions.

Following the characterization of GSTO1-1 as an efficient catalyst in the glutathionylation cycle, the physiological relevance of this function was further investigated in a biological setting. Since genetic variation in the Omega class GST genes has been associated with the age at onset of Alzheimer's and Parkinson's diseases and amyotrophic lateral sclerosis (ALS), and the last decade has accumulated indirect evidence for the involvement of GSTO1-1 in inflammation and inflammation associated diseases [210-217, 272], the project aimed at establishing a link between the implicated functions of GSTO1-1 and its role in the glutathionylation cycle. Interestingly, all the diseases that GSTO1-1 has been reported to influence are quite diverse in terms of symptoms, causes, tissues affected and pathways involved. However, inflammation is a common factor linking all the reported diseases that has been shown to exacerbate the underlying condition and its progression.. Neurodegeneration occurring in Alzheimer's' disease and Parkinson's disease is almost always is associated with hyper-activity of inflammatory signalling pathways. Increased cytokine secretion and ROS production by infiltrating neutrophils and macrophages aggravates tissue damage seen in neurodegenerative disease, thus exacerbating the disease and speeding up the progression and spread [280, 281, 287, 372]. Up-regulation of GSTO1-1 during inflammatory responses has been previously reported by independent studies though the mechanism of action is still open to speculation [213, 273]. Furthermore, the revelation by meta-studies that the polymorphisms, D140 in particular, associate quite strongly with the age at onset and progression of neurodegenerative diseases such as Alzheimer's

and Parkinson's disease further strengthens the evidence in support of a redox role for GSTO1-1 in inflammation associated diseases [210, 212, 272]. Increased ROS accompanying neurodegeneration not only causes excessive tissue damage but also disrupts protein activity by post translational modifications [148, 154, 341]. Over exposure of proteins to ROS results in the irreversible oxidation of protein thiols and subsequent loss of activity and proteosomal degradation. Hence, the results presented here suggesting that the polymorphic variants of GSTO1-1 have differential glutathionylating and deglutathionylating activities is a significant finding that may link all the previously implicated roles of GSTO1-1 in inflammatory diseases. It is not unreasonable to speculate that GSTO1-1 may either be glutathionylating proteins and protecting them from inflammation associated irreversible oxidation or deglutathionylating glutathionylate proteins and restoring their activity.

The D140 variant in particular was found to have lower deglutathionylating activity but higher glutathionylating activity. The reported linkage between D140 GSTO1-1 expression and progression of neurodegeneration may be attributed to increased protein glutathionylation and inhibition of the function of proteins that are required for normal physiological functioning in neural cells. Since GSTO1-1 was shown to have target specificity, the polymorphisms would impact only a few proteins and not all (de)glutathionylated proteins. It is curious that a single point mutation in GSTO1-1 (A140D) altered the activity of the protein significantly. In order to understand the nature of this polymorphism, a closer look into the structure of GSTO1-1 was warranted. Since the polymorphism encodes an alanine to an aspartic acid substitution, the change in the residue's charge (neutral to negative charge) was considered as a possible reason for the differential activity by a previously uncharacterized alteration in protein folding. In order to predict structural changes occurring due to the A140D substitution, and to evaluate the proximity of the alanine / aspartic residues on both subunits to the active site cysteines, a model of the GSTO1-1 dimer was constructed in *PyMOL* from the PDB coordinates *1EEM*. As shown in Figure 9.1A, the Ala /Asp residue resides towards the N-terminal end of helix 5 and is exposed to solvent. The residue at position 140 in the A subunit is 27.9A from the A subunit active site Cys 32 and 36.2A from the B subunit Cys 32. Due to the large distance between the residue at position 140 and the active site cysteine residues on either subunit, it is highly unlikely that the residue substitution could directly alter the structure or hinder the interaction of substrate proteins with GSTO1-1. The substrate peptide (SQLWCLSN) was modelled

on the active site of GSTO1-1 which presented a clear view of the distance between potential substrates and A140, further confirming that based on the crystal structure the lower deglutathionylating activity of D140 GSTO1-1 with the peptide is not due to an alteration in the protein structure resulting in direct steric hindrance, when alanine is substituted with aspartate (Figure 9.1B). Additionally, mutating the alanine to aspartate in Pymol showed no detectable difference in the positioning of the loop containing the residue except for a slight clash of the side chain of aspartate with the amino acid adjacent which wasn't considered significant enough to cause any structural alterations. However, when the factors contributing to the flexibility of crystal structures were considered, the loop between helix 4 and the residues at the start of helix 5 (containing A140) were found to have a high B-Factor and appeared to be relatively mobile (Figure 9.1C, in red). Since the assays were carried out with the purified proteins in solution, it is possible that the position of helix 5 may be altered by the charge change resulting from the A140D substitution, causing the loop and helix to move around more in solution and potentially dislodge or destabilize the interacting target protein from the active site crevice. The consequence of the A140D substitution on the structure of GSTO1-1 has not been characterized previously and warrants in depth structural analysis by techniques such as X-ray crystallography, NMR and circular dichroism. However since both the allelic variants were stable when purified (no precipitation observed), significant disruption to protein folding in solution seems unlikely. Hence the cause of the difference in glutathionylating and deglutathionylating activity of the two allelic variants remains unclear.

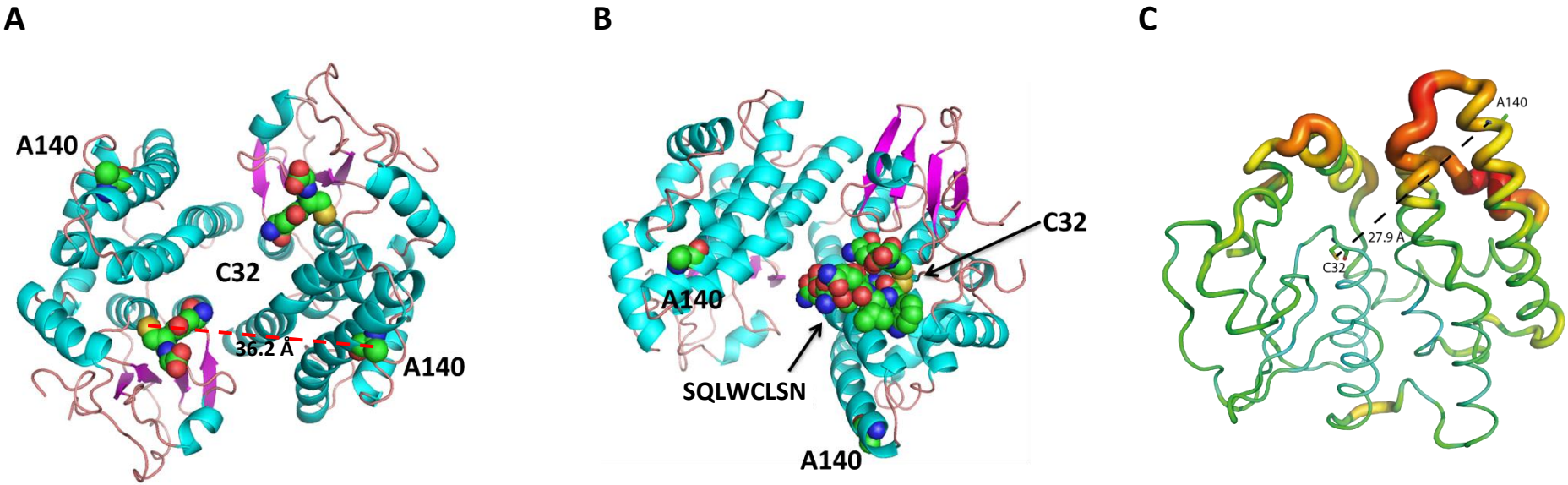

Figure 9.1: Structural implications of the A140D substitution in GSTO1-1
(A) GSTO1-1 dimer is presented in cartoon mode with the helices in blue, β-strands in pink. The alanine and cysteine residues on both monomers are highlighted in space-fill/sphere mode. (B) Interaction of the peptide SQLWCLSN with the active site Cys 32 is highlighted in sphere mode. (C) Evaluation of the B-factors (representing the flexibility/rigidity of the crystal structure identified the helix and loop containing A140 as highly dynamic (blue<green<yellow<orange<red).
Figure 9.1A,B were made by Emeritus Prof. Philip Board (Australian National University) and Assoc. Prof. Aaron Oakley (University of Wollongong); Figure 9.1C was designed with assistance from Dr. Soumya Jose, Australian National University)

As illustrated in Figure 9.2, the hypothesis that GSTO1-1 may be modulating proteins associated with inflammation was addressed by 4 aims. We first established that GSTO1-1 is an essential component in the TLR4 cascade required for the activation of pro-inflammatory responses including cytokine secretion and maintaining the oxidant/antioxidant axis for excessive anti-microbial ROS production in response to LPS in macrophages (Figure 9.2 aim 1). Furthermore, the inability of GSTO1-1 deficient cells to phagocytosize LPS coated beads is a clear indication of unresponsiveness of *Gsto1* knockdown cells to TLR4 activation.

Secondly, it was necessary to determine whether the catalytic activity of GSTO1-1 is required for the activation of pro-inflammatory responses of macrophages to LPS (Figure 9.2 aim 2). This would help rule out the possibility that GSTO1-1 mediates its effects on TLR4 signalling by physical interaction with protein(s) in the TLR4 signalling pathway without the requirement of a functional active site cysteine residue. To establish this point, the synthetic inhibitor ML175 previously shown to inhibit the catalytic activity of GSTO1-1 [350], was used on wildtype macrophages and their pro-inflammatory responses to LPS were compared with the response of the genetically modified *Gsto1* knockdown macrophages. As described in Chapters 5-7, all the effects resulting from knocking down GSTO1-1 in J774.1A macrophages were recapitulated in ML175 treated macrophages. Taken together these results suggested that the catalytic activity of GSTO1-1 is required for TLR4 signalling. Furthermore, the response to ML175 was always dose dependent, suggesting that GSTO1-1 is a strong target for pharmacological regulation of TLR4 signalling. The TLRs have been well recognized as targets for anti-inflammatory drugs and a recent review has listed over 20 compounds targeting TLRs in clinical trials for a variety of indications [163]. TLR4 specific compounds are currently being tested for the treatment of acute and chronic inflammation, chronic pain, allergic rhinitis and sepsis. Thus the discovery that the TLR4 pathway leading to the generation of ROS and the expression of pro inflammatory cytokines is dependent on GSTO1-1 activity has identified the potential of ML175 as a novel anti-inflammatory drug. Further investigations will be required to optimize the dosage in additional cell types apart from macrophages to minimize the observed toxicity. Alongside, it would be necessary to consider incorporating potential modifications in the compound, which would decrease the *in vitro* cytotoxicity of ML175 without compromising on its inhibitory property. Once a concentration range across multiple cell types *in vitro* is established, issues concerning drug toxicity (LD50)

and drug efficacy would be better understood. The next step in the bench to bedside protocol would be to extend the anti-inflammatory applications of ML175 to *in vivo* models. The translation of the use of synthetic compounds from *in vitro* to *in vivo* applications may be carried out as advised in the National Institute of Health, U.S.A (NIH) (http://www.epa.gov/hpv/pubs/general/nih2001b.pdf).

The third aim (Figure 9.2 aim 3) focussed on determining if multiple pathways independent of NFκB but responsive to TLR4 activation are impacted by GSTO1-1 deficiency. The metabolic profile of the cells was evaluated in order to further understand and characterize the phenotype and TLR4 mediated metabolic regulation in GSTO1-1 deficient macrophages. The Warburg effect was defined in 1954 by Otto Warburg as the metabolic deregulation observed in cancer cells where glycolysis is favoured by the cells even in the presence of oxygen. The occurrence of aerobic glycolysis in cancer cells was widely accepted however the possibility of a similar phenotype in other cell types such as immune cells and cancer associated invading macrophages was not initially accepted [400]. In the last decade, the exploitation of the metabolic profile of tumour associated macrophages has been shown to reduce the extent of tumour metastasis [401]. During tumour progression a gradual switching of macrophage polarization, from pro-inflammatory 'M1' to an anti-inflammatory phenotype 'M2' [402]. This transition establishes suitable conditions for tumour growth and metastasis. Excessive secretion of cytokines such as IL-1β has also been shown to exacerbate the progression of metabolic disorders. IL-1β secretion by activated macrophages has previously been linked to chronic inflammation associated with the development of insulin resistance in adipocytes and insulin secretion by pancreatic islets [172, 369, 374, 403-407]. Adipocytes themselves express TLR4 receptors on their surface and are highly responsive to LPS and free fatty acids (FFAs) [405, 407]. IL-1β secreted by adipocytes is sufficient to trigger the release of chemokines that attract activated pro-inflammatory macrophages, resulting in inflammation. Subsequently, IL-1β secreted by the infiltrating macrophages further exacerbates insulin resistance in adipocytes [172, 405-407].

The typical macrophage M1 phenotype characterized by increased glycolysis, accumulation of TCA intermediates, expression of NFκB dependent cytokines and ROS generation was absent in *Gsto1* deficient cells [1, 343, 344, 374, 375, 400, 408]. The attenuation of the glycolytic switch in GSTO1-1 deficient macrophages is believed to be a downstream effect of an upstream block in the TLR4 signalling pathway. Increased

phosphorylation of AMPKα in GSTO1-1 deficient cells was similar to the expression profile seen in macrophages treated with metformin [292, 298, 409]. Metformin is a well-known anti-diabetic drug which in recent times has gained recognition as a potential anti-cancer agent as well [410-413]. Metformin is a potent activator of AMPKα and has been shown to induce AMPKα phosphorylation in macrophages which in turn upregulates PGC1β levels [414]. The increased PGC1β expression resulted in the deacetylation and inhibition of NFκB nuclear translocation and eventually in the inhibition of IL-1β transcription [377, 414]. Though there is some dispute on the anti-inflammatory properties of metformin and the mechanism involved, it is certain that AMPKα activation is inhibitory to the pro-inflammatory responses in macrophages. Since GSTO1-1 deficient cells maintained activated AMPKα levels and high PGC1β transcript levels even in the absence of LPS, GSTO1-1 inhibition by synthetic inhibitors could not only be tested as anti-inflammatories but may also be considered for other metformin-like properties including the anti-cancer effects mediated via AMPKα.

The NLRP3 inflammasome has been shown to play a predominant role in modifying the pro-inflammatory state of both M1 and M2 macrophages [172] in response to ROS. Thus inhibiting TLR4 signalling with an inhibitor of GSTO1-1 would block the entire cascade of inflammatory events. The inhibition of TLR4 mediated pro-inflammatory responses by inhibiting GSTO1-1 in macrophages could possibly result in the reversal of insulin resistance and other IL-1β associated metabolic disorders.

Taken together, the three aims described above led to the conclusion that:

- GSTO1-1 is exclusive to TLR4 and plays an indispensable role in the activation of inflammatory signalling mediated via TLR4.

- The absence of IRAK4 phosphorylation which is an upstream signal for NFκB activation in *Gsto1* knockdown cells suggests that GSTO1-1 acts upstream of IRAK4, potentially in the Myddosome complex. As mentioned in Section 5.4 the presence of low levels of 'phosphorylated' IRAK4 in the unstimulated cells makes this piece of evidence slightly inconclusive. However, the failure of GSTO1-1 deficient cells to phagocytosize LPS coated beads is additional evidence pointing to the upstream activity of GSTO1-1 on LPS stimulation.

- Working around the above mentioned limitation, this study provided further evidence supporting the upstream positioning of GSTO1-1 in the TLR4 pathway

by determining the metabolic status of the GSTO1-1 deficient cells. Since the glycolytic switch triggered by LPS is not entirely dependent on IRAK4 phosphorylation and NFκB activation, the absence of a typical pro-inflammatory M1 glycolytic phenotype in *Gsto1* knockdown cell places GSTO1-1 above IRAK4.

Hence, the inhibition of downstream recruitment and activation of proteins initiating from IRAK4 in the TLR4 cascade that is required for cytokine secretion and ROS production and the complete absence of a classical M1 phenotype (phagocytic and glycolytic) suggests that GSTO1-1 may be a component of the Myddosome complex or act on proteins in the complex.

The fourth aim focussed on identifying potential targets of GSTO1-1 within the myddosome complex. LPS induced ROS has been shown to induce the post translational modification of proteins. Su *et al.* performed a large scale mass spectrometric analysis of glutathionylated proteins in RAW264.7 cells treated with LPS [415]. The study identified approximately 265 proteins that are differentially glutathionylated on LPS stimulation. MyD88 an essential component of the Myddsome complex was identified among the glutathionylated proteins in LPS treated cells. This is the first line of evidence suggesting that cysteines in MyD88 are susceptible to glutathionylation. However this is not unexpected as a previous study identified MyD88 to be nitrosylated upon activation with LPS [416]. Since MyD88 is a common accessory protein to multiple TLRs and the effect of GSTO1-1 was found to be specific to TLR4, the redox modifications of MyD88 were considered an unlikely cause for the downstream effects observed in GSTO1-1 deficient macrophages. Other proteins in this pathway that have been affected by glutathionylation include TRAF6, caspase-1, IKKβ and NFκB subunits p65 and p50 [61, 64, 118, 119, 160]. These proteins are all downstream of the target of GSTO1-1.While the glutathionylation of TRAF6 on LPS activation of TLR4 was catalysed by glutaredoxin; the glutathionylation of caspase-1 was dependent on the expression of the antioxidant SOD1. The experiments carried out in this study have placed GSTO1-1 upstream of IRAK4 and NFκB and demonstrated the attenuation of multiple pathways activated by LPS in macrophages. The induction of ROS and the subsequent glutathionylation of MAL were detected in macrophages expressing GSTO1-1 but not in GSTO1-1 deficient cells. Based on the discovery that GSTO1-1 has measurable deglutathionylating activity the initial hypothesis proposed

that GSTO1-1 may deglutathionylate protein(s) partaking in TLR4 signalling thereby contributing to the results described. However, initial analysis of the redox state of MAL suggests that GSTO1-1 may modulate the glutathionylation of MAL by either inducing ROS in response to LPS or may directly catalyse the glutathionylation of MAL. The difference in these two possibilities is significant. If MAL is glutathionylated by ROS that have been generated after LPS stimulation it seems unlikely that MAL is the target for the GSTO1-1 activity that regulates the pathway. In contrast, if GSTO1-1 is responsible for the direct glutathionylation of MAL then it is likely that MAL is the prime target for regulation by GSTO1-1. If MAL is not the target of GSTO1-1, it is important that the investigation focuses on TLR4. The cysteine residue Cys 747 in the TIR domain is critical for the homodimerization of TLR4 on LPS stimulation [395]. Since the deficiency of GSTO1-1 prevents the phosphorylation of IRAK4, it is possible that the Myddosome complex is recruited but does not correctly interact with the TIR domain of TLR4 due to the glutathionylation of Cys 747 in the absence of GSTO1-1.

The *Gsto1*$^{-/-}$ mice became available only towards the end of the project and hence characterization of the phenotype of these mice is incomplete. Since GSTO1-1 deficient macrophages remain unresponsive to TLR4 stimulation by LPS, it was hypothesized that *Gsto1*$^{-/-}$ mice would be tolerant to LPS and would fail to elicit typical pro-inflammatory responses including the secretion of cytokines and production of ROS. As expected, *Gsto1*$^{-/-}$ mice did not respond to sub lethal doses of LPS (5 mg/kg and 10 mg/kg) and failed to induce cytokines. In contrast, the wildtype counterparts experienced hypothermia within 9-12 hours post LPS injection and did not survive for more than 24-96 hours. An analysis of the histology of tissues extracted from LPS treated wildtype and *Gsto1*$^{-/-}$ mice revealed a remarkable difference in the morphology of the liver and spleen. The wildtype mice experienced severe necrosis and showed signs of acute inflammation including the infiltration of neutrophils and hepatic steatosis. The spleen in wildtype mice also showed acute inflammation in the red pulp regions along with the formation of tingable macrophage bodies. The knockout mice did not show any significant morphological changes while the extent of liver and spleen damage in heterozygotes were termed as ‘mild inflammation’ by Professor Jane Dahlstrom who analysed the samples.

Taken together, the absence of LPS induced tissue damage, failure to elicit cytokines, attenuation of the up-regulation of NOX1 transcription and the maintenance of a high

anti-oxidant redox environment in response to intra-peritoneally injected LPS strongly supports the novel role of GSTO1-1 in TLR4 pro-inflammatory signalling. However, the specificity of GSTO1-1 to TLR4 in vivo is yet to be fully investigated.

This study establishes an indispensable role for GSTO1-1 in TLR4 signalling and LPS associated inflammatory responses. Characterization of the glutathionylating and deglutathionylating activities of the polymorphic variants of GSTO1-1 revealed a significant difference which could explain the reported role of GSTO1-1 in inflammatory diseases. The effect of the polymorphic variant D140 on TLR4 signalling would be an interesting aspect to investigate. If TLR4 signalling is dependent on the polymorphic variant of GSTO1-1, it would further support the hypothesis that the regulatory effects of GSTO1-1 in inflammation are mediated by its (de)glutathionylation activity. We further conclude that this effect may be due to the glutathionylation of the upstream TLR4 specific adaptor MAL. However due to time constraints, this theory is yet to be fully investigated.

9.2 Future directions

9.2.1 Identifying the glutathionylation targets of GSTO1-1 in macrophages

A global mass spectrometry analysis of GSTO1-1 expressing versus deficient macrophages, similar to the work done on T47-D breast cancer cells (refer Chapter 4) would identify potential glutathionylation targets of GSTO1-1. This would include targets in the TLR4 cascade and other pathways that are regulated by GSTO1-1. A global increase in glutathionylation was measured in GSTO1-1 expressing macrophages in response to LPS induced ROS. Identification of these proteins could then be followed up by experimental validation as previously done.

9.2.2 In vivo validation of endotoxic responses to LPS

The susceptibility of *Gsto1*$^{-/-}$ mice to LPS was investigated towards the end of this project when the mice became available. Further studies are in place to characterize the phenotype of the mice. LPS response in the mice should be evaluated by measuring cytokine levels in the serum and in bone marrow derived and peritoneal macrophages. TLR4 signalling could be characterized further by determining the activation of intermediate signalling molecules that have been carried out in the J774.1A GSTO1-1 deficient macrophages. Since different types of immune cells respond to LPS in whole mice, it is important to determine their individual responses as it is possible that the effects observed in macrophages may not be occurring in other cell types. This would

also help narrow down the target of GSTO1-1 macrophages by comparing the activation of signalling molecules among different immune cells in response to LPS. Additionally, the specificity of GSTO1-1 to TLR4 in vivo needs to be investigated to confirm the results gathered from the macrophages *in vitro*.

9.2.3 Characterizing Gsto2$^{-/-}$ mice

With the intention to provide a 'negative control' group deficient in GSTO2-2, we had generated a V174A *Gsto2* mutant mouse model (available via the Australian Phenomics Facility ENU mutant library). Unfortunately, the homozygotes (mut/mut) were found to express GSTO2-2 in all tissues with considerable activity. Hence the data are not presented in this thesis. It would be interesting to characterize the response of *Gsto2*$^{-/-}$ mice to LPS. Based on the results described in this thesis, inhibition of TLR4 signalling is specific to GSTO1-1 and therefore *Gsto2*$^{-/-}$ mice are expected to be susceptible to LPS induced endotoxic shock unlike *Gsto1*$^{-/-}$ mice.

9.2.4 Testing disease models

The in vivo work thus far has been done using commercially available high purity LPS as a TLR4 stimulant. It would be necessary to test the susceptibility of Gsto1$^{-/-}$ mice to live bacteria such as *Salmonella typhimurium* to confirm the resistance of these mice to infection.

As over expression of cytokines has been reported to exacerbate diseases such as cancer and metabolic conditions, it would be interesting to use *Gsto1*$^{-/-}$ mice as an immune model to test the progression of inflammation associated diseases. Our laboratory has established a cancer model by injecting cancer cells such as 4T-1 (murine breast cancer) in normal mice and MDA-MB-231 (human breast cancer cells) in *Rag1*$^{-/-}$ immunocompromised mice. A similar approach would help understand if cancer cells are able to grow and metastasize in *Gsto1*$^{-/-}$ mice. Ideally, if *Gsto1*$^{-/-}$ mice are incapable of eliciting pro-inflammatory responses, the injected cancer cells wouldn't metastasize.

9.3 Conclusion

This study identifies a novel role of GSTO1-1 in the glutathionylation/deglutathionylation of proteins with target specificity. The regulatory role of GSTO1-1 was further elucidated as an essential component of TLR4 mediated inflammatory responses in macrophages stimulated by LPS. Blocking chronic oxidative stress associated with exacerbated cytokine secretion and neurodegeneration could therefore be of benefit in limiting the pathology and progression of Alzheimer's disease. This study also demonstrated that the inhibition of GSTO1-1 by ML175 mediates responses that are typical of reported anti-inflammatories, hence providing the first evidence that ML175 and related compounds are a new family of anti-inflammatory agents.

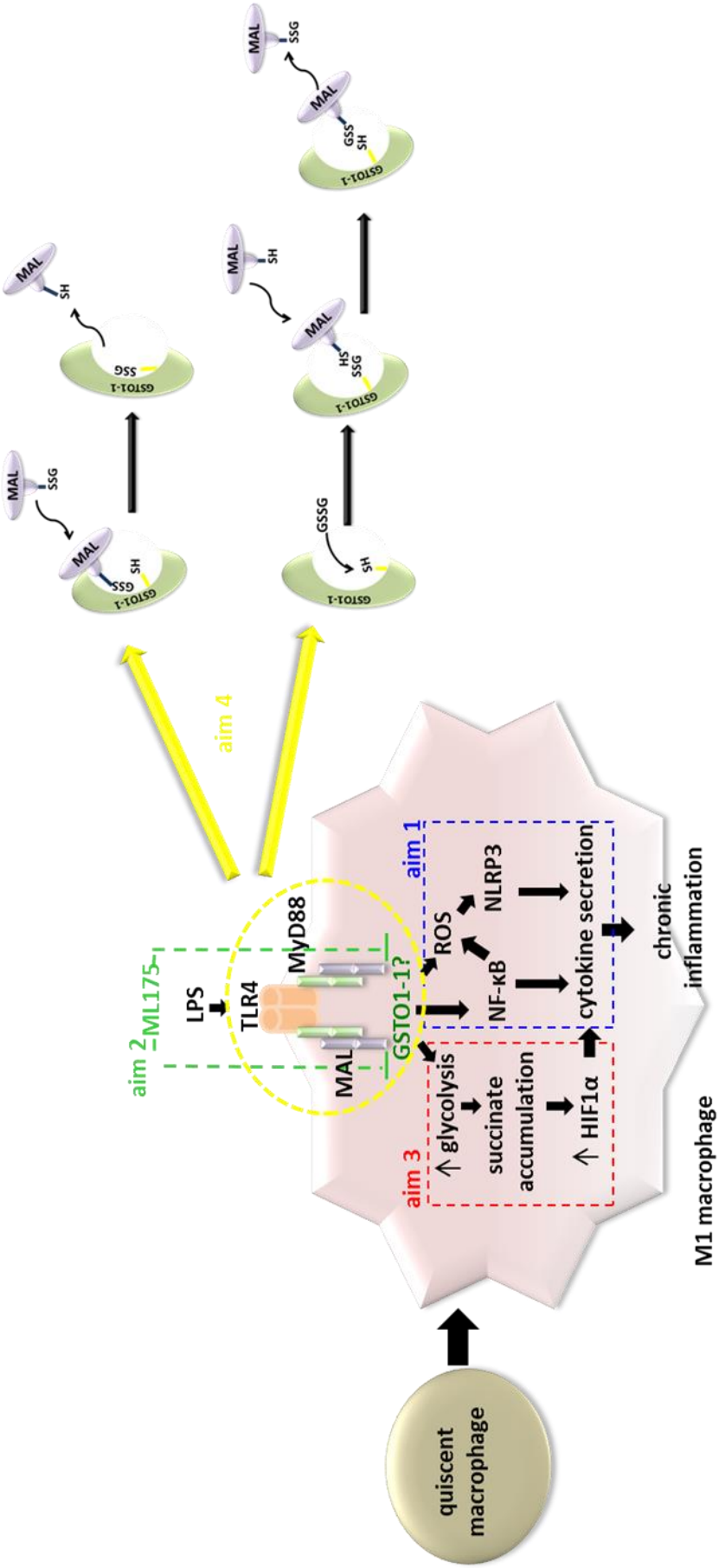

Figure 9.2: Working model: GSTO1-1 is necessary for the activation of LPS induced TLR4 signalling in macrophages

APPENDICES

Appendix A1: Common Reagents and their sources

Reagent	Source
Acetic acid	Chem-supply (Gillman) (Australia)
30% Acrylamide : Bisacrylamide	Biorad (U.S.A)
Agar	Amresco (USA)
Agarose	Amresco (USA)
Ammonium persulphate	Sigma (U.S.A)
Ampicillin	Sigma-Aldrich (USA)
Anti-rabbit IgG (peroxidase conjugated)	Dako Pty. Ltd. (Australia)
β-mercaptoethanol	Sigma (U.S.A)
Bovine Serum Albumin (BSA)	New England Biolabs (USA)
Chloroform	Sigma (U.S.A)
Coomasie Brilliant blue Phast Gel Blue R	Pharmacia Biotech (Sweden)
Ethanol	Ajax Finechem (Australia)
GelRed Dye	Jomar Biosciences (Australia)
Glycerol	Chem-supply (Gillman) (Australia)
Methanol	Chem-supply (Gillman) (Australia)
One Kb DNA ladder	Invitrogen (U.S.A)
One Kb Plus DNA ladder	Invitrogen(U.S.A.)
Rapid Step ECL Reagent	CalBiochem, Merck Pty Ltd (Australia)
Sodium Acetate	BDH AnalaR, Merck Pty Ltd (Australia)
Sodium Chloride	BDH AnalaR, Merck Pty Ltd (Australia)
Sodium di-hydrogen orthophosphate	Ajax Finechem (Australia)
Sodium Dodecyl Sulphate	Sigma (U.S.A)
Sodium Hydroxide	Ajax Finechem (Australia)
di-Sodium Hydrogen Orthophosphate	BDH AnalaR, Merck Pty Ltd (Australia)
Sucrose	Ajax Finechem (Australia)
Super RX Medical X-ray Film	Fuji (Japan)
TEMED	Sigma (U.S.A)
Tris	BioradSigma-Aldrich (USA)
Trypan Blue	Sigma (U.S.A)

Appendix A2: Consumables and their Sources:

Material	Source
Tissue Culture dishes	Nunc (USA)
96-well plates	Corning Costar (U.S.A)
Pipette tips	Axygen (U.S.A.)
Tissue culture Pipettor	Thermo Fischer Scientific (Australia)
Eppendorfs	Sarstedt (Germany)
Pipettes	Gilson (U.S.A)

Appendix A3: Enzymes and their Sources

Enzyme	Source
Restriction endonucleases and their 10X Buffers	New England Biolabs (U.S.A)
KOD Hot Start DNA Polymerase and 10X Buffer	Novagen (Japan)
T4 DNA Ligase and 10X Buffer	Promega (Australia)
Taq DNA Polymerase and 10X Buffer IV	ABGene (U.K.)

Appendix A4: Cell culture media and reagents

Media	Composition/Dilutions
Dulbecco's Modified Eagle Medium (DMEM)	H16 Powder Sodium hydrogen carbonate Sterile double distilled water
Luria Broth (LB)	Tryptone Yeast Extract Sodium Chloride
LB-Amp plates	LB 1.5% (w/v) Agar 100µg/ml Ampicillin
Roswell Park Memorial Institute- 1640 medium (RPM1-1640)	RPMI powder Sodium hydrogen carbonate Sterile double distilled water
PBS (Life technologies Catalogue number: 00-3002)	Dissolve 1 tablet/100ml double distilled water.
100X PSN (catalogue number: 15640-055)	Dilute 1/100 in sterile PBS
2.5% Trypsin (Catalog number: 15090-046)	Dilute 1/10 in sterile PBS
200mM Glutamine (Catalog number: 25030-081)	Dilute 1/100 in sterile PBS

Appendix A5: Buffers and solutions

Buffer/Solution	Composition
SDS-PAGE destaining solution	10% Acetic acid 30% Methanol
4X Resolving gel buffer	1.5M Tris pH 8.8 0.4% (w/v) SDS
10X Running Buffer	25mM Tris 192mM Glycine 0.1% (w/v) SDS
4X Stacking gel buffer	500mM Tris pH 6.8 0.4% (w/v) SDS
Coomasie blue protein staining Solution	0.2% stock solution: Phast Gel Blue R tablet : 60% Methanol Working solution: Mix with 20% acetic acid in a 1:1 dilution
SDS protein Loading dye	250 mM tris, pH 6.8 10% SDS 30% Glycerol 0.02% Bromophenol blue 5% β-Mercaptoethanol
Sucrose Gel Loading dye	15mM EDTA 60% (w/v) Sucrose A dash of Bromophenol Blue
1X TBE Buffer	900mM Tris-Borate 20mM EDTA pH 8.0
TFBI	30mM Potassium Acetate 50 mM $MnCl_2.4H_2O$ 100 mM KCl 10 mM $CaCl_2.2H_2O$ 15% Glycerol
TFBII	10 mM Sodium-MOPS 75 mM $CaCl_2.2H_2O$ 10 mM KCl 15% Glycerol
10X Transblot Buffer	12mM Tris 96mM Glycine 20% (v/v) Methanol
10X Tris buffered saline with tween Buffer (TBS-T)	50mM Tris,PH 7.4 150mM NaCl 0.1% Tween-20
Western blot blocking buffer	5% (w/v) skim milk powder in 1X TN buffer

Appendix A6: Primer sequences

Primer	Sequence
Catalase	5′ AGCGACCAGATGAAGCAGTG 3′ 5′ TCCGCTCTCTGTCAAAGTGTG 3′
COX2	5′ CCCTGAAGCCGTACACATCA 3′ 5′ TGTCACTGTAGAGGGCTTTCAATT 3′
GAPDH	5′ AGGTCGGTGTGAACGGATTTG 3′ 5′ TGTAGACCATGTAGTTGAGGTC 3′
GCLc	5′ GGGGTGACGAGGTGGAGTA 3′ 5′ GTTGGGGTTTGTCCTCTCCC 3′
GCLm	5′ AGGAGCTTCGGGACTGTATCC 3′ 5′ GGGACATGGTGCATTCCAAAA 3′
Gpx3	5′ GCCAGCTACTGAGGTCTGACAGA 3′ 5′ CAAATGGCCCAAGTTCTTCTTG 3′
HO-1	5′ GAGATAGAGCGCAACAAGCAG 3′ 5′ CTTGACCTCAGGTGTCATCTC 3′
IL-10	5′ GCT CTT ACT GAC TGG CAT GAG 3′ 5′ CGCAGCTCTAGGAGCATGTG 3′
iNOS	5′ CAGCACAGGAAATGTTTCAGC 3′ 5′ TAGCCAGCGTACCGGATGA 3′
NOX1	5′ TCCATTTCCTTCCTGGAGTGGCAT 3′ 5′ GGCATTGGTGAGTGCTGTTGTTCA 3′
NQO1	5′ GCCTGAGCCCAGATATTGTG 3′ 5′ GGAAAGGACCGTTGTCGT 3′
PGC1β	5′ TCCTGTAAAAGCCCGGAGTAT 3′ 5′ GCTCTGGTAGGGGCAGTGA 3′

Appendix A7

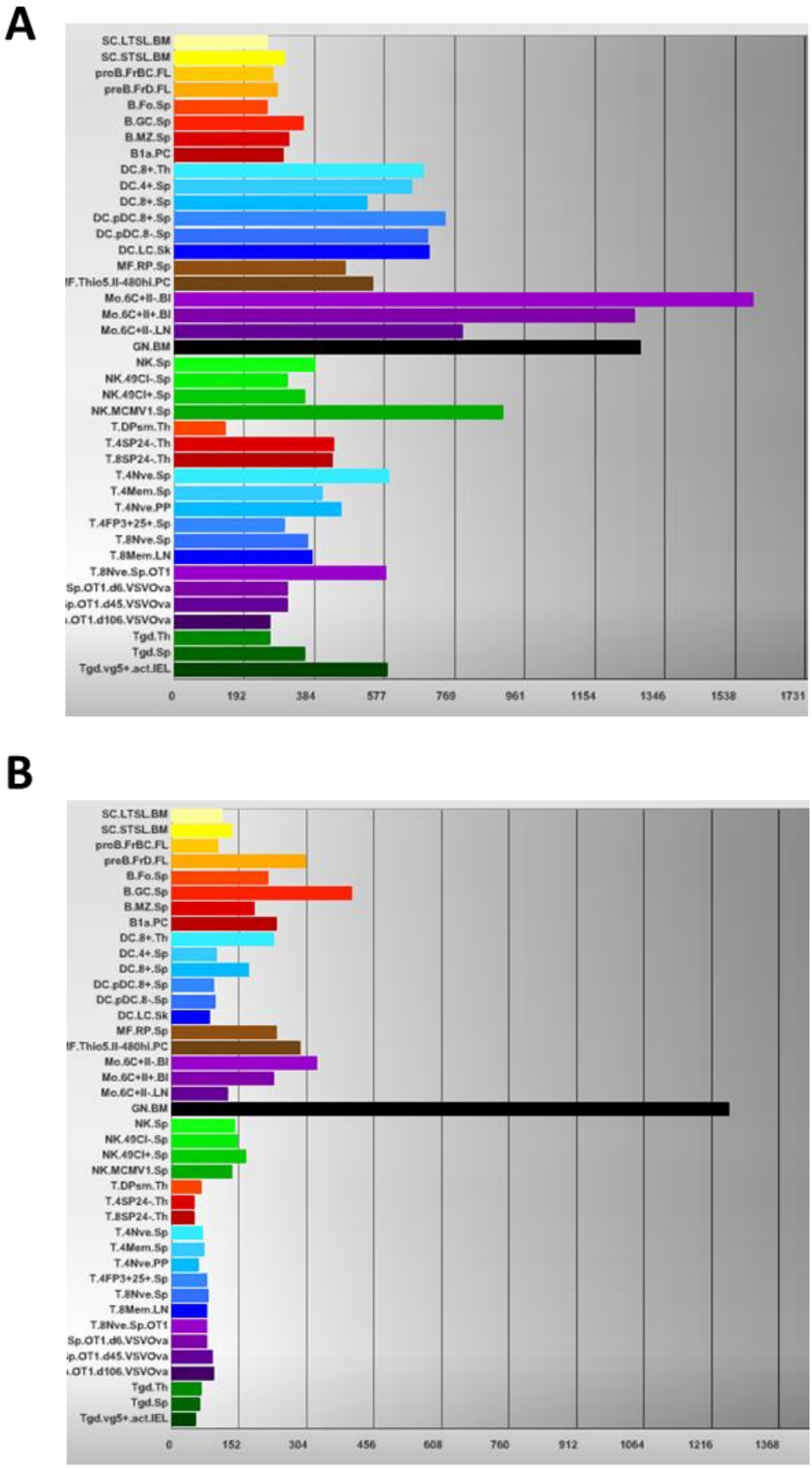

Figure 1: Expression profiling of *MyD88* (A) and *MAL* (B) in mouse immune cells (Immgen *www.immgen.org*).

C

Monocytes

Mo.6C+II-.BI	Classical Monocytes, MHCII-
Mo.6C+II+.BI	Classical Monocytes, MHCII+
Mo.6C-II-.BI	Nonclassical Monocytes, MHCII-
Mo.6C-II+.BI	Nonclassical Monocytes, MHCIIhi
Mo.6C-IIint.BI	Nonclassical Monocytes, MHCIIint
Mo.6C+II-.LN	Classical Monocytes, MHCII-
Mo.6C-II+.LN	Nonclassical Monocytes, MHCII+
Mo.6C+II-.BM	Classical Monocytes
Mo.6C-II-.BM	Nonclassical Monocytes

Macrophages

Lymphoid tissue

MF.RP.Sp	Red pulp MF

Non-lymphoid tissue

MF.11cloSer.SI	Small intestine serosal macrophage
MF.103-11b+.Salm3.SI	Small intestine CD103-CD11b+ MFs isolated from mice infected with salmonella typhimurium, day 3 P/I
MF.11cloSer.Salm3.SI	Small intestine serosal MFs isolated from mice infected with salmonella typhimurium, day 3 P/I
MF.103-11b+24-.Lu	Lung CD11b+24- macrophage
MF.II+480lo.PC	Peritoneal macrophage steady state
MF.Lu	Lung macrophage
MF.PPAR-.Lu	Lung macrophage from LysMcre PPARgfl/fl mice
MF.II-480hi.PC	Peritoneal MF steady state
MF.Thio5.II-480hi.PC	Peritoneal MF thio-elicited day 5
MF.Thio5.II+480int.PC	Peritoneal MF thio-elicited day 5
MF.Thio5.II-480int.PC	Peritoneal MF thio-elicited day 5
MF.Thio5.II+480lo.PC	Peritoneal DC thio-elicited day 5
MF.Microglia.CNS	Central nervous system microglia
MF.Microglia.DAP12-.CNS	Central nervous system microglia from DAP12 KO mice
MF.II-480hi.DAP12-.PC	Peritoneal MF steady state from DAP12 KO mice
MF.Lv	Liver macrophages (P6)
MF.AT.v2	Adipose Tissue Macrophage

Bone marrow

MF.BM	Bone marrow macrophages

Tumor-associated

MF.RTag.TI	Tumor, RIP-Tag2, macrophage

Figure 1C: Detailed description of subset nomenclature terminology used in Figure 5.1A-B, Appendix 7 Figure 1A-B)

Appendix A8

Antibody	Conditions
anti-glutathione	Virogen (101-A-100), mouse monoclonal 1/1000 dilution, 4°C overnight
anti-GSTO1-1	In-house antibody generated at JCSMR, rabbit polyclonal 1/1000 dilution, 2 hours room temperature
anti-β-actin	Abcam (ab8227), rabbit polyclonal 1/5000 dilution, 2 hours room temperature
anti-NOX1	Abcam (ab55831), rabbit polyclonal 1/1000 dilution, 4°C overnight
anti-p65	Santacruz (sc-372), rabbit polyclonal 1/1000 dilution, 4°C overnight
anti-glutaredoxin 1	Abcam (ab45953), rabbit polyclonal 1/1000 dilution, 4°C overnight
anti-IL-1β	R&D biosystems (AF-401-NA), goat polyclonal 1/1000 dilution, 4°C overnight
anti-PPARγ	Cell Signalling (C26H12), rabbit monoclonal 1/1000 dilution, 4°C overnight
anti-IRAK4	Cell Signalling (4363), rabbit polyclonal 1/1000 dilution, 4°C overnight
anti-phospho Thr/Ser	Cell Signalling (9631), rabbit polyclonal 1/1000 dilution, 4°C overnight
anti-AMPK	Cell Signalling (2532), rabbit polyclonal 1/1000 dilution, 4°C overnight
anti-pAMPK	Cell Signalling (2531), rabbit polyclonal 1/1000 dilution, 4°C overnight
anti-HIF1α	Abcam (ab51608), rabbit monoclonal 1/1000 dilution, 4°C overnight
anti-GSTO2-2	In-house antibody generated at JCSMR, rabbit polyclonal 1/1000 dilution, 2 hours room temperature
anti-GSTK	In-house antibody generated at JCSMR, rabbit polyclonal 1/1000 dilution, 2 hours room temperature
anti-GSTA1/2	In-house antibody generated at JCSMR, rabbit polyclonal 1/1000 dilution, 2 hours room temperature
anti-GSTZ1	In-house antibody generated at JCSMR, rabbit polyclonal 1/1000 dilution, 2 hours room temperature
anti-GSTP1/2	In-house antibody generated at JCSMR, rabbit polyclonal 1/1000 dilution, 2 hours room temperature
anti-GSTT2	In-house antibody generated at JCSMR, rabbit polyclonal 1/1000 dilution, 2 hours room temperature
anti-GSTM2	In-house antibody generated at JCSMR, rabbit polyclonal 1/1000 dilution, 2 hours room temperature
anti-GSTA4	In-house antibody generated at JCSMR, rabbit polyclonal 1/1000 dilution, 2 hours room temperature
anti-NQO1	Abcam (ab34173), rabbit polyclonal 1/1000 dilution, 4°C overnight
anti-GSTT1	In-house antibody generated at JCSMR, rabbit polyclonal 1/1000 dilution, 2 hours room temperature

anti-phospho p38 MAPK	Cell Signaling (9211), rabbit polyclonal 1/1000 dilution, 4°C overnight
anti-GCLm	Abcam (ab81445), rabbit polyclonal 1/1000 dilution, 4°C overnight
anti-HA	Sigma (H3663), mouse monoclonal 1/1000 dilution, 4°C overnight
anti-MAL	Abcam (ab17218), rabbit polyclonal 1/1000 dilution, 4°C overnight
anti-Myc	Sigma (C3956), rabbit polyclonal 1/1000 dilution, 4°C overnight

REFERENCES

1. Tannahill, G.M., et al., *Succinate is an inflammatory signal that induces IL-1beta through HIF-1alpha.* Nature, 2013. **496**(7444): p. 238-42.
2. Netto, L.E.S. and M.A. Oliveira, *Site-Directed Mutagenesis as a Tool to Characterize Specificity in Thiol-Based Redox Interactions Between Proteins and Substrates*, in *Genetic Manipulation of DNA and Protein - Examples from Current Research*, F. D., Editor 2013, Intech.
3. Broniowska, K.A., A.R. Diers, and N. Hogg, *S-nitrosoglutathione.* Biochim Biophys Acta, 2013. **1830**(5): p. 3173-81.
4. Lindahl, M., A. Mata-Cabana, and T. Kieselbach, *The Disulphide Proteome and other Reactive Cysteine Proteomes: Analysis and Fucntional Significance.* Antioxid Redox Signal, 2011. **14**(12): p. 2581-2642.
5. Chouchani, E.T., et al., *Proteomic approaches to the characterization of protein thiol modification.* Curr Opin Chem Biol., 2011. **15**(1): p. 120-128.
6. Trachootham, D., et al., *Redox Regulation of Cell Survival.* Antioxid Redox Signal., 2008. **10**(8): p. 1343–1374.
7. Le Bras, M., et al., *Reactive oxygen species and the mitochondrial signaling pathway of cell death.* Histol Histopathol, 2005. **20**(1): p. 205-19.
8. Fleury, C., B. Mignotte, and J.L. Vayssiere, *Mitochondrial reactive oxygen species in cell death signaling.* Biochimie, 2002. **84**(2-3): p. 131-41.
9. Anathy, V., et al., *Redox based regulation of apoptosis: S-glutathionylation as a regulatory mechanism to control cell death.* Antioxidants & Redox Signaling, 2011.
10. Bhatnagar, A. and B.G. Hill, *Protein S-glutathiolation: Redox sensitive regulation of protein function.* Journal of Molecular and Cellular Cardiology, 2011.
11. Meister, A. and M.E. Anderson, *Glutathione.* Annual Review Biochemistry, 1983. **52**: p. 711-760.
12. Richman, P.G. and A. Meister, *Regulation of Gamma Glutamyl-Cysteine Synthetase by Non-allosteric Feedback Inhibition by Glutathione.* The Journal of Biological Chemistry, 1975. **250**(4): p. 1422-1426.
13. Wu, G., et al., *Glutathione metabolism and its implications for health.* J Nutr, 2004. **134**(3): p. 489-92.
14. Lu, S.C., *Glutathione synthesis.* Biochim Biophys Acta, 2013. **1830**(5): p. 3143-53.
15. Garcia-Gimenez, J.L., et al., *Nuclear glutathione.* Biochim Biophys Acta, 2013. **1830**(5): p. 3304-16.
16. Chakravarthi, S., C.E. Jessop, and N.J. Bulleid, *The role of glutathione in disulphide bond formation and endoplasmic-reticulum-generated oxidative stress.* EMBO Rep, 2006. **7**(3): p. 271-5.
17. Hwang, C., A.J. Sinskey, and H.F. Lodish, *Oxidized redox state of glutathione in the endoplasmic reticulum.* Science, 1992. **257**(5076): p. 1496-502.
18. Chen, Y., et al., *Glutamate cysteine ligase catalysis: dependence on ATP and modifier subunit for regulation of tissue glutathione levels.* J Biol Chem, 2005. **280**(40): p. 33766-74.
19. Zhang, H., H.J. Forman, and J. Choi, *Gamma-glutamyl transpeptidase in glutathione biosynthesis.* Methods Enzymol, 2005. **401**: p. 468-83.
20. Townsend, D.M., et al., *Novel role for glutathione S-transferase pi. Regulator of protein S-Glutathionylation following oxidative and nitrosative stress.* J Biol Chem, 2009. **284**(1): p. 436-45.

21. Shelton, M.D., P.B. Chock, and J.J. Mieyal, *Glutaredoxin: Role in Reversible Protein S-glutathionlation and Regulaton of Redox Signal Transduction and Protein Translocation.* Antioxidants & Redox Signaling, 2005. **7**: p. 348-366.
22. Tew, K.D., *Redox in redux: Emergent roles for glutathione S-transferase P (GSTP) in regulation of cell signaling and S-glutathionylation.* Biochem Pharmacol, 2007. **73**(9): p. 1257-69.
23. Lo Conte, M. and K.S. Carroll, *The redox biochemistry of protein sulfenylation and sulfinylation.* J Biol Chem, 2013. **288**(37): p. 26480-8.
24. Roos, G. and J. Messens, *Protein sulfenic acid formation: from cellular damage to redox regulation.* Free Radic Biol Med, 2011. **51**(2): p. 314-26.
25. Lei, K., D.M. Townsend, and K.D. Tew, *Protein cysteine sulfinic acid reductase (sulfiredoxin) as a regulator of cell proliferation and drug response.* Oncogene, 2008. **27**: p. 4877-4887.
26. Allen, E.M. and J.J. Mieyal, *Protein-thiol oxidation and cell death: regulatory role of glutaredoxins.* Antioxid Redox Signal, 2012. **17**(12): p. 1748-63.
27. Cooper, A.J., J.T. Pinto, and P.S. Callery, *Reversible and irreversible protein glutathionylation: biological and clinical aspects.* Expert Opin Drug Metab Toxicol, 2011. **7**(7): p. 891-910.
28. Padgett, C.M. and A.R. Whorton, *Cellular responses to nitric oxide: role of protein S-thiolation/dethiolation.* Arch Biochem Biophys, 1998. **358**(2): p. 232-42.
29. Findlay, V.J., et al., *A Novel role for human Sulfiredoxin in the reversal of Glutathionylation.* Cancer Research, 2006. **66**(13): p. 6800-6804.
30. Grek, C.L., et al., *Causes and consequences of cysteine S-glutathionylation.* J Biol Chem, 2013. **288**(37): p. 26497-504.
31. Michelet, L., et al., *Thioredoxins, glutaredoxins, and glutathionylation: new crosstalks to explore.* Photosynth Res, 2006. **89**: p. 225–245.
32. Poole, L.B. and H.R. Ellis, *Identification of cysteine sulfenic acid in AhpC of alkyl hydroperoxide reductase.* Methods Enzymol, 2002. **348**: p. 122-36.
33. Jeong, W., et al., *Role of sulfiredoxin as a regulator of peroxiredoxin function and regulation of its expression.* Free Radic Biol Med, 2012. **53**(3): p. 447-56.
34. Chang, T.S., et al., *Characterization of mammalian sulfiredoxin and its reactivation of hyperoxidized peroxiredoxin through reduction of cysteine sulfinic acid in the active site to cysteine.* J Biol Chem, 2004. **279**(49): p. 50994-1001.
35. Woo, H.A., et al., *Reduction of cysteine sulfinic acid by sulfiredoxin is specific to 2-cys peroxiredoxins.* J Biol Chem, 2005. **280**(5): p. 3125-8.
36. Sivaramakrishnan, S., A.H. Cummings, and K.S. Gates, *Protection of a single-cysteine redox switch from oxidative destruction: On the functional role of sulfenyl amide formation in the redox-regulated enzyme PTP1B.* Bioorg Med Chem Lett, 2010. **20**(2): p. 444-7.
37. Chung, H.S., et al., *Cysteine oxidative posttranslational modifications: emerging regulation in the cardiovascular system.* Circ Res, 2013. **112**(2): p. 382-92.
38. Mustafa, A.K., et al., *H2S signals through protein S-sulfhydration.* Sci Signal, 2009. **2**(96): p. ra72.
39. Ishii, I., et al., *Cystathionine gamma-Lyase-deficient mice require dietary cysteine to protect against acute lethal myopathy and oxidative injury.* J Biol Chem, 2010. **285**(34): p. 26358-68.
40. Yang, G., et al., *H2S as a physiologic vasorelaxant: hypertension in mice with deletion of cystathionine gamma-lyase.* Science, 2008. **322**(5901): p. 587-90.

41. Krishnan, N., et al., *H2S-Induced sulfhydration of the phosphatase PTP1B and its role in the endoplasmic reticulum stress response.* Sci Signal, 2011. **4**(203): p. ra86.
42. Paul, B.D., et al., *Cystathionine gamma-lyase deficiency mediates neurodegeneration in Huntington's disease.* Nature, 2014. **509**(7498): p. 96-100.
43. Lee, Z.W., et al., *The cystathionine gamma-lyase/hydrogen sulfide system maintains cellular glutathione status.* Biochem J, 2014. **460**(3): p. 425-35.
44. Sen, N., et al., *Hydrogen sulfide-linked sulfhydration of NF-kappaB mediates its antiapoptotic actions.* Mol Cell, 2012. **45**(1): p. 13-24.
45. Mir, S., T. Sen, and N. Sen, *Cytokine-Induced GAPDH Sulfhydration Affects PSD95 Degradation and Memory.* Mol Cell, 2014. **56**(6): p. 786-95.
46. Guan, X. and C.A. Fierke, *Understanding Protein Palmitoylation: Biological Significance and Enzymology.* Sci China Chem, 2011. **54**(12): p. 1888-1897.
47. Linder, M.E. and R.J. Deschenes, *New insights into the mechanisms of protein palmitoylation.* Biochemistry, 2003. **42**(15): p. 4311-20.
48. Spurny, R., et al., *Oxidation and nitrosylation of cysteines proximal to the intermediate filament (IF)-binding site of plectin: effects on structure and vimentin binding and involvement in IF collapse.* J Biol Chem, 2007. **282**(11): p. 8175-87.
49. Chen Y.J., et al., *dbGSH: a database of S-glutathionylation Bioinformatics.* Bioinformatics, 2014. **30**(16): p. 2386-2388
50. Stamler, J.S., et al., *(S)NO signals: translocation, regulation, and a consensus motif.* Neuron, 1997. **18**(5): p. 691-6.
51. Song, S.P., et al., *Ras palmitoylation is necessary for N-Ras activation and signal propagation in growth factor signalling.* Biochem J, 2013. **454**(2): p. 323-32.
52. Cuiffo, B. and R. Ren, *Palmitoylation of oncogenic NRAS is essential for leukemogenesis.* Blood, 2010. **115**(17): p. 3598-605.
53. Altaany, Z., et al., *The coordination of S-sulfhydration, S-nitrosylation, and phosphorylation of endothelial nitric oxide synthase by hydrogen sulfide.* Sci Signal, 2014. **7**(342): p. ra87.
54. Hess, D.T., et al., *Protein S-nitrosylation: purview and parameters.* Nat Rev Mol Cell Biol, 2005. **6**(2): p. 150-66.
55. Kane, L.A. and J.E. Van Eyk, *Post-translational modifications of ATP synthase in the heart: biology and function.* J Bioenerg Biomembr, 2009. **41**(2): p. 145-50.
56. Wang, S.B., et al., *Redox regulation of mitochondrial ATP synthase: implications for cardiac resynchronization therapy.* Circ Res, 2011. **109**(7): p. 750-7.
57. Giustarini, D., et al., *S-nitrosation versus S-glutathionylation of protein sulfhydryl groups by S-nitrosoglutathione.* Antioxid Redox Signal, 2005. **7**(7-8): p. 930-9.
58. Konorev, E.A., B. Kalyanaraman, and N. Hogg, *Modification of creatine kinase by S-nitrosothiols: S-nitrosation vs. S-thiolation.* Free Radic Biol Med, 2000. **28**(11): p. 1671-8.
59. Xian, M., et al., *Inhibition of papain by S-nitrosothiols. Formation of mixed disulfides.* J Biol Chem, 2000. **275**(27): p. 20467-73.
60. Gergel, D. and A.I. Cederbaum, *Inhibition of the catalytic activity of alcohol dehydrogenase by nitric oxide is associated with S nitrosylation and the release of zinc.* Biochemistry, 1996. **35**(50): p. 16186-94.

61. Chantzoura, E., et al., *Glutaredoxin-1 regulates TRAF6 activation and the IL-1 receptor/TLR4 signalling.* Biochem Biophys Res Commun, 2010. **403**(3-4): p. 335-9.
62. Chung, S., et al., *Glutaredoxin 1 regulates cigarette smoke-mediated lung inflammation through differential modulation of IκB kinases in mice: impact on histone acetylation.* American Journal of Physiology-Lung Cellular and Molecular Physiology, 2010. **299**(2): p. L192-L203.
63. Gallogly, M.M., D.W. Starke, and J.J. Mieyal, *Mechanistic and kinetic details of catalysis of thiol-disulfide exchange by glutaredoxins and potential mechanisms of regulation.* Antioxid Redox Signal, 2009. **11**(5): p. 1059-81.
64. Liao, B.C., et al., *The glutaredoxin/glutathione system modulates NF-kappaB activity by glutathionylation of p65 in cinnamaldehyde-treated endothelial cells.* Toxicol Sci, 2010. **116**(1): p. 151-63.
65. Tsou, P.S., et al., *Role of Glutaredoxin-Mediated Protein S-Glutathionylation in Cellular Nitroglycerin Tolerance.* The Journal of Pharmacology and Experimental Therapeutics, 2009. **329**(2): p. 649-656.
66. Anathy, V., et al., *Redox based regulation of apoptosis: S-glutathionylation as a regulatory mechanism to control cell death.* Antioxidants & Redox Signaling, 2012. **16**(6): p. 496-505.
67. Cooper, A.J.L., J.T. Pinto, and P.S. Callery, *Reversible and irreversible protein glutathionylation: biological and clinical aspects.* Expert Opin. Drug Metab.Toxicol., 2011. **7**(7): p. 891-910.
68. Dalle-Donne, I., et al., *S-glutathionylation in protein redox regulation.* Free Radical & Medicine, 2007. **43**: p. 883-898.
69. Wang, J., et al., *Reversible glutathionylation regulates actin polymerization in A431 cells.* The Journal of Biologcal Chemistry, 2001. **276**(51): p. 47763-47766.
70. Nelson, K.J., et al., *Cysteine pK(a) values for the bacterial peroxiredoxin AhpC.* Biochemistry, 2008. **47**(48): p. 12860-8.
71. Naoi, M., et al., *Neuromelanin selectively induces apoptosis in dopaminergic SH-SY5Y cells by deglutathionylation in mitochondria: involvement of the protein and melanin component.* J Neurochem, 2008. **105**(6): p. 2489-500.
72. Mailloux, R.J., et al., *Glutaredoxin-2 is required to control oxidative phosphorylation in cardiac muscle by mediating deglutathionylation reactions.* J Biol Chem, 2014. **289**(21): p. 14812-28.
73. Holmgren, A., *Thioredoxin and glutaredoxin systems.* J Biol Chem, 1989. **264**(24): p. 13963-6.
74. Kim, H.S., et al., *Redox regulation of MAPK phosphatase 1 controls monocyte migration and macrophage recruitment.* Proc Natl Acad Sci U S A, 2012. **109**(41): p. E2803-12.
75. Reynaert, N.L., et al., *Dynamic redox control of NF-κB through glutaredoxin-regulated S-glutathionylation of inhibitory κB kinase β.* Proceedings of the National Academy of Sciences, 2006. **103**(35): p. 13086-13091.
76. Bedhomme, M., et al., *Glutathionylation of cytosolic glyceraldehyde-3-phosphate dehydrogenase from the model plant Arabidopsis thaliana is reversed by both glutaredoxins and thioredoxins in vitro.* Biochem J, 2012. **445**(3): p. 337-47.
77. Holmgren, A., *Hydrogen donor system for Escherichia coli ribonucleoside-diphosphate reductase dependent upon glutathione.* Proc Natl Acad Sci U S A, 1976. **73**(7): p. 2275-9.
78. Berglund, O. and A. Holmgren, *A thioredoxin induced by bacteriophage T4. 3. Amino acid sequence around the active center disulfide.* J Biol Chem, 1970. **245**(22): p. 6036-8.

79. Hall, D.E., et al., *Yeast thioredoxin. Amino-acid sequence around the active-center disulfide of thioredoxin I and II.* Eur J Biochem, 1971. **23**(2): p. 328-35.
80. Holmgren, A., *Thioredoxin. 5. Amino acid sequences of the tryptic peptides of peptide A.* Eur J Biochem, 1968. **6**(4): p. 467-74.
81. Holmgren, A., *Thioredoxin. 4. Amino acid sequence of peptide B.* Eur J Biochem, 1968. **5**(3): p. 359-65.
82. Holmgren, A., *Thioredoxin. 6. The amino acid sequence of the protein from escherichia coli B.* Eur J Biochem, 1968. **6**(4): p. 475-84.
83. Holmgren, A., *Glutathione-dependent enzyme reactions of the phage T4 ribonucleotide reductase system.* J Biol Chem, 1978. **253**(20): p. 7424-30.
84. Holmgren, A., R.N. Perham, and A. Baldesten, *Thioredoxin. 3. Amino acid sequences of the peptic peptides from S-aminoethylated peptide B.* Eur J Biochem, 1968. **5**(3): p. 352-8.
85. Holmgren, A. and P. Reichard, *Thioredoxin 2: cleavage with cyanogen bromide.* Eur J Biochem, 1967. **2**(2): p. 187-96.
86. Collinson, E.J. and C.M. Grant, *Role of Glutaredoxins as Glutathione S-transferases.* The Journal of Biologcal Chemistry, 2003. **278**(25): p. 22492-22497.
87. Peltoniemi, M.J., et al., *Insights into deglutathionylation reactions. Different intermediates in the glutaredoxin and protein disulfide isomerase catalyzed reactions are defined by the gamma-linkage present in glutathione.* J Biol Chem, 2006. **281**(44): p. 33107-14.
88. Peltoniemi, M., et al., *Insights into Deglutathionylation reactions: Different intermediates in the glutaredoxin and protein disulphide isomerase catalyzed reactions are defined by the gamma-linkage present in glutathione.* The Journal of Biologcal Chemistry, 2006. **281**(44): p. 33107-33114.
89. Al Khamici, H., et al., *Members of the chloride intracellular ion channel protein family demonstrate glutaredoxin-like enzymatic activity.* PLOS one, 2015. **10**(1): p. e115699.
90. Menon, D. and P.G. Board, *A role for Glutathione transferase Omega 1 (GSTO1-1) in the glutathionylation cycle.* Journal of Biological Chemistry, 2013. **288(36)**(36): p. 25769-79.
91. Rodriguez-Manzaneque, M.T., et al., *Grx5 glutaredoxin plays a central role in protection against protein oxidative damage in Saccharomyces cerevisiae.* Mol Cell Biol, 1999. **19**(12): p. 8180-90.
92. Tamarit, J., et al., *Biochemical characterization of yeast mitochondrial Grx5 monothiol glutaredoxin.* J Biol Chem, 2003. **278**(28): p. 25745-51.
93. Pai, H.V., et al., *What is the functional significance of the unique location of glutaredoxin 1 (GRx1) in the intermembrane space of mitochondria?* Antioxid Redox Signal, 2007. **9**(11): p. 2027-33.
94. Murphy, M.P., *Mitochondrial thiols in antioxidant protection and redox signaling: distinct roles for glutathionylation and other thiol modifications.* Antioxid Redox Signal, 2012. **16**(6): p. 476-95.
95. Hurd, T.R., et al., *Glutathionylation of mitochondrial proteins.* Antioxid Redox Signal, 2005. **7**(7-8): p. 999-1010.
96. Holmgren, A., *The function of thioredoxin and glutathione in deoxyribonucleic acid synthesis.* Biochem Soc Trans, 1977. **5**(3): p. 611-2.
97. Holmgren, A., *Glutathione-dependent synthesis of deoxyribonucleotides. Characterization of the enzymatic mechanism of Escherichia coli glutaredoxin.* J Biol Chem, 1979. **254**(9): p. 3672-8.

98. Luthman, M., et al., *Glutathione-dependent hydrogen donor system for calf thymus ribonucleoside-diphosphate reductase.* Proc Natl Acad Sci U S A, 1979. **76**(5): p. 2158-62.
99. Greetham, D., et al., *Thioredoxins function as deglutathionylase enzymes in the yeast Saccharomyces cerevisiae.* BMC Biochemistry 2010. **11**(3).
100. Freedman, R.B., T.R. Hirst, and M.F. Tuite, *Protein disulphide isomerase: building bridges in protein folding.* Trends Biochem Sci, 1994. **19**(8): p. 331-6.
101. Tu, B.P. and J.S. Weissman, *Oxidative protein folding in eukaryotes: mechanisms and consequences.* J Cell Biol, 2004. **164**(3): p. 341-6.
102. Wilkinson, B. and H.F. Gilbert, *Protein disulfide isomerase.* Biochim Biophys Acta, 2004. **1699**(1-2): p. 35-44.
103. Hawkins, H.C. and R.B. Freedman, *The reactivities and ionization properties of the active-site dithiol groups of mammalian protein disulphide-isomerase.* Biochem J, 1991. **275 (Pt 2)**: p. 335-9.
104. Grek, C. and D.M. Townsend, *Protein Disulfide Isomerase Superfamily in Disease and the Regulation of Apoptosis.* Endoplasmic Reticulum Stress Dis, 2014. **1**(1): p. 4-17.
105. Uys, J.D., Y. Xiong, and D.M. Townsend, *Nitrosative stress-induced S-glutathionylation of protein disulfide isomerase.* Methods Enzymol, 2011. **490**: p. 321-32.
106. Xiong, Y., et al., *S-Glutathionylation of Protein Disulfide Isomerase Regulates Estrogen Receptor alpha Stability and Function.* Int J Cell Biol, 2012. **2012**: p. 273549.
107. Townsend, D.M., et al., *Nitrosative stress-induced s-glutathionylation of protein disulfide isomerase leads to activation of the unfolded protein response.* Cancer Res, 2009. **69**(19): p. 7626-34.
108. Tew, K.D. and D.M. Townsend, *Glutathione-S-Transferases As Determinants of Cell Survival and Death.* Antioxid Redox Signal, 2012. **17(12)**(12): p. 1728-37.
109. Tew, K.D. and D.M. Townsend, *Regulatory functions of glutathione S-transferase P1-1 unrelated to detoxification.* Drug Metab Rev. **43**(2): p. 179-93.
110. Tew, K.D., et al., *The role of glutathione S-transferase P in signaling pathways and S-glutathionylation in cancer.* Free Radic Biol Med, 2011. **51**(2): p. 299-313.
111. Tew, K.D. and D.M. Townsend, *Regulatory functions of glutathione S-transferase P1-1 unrelated to detoxification.* Drug Metab Rev, 2011. **43**(2): p. 179-93.
112. Townsend, D.M., et al., *Novel role for Glutathione transferase Pi: Regulator of Protein S-glutathionylation following oxidative and nitrosative stress.* The Journal of Biologcal Chemistry, 2008.
113. Townsend, D.M. and K.D. Tew, *The role of glutathione-S-transferase in anti-cancer drug resistance.* Oncogene, 2003. **22**(47): p. 7369-75.
114. Biteau, B., J. Labarre, and M.B. Toledano, *ATP-dependent reduction of cysteine-sulphinic acid by S. cerevisiae sulphiredoxin.* Nature, 2003. **425**(6961): p. 980-4.
115. Perkins, A., L.B. Poole, and P.A. Karplus, *Tuning of peroxiredoxin catalysis for various physiological roles.* Biochemistry, 2014. **53**(49): p. 7693-705.
116. Jonsson, T.J., et al., *Structural basis for the retroreduction of inactivated peroxiredoxins by human sulfiredoxin.* Biochemistry, 2005. **44**(24): p. 8634-42.
117. Findlay, V.J., H. Tapiero, and D.M. Townsend, *Sulfiredoxin: a potential therapeutic agent?* Biomed Pharmacother, 2005. **59**(7): p. 374-9.

118. Reynaert, N.L., et al., *Dynamic redox control of NF-kappaB through glutaredoxin-regulated S-glutathionylation of inhibitory kappaB kinase beta.* Proc Natl Acad Sci U S A, 2006. **103**(35): p. 13086-91.
119. Pineda-Molina, E., et al., *Glutathionylation of the p50 subunit of NF-kappaB: a mechanism for redox-induced inhibition of DNA binding.* Biochemistry, 2001. **40**(47): p. 14134-42.
120. Elgan, T.H. and K.D. Berndt, *Quantifying Escherichia coli glutaredoxin-3 substrate specificity using ligand-induced stability.* J Biol Chem, 2008. **283**(47): p. 32839-47.
121. Dalle-Donne, I., et al., *Molecular mechanisms and potential clinical significance of S-glutathionylation.* Antioxid Redox Signal, 2008. **10**(3): p. 445-73.
122. Stone, R.L. and J.E. Dixon, *Protein-tyrosine phosphatases.* J Biol Chem, 1994. **269**(50): p. 31323-6.
123. Fritz-Wolf, K., et al., *Structure of mitochondrial creatine kinase.* Nature, 1996. **381**(6580): p. 341-5.
124. Furter, R., E.M. Furter-Graves, and T. Wallimann, *Creatine kinase: the reactive cysteine is required for synergism but is nonessential for catalysis.* Biochemistry, 1993. **32**(27): p. 7022-9.
125. Wang, P.F., et al., *An unusually low pK(a) for Cys282 in the active site of human muscle creatine kinase.* Biochemistry, 2001. **40**(39): p. 11698-705.
126. Mohr, S., et al., *Nitric oxide-induced S-glutathionylation and inactivation of glyceraldehyde-3-phosphate dehydrogenase.* J Biol Chem, 1999. **274**(14): p. 9427-30.
127. Choi, H.J., et al., *Crystal structure of a novel human peroxidase enzyme at 2.0 A resolution.* Nat Struct Biol, 1998. **5**(5): p. 400-6.
128. Hayano, T., et al., *PDI and glutathione-mediated reduction of the glutathionylated variant of human lysozyme.* FEBS, 1993. **328**(1.2): p. 203-208.
129. Shelton, M.D. and J.J. Mieyal, *Regulation by reversible S-glutathionylation: molecular targets implicated in inflammatory diseases.* Molecules and cells, 2008. **25**(3): p. 332.
130. Ghezzi, P., et al., *Redox regulation of cyclophilin A by glutathionylation.* Proteomics, 2006. **6**(3): p. 817-25.
131. Gravina, S.A. and J.J. Mieyal, *Thioltransferase is a specific glutathionyl mixed disulfide oxidoreductase.* Biochemistry, 1993. **32**(13): p. 3368-76.
132. Yang, Y., et al., *Reactivity of the human thioltransferase (glutaredoxin) C7S, C25S, C78S, C82S mutant and NMR solution structure of its glutathionyl mixed disulfide intermediate reflect catalytic specificity.* Biochemistry, 1998. **37**(49): p. 17145-56.
133. Klatt, P., et al., *Novel application of S-nitrosoglutathione-Sepharose to identify proteins that are potential targets for S-nitrosoglutathione-induced mixed-disulphide formation.* Biochem J, 2000. **349**(Pt 2): p. 567-78.
134. Hill, B.G. and A. Bhatnagar, *Protein S-glutathiolation: Redox-sensitive regulation of protein function.* Journal of Molecular and Cellular Cardiology, 2011. **52**(3): p. 559-67.
135. Nulton-Persson, A.C., et al., *Reversible inactivation of alpha-ketoglutarate dehydrogenase in response to alterations in the mitochondrial glutathione status.* Biochemistry, 2003. **42**(14): p. 4235-42.
136. Shenton, D. and C.M. Grant, *Protein S-thiolation targets glycolysis and protein synthesis in response to oxidative stress in the yeast Saccharomyces cerevisiae.* Biochem J, 2003. **374**(Pt 2): p. 513-9.

137. Velu, C.S., et al., *Human p53 is inhibited by glutathionylation of cysteines present in the proximal DNA-binding domain during oxidative stress.* Biochemistry, 2007. **46**: p. 7765-7780.
138. Jalilian, C., et al., *Redox potential and the response of cardiac ryanodine receptors to CLIC-2, a member of the glutathione S-transferase structural family.* Antioxid Redox Signal, 2008. **10**(10): p. 1675-86.
139. Lock, J.T., W.J.a. Sinkins, and W.P. Schilling, *Effect of protein S-glutathionylation on Ca2+ homeostasis in cultured aortic endothelial cells* Am J Physiol Heart Circ Physiol, 2011. **300**: p. 493-506.
140. Terentyev, D., et al., *Redox modification of ryanodine receptors contributes to sarcoplasmic reticulum Ca2+ leak in chronic heart failure.* Circ Res. , 2008. **103**(12): p. 1466-72.
141. Luca, A.D., et al., *Treatment of Doxorubicin resistant MCF7/Dx cells with Nitric Oxide causes histone glutathionylation and reversal of drug resistance.* Biochemical Journal, 2011. **440**(2): p. 175-83.
142. Shelton, M.D. and J.J. Mieyal, *Regulation by reversible S-glutathionylation: molecular targets implicated in inflammatory diseases.* Mol Cells, 2008. **25**(3): p. 332-46.
143. Di Domenico, F., et al., *Glutathionylation of the pro-apoptotic protein p53 in Alzheimer's disease brain: implications for AD pathogenesis.* Neurochem Res, 2009. **34**(4): p. 727-33.
144. Lim, S.Y., et al., *S-glutathionylation regulates inflammatory activities of S100A9.* Journal of Biological Chemistry, 2010. **285**(19): p. 14377-14388.
145. Sanchez-Gomez, F.J., et al., *S-glutathionylation: relevance in diabetes and potential role as a biomarker.* Biol Chem, 2013. **394**(10): p. 1263-80.
146. Burgoyne, J.R., et al., *Redox signaling in cardiac physiology and pathology.* Circ Res, 2012. **111**(8): p. 1091-106.
147. Bedard, K. and K.H. Krause, *The NOX family of ROS-generating NADPH oxidases: physiology and pathophysiology.* Physiol Rev, 2007. **87**(1): p. 245-313.
148. Forman, H.J. and M. Torres, *Redox signaling in macrophages.* Mol Aspects Med, 2001. **22**(4-5): p. 189-216.
149. Maitra, U., et al., *IRAK-1 contributes to lipopolysaccharide-induced reactive oxygen species generation in macrophages by inducing NOX-1 transcription and Rac1 activation and suppressing the expression of antioxidative enzymes.* Journal of Biological Chemistry, 2009. **284**(51): p. 35403-35411.
150. van Bruggen, R., et al., *Human NLRP3 inflammasome activation is Nox1-4 independent.* Blood, 2010. **115**(26): p. 5398-400.
151. Gebhardt, C., et al., *S100A8 and S100A9 in inflammation and cancer.* Biochem Pharmacol, 2006. **72**(11): p. 1622-31.
152. Gomes, L.H., et al., *S100A8 and S100A9-oxidant scavengers in inflammation.* Free Radic Biol Med, 2013. **58**: p. 170-86.
153. Ryckman, C., et al., *Proinflammatory activities of S100: proteins S100A8, S100A9, and S100A8/A9 induce neutrophil chemotaxis and adhesion.* J Immunol, 2003. **170**(6): p. 3233-42.
154. Lim, S.Y., et al., *S-glutathionylation regulates inflammatory activities of S100A9.* J Biol Chem, 2010. **285**(19): p. 14377-88.
155. Bowers, R.R., et al., *Sulfiredoxin redox-sensitive interaction with S100A4 and non-muscle myosin IIA regulates cancer cell motility.* Biochemistry, 2012. **51**(39): p. 7740-54.

156. Ullevig, S., et al., *NADPH oxidase 4 mediates monocyte priming and accelerated chemotaxis induced by metabolic stress.* Arterioscler Thromb Vasc Biol, 2012. **32**(2): p. 415-26.
157. Lee, C.F., et al., *Regulation of Monocyte Adhesion and Migration by Nox4.* PLOS one, 2013. **8**(6): p. e66964.
158. Takashima, Y., et al., *Differential expression of glutaredoxin and thioredoxin during monocytic differentiation.* Immunol Lett, 1999. **68**(2-3): p. 397-401.
159. Salzano, S., et al., *Linkage of inflammation and oxidative stress via release of glutathionylated peroxiredoxin-2, which acts as a danger signal.* Proc Natl Acad Sci U S A, 2014. **111**(33): p. 12157-62.
160. Meissner, F., K. Molawi, and A. Zychlinsky, *Superoxide dismutase 1 regulates caspase-1 and endotoxic shock.* Nat Immunol, 2008. **9**(8): p. 866-72.
161. Coll, R.C. and L.A. O'Neill, *New insights into the regulation of signalling by toll-like receptors and nod-like receptors.* Journal of innate immunity, 2010. **2**(5): p. 406-421.
162. Doyle, S.L. and L.A. O'Neill, *Toll-like receptors: from the discovery of NFκB to new insights into transcriptional regulations in innate immunity.* Biochemical pharmacology, 2006. **72**(9): p. 1102-1113.
163. Hennessy, E.J., A.E. Parker, and L.A. O'Neill, *Targeting Toll-like receptors: emerging therapeutics?* Nat Rev Drug Discov, 2010. **9**(4): p. 293-307.
164. Baeuerle, P.A. and T. Henkel, *Function and activation of NF-kappaB in the immune system.* Annual review of immunology, 1994. **12**(1): p. 141-179.
165. Cogswell, J.P., et al., *NF-kappa B regulates IL-1 beta transcription through a consensus NF-kappa B binding site and a nonconsensus CRE-like site.* The Journal of immunology, 1994. **153**(2): p. 712-723.
166. D'Acquisto, F., et al., *Involvement of NF-kappaB in the regulation of cyclooxygenase-2 protein expression in LPS-stimulated J774 macrophages.* FEBS Lett, 1997. **418**(1-2): p. 175-8.
167. Ghosh, S. and M.S. Hayden, *New regulators of NF-kappaB in inflammation.* Nat Rev Immunol, 2008. **8**(11): p. 837-48.
168. Palsson-McDermott, E.M. and L.A. O'Neill, *Signal transduction by the lipopolysaccharide receptor, Toll-like receptor-4.* Immunology, 2004. **113**(2): p. 153-62.
169. Asmis, R., et al., *A novel thiol oxidation-based mechanism for adriamycin-induced cell injury in human macrophages.* FASEB J, 2005. **19**(13): p. 1866-8.
170. Asmis, R., et al., *Adriamycin promotes macrophage dysfunction in mice.* Free Radic Biol Med, 2006. **41**(1): p. 165-74.
171. Lane, T., et al., *TXNIP shuttling: missing link between oxidative stress and inflammasome activation.* Front Physiol, 2013. **4**: p. 50.
172. Vandanmagsar, B., et al., *The NLRP3 inflammasome instigates obesity-induced inflammation and insulin resistance.* Nature medicine, 2011. **17**(2): p. 179-188.
173. Townsend, D.M., C.J. Pazoles, and K.D. Tew, *NOV-002, a mimetic of glutathione disulfide.* Expert Opin Investig Drugs, 2008. **17**(7): p. 1075-83.
174. Townsend, D.M., et al., *NOV-002, a glutathione disulfide mimetic, as a modulator of cellular redox balance.* Cancer Res, 2008. **68**(8): p. 2870-7.
175. Townsend, D.M. and K.D. Tew, *Pharmacology of a mimetic of glutathione disulfide, NOV-002.* Biomed Pharmacother, 2009. **63**(2): p. 75-8.
176. Diaz-Montero, C.M., et al., *The glutathione disulfide mimetic NOV-002 inhibits cyclophosphamide-induced hematopoietic and immune suppression by reducing oxidative stress.* Free Radic Biol Med, 2012. **52**(9): p. 1560-8.
177. Board, P.G. and M.W. Anders, *Human glutathione transferase zeta.* Methods Enzymol, 2005. **401**: p. 61-77.

178. Board, P.G. and M.W. Anders, *Glutathione transferase zeta: discovery, polymorphic variants, catalysis, inactivation, and properties of Gstz1-/- mice.* Drug Metab Rev, 2011. **43**(2): p. 215-25.
179. Board, P.G., *The Omega-class glutathione transferases: structure, function and genetics.* Drug Metabolism Reviews, 2011. **43**(2): p. 226-235.
180. Board, P.G. and D. Menon, *Glutathione transferases, regulators of cellular metabolism and physiology.* Biochimica et Biophysica Acta (BBA)-General Subjects, 2012. **1830**(5): p. 3267–328.
181. Litwack, G., B. Ketterer, and I.M. Arias, *Ligandin: a hepatic protein which binds steroids, bilirubin, carcinogens and a number of exogenous organic anions.* Nature, 1971. **234**(5330): p. 466-7.
182. Arias, I.M., *Ligandin: review and update of a multifunctional protein.* Med Biol, 1979. **57**(5): p. 328-34.
183. Fleischner, G.M. and I.M. Arias, *Structure and function of ligandin (Y protein, GSH transferase B) and Z protein in the liver: a progress report.* Prog Liver Dis, 1976. **5**: p. 172-82.
184. Kamisaka, K., et al., *The binding of bilirubin and other organic anions to serum albumin and ligandin (Y protein).* Birth Defects Orig Artic Ser, 1976. **12**(2): p. 156-67.
185. Habig, W.H., et al., *The identity of glutathione S-transferase B with ligandin, a major binding protein of liver.* Proc Natl Acad Sci U S A, 1974. **71**(10): p. 3879-82.
186. Kamisaka, K., et al., *Multiple forms of human glutathione S-transferase and their affinity for bilirubin.* Eur J Biochem, 1975. **60**(1): p. 153-61.
187. Alin, P., et al., *Purification of major basic glutathione transferase isoenzymes from rat liver by use of affinity chromatography and fast protein liquid chromatofocusing.* Anal Biochem, 1985. **146**(2): p. 313-20.
188. Jakoby, W.B., *The glutathione S-transferases: a group of multifunctional detoxification proteins.* Adv Enzymol Relat Areas Mol Biol, 1978. **46**: p. 383-414.
189. Jakoby, W.B. and D.M. Ziegler, *The enzymes of detoxication.* J Biol Chem, 1990. **265**(34): p. 20715-8.
190. Ketley, J.N., W.H. Habig, and W.B. Jakoby, *Binding of nonsubstrate ligands to the glutathione S-transferases.* J Biol Chem, 1975. **250**(22): p. 8670-3.
191. Marcus, C.J., W.H. Habig, and W.B. Jakoby, *Glutathione transferase from human erythrocytes. Nonidentity with the enzymes from liver.* Arch Biochem Biophys, 1978. **188**(2): p. 287-93.
192. Pabst, M.J., W.H. Habig, and W.B. Jakoby, *Glutathione S-transferase A. A novel kinetic mechanism in which the major reaction pathway depends on substrate concentration.* J Biol Chem, 1974. **249**(22): p. 7140-7.
193. Wolkoff, A.W., R.A. Weisiger, and W.B. Jakoby, *The multiple roles of the glutathione transferases (ligandins).* Prog Liver Dis, 1979. **6**: p. 213-24.
194. Mannervik, B., et al., *Nomenclature for Mammalian Soluble Glutathione Transferases.* Methods in Enzymology, 2005. **401**: p. 1-8.
195. Hayes, J.D., J.U. Flanagan, and I.R. Jowsey, *Glutathione transferases.* Annu Rev Pharmacol Toxicol, 2005. **45**: p. 51-88.
196. Jowsey, I.R., et al., *Mammalian class Sigma glutathione S-transferases: catalytic properties and tissue-specific expression of human and rat GSH-dependent prostaglandin D2 synthases.* Biochem J, 2001. **359**(Pt 3): p. 507-16.
197. Whitbread, A.K., et al., *Characterization of the omega class of glutathione transferases.* Methods Enzymol, 2005. **401**: p. 78-99.

198. Giffen, P.S., et al., *Alpha-glutathione S-transferase in the assessment of hepatotoxicity--its diagnostic utility in comparison with other recognized markers in the Wistar Han rat.* Toxicol Pathol, 2002. **30**(3): p. 365-72.
199. Abdellatif, Y., et al., *The Mu class glutathione transferase is abundant in striated muscle and is an isoform-specific regulator of ryanodine receptor calcium channels.* Cell Calcium, 2007. **41**(5): p. 429-40.
200. Adler, V., et al., *Regulation of JNK signaling by GSTp.* . EMBO J, 1999. **18**(5): p. 1321-1334.
201. Beuckmann, C.T., et al., *Identification of mu-class glutathione transferases M2-2 and M3-3 as cytosolic prostaglandin E synthases in the human brain.* Neurochem Res, 2000. **25**(5): p. 733-8.
202. Board, P.G., et al., *CLIC-2 modulates cardiac ryanodine receptor Ca2+ release channels.* Int J Biochem Cell Biol, 2004. **36**(8): p. 1599-612.
203. Bogaards, J.J., J.C. Venekamp, and P.J. van Bladeren, *Stereoselective conjugation of prostaglandin A2 and prostaglandin J2 with glutathione, catalyzed by the human glutathione S-transferases A1-1, A2-2, M1a-1a, and P1-1.* Chem Res Toxicol, 1997. **10**(3): p. 310-7.
204. Fernandez-Canon, J.M., et al., *Maleylacetoacetate isomerase (MAAI/GSTZ)-deficient mice reveal a glutathione-dependent nonenzymatic bypass in tyrosine catabolism.* Mol Cell Biol, 2002. **22**(13): p. 4943-51.
205. Dulhunty, A., et al., *The glutathione transferase structural family includes a nuclear chloride channel and a ryanodine receptor calcium release channel modulator.* J Biol Chem, 2001. **276**(5): p. 3319-23.
206. Witham, S., et al., *A missense mutation in CLIC2 associated with intellectual disability is predicted by in silico modeling to affect protein stability and dynamics.* Proteins, 2011. **79**(8): p. 2444-54.
207. Dulhunty, A.F., et al., *Regulation of the cardiac muscle ryanodine receptor by glutathione transferases.* Drug Metab Rev, 2011. **43**(2): p. 236-52.
208. Liu, D., et al., *Dissection of the inhibition of cardiac ryanodine receptors by human glutathione transferase GSTM2-2.* Biochem Pharmacol, 2009. **77**(7): p. 1181-93.
209. Wei, L., et al., *Muscle-specific GSTM2-2 on the luminal side of the sarcoplasmic reticulum modifies RyR ion channel activity.* Int J Biochem Cell Biol, 2008. **40**(8): p. 1616-28.
210. Allen, M., et al., *Glutathione S-transferase omega genes in Alzheimer and Parkinson disease risk, age-at-diagnosis and brain gene expression: an association study with mechanistic implications.* Mol Neurodegener, 2012. **7**(1): p. 13.
211. Capurso, C., et al., *Polymorphisms in Glutathione S-Transferase Omega-1 Gene and Increased Risk of Sporadic Alzheimer Disease.* Rejuvenation Research 2010. **13**(6): p. 645-652.
212. Escobar-Garcia, D.M., et al., *Association of glutathione S-transferase Omega 1-1 polymorphisms (A140D and E208K) with the expression of interleukin-8 (IL-8), transforming growth factor beta (TGF-beta), and apoptotic protease-activating factor 1 (Apaf-1) in humans chronically exposed to arsenic in drinking water.* Arch Toxicol, 2012. **86**(6): p. 857-68.
213. Harju, T.H., et al., *Glutathione S-transferase omega in the lung and sputum supernatants of COPD patients.* Respiratiory Research, 2007. **8**(1): p. 48.
214. Kölsch, H., et al., *Polymorphisms in glutathione S-transferase omega-1 and AD, vascular dementia, and stroke.* Neurology, 2004. **63**(12): p. 2255-60.

215. Li YJ, et al., *Glutathione S-transferase omega-1 modifies age-at-onset of Alzheimer disease and Parkinson disease.* Hum Mol Genet. , 2003. **12**(24): p. 3259-3267.
216. Li, Y.J., et al., *Revealing the role of glutathione S-transferase omega in age-at-onset of Alzheimer and Parkinson diseases.* Neurobiol Aging, 2006. **27**(8): p. 1087-1093.
217. Van De Giessen, E., et al., *Association study on glutathione S-transferase omega 1 and 2 and familial ALS.* Amyotrophic Lateral Sclerosis, 2008. **9**(2): p. 81-84.
218. Pearson, W.R., *Phylogenies of glutathione transferase families.* Methods Enzymol, 2005. **401**: p. 186-204.
219. Blackburn, A.C., et al., *Deficiency of glutathione transferase zeta causes oxidative stress and activation of antioxidant response pathways.* Mol Pharmacol, 2006. **69**(2): p. 650-7.
220. Johansson, K., et al., *Microsomal glutathione transferase 1 in anticancer drug resistance.* Carcinogenesis, 2007. **28**(2): p. 465-70.
221. Johansson, A.S. and B. Mannervik, *Human glutathione transferase A3-3, a highly efficient catalyst of double-bond isomerization in the biosynthetic pathway of steroid hormones.* J Biol Chem, 2001. **276**(35): p. 33061-5.
222. Ohno, K., et al., *Effect of glutathione content on cellular uptake and growth inhibitory activity of prostaglandin A2 in L-1210 cells.* Eicosanoids, 1992. **5**(2): p. 81-5.
223. Atsmon, J., et al., *Formation of thiol conjugates of 9-deoxy-delta 9,delta 12(E)-prostaglandin D2 and delta 12(E)-prostaglandin D2.* Biochemistry, 1990. **29**(15): p. 3760-5.
224. Atsmon, J., et al., *Conjugation of 9-deoxy-delta 9,delta 12(E)-prostaglandin D2 with intracellular glutathione and enhancement of its antiproliferative activity by glutathione depletion.* Cancer Res, 1990. **50**(6): p. 1879-85.
225. Kanaoka, Y., et al., *Cloning and crystal structure of hematopoietic prostaglandin D synthase.* Cell, 1997. **90**(6): p. 1085-95.
226. Anderson, W.B., et al., *Inactivation of Glutathione Transferase Zeta by Dichloroacetic Acid and Other Fluorine-Lacking alpha-Haloalkanoic Acids.* Chem. Res. Toxicol., 1999. **12**: p. 1144-1149.
227. Stacpoole, P.W., *The dichloroacetate dilemma: environmental hazard versus therapeutic goldmine--both or neither?* Environ Health Perspect, 2011. **119**(2): p. 155-8.
228. Lantum, H.B., et al., *Alkylation and inactivation of human glutathione transferase zeta (hGSTZ1-1) by maleylacetone and fumarylacetone.* Chem Res Toxicol, 2002. **15**(5): p. 707-16.
229. Bonnet, S., et al., *A mitochondria-K+ channel axis is suppressed in cancer and its normalization promotes apoptosis and inhibits cancer growth.* Cancer Cell, 2007. **11**(1): p. 37-51.
230. Sun, R.C., et al., *Reversal of the glycolytic phenotype by dichloroacetate inhibits metastatic breast cancer cell growth in vitro and in vivo.* Breast Cancer Res Treat, 2010. **120**(1): p. 253-60.
231. Sun, R.C., P.G. Board, and A.C. Blackburn, *Targeting metabolism with arsenic trioxide and dichloroacetate in breast cancer cells.* Mol Cancer, 2011. **10**: p. 142.
232. Ishiguro, T., et al., *Cotreatment with dichloroacetate and omeprazole exhibits a synergistic antiproliferative effect on malignant tumors.* Oncol Lett, 2012. **3**(3): p. 726-728.

233. Sutendra, G., et al., *Mitochondrial activation by inhibition of PDKII suppresses HIF1a signaling and angiogenesis in cancer.* Oncogene, 2013. **32**(13): p. 1638-50.
234. Lim, C., et al., *Mice deficient in Glutathione Transferase Zeta/ Maleylacetoacetate isomerase exhibit a Range of Pathology Changes and Elevated Expression of Alpha, Mu and Pi Class Glutathione Transferases.* American Journal of Pathology, 2004. **165**(2): p. 679-693.
235. Theodoratos, A., et al., *Phenylalanine-induced leucopenia in genetic and dichloroacetic acid generated deficiency of glutathione transferase Zeta.* Biochem Pharmacol, 2009. **77**(8): p. 1358-63.
236. Tew, K.D. and D.M. Townsend, *Regulatory functions of glutathione S-transferase Pi-1 unrelated to detoxification.* Drug Metabolsim Reviews, 2011. **43**(2): p. 179-193.
237. Lacave, R., et al., *Comparative evaluation by semiquantitative reverse transcriptase polymerase chain reaction of MDR1, MRP and GSTp gene expression in breast carcinomas.* Br J Cancer, 1998. **77**(5): p. 694-702.
238. Adler, V., et al., *Regulation of JNK signaling by GSTp.* EMBO J, 1999. **18**(5): p. 1321-34.
239. Elsby, R., et al., *Increased constitutive c-Jun N-terminal kinase signaling in mice lacking glutathione S-transferase Pi.* J Biol Chem, 2003. **278**(25): p. 22243-9.
240. Gate, L., et al., *Increased myeloproliferation in glutathione S-transferase pi-deficient mice is associated with a deregulation of JNK and Janus kinase/STAT pathways.* J Biol Chem, 2004. **279**(10): p. 8608-16.
241. Castro-Caldas, M., et al., *Glutathione S-Transferase pi Mediates MPTP-Induced c-Jun N-Terminal Kinase Activation in the Nigrostriatal Pathway.* Mol Neurobiol, 2012. **45**(3): p. 466-77.
242. Wu, Y., et al., *Human glutathione S-transferase P1-1 interacts with TRAF2 and regulates TRAF2-ASK1 signals.* Oncogene, 2006. **25**(42): p. 5787-800.
243. Romero, L., et al., *Human GSTA1-1 reduces c-Jun N-terminal kinase signalling and apoptosis in Caco-2 cells.* Biochem J, 2006. **400**(1): p. 135-41.
244. Sharma, A., et al., *Glutathione S-transferases as antioxidant enzymes: small cell lung cancer (H69) cells transfected with hGSTA1 resist doxorubicin-induced apoptosis.* Arch Biochem Biophys, 2006. **452**(2): p. 165-73.
245. Dorion, S., H. Lambert, and J. Landry, *Activation of the p38 signaling pathway by heat shock involves the dissociation of glutathione S-transferase Mu from Ask1.* J Biol Chem, 2002. **277**(34): p. 30792-7.
246. Arakawa, S., et al., *Resistance to acetaminophen-induced hepatotoxicity in glutathione S-transferase Mu 1 null mice.* J Toxicol Sci, 2012. **37**(3): p. 595-605.
247. Dulhunty, A.F., et al., *Regulation of the cardiac muscle ryanodine receptor by glutathione transferases.* Drug Metab Rev., 2011. **43**(2): p. 236-252.
248. Lanner, J.T., et al., *Ryanodine receptors: structure, expression, molecular details, and function in calcium release.* Cold Spring Harb Perspect Biol. **2**(11): p. a003996.
249. Hool, L.C. and B. Corry, *Redox control of calcium channels: from mechanisms to therapeutic opportunities.* Antioxid Redox Signal, 2007. **9**(4): p. 409-35.
250. Turan, B. and G. Vassort, *Ryanodine receptor: a new therapeutic target to control diabetic cardiomyopathy.* Antioxid Redox Signal, 2011. **15**(7): p. 1847-61.

251. Liu, D., et al., *The inhibitory glutathione transferase M2-2 binding site is located in divergent region 3 of the cardiac ryanodine receptor.* Biochem Pharmacol. **83**(11): p. 1523-9.
252. Henderson, C.J., et al., *Increased skin papilloma formation in mice lacking glutathione transferase GSTP.* Cancer Res, 2011. **71**(22): p. 7048-60.
253. Mannervik, B., et al., *Expression of class Pi glutathione transferase in human malignant melanoma cells.* Carcinogenesis, 1987. **8**(12): p. 1929-32.
254. Shea, T.C., S.L. Kelley, and W.D. Henner, *Identification of an anionic form of glutathione transferase present in many human tumors and human tumor cell lines.* Cancer Res, 1988. **48**(3): p. 527-33.
255. Tidefelt, U., et al., *Expression of glutathione transferase pi as a predictor for treatment results at different stages of acute nonlymphoblastic leukemia.* Cancer Res, 1992. **52**(12): p. 3281-5.
256. Lien, S., A.K. Larsson, and B. Mannervik, *The polymorphic human glutathione transferase T1-1, the most efficient glutathione transferase in the denitrosation and inactivation of the anticancer drug 1,3-bis(2-chloroethyl)-1-nitrosourea.* Biochem Pharmacol, 2002. **63**(2): p. 191-7.
257. Morrow, C.S., et al., *Coordinated action of glutathione S-transferases (GSTs) and multidrug resistance protein 1 (MRP1) in antineoplastic drug detoxification. Mechanism of GST A1-1- and MRP1-associated resistance to chlorambucil in MCF7 breast carcinoma cells.* J Biol Chem, 1998. **273**(32): p. 20114-20.
258. Kodym, R., P. Calkins, and M. Story, *The Cloning and Characterization of a New Stress Response Protein. A mammalian member of a family of tetha class of glutathione transferase-like proteins.* The Journal of Biological Chemistry, 1999. **274**(8): p. 5131-5137.
259. Yan, X.D., et al., *Identification of Platinum-Resistance Associated Proteins through Proteomic Analysis of Human Ovarian Cancer Cells and Their Platinum-Resistant Sublines.* J Proteome Res., 2007. **6**(2): p. 772-780.
260. Piaggi, S., et al., *Glutathione transferase omega 1-1 (GSTO1-1) plays an anti-apoptotic role in cell resistance to cisplatin toxicity.* Carcinogenesis, 2010. **31**(5): p. 804-811.
261. Kim, K., et al., *Glutathione s-transferase omega 1 activity is sufficient to suppress neurodegeneration in a Drosophila model of Parkinson disease.* J Biol Chem, 2012. **287**(9): p. 6628-41.
262. Board, P.G., et al., *Identification, Characterization and Crystal Structure of the Omega Class Glutathione Transferases.* The Journal of Biological Chemistry, 2000. **275**(32): p. 24798-24806.
263. Yin, Z.L., et al., *Immunohistochemistry of omega class glutathione S-transferase in human tissues.* J Histochem Cytochem, 2001. **49**(8): p. 983-7.
264. Laliberte, R.E., et al., *Glutathione S-Transferase Omega 1-1 Is a Target of Cytokine Release Inhibitory Drugs and May Be Resposible for their Effect on Interleukin-1Beta Posttranslational processing.* The Journal of Biological Chemistry, 2003. **278**(19): p. 16567-16578.
265. Coll, R.C. and L.A.J. O'Neill, *The Cytokine Release Inhibitory Drug CRID3 Targets ASC Oligomerisation in the NLRP3 and AIM2 Inflammasomes.* PLOS one, 2011. **6**(12): p. e29539.
266. Board, P.G., *The omega-class glutathione transferases: structure, function, and genetics.* Drug Metab Rev., 2011. **43**(2): p. 226-235.
267. Burmeister, C., et al., *Oxidative stress in Caenorhabditis elegans: protectve effects of the Omega class glutathione transferase (GSTO-1).* The FASEB Journal, 2008. **22**: p. 343-354.

268. Story, M.D. and R.E. Meyn, *Modulation of apoptosis and enhancement of chemosensitivity by decreasing cellular thiols in a mouse B-cell lymphoma cell line that overexpresses bcl-2.* Cancer Chemother Pharmacol, 1999. **44**: p. 362-366.
269. Dulhunty, A., et al., *The glutathione transferase structural family includes a nuclear chloride channel and a ryanodine receptor calcium release channel modulator.* J Biol Chem. , 2001. **276**(5): p. 3319-23.
270. Board, P.G. and M.W. Anders, *Glutathione transferase omega 1 catalyzes the reduction of S-(phenacyl)glutathiones to acetophenones.* Chem Res Toxicol, 2007. **20**(1): p. 149-54.
271. Kitada, M., J.C. McLenithan, and M.W. Anders, *Purification and characterization of S-phenacylglutathione reductase from rat liver.* J Biol Chem, 1985. **260**(21): p. 11749-54.
272. Piacentini, S., et al., *GSTO1*E155del polymorphism associated with increased risk for late-onset Alzheimer's disease: Association hypothesis for an uncommon genetic variant.* Neurosci Lett., 2012. **506**(2): p. 203-207.
273. Dittrich, A.M., et al., *Glutathione Peroxidase-2 Protects from Allergen-Induced Airway Inflammation in mice.* Eur Respir J. , 2010. **35**(5): p. 1148–1154.
274. Chowdhury, U.K., et al., *Glutathione transferase omega [MMA(V) reductase] knockout mice: Enzyme and arsenic species concentrations in tissues after arsenate administration.* Toxicology and Applied Pharmacology, 2006. **216**: p. 446-457.
275. Schmuck, E.M., et al., *Characterization of the monomethylarsonate reductase and dehydroascorbate reductase activities of Omega class glutathione transferase variants: implications for arsenic metabolism and the age-at-onset of Alzheimer's and Parkinson's diseases.* Pharmacogenetics and Genomics 2005. **15**: p. 493–501.
276. Ozinsky, A., et al., *The repertoire for pattern recognition of pathogens by the innate immune system is defined by cooperation between toll-like receptors.* Proceedings of the National Academy of Sciences, 2000. **97**(25): p. 13766-13771.
277. Schmidt, M., et al., *Crucial role for human Toll-like receptor 4 in the development of contact allergy to nickel.* Nat Immunol, 2010. **11**(9): p. 814-9.
278. Stoll, L.L., G.M. Denning, and N.L. Weintraub, *Endotoxin, TLR4 signaling and vascular inflammation: potential therapeutic targets in cardiovascular disease.* Current pharmaceutical design, 2006. **12**(32): p. 4229-4245.
279. Zhang, G. and S. Ghosh, *Toll-like receptor–mediated NF-κB activation: a phylogenetically conserved paradigm in innate immunity.* Journal of Clinical Investigation, 2001. **107**(1): p. 13-19.
280. Gill, R., A. Tsung, and T. Billiar, *Linking oxidative stress to inflammation: Toll-like receptors.* Free Radical Biology and Medicine, 2010. **48**(9): p. 1121-1132.
281. Zhou, R., et al., *Thioredoxin-interacting protein links oxidative stress to inflammasome activation.* Nature immunology, 2009. **11**(2): p. 136-140.
282. Valkov, E., et al., *Crystal structure of Toll-like receptor adaptor MAL/TIRAP reveals the molecular basis for signal transduction and disease protection.* Proc Natl Acad Sci U S A, 2011. **108**(36): p. 14879-84.
283. Haneklaus, M., L.A. O'Neill, and R.C. Coll, *Modulatory mechanisms controlling the NLRP3 inflammasome in inflammation: recent developments.* Curr Opin Immunol, 2013. **25**(1): p. 40-5.
284. Zhou, R., et al., *A role for mitochondria in NLRP3 inflammasome activation.* Nature, 2011. **469**(7329): p. 221-5.

285. Dostert, C., et al., *Innate immune activation through Nalp3 inflammasome sensing of asbestos and silica.* Science, 2008. **320**(5876): p. 674-7.
286. Hornung, V., et al., *Silica crystals and aluminum salts activate the NALP3 inflammasome through phagosomal destabilization.* Nat Immunol, 2008. **9**(8): p. 847-56.
287. Kim, S.R., et al., *NLRP3 inflammasome activation by mitochondrial ROS in bronchial epithelial cells is required for allergic inflammation.* Cell Death Dis, 2014. **5**: p. e1498.
288. Hua, K.F., et al., *Cyclooxygenase-2 Regulates NLRP3 Inflammasome-Derived IL-1beta Production.* J Cell Physiol, 2015. **230**(4): p. 863-74.
289. Zhong, Z., et al., *TRPM2 links oxidative stress to NLRP3 inflammasome activation.* Nat Commun, 2013. **4**: p. 1611.
290. Axline, S.G. and E.P. Reaven, *Inhibition of phagocytosis and plasma membrane mobility of the cultivated macrophage by cytochalasin B. Role of subplasmalemmal microfilaments.* J Cell Biol, 1974. **62**(3): p. 647-59.
291. Sung, S.J. and S.C. Silverstein, *Inhibition of macrophage phagocytosis by methylation inhibitors. Lack of correlation of protein carboxymethylation and phospholipid methylation with phagocytosis.* J Biol Chem, 1985. **260**(1): p. 546-54.
292. Mo, C., et al., *The Crosstalk Between Nrf2 and AMPK Signal Pathways Is Important for the Anti-Inflammatory Effect of Berberine in LPS-Stimulated Macrophages and Endotoxin-Shocked Mice.* Antioxidants & redox signaling, 2013. **20**(4): p. 574-88.
293. Sakai, J., et al., *Reactive oxygen species-induced actin glutathionylation controls actin dynamics in neutrophils.* Immunity, 2012. **37**(6): p. 1037-49.
294. Baker, R.T., et al., *Using deubiquitylating enzymes as research tools.* Methods Enzymol, 2005. **398**: p. 540-54.
295. Towbin, H., T. Staehelin, and J. Gordon, *Electrophoretic transfer of proteins from polyacrylamide gels to nitrocellulose sheets: procedure and some applications.* Proc Natl Acad Sci U S A, 1979. **76**(9): p. 4350-4.
296. Rahman, I., A. Kode, and S.K. Biswas, *Assay for quantitative determination of glutathione and glutathione disulfide levels using enzymatic recycling method.* Nature Protocol, 2006. **1**(6): p. 3159-3165.
297. Hill, B.G. and A. Bhatnagar, *Role of Glutathiolation in Preservation, Restoration and Regulation of Protein function.* IUBMB Life, 2007. **59**(1): p. 21-26.
298. O'Neill, L.A. and D.G. Hardie, *Metabolism of inflammation limited by AMPK and pseudo-starvation.* Nature, 2013. **493**(7432): p. 346-355.
299. Vivancos, P.D., et al., *A nuclear glutathione cycle within the cell cycle.* Biochem. J., 2010. **431**: p. 169-178.
300. Awasthi, Y.C., R.a. Sharma, and S.S. Singhal, *Human Glutathione S-Transferases.* Int. J. Biochem., 1994. **26**(3): p. 295-308.
301. Eaton, D.L. and K.T. Bammler, *Concise Review of the Glutathione S-Transferases and their Significance to Toxicology.* Toxicological Sciences, 1999. **49**: p. 156-164.
302. Fratelli, M., et al., *Identification of proteins undergoing glutathionylation in oxidatively stressed hepatocytes and hepatoma cells.* Proteomics, 2003. **3**: p. 1154-1161.
303. Gilge, J.L., M. Fisher, and Y.-C. Chai, *The effect of Oxidant and the Non-oxidant Alteration of Cellular Thiol Concentration on the formation of protein mixed disulphides in HEK 293 cells.* PLOS one, 2008. **3**(12): p. e4015.

304. Jung, C.H. and J.A. Thomas, *S-Glutathiolated Hepatocyte Proteins and Insulin Disulfides as Substrates for Reduction by Glutaredoxin, Thioredoxin, Protein Disulfide Isomerase, and Glutathione.* Arch. Biochem. Biophys., 1996. **335**: p. 61-72.
305. Dalle-Donne, I., et al., *Protein S-glutathionylation: a regulatory device from bacteria to humans.* Trends Biochem Sci, 2009. **34**(2): p. 85-96.
306. Lind, C., et al., *Identification of S-glutathionylated cellular proteins during oxidative stress and constitutive metabolism by affinity purification and proteomic analysis.* Archives of Biochemistry and Biophysics, 2002. **406**(2): p. 229-240.
307. Su, D., et al., *Proteomic Identification and Quantification of S-glutathionylation in Mouse Macrophages Using Resin-Assisted Enrichment and Isobaric Labeling.* Free Radical Biology and Medicine, 2014. **67**: p. 460-70.
308. Cheng, G., et al., *A novel method to detect S-glutathionylated proteins by Glutathione S-transferase.* Archives of Biochemistry and Biophysics 2005. **435**(1): p. 42-49.
309. Gao, X.-H., et al., *Methods for Analysis of Protein Glutathionylation and their Application to Photosynthetic Organisms.* Mol. Plant, 2009. **2**(2): p. 218-235.
310. Sullivan, D.M., et al., *Identification of Oxidant-Sensitive Proteins: TNF-R Induces Protein Glutathiolation.* Biochemistry, 2000. **39**: p. 11121-11128.
311. Zhang, C., et al., *S-Glutathionyl quantification in the attomole range using glutaredoxin-3-catalyzed cysteine derivatization and capillary gel electrophoresis with laser-induced fluorescence detection.* Anal Bioanal Chem. **401**(7): p. 2165-75.
312. Orwar, O., et al., *Use of 2,3-naphthalenedicarboxaldehyde derivatization for single-cell analysis of glutathione by capillary electrophoresis and histochemical localization by fluorescence microscopy.* Anal Chem, 1995. **67**(23): p. 4261-8.
313. White, C.C., et al., *Fluorescence-based microtiter plate assay for glutamate-cysteine ligase activity.* Anal Biochem, 2003. **318**(2): p. 175-80.
314. de Luca, A., et al., *Treatment of doxorubicin-resistant MCF7/Dx cells with nitric oxide causes histone glutathionylation and reversal of drug resistance.* Biochem J, 2011. **440**(2): p. 175-83.
315. Wang, S., et al., *Doxorubicin induces apoptosis in normal and tumor cells via distinctly different mechanisms. intermediacy of H(2)O(2)- and p53-dependent pathways.* J Biol Chem, 2004. **279**(24): p. 25535-43.
316. Zhou, S., C.M. Palmeira, and K.B. Wallace, *Doxorubicin-induced persistent oxidative stress to cardiac myocytes.* Toxicol Lett, 2001. **121**(3): p. 151-7.
317. Oakley, A.J., et al., *The identification and structural characterization of C7orf24 as gamma-glutamyl cyclotransferase. An essential enzyme in the gamma-glutamyl cycle.* J Biol Chem, 2008. **283**(32): p. 22031-42.
318. Hakanson, R. and A.L. Ronnberg, *Improved fluorometric assay of histamine: condensation with O-phthalaldehyde at -20 degrees C.* Anal Biochem, 1974. **60**(2): p. 560-7.
319. Dalle-Donne, I., et al., *Protein S-glutathionylation: a regulatory device from bacteria to humans.* Trends in Biochemical Sciences, 2009. **34**(2): p. 85-96.
320. Mieyal, J.J., et al., *Molecular mechanisms and clinical implications of reversible protein S-glutathionylation.* Antioxid Redox Signal, 2008. **10**(11): p. 1941-88.
321. Schmuck, E., et al., *Deletion of Glu155 causes a deficiency of glutathione transferase Omega 1-1 but does not alter sensitivity to arsenic trioxide and other cytotoxic drugs.* Int J Biochem Cell Biol., 2008. **40**(11): p. 2553-2559.

322. Menon, D. and P.G. Board, *A fluorometric method to quantify protein glutathionylation using glutathione derivatization with 2,3-naphthalenedicarboxaldehyde.* Anal Biochem, 2013. **433**(2): p. 132-6.
323. Schmuck, E.M., et al., *Characterization of the monomethylarsonate reductase and dehydroascorbate reductase activities of Omega class glutathione transferase variants: implications for arsenic metabolism and the age-at-onset of Alzheimer's and Parkinson's diseases.* Pharmacogenet Genomics, 2005. **15**(7): p. 493-501.
324. Robinson, A., et al., *Modelling and bioinformatics studies of the human Kappa-class glutathione transferase predict a novel third glutathione transferase family with similarity to prokaryotic 2-hydroxychromene-2-carboxylate isomerases.* Biochem J, 2004. **379**(Pt 3): p. 541-52.
325. Starke, D.W., P.B. Chock, and J.J. Mieyal, *Glutathione-thiyl radical scavenging and transferase properties of human glutaredoxin (thioltransferase). Potential role in redox signal transduction.* J Biol Chem, 2003. **278**(17): p. 14607-13.
326. Findlay, V.J., et al., *A novel role for human sulfiredoxin in the reversal of glutathionylation.* Cancer Res, 2006. **66**(13): p. 6800-6.
327. Robinson, A., et al., *Modelling and bioinformatics studies of the human Kappa class Glutathione Transferase predict a novel third Glutathione Transferase family with homology to prokaryotic 2-hydroxychromene-2-carboxylate (HCCA) Isomerases.* Biochem J, 2004. **379**(Pt3): p. 541-52.
328. Staab, C.A., et al., *Reduction of S-nitrosoglutathione by alcohol dehydrogenase 3 is facilitated by substrate alcohols via direct cofactor recycling and leads to GSH-controlled formation of glutathione transferase inhibitors.* Biochem J, 2008. **413**(3): p. 493-504.
329. Klatt, P. and S. Lamas, *Regulation of protein function by S-glutathiolation in response to oxidative and nitrosative stress.* Eur J Biochem, 2000. **267**(16): p. 4928-44.
330. Park, J.-W., *Reaction of S-Nitrosoglutathione with Sulfhydryl Groups in Protein.* Biochemical and Biophysical Research Communications, 1988. **152**(2): p. 916-920.
331. Lee, K.K., et al., *Novel function of glutathione transferase in rat liver mitochondrial membrane: role for cytochrome c release from mitochondria.* Toxicol Appl Pharmacol, 2008. **232**(1): p. 109-18.
332. Listowsky, I., *Proposed intracellular regulatory functions of glutathione transferases by recognition and binding to S-glutathiolated proteins.* J.Peptide Res., 2005. **65**: p. 42-46.
333. Laborde, E., *Glutathione transferases as mediators of signaling pathways involved in cell proliferation and cell death.* Cell Death Differ., 2010. **17**(9): p. 1373-80.
334. Klaus, A., et al., *Glutathione S-transferases interact with AMP-activated protein kinase: evidence for S-glutathionylation and activation in vitro.* PLOS one, 2013. **8**(5): p. e62497.
335. Zhou, H., et al., *Novel folding and stability defects cause a deficiency of human glutathione transferase omega 1.* J Biol Chem., 2011. **286**(6): p. 4271-4279.
336. Schmuck, E., et al., *Deletion of Glu155 causes a deficiency of glutathione transferase Omega 1-1 but does not alter sensitivity to arsenic trioxide and other cytotoxic drugs.* Int J Biochem Cell Biol, 2008. **40**(11): p. 2553-9.
337. Carletti, B., et al., *Effect of protein glutathionylation on neuronal cytoskeleton: a potential link to neurodegeneration.* Neuroscience, 2011. **192**: p. 285-94.
338. Cordes, C.M., et al., *Redox regulation of insulin degradation by insulin-degrading enzyme.* PLoS One, 2011. **6**(3): p. e18138.

339. Sabens Liedhegner, E.A., X.H. Gao, and J.J. Mieyal, *Mechanisms of altered redox regulation in neurodegenerative diseases--focus on S--glutathionylation.* Antioxid Redox Signal, 2012. **16**(6): p. 543-66.
340. Gauss, K.A., et al., *Role of NF-κB in transcriptional regulation of the phagocyte NADPH oxidase by tumor necrosis factor-α.* Journal of leukocyte biology, 2007. **82**(3): p. 729-741.
341. Mittal, M., et al., *Reactive Oxygen Species in Inflammation and Tissue Injury.* Antioxidants & redox signaling, 2013. **20**(7): p. 1126-67.
342. Wood, L.G., P.A. Wark, and M.L. Garg, *Antioxidant and anti-inflammatory effects of resveratrol in airway disease.* Antioxidants & redox signaling, 2010. **13**(10): p. 1535-1548.
343. West, A.P., et al., *TLR signalling augments macrophage bactericidal activity through mitochondrial ROS.* Nature, 2011. **472**(7344): p. 476-480.
344. Matsuzawa, A., et al., *ROS-dependent activation of the TRAF6-ASK1-p38 pathway is selectively required for TLR4-mediated innate immunity.* Nature immunology, 2005. **6**(6): p. 587-592.
345. Menon, D., et al., *Glutathione transferase Omega 1 is required for the LPS stimulated induction of NADPH oxidase 1 and the production of reactive oxygen species in macrophages.* Free Radical Biology and Medicine, 2014. **73**: p. 318-327.
346. Bokoch, G.M. and T. Zhao, *Regulation of the phagocyte NADPH oxidase by Rac GTPase.* Antioxidants & redox signaling, 2006. **8**(9-10): p. 1533-1548.
347. Sinha, A.K., *Colorimetric assay of catalase.* Analytical biochemistry, 1972. **47**(2): p. 389-394.
348. Board, P.G., et al., *S-(4-Nitrophenacyl)glutathione is a specific substrate for glutathione transferase omega 1-1.* Anal Biochem, 2008. **374**(1): p. 25-30.
349. Zandi, E., et al., *The IκB kinase complex (IKK) contains two kinase subunits, IKKα and IKKβ, necessary for IκB phosphorylation and NF-κB activation.* Cell, 1997. **91**(2): p. 243-252.
350. Tsuboi, K., et al., *Optimization and Characterization of an Inhibitor for Glutathione S-Tranferase Omega 1 (GSTO1)*, in *Probe Reports from the NIH Molecular Libraries Program*, N.C.B.I. (US), Editor 2010: Bethesda (MD).
351. van den Bosch, M.W.M., et al., *LPS induces the degradation of PDCD4 to release Twist2, activating c-Maf transcription to promote IL-10.* J Biol Chem, 2014. **289**(33): p. 22980-90.
352. Park, E.Y., I.J. Cho, and S.G. Kim, *Transactivation of the PPAR-responsive enhancer module in chemopreventive glutathione S-transferase gene by the peroxisome proliferator-activated receptor-γ and retinoid X receptor heterodimer.* Cancer Research, 2004. **64**(10): p. 3701-3713.
353. Cho, H.-Y., S.P. Reddy, and S.R. Kleeberger, *Nrf2 defends the lung from oxidative stress.* Antioxidants & redox signaling, 2006. **8**(1-2): p. 76-87.
354. Feingold, K.R., et al., *LPS decreases fatty acid oxidation and nuclear hormone receptors in the kidney.* J Lipid Res, 2008. **49**(10): p. 2179-87.
355. Hayden, M.S. and S. Ghosh, *Shared principles in NF-κB signaling.* Cell, 2008. **132**(3): p. 344-362.
356. Sun, S.-C., et al., *NF-kappa B controls expression of inhibitor I kappa B alpha: evidence for an inducible autoregulatory pathway.* Science, 1993. **259**(5103): p. 1912-1915.
357. Zandi, E., et al., *The IkappaB kinase complex (IKK) contains two kinase subunits, IKKalpha and IKKbeta, necessary for IkappaB phosphorylation and NF-kappaB activation.* Cell, 1997. **91**(2): p. 243-52.

358. DiDonato, J.A., et al., *A cytokine-responsive IkappaB kinase that activates the transcription factor NF-kappaB.* Nature, 1997. **388**(6642): p. 548-54.
359. Cordle, S.R., et al., *Lipopolysaccharide induces phosphorylation of MAD3 and activation of c-Rel and related NF-kappa B proteins in human monocytic THP-1 cells.* Journal of Biological Chemistry, 1993. **268**(16): p. 11803-11810.
360. Donald, R., D.W. Ballard, and J. Hawiger, *Proteolytic Processing of NF-B/IB in Human Monocytes ATP-dependent induction by pro-inflammatory mediators.* Journal of Biological Chemistry, 1995. **270**(1): p. 9-12.
361. Gay, N.J., M. Gangloff, and L.A. O'Neill, *What the Myddosome structure tells us about the initiation of innate immunity.* Trends Immunol, 2011. **32**(3): p. 104-9.
362. Lin, Z., et al., *Structural insights into TIR domain specificity of the bridging adaptor Mal in TLR4 signaling.* PLOS one, 2012. **7**(4): p. e34202.
363. Dowling, J.K. and L.A. O'Neill, *Biochemical regulation of the inflammasome.* Critical Reviews in Biochemistry and Molecular Biology, 2012. **47**(5): p. 424-443.
364. Franchi, L., et al., *The inflammasome: a caspase-1-activation platform that regulates immune responses and disease pathogenesis.* Nature immunology, 2009. **10**(3): p. 241-247.
365. Necela, B.M., W. Su, and E.A. Thompson, *Toll-like receptor 4 mediates cross-talk between peroxisome proliferator-activated receptor γ and nuclear factor-κB in macrophages.* Immunology, 2008. **125**(3): p. 344-358.
366. Raso, G.M., et al., *Inhibition of inducible nitric oxide synthase and cyclooxygenase-2 expression by flavonoids in macrophage J774A.1.* Life Sci, 2001. **68**(8): p. 921-31.
367. Thimmulappa, R.K., et al., *Nrf2-dependent protection from LPS induced inflammatory response and mortality by CDDO-Imidazolide.* Biochemical and biophysical research communications, 2006. **351**(4): p. 883-889.
368. Sekhar, K.R., et al., *Redox-sensitive interaction between KIAA0132 and Nrf2 mediates indomethacin-induced expression of γ-glutamylcysteine synthetase.* Free Radical Biology and Medicine, 2002. **32**(7): p. 650-662.
369. Suzawa, M., et al., *Cytokines suppress adipogenesis and PPAR-γ function through the TAK1/TAB1/NIK cascade.* Nature cell biology, 2003. **5**(3): p. 224-230.
370. Adamik, J., et al., *Distinct Mechanisms for Induction and Tolerance Regulate the Immediate Early Genes Encoding Interleukin 1β and Tumor Necrosis Factor α.* PLOS one, 2013. **8**(8): p. e70622.
371. Heneka, M.T., et al., *NLRP3 is activated in Alzheimer's disease and contributes to pathology in APP/PS1 mice.* Nature, 2013. **493**(7434): p. 674-8.
372. Mrak, R.E. and W.S. Griffin, *Interleukin-1, neuroinflammation, and Alzheimer's disease.* Neurobiol Aging, 2001. **22**(6): p. 903-8.
373. Haschemi, A., et al., *The sedoheptulose kinase CARKL directs macrophage polarization through control of glucose metabolism.* Cell Metab, 2012. **15**(6): p. 813-26.
374. Freemerman, A.J., et al., *Metabolic reprogramming of macrophages: glucose transporter 1 (GLUT1)-mediated glucose metabolism drives a proinflammatory phenotype.* J Biol Chem, 2014. **289**(11): p. 7884-96.
375. Marsin, A.-S., et al., *The stimulation of glycolysis by hypoxia in activated monocytes is mediated by AMP-activated protein kinase and inducible 6-phosphofructo-2-kinase.* Journal of Biological Chemistry, 2002. **277**(34): p. 30778-30783.

376. Chen, C., Y.H. Chen, and W.W. Lin, *Involvement of p38 mitogen-activated protein kinase in lipopolysaccharide-induced iNOS and COX-2 expression in J774 macrophages.* Immunology, 1999. **97**(1): p. 124-9.
377. McGettrick, A.F. and L.A. O'Neill, *How metabolism generates signals during innate immunity and inflammation.* Journal of Biological Chemistry, 2013. **288**(32): p. 22893-22898.
378. Demas, G.E., et al., *Metabolic costs of mounting an antigen-stimulated immune response in adult and aged C57BL/6J mice.* Am J Physiol, 1997. **273**(5): p. 1631-7.
379. Infantino, V., et al., *The mitochondrial citrate carrier: a new player in inflammation.* Biochem J, 2011. **438**(3): p. 433-6.
380. Hoshino, K., et al., *Cutting edge: Toll-like receptor 4 (TLR4)-deficient mice are hyporesponsive to lipopolysaccharide: evidence for TLR4 as the Lps gene product.* J Immunol, 1999. **162**(7): p. 3749-52.
381. Kawai, T., et al., *Unresponsiveness of MyD88-deficient mice to endotoxin.* Immunity, 1999. **11**(1): p. 115-22.
382. Fitzgerald, K.A., et al., *Mal (MyD88-adapter-like) is required for Toll-like receptor-4 signal transduction.* Nature, 2001. **413**(6851): p. 78-83.
383. Horng, T., et al., *The adaptor molecule TIRAP provides signalling specificity for Toll-like receptors.* Nature, 2002. **420**(6913): p. 329-33.
384. Horng, T., G.M. Barton, and R. Medzhitov, *TIRAP: an adapter molecule in the Toll signaling pathway.* Nat Immunol, 2001. **2**(9): p. 835-41.
385. Bentala, H., et al., *Removal of phosphate from lipid A as a strategy to detoxify lipopolysaccharide.* Shock, 2002. **18**(6): p. 561-6.
386. Lim, C.E., et al., *Mice deficient in glutathione transferase zeta/maleylacetoacetate isomerase exhibit a range of pathological changes and elevated expression of alpha, mu, and pi class glutathione transferases.* Am J Pathol, 2004. **165**(2): p. 679-93.
387. Groeneveld, P.H., T. Erich, and G. Kraal, *The differential effects of bacterial lipopolysaccharide (LPS) on splenic non-lymphoid cells demonstrated by monoclonal antibodies.* Immunology, 1986. **58**(2): p. 285-90.
388. Chanas, S.A., et al., *Loss of the Nrf2 transcription factor causes a marked reduction in constitutive and inducible expression of the glutathione S-transferase Gsta1, Gsta2, Gstm1, Gstm2, Gstm3 and Gstm4 genes in the livers of male and female mice.* Biochem J, 2002. **365**(Pt 2): p. 405-16.
389. Hayes, J.D., et al., *The Nrf2 transcription factor contributes both to the basal expression of glutathione S-transferases in mouse liver and to their induction by the chemopreventive synthetic antioxidants, butylated hydroxyanisole and ethoxyquin.* Biochem Soc Trans, 2000. **28**(2): p. 33-41.
390. Henderson, C.J., A.W. McLaren, and C.R. Wolf, *In vivo regulation of human glutathione transferase GSTP by chemopreventive agents.* Cancer Res, 2014. **74**(16): p. 4378-87.
391. Gambhir, L., et al., *1,4-Naphthoquinone, a pro-oxidant, suppresses immune responses via KEAP-1 glutathionylation.* Biochem Pharmacol, 2014. **88**(1): p. 95-105.
392. Planson, A.G., et al., *Sulfiredoxin protects mice from lipopolysaccharide-induced endotoxic shock.* Antioxid Redox Signal, 2011. **14**(11): p. 2071-80.
393. Ferrao, R., et al., *IRAK4 dimerization and trans-autophosphorylation are induced by Myddosome assembly.* Mol Cell, 2014. **55**(6): p. 891-903.
394. Klomsiri, C., et al., *Use of dimedone-based chemical probes for sulfenic acid detection evaluation of conditions affecting probe incorporation into redox-sensitive proteins.* Methods Enzymol, 2010. **473**: p. 77-94.

395. Matsunaga, N., et al., *TAK-242 (resatorvid), a small-molecule inhibitor of Toll-like receptor (TLR) 4 signaling, binds selectively to TLR4 and interferes with interactions between TLR4 and its adaptor molecules.* Mol Pharmacol, 2011. **79**(1): p. 34-41.
396. Piao, W., et al., *Tyrosine phosphorylation of MyD88 adapter-like (Mal) is critical for signal transduction and blocked in endotoxin tolerance.* J Biol Chem, 2008. **283**(6): p. 3109-19.
397. Hanna, M.E., et al., *Perturbations in dopamine synthesis lead to discrete physiological effects and impact oxidative stress response in Drosophila.* J Insect Physiol, 2015. **73C**: p. 11-19.
398. Kuroda, N., et al., *Apoptotic response through a high mobility box 1 protein-dependent mechanism in LPS/GalN-induced mouse liver failure and glycyrrhizin-mediated inhibition.* PLOS one, 2014. **9**(4): p. e92884.
399. Yang, H., et al., *MD-2 is required for disulfide HMGB1-dependent TLR4 signaling.* J Exp Med, 2015. **212**(1): p. 5-14.
400. Palsson-McDermott, E.M. and L.A. O'Neill, *The Warburg effect then and now: from cancer to inflammatory diseases.* Bioessays, 2013. **35**(11): p. 965-73.
401. Apte, R.N., et al., *The involvement of IL-1 in tumorigenesis, tumor invasiveness, metastasis and tumor-host interactions.* Cancer Metastasis Rev, 2006. **25**(3): p. 387-408.
402. Sica, A., et al., *Macrophage polarization in tumour progression.* Semin Cancer Biol, 2008. **18**(5): p. 349-55.
403. Stienstra, R., et al., *The inflammasome-mediated caspase-1 activation controls adipocyte differentiation and insulin sensitivity.* Cell metabolism, 2010. **12**(6): p. 593-605.
404. Wen, H., et al., *Fatty acid-induced NLRP3-ASC inflammasome activation interferes with insulin signaling.* Nature immunology, 2011. **12**(5): p. 408-415.
405. Weisberg, S.P., et al., *Obesity is associated with macrophage accumulation in adipose tissue.* Journal of Clinical Investigation, 2003. **112**(12): p. 1796-1808.
406. Cani, P.D., et al., *Metabolic endotoxemia initiates obesity and insulin resistance.* Diabetes, 2007. **56**(7): p. 1761-1772.
407. Xu, H., et al., *Chronic inflammation in fat plays a crucial role in the development of obesity-related insulin resistance.* Journal of Clinical Investigation, 2003. **112**(12): p. 1821-1830.
408. O'Leary, D.P., et al., *TLR-4 Signalling Accelerates Colon Cancer Cell Adhesion via NF-κB Mediated Transcriptional Up-Regulation of Nox-1.* PLOS one, 2012. **7**(10): p. e44176.
409. Kim, J., et al., *Metformin suppresses lipopolysaccharide (LPS)-induced inflammatory response in murine macrophages via activating transcription factor-3 (ATF-3) induction.* J Biol Chem, 2014. **289**(33): p. 23246-55.
410. Leone, A., et al., *New perspective for an old antidiabetic drug: metformin as anticancer agent.* Cancer Treat Res, 2014. **159**: p. 355-76.
411. Goodwin, P.J., et al., *Evaluation of metformin in early breast cancer: a modification of the traditional paradigm for clinical testing of anti-cancer agents.* Breast Cancer Res Treat, 2011. **126**(1): p. 215-20.
412. Fryer, L.G., A. Parbu-Patel, and D. Carling, *The Anti-diabetic drugs rosiglitazone and metformin stimulate AMP-activated protein kinase through distinct signaling pathways.* J Biol Chem, 2002. **277**(28): p. 25226-32.
413. Zou, M.H., et al., *Activation of the AMP-activated protein kinase by the anti-diabetic drug metformin in vivo. Role of mitochondrial reactive nitrogen species.* J Biol Chem, 2004. **279**(42): p. 43940-51.

414. Zhou, G., et al., *Role of AMP-activated protein kinase in mechanism of metformin action.* J Clin Invest, 2001. **108**(8): p. 1167-74.
415. Su, D., et al., *Proteomic identification and quantification of S-glutathionylation in mouse macrophages using resin-assisted enrichment and isobaric labeling.* Free Radic Biol Med, 2014. **67**: p. 460-70.
416. Into, T., et al., *Regulation of MyD88-dependent signaling events by S nitrosylation retards toll-like receptor signal transduction and initiation of acute-phase immune responses.* Mol Cell Biol, 2008. **28**(4): p. 1338-47.